Universidade de Aveiro
2011

Departamento de Química

Patrícia Sofia Matos dos Santos

Origem, sazonalidade e características químicas da água da chuva em Aveiro

Origin, seasonality and chemical characteristics of rainwater in Aveiro

Universidade de Aveiro
2011

Departamento de Química

Patrícia Sofia Matos dos Santos

Origem, sazonalidade e características químicas da água da chuva em Aveiro

Origin, seasonality and chemical characteristics of rainwater in Aveiro

Dissertação apresentada à Universidade de Aveiro para cumprimento dos requisitos necessários à obtenção do grau de Doutor em Química, realizada sob a orientação científica do Doutor Armando da Costa Duarte, Professor Catedrático do Departamento de Química da Universidade de Aveiro e da Doutora Maria Eduarda Bastos Henriques dos Santos, Professora Auxiliar do Departamento de Química da Universidade de Aveiro

Apoio financeiro da FCT e do FSE no âmbito do QREN - POPH – Tipologia 4.1 – Formação Avançada.

o júri

presidente

Prof. Doutora Celeste de Oliveira Alves Coelho
professora catedrática da Universidade do Aveiro

Prof. Doutora Maria Isabel Almeida Ferra
professora catedrática da Universidade da Beira Interior

Prof. Doutor Armando da Costa Duarte
professor catedrático da Universidade de Aveiro

Prof. Doutor Joaquim Carlos Gomes Esteves da Silva
professor associado com agregação da Faculdade de Ciências da Universidade do Porto

Prof. Doutora Maria Cristina Guiomar Antunes
professora auxiliar da Universidade de Trás-os-Montes e Alto Douro

Prof. Doutora Maria Eduarda Bastos Henriques dos Santos
professor auxiliar da Universidade de Aveiro

agradecimentos

Aos meus orientadores, Professor Doutor Armando Duarte e Professora Doutora Eduarda Santos, pela orientação científica, disponibilidade, confiança e simpatia que demonstraram ao longo da realização deste trabalho.

À Doutora Marta Otero, pelo apoio, disponibilidade e amizade que demonstrou durante a realização deste trabalho.

Ao grupo de Química Orgânica, do Departamento de Química da Universidade de Aveiro, em particular à Professora Doutora Amparo Faustino e ao Professor Doutor Artur Silva, pela disponibilidade e cedência de equipamento para as análises de fluorescência.

Ao Professor Doutor Eduardo Silva e à Doutora Carla Patinha, do Departamento de Geociências da Universidade de Aveiro, pela disponibilidade e cedência de equipamento para a determinação de iões.

À Professora Doutora Maria de Los Dolores Orgaz, do Departamento de Física, pela disponibilidade e cedência do espaço para amostragem da água da chuva e pelos dados meteorológicos.

À Dra. Ana Maria Félix e à Dra. Rosário Figueiredo, do Laboratório da Administração Regional de Saúde de Aveiro, pela disponibilidade e cedência de equipamento para a determinação do carbono orgânico dissolvido.

À Dra. Teresa Caldeira, ao Sr. Ivo Mateus, ao Dr. Hilário Tavares, e a todos os que contribuíram para a realização deste trabalho.

Aos tantos colegas e amigos, em particular à Joana Coimbra, à Olga Filipe, à Vânia Calisto, pela força e amizade que demonstraram durante a realização deste trabalho.

À minha irmã, cunhado e sobrinha pela força…

Aos melhores pais do mundo, os meus, por tudo...

Ao Pedro, pelo amor incondicional…

À Fundação para a Ciência e Tecnologia, pela atribuição de uma Bolsa de Doutoramento (Referência SFRH/BD/27379/2006) que permitiu a realização deste trabalho.

palavras-chave

água da chuva, composição química, matéria orgânica dissolvida, caracterização estrutural, variação sazonal, trajectórias das massas de ar.

resumo

Este trabalho teve como objectivo caracterizar quimicamente a água da chuva recolhida na cidade de Aveiro, localizada a sudoeste da Europa, no período de Setembro de 2008 a Setembro de 2009.

Para matrizes diluídas como a da água da chuva, as metodologias analíticas a utilizar para se conseguir uma rigorosa caracterização química são de grande importância e ainda não estão uniformizadas. Assim, para caracterizar a fracção orgânica, primeiramente foram comparadas duas metodologias de filtração (0.22 e 0.45 µm) e foram estudados dois procedimentos de preservação da água da chuva (refrigeração e congelação), utilizando a espectroscopia de fluorescência molecular. Além disso, foram comparados dois procedimentos de isolamento e extracção da matéria orgânica dissolvida (DOM) da água da chuva, baseados na sorção nos sorbentes DAX-8 e C-18, utilizando as espectroscopias de ultravioleta-visível e fluorescência molecular. Relativamente aos resultados das metodologias de filtração e preservação, é recomendada a filtração por 0.45 µm, assim como, as amostras de água da chuva deverão ser mantidas no escuro a 4ºC, no máximo até 4 dias, até às análises espectroscópicas. Relativamente à metodologia de isolamento e extracção da DOM, os resultados mostraram que o procedimento de isolamento baseado na C-18 extraiu a DOM que é representativa da matriz global, enquanto que o procedimento da DAX-8 extraiu preferencialmente a fracção do tipo húmico. Como no presente trabalho pretendíamos caracterizar a fracção do tipo húmico da DOM da água da chuva, foi escolhida a metodologia de isolamento e extracção baseada na sorção no sorvente DAX-8. Previamente ao isolamento e extracção da DOM da água da chuva, toda a fracção orgânica das amostras de água da chuva foi caracterizada pelas técnicas de ultravioleta-visível e de fluorescência molecular. As amostras mostraram características semelhantes às de outras águas naturais, e a água da chuva do Verão e Outono apresentou maior conteúdo da matéria orgânica dissolvida cromofórica que a do Inverno e Primavera. Posteriormente, a fracção do tipo húmico de algumas amostras de água da chuva, isolada e extraída pelo procedimento baseado na DAX-8, foi caracterizada utilizando as técnicas espectroscópicas de ultravioleta-visível, fluorescência molecular e ressonância magnética nuclear de protão. Todos os extractos continham uma mistura complexa de compostos hidroxilados e ácidos carboxílicos, com uma predominância da componente alifática e um baixo conteúdo da componente aromática.

A fracção inorgânica da água da chuva foi caracterizada determinando a concentração das seguintes espécies iónicas: H^+, NH_4^+, Cl^-, NO_3^-, SO_4^{2-}. Os resultados foram comparados com os obtidos na chuva colectada no mesmo local entre 1986-1989 e mostraram que de todos os iões determinados a concentração de NO_3^- foi a única que aumentou (cerca do dobro) em 20 anos, tendo sido atribuído ao aumento de veículos e emissões industriais na área de amostragem.

resumo

Durante o período de amostragem cerca de 80% da precipitação esteve associada a massas de ar oceânicas, enquanto a restante esteve relacionada com massas que tiveram uma influência antropogénica e terrestre. De um modo geral, para as fracções orgânica e inorgânica da água da chuva analisadas, o conteúdo químico foi menor para as amostras que estiveram associadas a massas de ar marítimas do que para as amostras que tiveram contribuições terrestres e antropogénicas.

keywords

rainwater, chemical composition, dissolved organic matter, estrutural characterization, seasonal variation, air mass trajectories.

abstract

The aim of this work was to characterize chemically the rainwater collected in the town of Aveiro, at the southwest of Europe. Rainwater samples were collected between September 2008 and September 2009.

For matrixes diluted as rainwater is, the analytical methodologies used to perform a rigorous chemical characterization are of extreme importance and are not still standardized. Thus, for characterizing the organic fraction, firstly were compared two methodologies of filtration (0.22 and 0.45 μm) and were studied two preservation procedures of rainwater (refrigeration and freezing), using the molecular fluorescence spectroscopy. Moreover, were compared two procedures of isolation and extraction of dissolved organic matter (DOM) from rainwater, based on sorption on the DAX-8 and the C-18 sorbents, using the ultraviolet-visible and molecular fluorescence spectroscopies. Regarding to the results of filtration and preservation methodologies, filtration through 0.45 μm is recommended, as well as, rainwater samples should be kept in the dark at 4ºC, no longer than 4 days, until spectroscopic analysis. Regarding to the methodologies of isolation and extraction of DOM, results showed that the C-18 based isolation procedure allow concentrating DOM that is more representative of the global matrix, while the DAX-8 procedure extracts preferentially the humic-like fraction. As in the present work we were interested in characterizing the humic-like fraction of rainwater DOM, it was chosen the methodology isolation and extraction based on sorption on the DAX-8 sorbent.

Previously to the isolation and extraction of rainwater DOM, the bulk organic fraction was characterized by ultraviolet-visible and molecular fluorescence techniques. Samples showed to have similar characteristics to other natural waters and rainwater from summer and autumn presented more content of chromophoric dissolved organic matter than that from winter and spring. Then, the humic-like fraction of some rainwater samples, isolated and extracted by the DAX-8 based procedure, was characterized by the spectroscopic techniques of ultraviolet-visible, molecular fluorescence and ^{1}H NMR, and results showed that the extracts consist of a complex mixture of hydroxylated compounds and carboxylic acids with a predominantly aliphatic character, containing a minor component of aromatics.

The inorganic fraction of the rainwater samples was characterized determining the concentration of the following ionic species: H^+, NH_4^+, Cl^-, NO_3^-, SO_4^{2-}. Results were compared with those obtained for rain collected at the same site between 1986-1989, and showed that of all the ions determined the concentration of NO_3^- was the only that increased (about twice) in twenty years, and it was attributed to the increase of local vehicular and industrial emissions in the sampling area.

resumo

During the sampling period, about 80 % of precipitation was associated to oceanic air masses, while the rest was related with air masses having more anthropogenic and terrestrial influence. Generally, for the organic and inorganic fractions analysed, the chemical content in rainwater was lower when samples were associated to maritime air masses than when samples were associated to terrestrial and anthropogenic air masses.

Index

Index xv

List of Symbols and Abbreviations xix

List de Tables xxi

List of Figures xxiii

1. Introduction 1

1.1 Rainwater: general grounds 1

1.2 Chemical composition of rainwater 4

1.2.1 Organic composition of rainwater 4

1.2.2 Inorganic composition of rainwater 7

1.2.3 Rainwater chemical composition measurements 9

1.3 Effects of chemical composition of rainwater in climate and human health 10

1.4 Main purposes of the work 11

References 13

2. Rainwater sampling and characterization of atmospheric conditions 21

2.1 Rainwater sampling in Aveiro 21

2.2. Atmospheric conditions associated to rainwater samples 24

3. Molecular fluorescence analysis of rainwater: effects of sample preservation 41

3.1 Introduction 42

3.2 Experimental 44

3.2.1 Rainwater sampling and preservation 44

3.2.2 Laboratory analytical procedures 46

3.3 Results and discussion 47
3.4 Conclusions 52
References 53
4. Comparison between DAX-8 and C-18 solid phase extraction of rainwater dissolved organic matter 57
4.1 Introduction 58
4.2 Experimental 60
4.2.1 Rainwater sampling and sample preparation 60
4.2.2 Fulvic acids solution preparation 60
4.2.3 Extraction of dissolved organic matter (DOM) 61
4.2.3 Optical analysis 63
4.3 Results and discussion 64
4.4 Conclusions 73
References 74
5. Seasonal and air mass trajectory effects on rainwater dissolved organic matter at a coastal town on the southwest of Europe 77
5.1 Introduction 78
5.2 Experimental 80
5.2.1 Rainwater sampling and sample preparation 80
5.2.3 Measurements of dissolved organic carbon (DOC) 80
5.2.4 Optical analysis 81
5.2.5 Air mass trajectories origin and meteorological data 82
5.3 Results and discussion 83
5.4 Conclusions 96
References 98
6. Chemical features and seasonal variation of dissolved organic matter isolated from rainwater 101
6.1 Introduction 102
6.2 Experimental 103
6.2.1. Rainwater sampling and sample preparation 103
6.2.2. Extraction of dissolved organic matter (DOM) 104
6.2.3 Measurements of dissolved organic carbon (DOC) 105

6.2.4 Optical analysis 105
6.2.5 ^{1}H NMR spectroscopy 107
6.2.6 Air mass trajectories origin and meteorological data 107
6.3 Results and discussion 108
6.3.1 UV-visible spectra 109
6.3.2 Excitation-emission matrix fluorescence spectra 111
6.3.3 ^{1}H NMR spectra 114
6.4 Conclusions 118
References 119
7. Chemical composition of rainwater at a coastal town on the southwest of Europe: What changes in 20 years? 123
7.1 Introduction 124
7.2 Experimental 125
7.2.1 Rainwater sampling and analysis 125
7.2.2 Air mass trajectories and meteorological data 126
7.3 Results and discussion 127
7.4 Conclusions 134
References 135
8. Final considerations 139
Annex I. Air mass trajectories calculated for events whose rainwater was not collected between September 2008 and September 2009 145
Annex II. Excitation-emission matrix fluorescence contour and surface profiles of the collected rainwater samples 153
Annex III. Excitation-emission matrix fluorescence contour and surface profiles of the eluates of rainwater samples 161

List of Symbols and Abbreviations

CCN	- cloud condensation nuclei
CDOM	- chromophoric dissolved organic matter
DMSO	- dimethylsulfoxide
DOC	- dissolved organic carbon
DOM	- dissolved organic matter
EC	- electrical conductivity
EEM	- excitation-emission matrix
e.g.	- for example
ELIX	- electronic ion exchange
FA	- fulvic acids
FI	- fluorescence intensitie
FTIR	- “Fourier” transform infrared
HULIS	- humic like substances
IC	- inorganic carbon
IHSS	- international humic substance society
MW	- molecular weight
NMR	- nuclear magnetic resonance
QS	- quinine sulphate
OM	- organic matter
RS	- rainwater sample
RS1…RS40	- rainwater sample RS1…rainwater sample RS40
S	- spectral slope coefficients
SFI	- specific fluorescence intensity
TC	- total carbon

TFC	- thin film composite
UV-Visible	- ultraviolet-visible
UV	- ultravioleta
UV_{250}	- absorbance at 250 nm
VOC	- volatile organic carbon
VWA	- volume weighted average
WSOM	- water-soluble organic matter
ε	- specific absorptivity
ε_{280}	- specific absorptivity at 280 nm
δ_H	- chemical shift
$\Delta\lambda$	- wavelength variation
λ	- wavelength
λ_{ex}	- excitation wavelength
λ_{em}	- emission wavelength

List of Tables

Table 2.1 - Rainwater samples collected, sampling date and season.

Table 2.2 - Summer of meteorological data observed for each rainwater sample.

Table 2.3 - Percentage of total and seasonal rainwater amount discriminated according to air-mass trajectories for all precipitation events between September 2008 and September 2009.

Table 2.4 - Percentage of total and seasonal rainwater amount discriminated according to air-mass trajectories for collected rainwater events between September 2008 and September 2009.

Table 3.1 - Works published on the rainwater dissolved organic fraction during the last decade.

Table 4.1 - Spectral slope coefficients (μm^{-1}) calculated for the different fractions of FA solution and rainwater, obtained by the DAX-8 and C-18 isolation procedures.

Table 4.2 - Band, excitation/emission wavelength maxima range and attribution of fluorescent DOM in rainwater based in previous works (Kieber et al., 2006; Muller et al., 2008; Santos et al., 2009a,b).

Table 4.3 - Percentages of DOM retention and recovery obtained from the DAX-8 and C-18 isolation procedures.

Table 5.1 - Rainwater VWA DOC concentrations (mg L^{-1}), UV absorbance at 250 nm (UV_{250nm}; absorbance units), specific absorptivity at 280 nm

(ε_{280nm}; $Lg^{-1}C\ cm^{-1}$), spectral slope coefficient (μm^{-1}), integrated fluorescence for the entire scan (integrated fluorescence units) and A:M ratio for the total of samples collected, for the samples of the hydrological year 2009, for samples grouped by seasons and for samples grouped by air masses trajectories (class).

Table 5.2 - Average excitation and emission wavelength maxima (± standard deviation) of the fluorescence of humic-like bands and its VWA of fluorescence intensity (FI; ppb QS) for samples collected at the different seasons and for samples grouped by air masses trajectories (class). The standard deviations of VWA FI and VWA SFI are indicated between brackets.

Table 6.1 - Rainwater samples subjected to the DAX-8 based isolation procedure, classified according to the season and air mass trajectory associated, eluate DOC and percentage of recoveries of rainwater organic matter resulting from the isolation procedure.

Table 7.1 - Rainwater VWA EC and ion concentrations for the total of samples collected, for the samples of the hydrological year (2009) and for samples collected at the different seasons. Results obtained in this study are compared with those reported in the literature for rainwater collected in Aveiro and for rainwater collected at different sites on the south-western coast of Europe.

Table 7.2 - Rainwater VWA ion concentrations and EC calculated corresponding to rainwater classified by dominant air masses trajectories.

Table 7.3 - Pearson correlation coefficients for rainwater volume, EC and ions concentrations.

Table 7.4 - Varimax rotated factor matrix and communalities of metals in rainwater samples.

List of Figures

Figure 1.1 - Conceptual framework of wet deposition processes (adapted from Seinfeld and Pandis, 1998)

Figure 2.1 - Schematic maps of Portugal and Aveiro showing the location of the sampling site (orange arrow).

Figure 2.2 - Photographs of the sampling station and of the collectors of rainwater.

Figure 2.3 - Values of accumulated precipitation, values of minimum, median (●) and maximum of temperature (ºC), and values of minimum, median (○) and maximum of relative humidity (%) associated to each rainwater sample.

Figure 2.4 - Wind Roses, with indication of percentages of distribution of wind velocity in function of its direction, associated to each rainwater sample.

Figure 2.5 - Air mass trajectories generated for a 48 h hind-cast starting at 10 and 500 m level, calculated every 6 h for each rainwater sample.

Figure 2.6 - The air mass trajectory analysis at 500 m level, for the rainwater sample RS1 collected at 04 September 2008, to exemplify the classification of rainwater according to air-mass origins and trajectories.

Figure 3.1 - Schematic diagram of the experimental procedure adopted.

Figure 3.2 - EEM fluorescence contour profiles of a) A08 and b) O08 rainwater

samples. Fluorescence intensities are presented in ppb QS. The line S indicates the spectral range covered by the synchronous mode using $\Delta\lambda$ = 70 nm. The line E corresponds to the excitation spectrum at λ_{em}=415 nm.

Figure 3.3 - Excitation, (a) and (b), and synchronous, (c) and (d), fluorescence spectra corresponding to O08 rainwater analysed after refrigeration (1 to 7 days), for the two filtrates (0.22 and 0.45 µm).

Figure 3.4 - Excitation, (a) and (b), and synchronous, (c) and (d), fluorescence spectra corresponding to O08 rainwater analysed after freezing (1 to 4 weeks), for the two filtrates (0.22 and 0.45 µm).

Figure 4.1 - Schematic diagram of the experimental procedures adopted for DOM isolation.

Figure 4.2 - UV-Vis spectra, with blank subtraction, obtained for the different fractions of FA solution (averages spectrum; a) and b)) and rainwater (J09, c) and d); O09a, e) and f); O09b, g) and h)), by each of the isolation procedures considered. The blanks of the procedures (averages spectrum) are presented in the graphs i) and j).

Figure 4.3 - Figure 4.3 Synchronous spectra of fluorescence, with blank subtraction, obtained for the different fractions of FA solutions (averages spectrum; a) and b)), rainwater (J09, c) and d); O09a, e) and f); O09b, g) and h)), by each of the isolation procedures considered. The blanks of the procedures (averages spectrum) are presented in the graphs i) and j).

Figure 5.1 - The air mass trajectory analysis at 10 m (a) and 500 m (b) level, for the rainwater sample (RS1) collected at 04 September 2008, to exemplify the classification of rainwater according to air-mass origins and trajectories.

Figure 5.2 - Volume-weighted average (VWA) UV-Visible spectra (absorbance units) versus wavelength (nm) of rainwater from: Autumn, Winter,

Spring, Summer and all events (a); classes of trajectories A, B, D and all events (b).

Figure 5.3 - Representative EEM fluorescence spectrum of rainwater CDOM. The scale is in ppb QS. The EEM spectrum is from rainwater sample RS39, which was collected in summer and was associated with air-mass trajectories with a maritime origin (class A). The sample had [DOC] = 0.66 mg L^{-1}, UV_{250nm} = 0.009 (a.u.), ε_{280nm} = 18.6 $Lg^{-1}C\ cm^{-1}$, spectral slope coefficient = 11.5 μm^{-1}, entire scan integrated fluorescence = 33.8 x 103, and A:M ratio = 1.7.

Figure 5.4 - The relationships between absorbance at 250nm and DOC (absorbance units; $r = 0.826$, $p < 0.001$), and between entire scan integrated EEM fluorescence and DOC (integrated fluorescence units; $r = 0.832$, $p < 0.001$). b) The relationship between the entire scan integrated EEM fluorescence (integrated fluorescence units) with the absorbance at 250nm (absorbance units) ($r = 0.819$, $p < 0.001$).

Figure 5.5 - The relationships between the DOC concentration (mg L^{-1}), the absorbance at 250 nm (absorbance units) and the entire scan integrated EEM fluorescence (integrated fluorescence units) with rainwater volume (mm).

Figure 6.1 - UV-visible spectra of rainwater eluates obtained from the isolation procedure of the rainwater DOM, grouped by seasons and presented as specific absorptivity (g^{-1} C L cm^{-1}).

Figure 6.2 - Specific absorptivity at 280 nm (ε_{280}, g^{-1} C L cm^{-1}) and spectral slope coefficient (S, μm^{-1}) of eluates obtained from the isolation procedure of the rainwater DOM.

Figure 6.3 - EEM fluorescence spectrum of the eluate from the sample 11 December 2008, presented as specific fluorescence intensity (g^{-1} C L ppb QS).

Figure 6.4 - Excitation (left) and synchronous (right) fluorescence spectra for

the eluates obtained from the isolation procedure of the rainwater DOM, grouped by seasons and presented as specific fluorescence intensity ($g^{-1}C$ L ppb QS).

Figure 6.5 - ^{1}H NMR spectra of the groups of extracted samples (Autumn–Class A; Winter–Class D; Winter–Class A; Spring–Class A; Summer–Class A). The peak at 4.7 ppm indicate the water signal.

Figure 6.6 - Functional group composition of the extracted samples: Autumn–Class A; Winter–Class D; Winter–Class A; Spring–Class A; Summer–Class A. Relative abundance of each functional group estimated as the partial integrals of the spectra reported in Figure 6.5. H-C: purely alkylic hydrogen atoms; H-C-C=: hydrogen atoms in α position to C=C or C=O groups; H-C-O: aliphatic C-H directly bound to an oxygen atom; H-Ar: aromatic hydrogen atoms.

1. Introduction

1.1 Rainwater: general grounds

Precipitation (including rain, snow and hail) is the primary mechanism for transporting water from the atmosphere back to the Earth's surface. It is also the key physical process that links aspects of climate, weather and the global hydrological cycle. Moreover, precipitation is the parameter that has the most direct and significant influence on the quality of human life through the availability of freshwater (Levsen and Cotton, 2009).

The importance of freshwater to the human life has been highlighted in the studies and reports of international organisations (e.g., Agenda 21, World Water Forum, the Millennium Ecosystem Assessment, and the World Water Development Report). Freshwater is indispensable for all forms of life and needed in almost all human activities. The challenges in quantity and quality related to freshwater are: having too much water (floods), having too little water (droughts), and having too much contamination (pollution). Each of these problems may be exacerbated by climate change. Therefore, the relationship between climate change and freshwater resources is of primary concern and interest (IPCC, 2008).

The hydrological cycle affects and interacts with some of the components of the climate system, such as the hydrosphere, the cryosphere, the land surface, the biosphere, and the atmosphere, where the atmospheric aerosols play an important role. In the context of atmospheric science, aerosol is a collective name for suspended particulate matter that ranges in size from molecular clusters of 1 nm to particles as big as approximately ~20 μm in diameter (Levsen and Cotton, 2009). The variation of aerosol size distribution and composition in the atmosphere depends on a complex combination of processes involving primary (direct release

to the atmosphere) and secondary (formed in the atmosphere from gas to particle conversion) sources, transport, dispersion, cloud processing, and removal by precipitation (Levsen and Cotton, 2009).

Dry and wet depositions are the ultimate paths by which trace gases and particles are removed from the atmosphere. The relative importance of dry deposition, as compared to wet deposition, for removal of a particular species depends on the following factors: whether the substance is present in the gaseous or particulate form; the solubility of the species in water; the amount of precipitation in the region; the terrain and type of surface cover (Seinfeld and Pandi, 1998).

Dry deposition is the transport of gaseous and particulate species from the atmosphere onto surfaces in the absence of precipitation. The factors that control the dry deposition of a gaseous species or a particle are the level of atmospheric turbulence, the chemical properties of the depositing species, and the nature of the surface itself. The level of turbulence in the atmosphere, especially in the layer nearest the ground, defines the rate at which species are delivered down to the surface, while for gases, solubility and chemical reactivity may affect uptake at the surface. For particles, size, density, and shape may determine whether capture by the surface occurs. The surface itself is a factor in dry deposition: a non-reactive surface may not permit absorption or adsorption of certain gases; a smooth surface may lead to particle bounce-off. Natural surfaces, such as vegetation, whereas highly variable and often difficult to describe theoretically, generally promote dry deposition (Seinfeld and Pandi, 1998).

Wet deposition is the natural processes by which atmospheric material is scavenged by atmospheric hydrometeors (cloud and fog drops, rain, snow) and is consequently delivered to the Earth's surface. A number of different terms are used, more or less synonymously, to signifying wet deposition including precipitation scavenging, wet removal, washout, and rainout. Washout usually refers to in-cloud scavenging, and rainout to below-cloud scavenging by falling rain or other hydrometeor. Three steps are necessary for wet removal of an atmospheric material: the species (gas or aerosol) must first be brought into the presence of condensed water; then, the species must be scavenged by the

hydrometeors; and finally, it needs to be delivered to the Earth's surface. Moreover, the compounds may also undergo chemical transformations during each one of the above mentioned steps. All the wet deposition processes are reversible as shown in Figure 1.1.. For example, rain may scavenge particles below cloud, but raindrops that evaporate produce new aerosols (Seinfeld and Pandi, 1998).

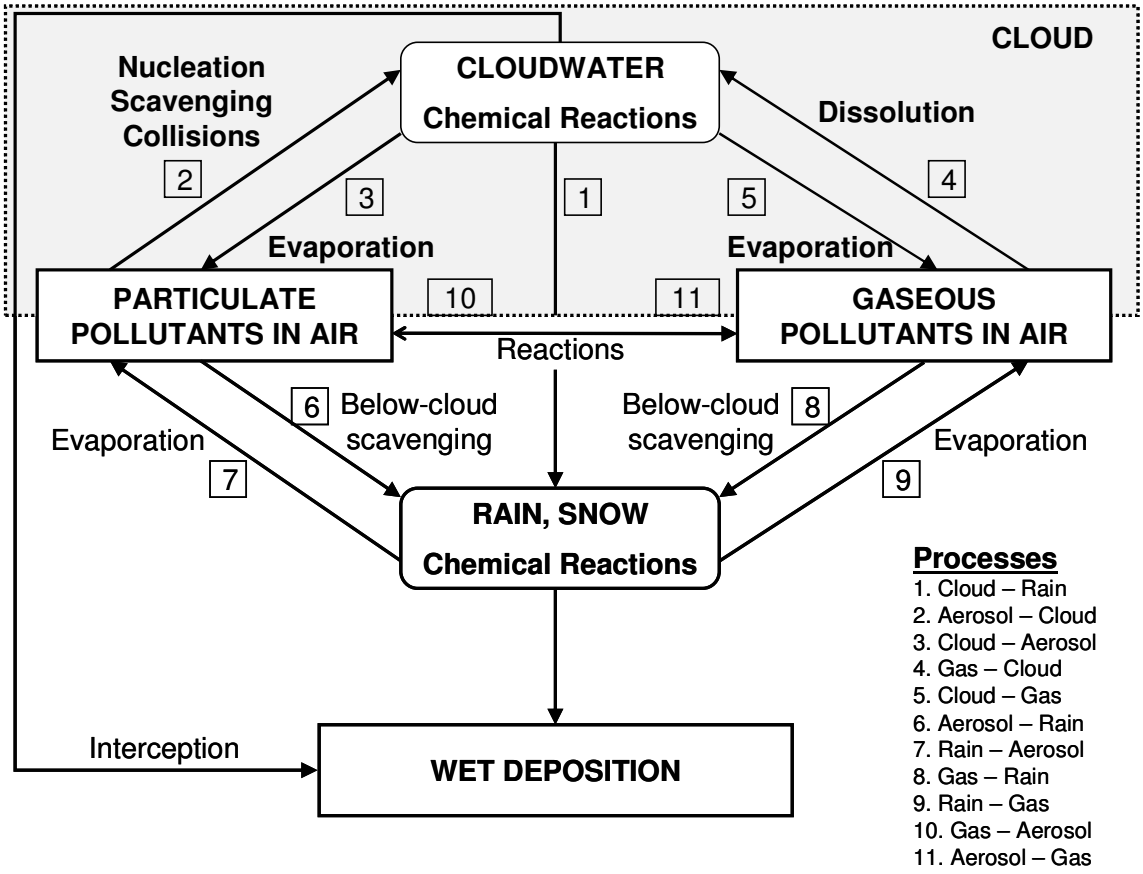

Figure 1.1 Conceptual framework of wet deposition processes (adapted from Seinfeld and Pandis, 1998)

1.2 Chemical composition of rainwater

During precipitation, rainwater dissolves and scavenges from atmosphere gases as well as from aerosols that contain a large array of inorganic and organic materials. Although several studies (e.g. Zunckel et al., 2003; Zhang et al., 2007a; Calvo et al., 2010; Huang et al., 2010) have been conducted on the inorganic chemistry of rainwater, little attention has been paid so far to the organic compounds. The results from rainwater characterization are of utmost importance because they are indicative of the air quality and allow inferring effects on receiving ecosystems.

1.2.1 Organic composition of rainwater

Dissolved organic carbon (DOC) is a ubiquitous component of rainwater (Willey et al., 2000), and the operational boundary between DOC and particulate organic carbon is set as that which will pass through a 0.45 μm filter (Peuravuori and Pihlaja, 2007).

With the perception of the low concentration of all rainwater constituents, DOC is a major component of both marine (23 μM) and continental rain (161 μM) (Willey et al., 2000). Furthermore, rainwater is a globally important removal mechanism for atmospheric DOC with a carbon flux (0.3 Gt C yr^{-1}) equal to approximately 6% of the fossil fuel influx (5.5 Gt C yr^{-1}) to the atmosphere (Willey et al., 2000).

Recent studies (Campos et al., 2007; Avery et al., 2009) have shown that volatile organic carbon (VOC) is an important fraction of the DOC pool in rainwater (0-56%). Therefore, rainwater DOC measurements should also account for such water soluble volatile compounds.

The removal process of the atmospheric DOC by rain prior to its oxidation to carbon dioxide is of great importance when evaluating the global carbon biogeochemical cycle. It has been estimated that the organic carbon fraction may account for 80% of the global flux of rainwater carbon (Willey et al., 2000), and it

can be of greater bioavailability to the oceanic biota than that derived from river water (Avery et al., 2003).

The concentrations of DOC in rainwater from urban areas or from places impacted with biomass burning can reach relatively high values (> 50 μmol C L^{-1}; e.g. Willey et al., 2006; Lara et al., 2001), while in remote areas they can be as low as 10 μmol C L^{-1} (Kieber et al., 2002). In deep seawater, DOC concentrations are about 30-40 μmol C L^{-1} (Aminot and Kerouel, 2004) and such low concentrations of organic carbon in natural waters enhance the importance of analytical accuracy besides the care needed to avoid contamination through all the sampling and analytical steps, including sample preservation (Campos et al., 2007; Santos et al., 2010).

In rainwater, DOC refers to a plethora of dissolved compounds that derive from organic materials, and is composed of 'organic acids', 'organic bases', and neutral compounds (Seitzinger et al., 2003). Over the past decade, a handful of compounds such as organic acids (e.g. acetic, formic and oxalic), aldehydes (e.g. formaldehyde and acroleine), polycyclic aromatic hydrocarbons (e.g. fluoranthene and pyrene) and organochlorine pesticides (e.g. lindane and aldrin) have been identified in some rainwater samples (Kawamura et al., 2001; Kieber et al., 2002; Peña et al., 2002; Basheer et al., 2003; Seitzinger et al., 2003).

Few studies of rainwater dissolved organic matter (DOM) have related the individual compounds detected to the total DOM. Willey et al. (2000) in North Carolina reported organic acids as the largest contributor (40%) to the total rainwater DOC with total aldehydes and amino acids contributing 8% and 2% of the total DOC. However, approximately 50% of rainwater DOC is considered uncharacterized at both the compound class and at the individual compound level (Willey et al., 2000).

The complexity of rainwater DOM and the large percent considered uncharacterized has made it difficult to determine the role of rainwater DOM in regional and global carbon budgets (Raymond, 2005). Consequently, more recent efforts have concentrated on the structural characteristics of the bulk DOM in rainwater (Wang et al., 2004; Decesari et al., 2005; Kieber et al., 2006; Miller et al., 2009; Santos et al., 2009a,b) and these studies have reported the prevalence

of DOM with characteristics resembling those of terrestrial and aquatic humic substances. This organic material has been termed humic like substances (HULIS), designation also used for similar substances found in atmospheric aerosols, fog water and cloud water (Zappoli et al., 1999; Krivacsy et al., 2000; Feng and Moller, 2004; Graber and Rudich, 2006). One of the most important uncertainties in the study of this poorly defined class of compounds relates to their origin. HULIS bear some resemblance to terrestrial and aquatic humic material, namely the presence of some similar functional groups, such as carboxyl, hydroxyl and carbonyl, and also similar properties in terms of fluorescence and UV-visible spectra. However, in some other aspects HULIS are quite different from terrestrial and aquatic humic material. One important difference is that the average molecular weight of atmospheric HULIS is typically smaller than the terrestrial and aquatic humic substances (Graber and Rudich 2006). The reasons behind this size discrepancy are not clear but may involve photodegradation of larger HULIS into smaller molecular weight entities (Graber and Rudich 2006) similar to what has been observed for humic substances in surface waters. Kieber et al. (2007) have shown that significant photodegradation of chromophoric dissolved organic matter (CDOM; term frequently used to refer the bulk DOM which absorbs UV-visible radiation) occurs after exposure to simulated sunlight suggesting that these chromophoric compounds could be involved in a variety of photo mediated processes. Moreover, Kieber et al. (2010) showed that photolysis of rainwater DOC produces significant amounts of formaldehyde, and possibly other low molecular weight organic compounds, which are likely to increase its reactivity and bioavailability

The complexity of HULIS in atmospheric waters (aerosol water, rainwater, and cloud water) poses a significant analytical challenge, and thus the sources of HULIS to the atmosphere are not well understood (Altieri et al., 2008). Possibilities include primary terrestrial and marine sources, biomass burning, and secondary organic aerosol (SOA) formation mechanisms such as oligomerization (Graber and Rudich, 2006).

The bulk chemical characterization of the DOM in rainwater in different areas with distinct climate patterns and different levels of pollution is of relevance

since rain is the predominant source of all the freshwater and may affect both the terrestrial and aquatic ecosystems.

1.2.2 Inorganic composition of rainwater

Rainwater has been collected and analyzed routinely worldwide to determine air quality trends and understand the effects of atmospherically derived inorganic chemical substances (e.g. sulfate, nitrate, ammonium) on receiving ecosystems. Many studies have demonstrated the influence of different natural and anthropogenic sources on the inorganic chemical composition of precipitation (e.g. Zunckel et al., 2003; Zhang et al., 2007a; Calvo et al., 2010; Huang et al., 2010). For example, sea-salt aerosol (mainly sodium and chloride) dominates precipitation chemistry in coastal areas (Ceron et al., 2002: Zhang et al., 2007b), wind-borne dust and soil are important sources of many ions present in rainwater, such as calcium and aluminium (e.g. Al-Momani, 2003; Al-Khashman, 2005), and most of the anthropogenic influences on atmospheric chemistry are due to emissions of nitrogen and sulfur compounds (e.g. Al-Momani, 2003; Das et al., 2005).

Inorganic nitrogen species, including nitrate (NO_3^-) and ammonium (NH_4^+), are among the most widely measured analytes in precipitation. The majority of the atmospheric nitrate is formed by oxidation of NO and NO_2, emitted primarily from fossil fuel combustion, forming nitric acid HNO_3 (g) which is subsequently scavenged into the aqueous phase. Ammonia (NH_3) is emitted from numerous sources including both natural and anthropogenic, and in acidic conditions contribute to the NH_4^+ formation. The main natural sources include emission from vegetation and the oceans (e.g. biological decomposition) and wild animal excreta while the main anthropogenic sources are agriculturally based including domestic animal excreta, fertilizers and biomass burning (Seinfeld and Pandis, 1998)

Inorganic sulphur species including sulphate (SO_4^{2-}) are also widely measured analytes in precipitation. Sulphate may be emitted directly to the atmosphere, through sources such as fossil-fuel combustion, industry, biomass burning, oceans, plants, soils, volcanoes, or may be formed by oxidation of SO_2,

emitted to the atmosphere through sources such as fossil-fuel combustion, industry, biomass burning and volcanoes (Seinfeld and Pandis, 1998).

Acid rain has been one of the major global environmental problems because of its important impact on the Earth's ecosystems, especially on vegetation and aquatic environments. Acidic precipitation is primarily caused by the incorporation of anthropogenic SO_x, NO_x, and other acid precursors. However, the acidity values depend on the neutralization produced by certain components such as mineral components, especially carbonates, and/or dissolved gases (e.g., NH_3), before reaching the ground or before their collection (e.g. Flues et al. 2002; Migliavacca et al. 2005; Prathibha et al., 2009; Calvo et al., 2010; Das et al., 2010). In the past, more and more studies have been conducted in order to better understand the characteristics and mechanisms of acid rain (e.g., Al-Momani et al., 1995; Lee et al., 2000; Okuda et al., 2005; Huang et al., 2010).

Besides the importance of studying the major inorganic ions present in rainwater that include the major cations, such as calcium, magnesium, sodium and potassium, and the major anions, such as chloride, nitrate and sulphate, the trace metal ions are also of utmost importance.

The trace metals, particularly the potentially toxic metals, are contaminants and pollutants increasingly being introduced into the environment as, by-products of industry and human civilization. There is considerable research interest in the atmospheric trace metals for of a number of reasons (Hu and Balasubramanian, 2003). Firstly, atmospheric deposition is considered to be a major source of toxic metals, such as Hg, Cd, Pb, and other trace metals to ecosystems. Secondly, in atmospheric water droplets, trace metals such as Fe, Mn and Cu have been implicated in the catalysis of SO_2 oxidation, leading to enhanced acidity of hydrometeors. Thirdly, certain trace metals, emitted from particular source types, can be used to help identifying the origin of the precipitating air mass and the sources from which the acid precipitation is derived. Furthermore, the contribution of wet deposition to the mass balance of some elements in surface water run-off has been recognized as an important aspect of water quality. As a result of these reasons, field studies to measure the levels of trace metals in hydrometeors, particularly in rainwater, have been actively determined in urban, rural, and remote

sites at different parts of the world (Hu and Balasubramanian, 2003). The various monitoring programmes and research studies for measuring trace metal concentrations in rainwater concluded that highest concentrations are observed in industrialized and densely populated areas (e.g., Kaya and Tuncel, 1997; Takeda et al., 2000; Al-Momani, 2003; Hou et al., 2005).

1.2.3 Rainwater chemical composition measurements

Rainwater chemical measurements are usually reported as volume weighted averages. The volume weighted average (VWA), assuming that the species are conserved during mixing, is the concentration that would result if the samples from all events were physically mixed and the resulting concentration measured (Seinfeld and Pandis, 1996). VWA of the chemical measurements and the corresponding standard deviations (SD_{VWA}; Hu and Balasubramanian, 2003) must be calculated accordingly to the following formulae:

$$VWA = \frac{\sum_{i=1}^{n} X_i P_i}{\sum_{i=1}^{n} P_i}$$

$$SD_{VWA} = \left[\frac{n\sum_{i=1}^{n} P_i^2 (X)_i^2 - \left(\sum_{i=1}^{n} P_i X_i \right)^2}{\left(\sum_{i=1}^{n} P_i \right)^2 \times (n-1)} \right]^{1/2}$$

where P_i is the precipitation amount corresponding to the *i*th sample, X_i is the signal corresponding to a given measurement in that sample, and n is the number of samples.

1.3 Effects of chemical composition of rainwater in climate and human health

The study of precipitation chemistry was initially developed in response to the adverse effects of acidic rain on vegetation, animals, soil, water, fish and buildings (e.g. Dangles et al., 2004; Menz and Seip, 2004). Currently, studies of atmospheric constituents, and their relationship with precipitation chemistry, have been considered of greater importance due to their harmful effects in climate and human health (e.g. Macdonald et al., 2005; Schiedek et al., 2007; Noyes et al., 2009).

The presence of trace metals in rainwater also has effects on aquatic and terrestrial ecosystems, but affects human health through the consumption of drinking water and food (e.g. Seinfeld and Pandi, 1998). Many rainwater trace metals have ecological interest due to their necessity as nutrients by the ecosystems but also due to their toxicity as pollutants (e.g. He et al., 2005). For example, nutrient trace elements include Mg, Mn, Cu, Zn, some of which become toxic at high concentrations (e.g. Mohamed et al., 2003). On other hand, elements, such as Hg, Cd, As and Pb are of environment concern due to their high toxicity even at trace levels (e.g. Kieber et al., 2008).

Regarding the organic composition, there are additional toxic effects in aquatic and terrestrial ecosystems to that caused by the presence of high concentrations of DOM in rainwater that may become toxic, as in the case of persistent organic pollutants (Noyes et al., 2009). As already mentioned in point 1.2.1, the chromophoric organic constituents are an important subset of rainwater DOM (Kieber et al. 2006; Santos et al., 2009b), and an important fraction of the water-soluble organic matter (WSOM) in atmospheric particles (Facchini et al. 1999; Zappoli et al. 1999; Decesari et al. 2000). The aerosol WSOM exhibit intense absorbance in the lower visible to ultraviolet range and, therefore, they might also be important in atmospheric absorption of solar radiation (Hoffer et al. 2004). Moreover, apart from inorganic salts, these organic constituents were found to be important contributors to cloud condensation nuclei (CCN) (Facchini et al. 1999; Gysel et al. 2004). Droplet clouds are effective reflectors of incoming solar

radiation and small perturbations in their properties (size and number) can significantly impact the amount of solar radiation absorbed by the planet (Andreae et al. 2005). The solar radiation absorbed by the planet influence directly the radiation budget, atmospheric temperatures, land-surface and ocean temperatures, and thus affect climate (Levson and Cotton, 2009). In view of the potentially important role played by WSOM in the environmental impact of atmospheric particles, one can anticipate that DOM in rainwater may perform similar functions of absorbance and reflectance of solar radiation.

Climate change is an increasingly urgent problem with potentially far-reaching consequences for life on Earth. One of the consequences of climate change that has recently attracted attention is its potential to alter the environmental distribution and biological effects of chemical toxicants. There is a growing concern on anticipating the effects of chemical pollution in the rapidly changing environment and on identifying and mitigating the effects in humans and ecosystems most vulnerable (Noyes et al., 2009).

Human health, incorporating physical, social and psychological well-being, depends on an adequate supply of potable water and a safe environment. Human beings are exposed to climate change directly through weather patterns (more intense and frequent extreme events), and indirectly through changes in water, air, food quality and quantity, ecosystems, agriculture and infrastructure (IPCC, 2008).

1.4 Main purposes of the work

Rainwater removes air pollutants that may be in gaseous and liquid phase or associated to atmospheric particulates. The determination of the pollutant levels in rainwater could be of interest as a screening of air quality in different areas (Guidotti et al. 2000) but also to evaluate its role in climate and human health.

The chemical composition of the rainwater depends on local emissions, pollutants transport, meteorological conditions, sea level elevation and drop size, which in turn influence the rainout and the washout (Flues et al., 2002). Thus, the composition of rainwater varies from site to site, and from region to region.

Being the atmosphere a dynamic system, the complete knowledge of chemical composition of rainwater is very far from the end. However, the knowledge of chemical composition of rainwater in one local together with physical models, may contribute to the definition of strategies that control the existence of atmospheric compounds adverse to the environment and human health.

The present study aims at contributing to the knowledge of chemical composition of rainwater in the costal town of Aveiro, Portugal, located in southwest of Europe. In this study, the organic and inorganic composition of rainwater was evaluated between September 2008 and September 2009. The influence of seasonality and air masses trajectories were assessed.

Due to the low concentrations of organic matter in rainwater, the importance of analytical accuracy, and the care needed to avoid contamination through all the sampling and analytical steps, the effects of rainwater preservation on DOM were assessed by fluorescence spectroscopy (Chapter 3).

Since rainwater is a very low concentrated matrix and, for DOM characterization, an efficient extraction procedure is essential, a comparison was performed between two isolation procedures based on the adsorption onto XAD-8 and C-18 sorbents, both used in the literature for rainwater DOM isolation (Chapter 4).

The effects of seasonality and air mass trajectory on the original rainwater DOM in Aveiro were assessed using the UV-visible and molecular fluorescence spectroscopies, besides the determination of its DOC content (Chapter 5).

The influence of the seasons into the chemical properties of rainwater DOM isolated by adsorption onto DAX-8 resin, was also assessed in this work, recurring by UV-visible, molecular fluorescence and ^{1}H NMR spectroscopies (Chapter 6).

The inorganic composition was evaluated determining the concentration of some ionic species (H^+, NH_4^+, Cl^-, NO_3^-, SO_4^{2-}) and comparing the results with those obtained for rain collected at the same site between 1986-1989 (Pio et al., 1991) (Chapter 7).

The determination of chemical composition of rainwater in Aveiro, provides an understanding of the source types that contribute to rainwater chemistry, and enhances the understanding of the local and regional dispersion of pollutants and

their potential impacts on ecosystems through deposition processes (Chapter 8 – Final considerations).

The present work is organized by articles, from the chapter 3 until the chapter 7. The work contained in chapters 3 and 4 has been published in Talanta (Santos et al., 2010a; Santos et al., 2010b). The work of chapters 5, 6 and 7 has submitted in international scientific journals with peer reviewing.

References

Al-Khashman, O.A., 2005. Study of chemical composition in wet atmospheric precipitation in Eshidiya area, Jordan. Atmos. Environ. 39, 6175–6183.

Al-Momani, I.F., Tuncel, S., Eler, U., Ortel, E., Sirin, G., Tuncel, G., 1995. Major ion composition of wet and dry deposition in the eastern Mediterranean basin. Sci. Total Environ. 164, 75–85.

Al-Momani, I.F., 2003. Trace elements in atmospheric precipitation at Northern Jordan measured by ICPMS: acidity and possible sources. Atmos. Environ. 37, 4507–4515.

Altieri, K.E., Turpin, B.J., Seitzinger, S.P., 2008. Oligomers, organosulfates, and nitroxy organosulfates in rainwater identified by ultra-high resolution electrospray ionization FT-ICR mass spectrometry. Atmos. Chem. Phys. Discuss. 8, 17439–17466.

Aminot, A., Kerouel, R., 2004. Dissolved organic carbon, nitrogen and phosphorus in the N–E Atlantic and the N–W Mediterranean with particular reference to non-refractory fractions and degradation. Deep-Sea Res. Part I — Oceanogr. Res. Pap. 51, 1975–1999.

Andreae, M.O., Jones, C.D., Cox, P.M., 2005. Strong present-day aerosol cooling implies a hot future. Nature 435, 1187–1190.

Avery, G.B., Willey, J.D., Kieber, R.J., Shank, G.C., Whitehead, R.F., 2003. Flux and bioavailability of Cape Fear River and rainwater dissolved organic carbon to Long Bay, southeastern United States. Global Biogeochem. Cy. 17, 1042, doi:10.1029/2002GB001964.

Avery, Jr. G.B., Dickson Brown, J.L., Willey, J.D., Kieber, R.J.. 2009. Assessment of rainwater volatile organic carbon in southeastern North Carolina, USA. Atmos. Environ. 43, 2678–2681.

Basheer, C., Balasubramanian, R., Lee, H.K., 2003. Determination of organic pollutants in rainwater using hollow fibre membrane/liquid-phase microextraction combined with gas chromatography-mass spectrometry. J. Chrom. A 1016, 11–20.

Calvo, A.I., Olmo, F.J., Lyamani, H., Alados-Arboledas, L., Castro, A., Fernández-Raga, M., Fraile, R., 2010. Chemical composition of wet precipitation at the background EMEP station in Víznar (Granada, Spain) (2002–2006). Atmos. Res. 96, 408–420.

Campos, M.L.A.M., Nogueira, R.F.P., Dametto, P.R., Francisco, J.G., Coelho, C.H., 2007. Dissolved organic carbon in rainwater: Glassware decontamination and sample preservation and volatile organic carbon. Atmos. Environ. 41, 8924–8931.

Ceron, R.M.B., Padilla, H.G., Belmont, R.D., Torres, M.C.B., García, R.M., Báez, A.P., 2002. Rainwater chemical composition at the end of the mid-summer drought in the Caribbean shore of the Yucatan Peninsula. Atmos. Environ. 36 (2), 2367–2374.

Dangles, O., Malmqvist, B., Laudon, H., 2004. Naturally acid freshwater ecosystems are diverse and functional: evidence from boreal streams. OIKOS 104, 149–155.

Das, R., Das, S.N., Misra, V.N., 2005. Chemical composition of rainwater and dustfall at Bhubaneswar in the east coast of India. Atmos. Environ. 39, 5908–5916.

Das, N., Das, R., Chaudhury, G.R., Das, S.N., 2010. Chemical composition of precipitation at background level. Atmos. Res. 95, 108–113.

Decesari, S., Facchini, M.C., Fuzzi, S., Tagliavini, E., 2000. Characterization of water-soluble organic compounds in atmospheric aerosols: a new approach. J. Geophys. Res. 105, 1481–1489.

Decesari, S., Facchini, M.C., Fuzzi, S., McFiggans, G.B., Coe, H., Bower, K.N., 2005. The water-soluble organic component of size-segregated aerosol,

cloud water and wet deposition from Jeju Island during ACE-Asia. Atmos. Environ. 39, 211–222.

Facchini, M.C., Fuzzi, S., Zappoli, S., Andracchio, A., Gelencsér, A., Kiss, G., Krivácsy, Z., Mészáros, E., Hansson, H.C., Alsberg, T., Zebühr, Y., 1999. Partitioning of the organic aerosol component between fog droplets and interstitial air. J. Geophys. Res. 104(26), 26 821–26 832.

Facchini, M.C., Decesari, S., Mircea, M., Fuzzi, S., Loglio, G., 2000. Surface tension of atmospheric wet aerosol and cloud/fog droplets in relation to their organic carbon content and chemical composition. Atmos. Environ. 34, 4853–4857.

Feng, J. S. and Moller, D., 2004. Characterization of water-soluble macromolecular substances in cloud water, J. Atmos. Chem., 48, 217–233.

Flues, M., Hamma, P., Lames, M.J.L., Dantas, E.S.K., Fornaro, A., 2002. Evaluation of rainwater acidity of a rural region due to a coal-fired power plant in Brazil. Atmos. Environ. 36, 2397–2404.

Guidotti, M., Giovinazzo, R., Cedrone, O., Vitali, M., 2000. Determination of organic micropollutants in rain water for laboratory screening of air quality in urban environment. Environ. Int. 26, 23–28

Gysel, M., Weingartner, E., Nyeki, S., Paulsen, D., Baltensperger, U., Galambos, I., Kiss, G., 2004. Hygroscopic properties of water-soluble matter and humic-like organics in atmospheric fine aerosol. Atmos. Chem. Phys. 4, 35–50.

He, Z.L., Yang, X.E., Stoffella, P.J., 2005. Trace elements in agroecosystems and impacts on the environment. J. Trace Elem. Med. Biol. 19, 125–140.

Hoffer, A., Kiss, G., Blazsó, M., Gelencsér, A., 2004. Chemical characterization of humic-like substances (HULIS) formed from a lignin-type precursor in model cloud water. Geophys. Res. Lett. 31, L06115 (2004). doi:10.1029/2003GL018962

Hou, H., Takamatsu, T., Koshikawa, M.K., Hosomi, M., 2005. Trace metals in bulk precipitation and throughfall in a suburban area of Japan. Atmos. Environ. 39, 3583-3595.

Hu, G.-P., Balasubramanian, R., 2003. Wet deposition of trace metals in Singapure. Water, Air, and Soil Pollut. 144, 285–300.

Huang, X.-F., Li, X., He, L.-Y., Feng, N., Hub, M., Niu, Y.-W., Zeng, L.-W., 2010. 5-Year study of rainwater chemistry in a coastal mega-city in South China. Atmos. Res. 97, 185–193.

Intergovernmental Panel on Climate Change (IPCC), 2008. Climate change and water, IPCC Technical Paper VI.

Kawamura, K., Steinberg, S., Ng, L., Kaplan, I.R., 2001. Wet deposition of low molecular weight mono- and dicarboxylic acids, aldehydes and inorganic species in Los Angeles. Atmos. Environ. 35, 3917–3926.

Kaya, G., Tuncel, G., 1997, Trace element and major ion composition of wet and dry deposition in Ankara, Turkey. Atmos. Environ. 31, 3985–3998.

Kieber, R.J., Peake, B., Willey, J.D., Avery, G.B., 2002. Dissolved organic carbon and organic acids in coastal New Zealand rainwater. Atmos. Environ. 26, 3557–3563.

Kieber, R.J., Whitehead, R.F., Reid, S.N., Willey, J.D., Seaton, P.J., 2006. Chromophoric dissolved organic matter (CDOM) in rainwater, Southeastern North Carolina, USA. J. Atmos. Chem. 54, 21–41.

Kieber, R.J., Willey, J.D., Whitehead, R.F., Reid, S., 2007. Photochemistry of chromophoric dissolved organic matter (CDOM) in rainwater. J. Atmos. Chem. 58, 219–235.

Kieber, R.J., Parler, N.E., Skrabal, S.A., Willey, J.D., 2008. Speciation and photochemistry of mercury in rainwater. J. Atmos. Chem. 60, 153–168.

Kiss, G., Tombacz, E., Hannsson, H.C., 2005. Surface tension effects of humic like substances in the aqueous extract of tropospheric fine aerosol. Global Biogeochem. Cy. 50, 279–294.

Krivacsy, Z., Kiss, G., Varga, B., Galambos, I., Sarvari, Z., Gelencser, A., Molnar, A., Fuzzi, S., Facchini, M. C., Zappoli, S., Andracchio, A., Alsberg, T., Hansson, H. C., and Persson, L., 2000. Study of humic-like substances in fog and interstitial aerosol by size-exclusion chromatography and capillary electrophoresis, Atmos. Environ., 34, 4273–4281.

Lara, L.B.L.S., Artaxo, P., Martinelli, L.A., Victoria, R.L., Camargo, P.B., Krusche, A., Ayers, G.P., Ferraz, E.S.B., Ballester, M.V., 2001. Chemical composition of rainwater and anthropogenic influences in the Piracicaba River Basin, Southeast Brazil. Atmos. Environ. 35, 4937–4945.

Lee, B.K., Hong, S.H., Lee, D.S., 2000. Chemical composition of precipitation and wet deposition of major ions on the Korean peninsula. Atmos. Environ. 34, 563–575.

Levin, Z., Cotton, W.R., 2009. Aerosol Pollution Impact on Precipitation: A Scientific Review, Springer, ISBN: 978-1-4020-8689-2.

Macdonald, R.W., Harner, T., Fyfe, J., 2005. Recent climate change in the Arctic and its impact on contaminant pathways and interpretation of temporal trend data. Sci. Total Environ. 342, 5–86.

Menz, F.C., Seip, H.M., 2004. Acid rain in Europe and the United States: an update. Environ. Sci. Policy 7, 253–265.

Migliavacca, D., Teixeira, E.C., Wiegand, F., Machado, A.C.M., Sanchez, J., 2005. Atmospheric precipitation and chemical composition of an urban site, Guaiba hydrographic basin, Brazil. Atmos. Environ. 39, 1829–1844.

Miller, C., Gordon, K.G., Kieber, R.J., Willey, J.D., Seaton, P.J., 2009. Chemical characteristics of chromophoric dissolved organic matter in rainwater. Atmos. Environ. 43, 2497-2502.

Mohamed, A.E., Rashed, M.N., Mofty A., 2003. Assessment of essential and toxic elements in some kinds of vegetables. Ecotox. Environ. Safety 55, 251–260.

Muller, C.L., Baker, A., Hutchinson, R., Fairchild, I.J., Kidd, C., 2008. Analysis of rainwater dissolved organic carbon compounds using fluorescence spectroscopy. Atmos. Environ. 42, 8036–8045. Environ. Int. 35, 971–986.

Noyes, P.D., McElwee, M.K., Miller, H.D., Clark, B.W., Tiem, L.A.V., Walcott, K.C., Erwin, K.N., Levin, E.D., 2009. The toxicology of climate change: Environmental contaminants in a warming world.

Okuda, T., Iwase, T., Ueda, H., Suda, Y., Tanaka, S., Dokiya, Y., Fushimi, K., Hosoe, M., 2005. Long-term trend of chemical constituents in precipitation

in Tokyo metropolitan area, Japan, from 1990–2002. Sci. Total Environ. 339, 127–141.

Peña, R.M., García, S., Herrero, C., Losada, M., Vasquez, A., Lucas, T., 2002. Organic acids and aldehydes in rainwater in a northwest region of Spain. Atmos. Environ. 36, 5277–5288.

Peuravuori, J., Pihlaja, K., 2007. Characterization of Freshwater Humic Matter. In: Handbook of Water Analysis. Editor Leo M.L. Nollet. CRC Press. Taylor & Francis Group LLC, Boca Raton, 2nd Edition, pp. 436-437.

Pio, C.A., Salgueiro, M.L., Nunes, T.V., 1991. Seasonal and air-mass trajectory effects on rainwater quality at the south-western european border. Atmos. Env. 25A (10), 2259-2266.

Prathibha, P., Kothai, P., Saradhi, I.V., Pandit, G.G., Puranik, V.D., 2009. Chemical characterization of precipitation at a coastal site in Trombay, Mumbai, India. Environ. Monit. Assess. doi:10.1007/s10661-009-1090-7.

Raymond, P. A.: The composition and transport of organic carbon in rainfall: Insights from the natural (C-13 and C-14) isotopes of carbon, Geophys. Res. Lett., 32, doi:10.1029/2005GL022879, 2005.

Roy, S., Négrel, P., 2001. A Pb isotope and trace element study of rainwater from the Massif Central (France). Sci. Total Environ. 277, 225-239.

Santos, P.S.M., Otero, M., Duarte, R.M.B.O., Duarte, A.C., 2009a. Spectroscopic characterization of dissolved organic matter isolated from rainwater. Chemosphere 74(8), 1053–1061.

Santos, P.S.M., Duarte, R.M.B.O., Duarte, A.C., 2009b. Absorption and fluorescence properties of rainwater during the cold season at a town in Western Portugal. J. Atmos. Chem. 62, 45-57.

Santos, P.S.M., Otero, M., Santos, E.B.H, Duarte, A.C., 2010a. Rainwater preservation: effects on fluorescence properties of dissolved organic matter. Talanta 82, 1616–1621.

Santos, P.S.M., Otero, M., Filipe, O.M.S., Santos, E.B.H., Duarte, A.C., 2010b. Comparison between DAX-8 and C-18 solid phase extraction of rainwater dissolved organic matter. Talanta 83, 505–512.

Schiedek, D., Sundelin, B., Readman, J.W., Macdonald, R.W., 2007. Interactions between climate change and contaminants. Mar. Pollut. Bull. 54, 1845–1856

Seinfeld, J.H., Pandis, S.N., 1998. Atmospheric Chemistry and Physics: From air pollution to climate change. 1st ed., John Wiley & Sons, Inc, New York (United States of America).

Seitzinger, S.P., Styles, R.M., Lauck, R., Mazurek, M.A., 2003. Atmospheric pressure mass spectrometry: a new analytical chemical characterization method for dissolved organic matter in rainwater. Environ. Sci. Technol. 37, 131–137.

Takeda, K., Marumoto, K., Minamikawa, T., Sakugawa, H. and Fujiwara, K., 2000, Three-year determination of trace metals and the lead isotope ratio in rain and snow depositions collected in Higashi-Hiroshima, Japan, Atmos. Environ. 34, 4525–4535.

Wang, M.C., Liu, C.P., Sheu, B.H., 2004. Characterization of organic matter in rainfall, throughfall, stemflow, and streamwater from three subtropical forest ecosystems. J. Hydrol. 289, 275–285.

Willey, J.D., Kieber, R.J., Eyman, M.S., Avery, G.B., 2000. Rainwater dissolved organic carbon: concentrations and global flux. Global Biogeochem. Cy. 14, 139–148.

Willey, J.D., Kieber, R.J., Avery, G.B., 2006. Changing chemical composition of precipitation in Wilmington, North Carolina, USA: implications for the continental USA. Environ. Sci. Technol. 40, 5675–5680.

Zappoli, S., Andracchio, A., Fuzzi, S., Facchini, M.C., Gelencsér, A., Kiss, G., Krivácsy, Z., Molnár, Á., Mészáros, E., Hansson, H.C., Rosman, K., Zebühr, Y., 1999. Inorganic, organic and macromolecular components of fine aerosol in different areas of Europe in relation to their water solubility. Atmos. Environ. 33, 2733–2743.

Zhang, M.Y., Wang, S.J., Wu, F.C., Yuan, X.H., Zhang, Y., 2007a. Chemical compositions of wet precipitation and anthropogenic influences at a developing urban site in southeastern China. Atmos. Res. 84, 311–322.

Zhang, G.S., Zhang, J., Liu, S.M., 2007b. Chemical composition of atmospheric wet depositions from the Yellow Sea and East China Sea. Atmos. Res. 85, 84–97.

Zunckel, M., Saizar, C., Zarauz, J., 2003. Rainwater composition in northeast Uruguay. Atmos. Environ. 37, 1601–1611.

2. Rainwater sampling and characterization of atmospheric conditions

2.1 Rainwater sampling in Aveiro

Rainwater was collected at a sampling station located in the western part of the town of Aveiro, Portugal, on the university campus, with the geographical coordinates 40º38'N and 8º39'W. The town of Aveiro has an area of 197.5 Km^2 and a population of around 72,919 ("Instituto Nacional de Estatística", www.ine.pt, site visited in November 2010). Near the sampling site there is a road that is used daily on a large scale and that may influence the local atmospheric composition and hence the composition of rainwater. Aveiro, being located in the southwest coast of Europe, is presumably less affected by anthropogenic emissions from the European continent, because this location is frequently subjected to relatively clean air masses transported from the Atlantic Ocean.

Figure 2.1 presents two maps, one schematic map of Portugal and other map of the city of Aveiro, which shows the location of the sampling site.

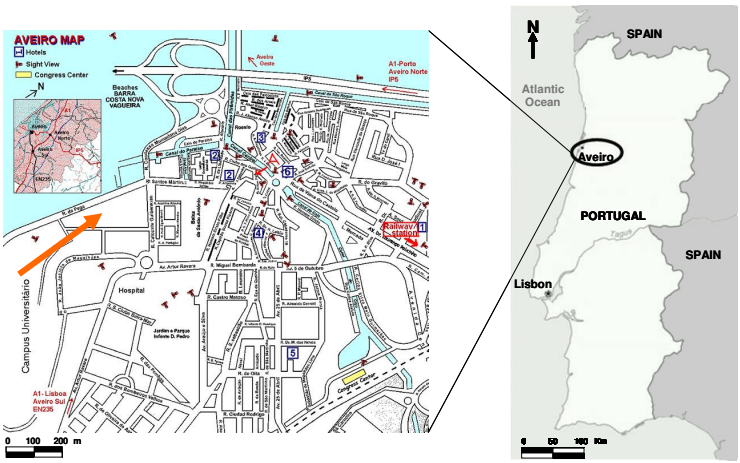

Figure 2.1 Schematic maps of Portugal and Aveiro showing the location of the sampling site (orange arrow).

Rainwater collection was carried out 70 cm above the ground, to avoid the effect of any resuspension that might contaminate the sample. Collection was carried out through glass funnels (30 cm diameter) into glass bottles (5 L). The bottles were placed inside a PVC opaque tube, being protected from direct sunlight. The sampling was performed with several collectors of rainwater at the same time, as shown in Figure 2.2.

Figure 2.2 Photographs of the sampling station and of the collectors of rainwater.

Prior to use, all glass materials were immersed for 30 min, in a solution of NaOH (0.1 M), then rinsed with distilled water, followed by another immersion for 24 hours in a solution of HNO_3 (4 M), and finally rinsed with ultrapure water. Ultrapure water was produced with a Millipore water purification system, which combines the module of reverse osmosis TFC (thin film composite) with the technology of deionization auto-regenerable ELIX ("Electronic Ion Exchange") of ionic resins and uses a UV lamp, to reduce the microbiological content.

For the study of the origin, seasonality and chemical characteristics of rainwater in Aveiro, rainwater was collected between September 2008 and September 2009. Nevertheless, more two samples were collected in October of 2009 to complete the study of comparison between DAX-8 and C-18 solid phase extraction of rainwater DOM.

Sampling containers were left out open, at 8:30h local hour, in order to collect both wet and dry depositions on a 24 h basis. During the sampling period of

September 2008 and September 2009, forty rainwater samples were collected and are these ones that will be following presented.

Table 2.1 presents the rainwater samples (RS) collected as well as the sampling date and season.

Table 2.1 Rainwater samples collected, sampling date and season.

Sample	Sampling date	Season
RS1	03-04 of September 2008	Summer 2008
RS2	05-06 of September 2008	
RS3	20-21 of September 2008	
RS4	21-22 of September 2008	Autumn 2008
RS5	22-23 of September 2008	
RS6	07-08 of October 2008	
RS7	29-30 of October 2008	
RS8	30-31 of October 2008	
RS9	04-05 of November 2008	
RS10	24-25 of November 2008	
RS11	11-12 of December 2008	
RS12	12-13 of December 2008	
RS13	13-14 of December 2008	
RS14	14-15 of December 2008	
RS15	12-13 of January 2009	Winter 2009
RS16	14-15 of January 2009	
RS17	15-16 of January 2009	
RS18	18-19 of January 2009	
RS19	19-20 of January 2009	
RS20	20-21 of January 2009	
RS21	01-02 of February 2009	
RS22	03-04 of February 2009	
RS23	04-05 of February 2009	
RS24	09-10 of February 2009	
RS25	04-05 of March 2009	
RS26	05-06 of March 2009	
RS27	06-07 of April 2009	Spring 2009
RS28	14-15 of April 2009	
RS29	15-16 of April 2009	
RS30	16-17 of April 2009	
RS31	29-30 of April 2009	
RS32	10-11 of May 2009	
RS33	08-09 of May 2009	
RS34	23-24 of May 2009	
RS35	04-05 of June 2009	
RS36	05-06 of June 2009	
RS37	07-08 of June 2009	
RS38	27-28 of June 2009	Summer 2009
RS39	22-23 of July 2009	
RS40	18-19 of September 2009	

Regarding to the samples collected by season, 6 samples were collected in summer, 11 samples in autumn, 12 in winter and 11 in spring. The lower number of rainwater samples collected in summer was because lower number of rain events occurs during this season in Aveiro comparatively with the other seasons.

After collection, samples were transported to the laboratory and divided into three aliquots.

An aliquot was used for the measurements of pH and electrical conductivity (EC).

A second aliquot, used for analysis of organics, was filtered through hydrophilic PVDF Millipore membrane filters of 0.45 µm pore size, and one fraction was stored in glass vials in the dark at 4ºC, for a maximum of four days, until the subsequent analysis of organic composition, and another fraction was frozen for subsequent analysis of DOC.

A third aliquot was filtered through sterilized nitrocellulose filters (Millipore) of 0.45 µm pore size and frozen for further determination of ion composition.

2.2 Atmospheric conditions associated to rainwater samples

In order to evaluate how atmospheric conditions affect the organic and ion composition of rainwater the following meteorological data were recorded: volume of precipitation, temperature, relative humidity, velocity and direction of wind at 10 m of height.

Figure 2.3 shows the values of accumulated precipitation, temperature and relative humidity for each collected rainwater sample.

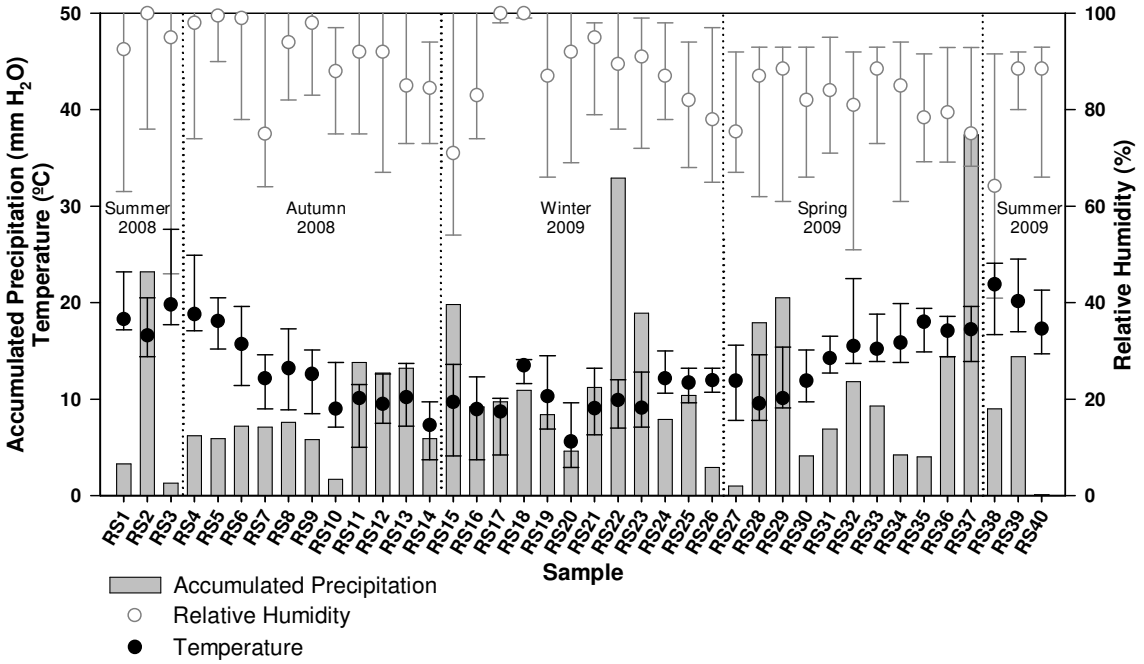

Figure 2.3 Values of accumulated precipitation, values of minimum, median (●) and maximum of temperature (ºC), and values of minimum, median (○) and maximum of relative humidity (%) associated to each rainwater sample.

During the sampling period from September 2008 to September 2009 were collected 417 mm of precipitation, which represents approximately 50% of the total precipitation, 839 mm H_2O.

As shown in Figure 2.3, the accumulated precipitation varied from sample to sample between a minimum of 0.1 mm H_2O for sample RS40 and a maximum of 37.4 mm H_2O for sample RS37. The samples with highest levels of accumulated precipitation were RS2 (27.0 mm H_2O), RS22 (32.9 mm H_2O) and RS37 (37.7 mm H_2O), and occurred in summer 2008, winter 2009 and spring 2009, respectively.

The medians of temperatures associated to summer samples ranged between 18.3-21.9 ºC and were generally higher than for the other samples, except for samples RS2 (16.6 ºC) and RS40 (17.3 ºC). The medians of temperatures of autumn samples tended to decrease from the beginning (18.8 ºC) to the end (7.3 ºC) of autumn, while the medians of temperatures of spring samples tended to increase from the beginning to the end of spring (the range observed was 9.6-18.0 ºC). On other hand, the medians of temperatures of winter

samples varied less than for autumn and spring samples and tended to be lower than for the other samples, ranging between 5.6-13.5 ºC.

The medians of relative humidity associated to rainwater samples were generally higher than 80%, except for samples RS7, RS15, RS26, RS27, RS35, RS36, RS37 and RS38, for which the values were slightly lower.

Figure 2.4 shows the wind roses, with the direction and velocity of winds at 10 m of height, associated to each rainwater sample.

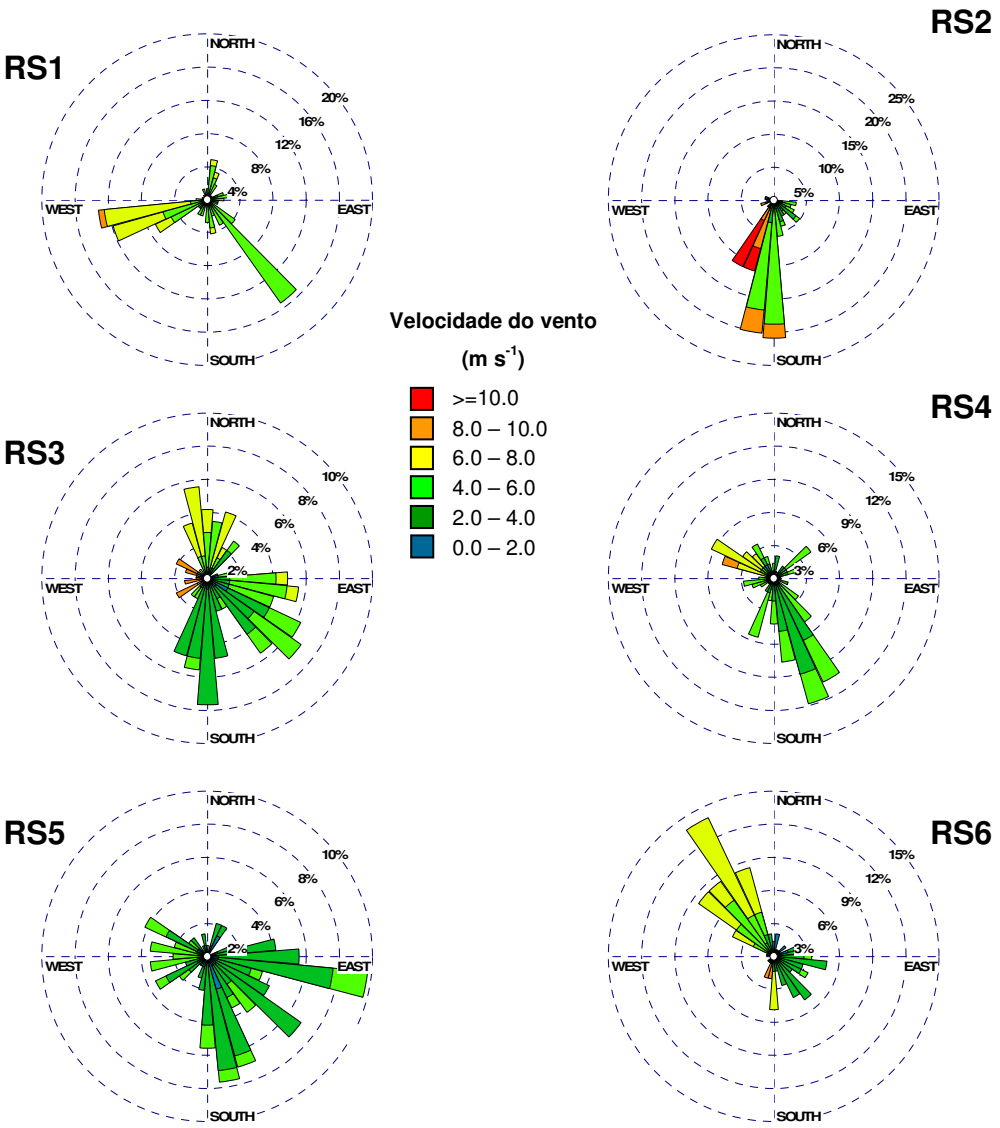

Figure 2.4 Wind Roses, with indication of percentages of distribution of wind velocity in function of its direction, associated to each rainwater sample.

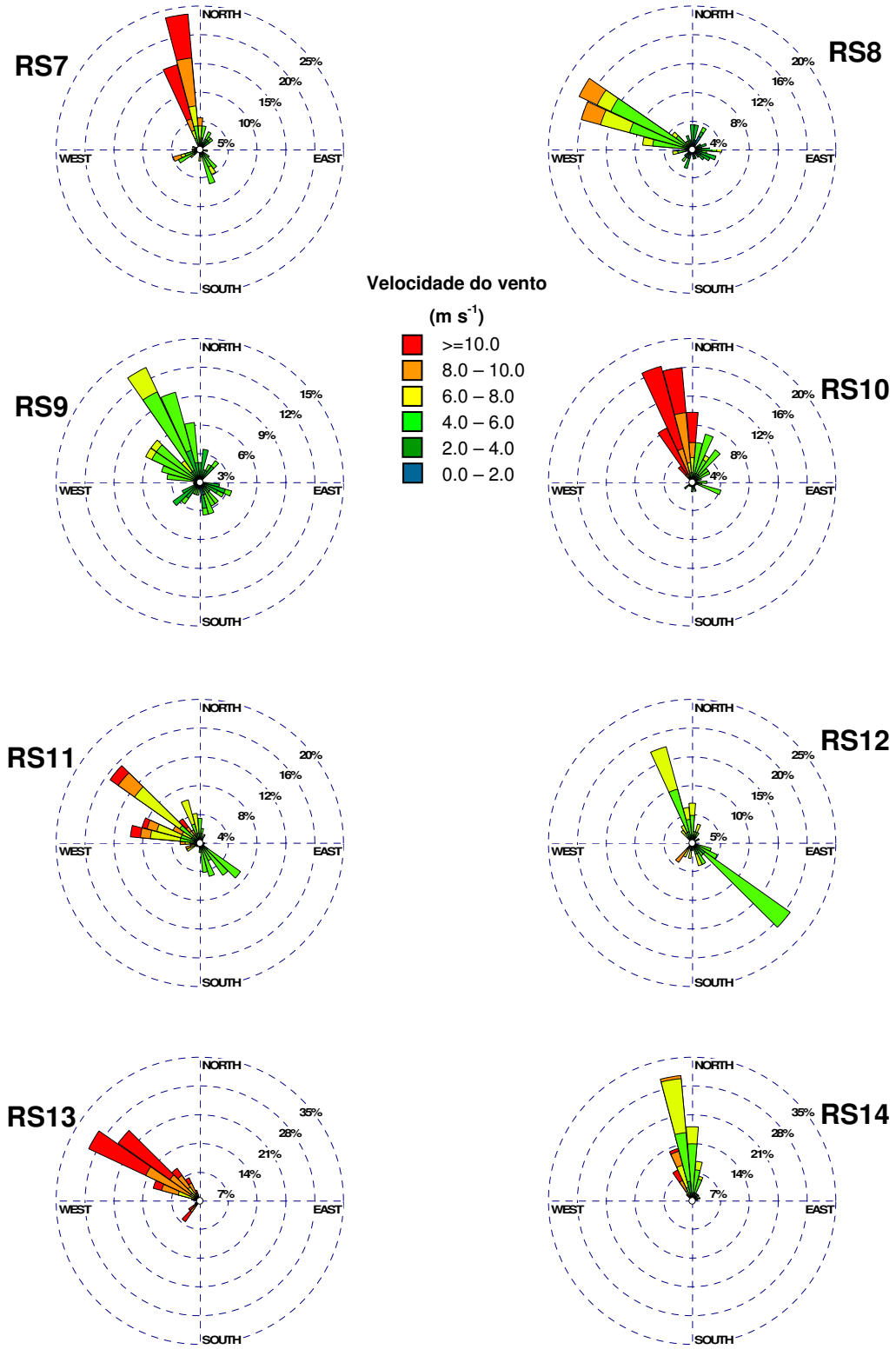

Figure 2.4 Wind Roses, with indication of percentages of distribution of wind velocity in function of its direction, associated to each rainwater sample (to be continued).

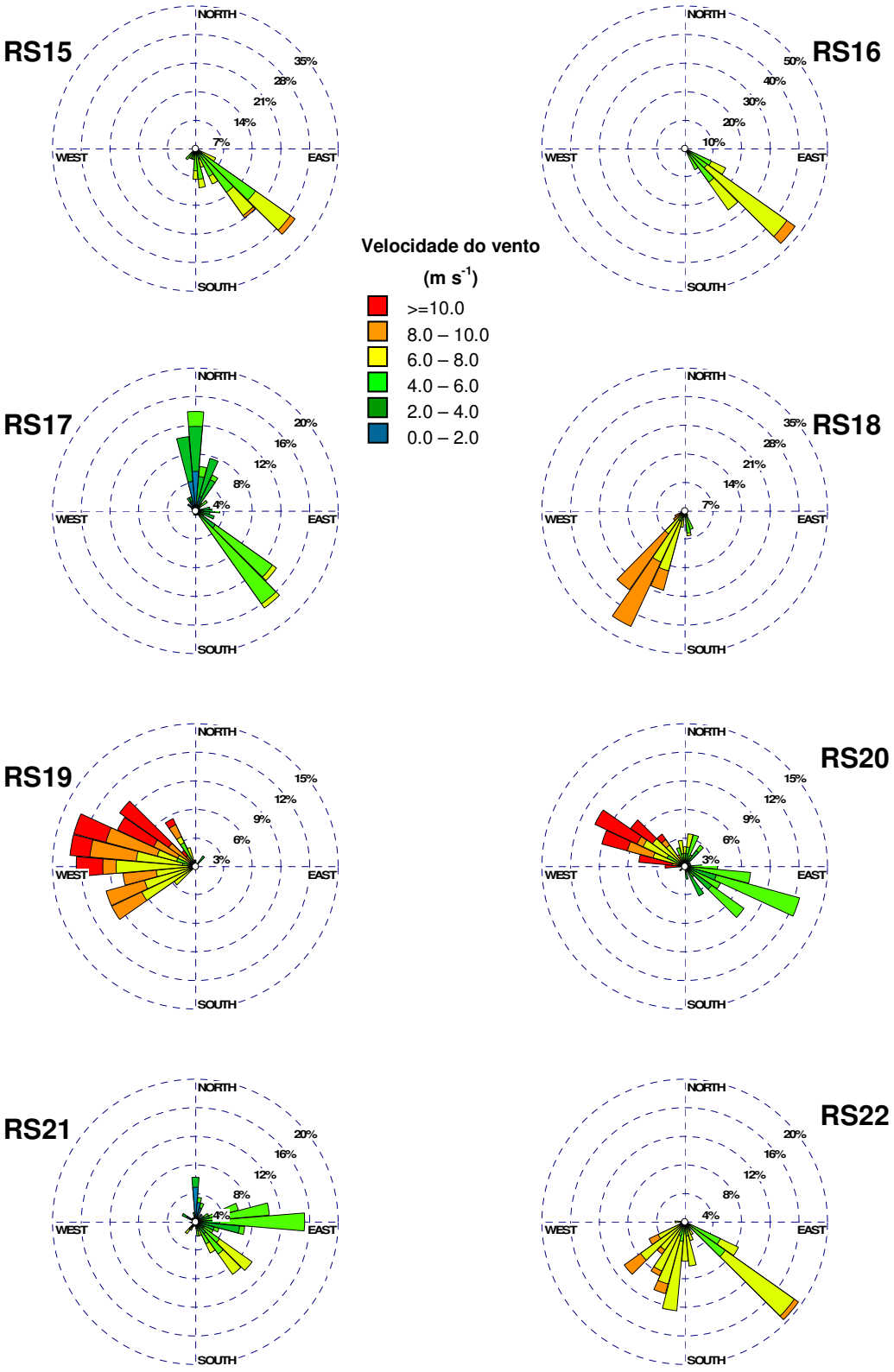

Figure 2.4 Wind Roses, with indication of percentages of distribution of wind velocity in function of its direction, associated to each rainwater sample (to be continued).

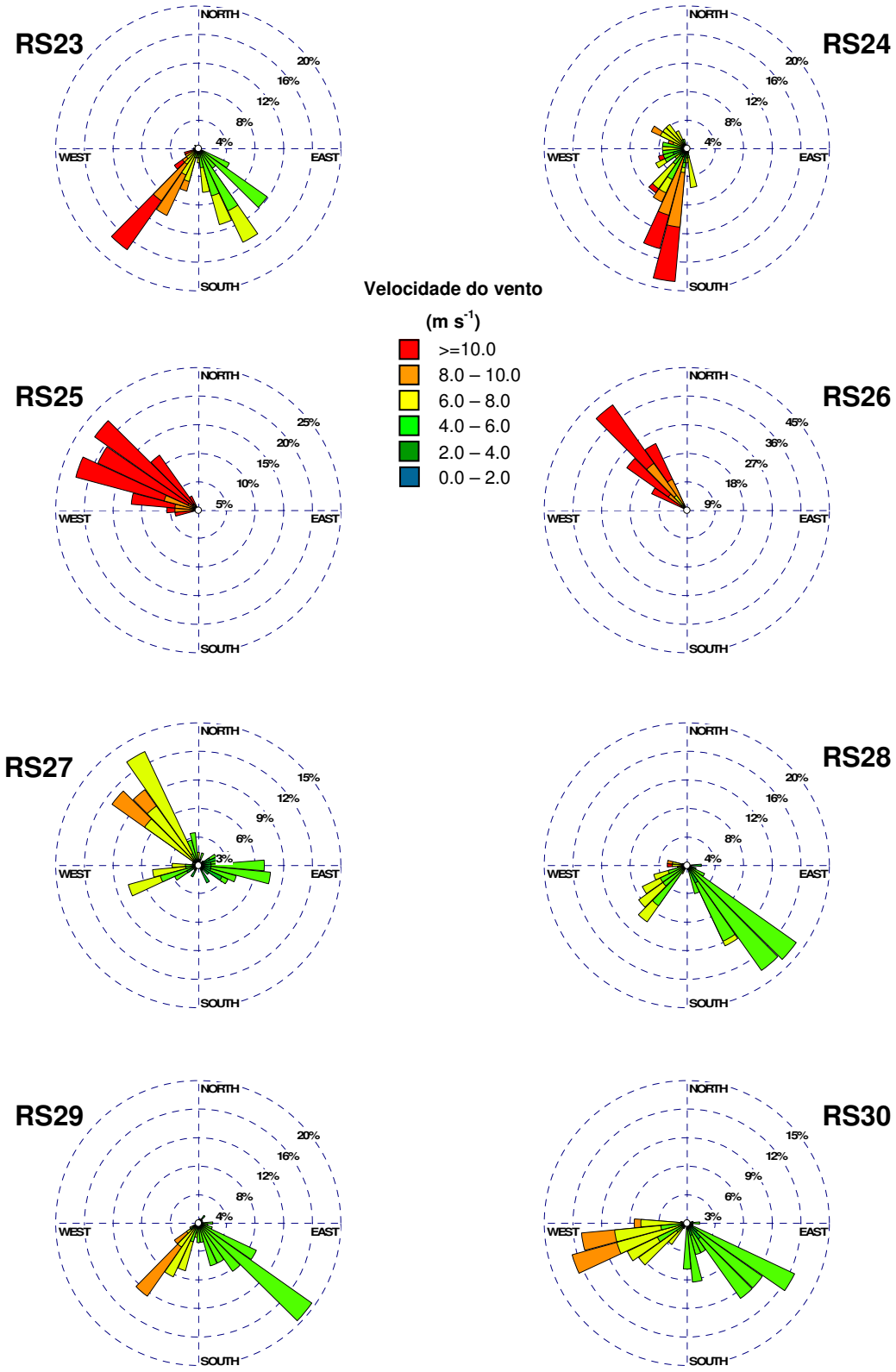

Figure 2.4 Wind Roses, with indication of percentages of distribution of wind velocity in function of its direction, associated to each rainwater sample (to be continued).

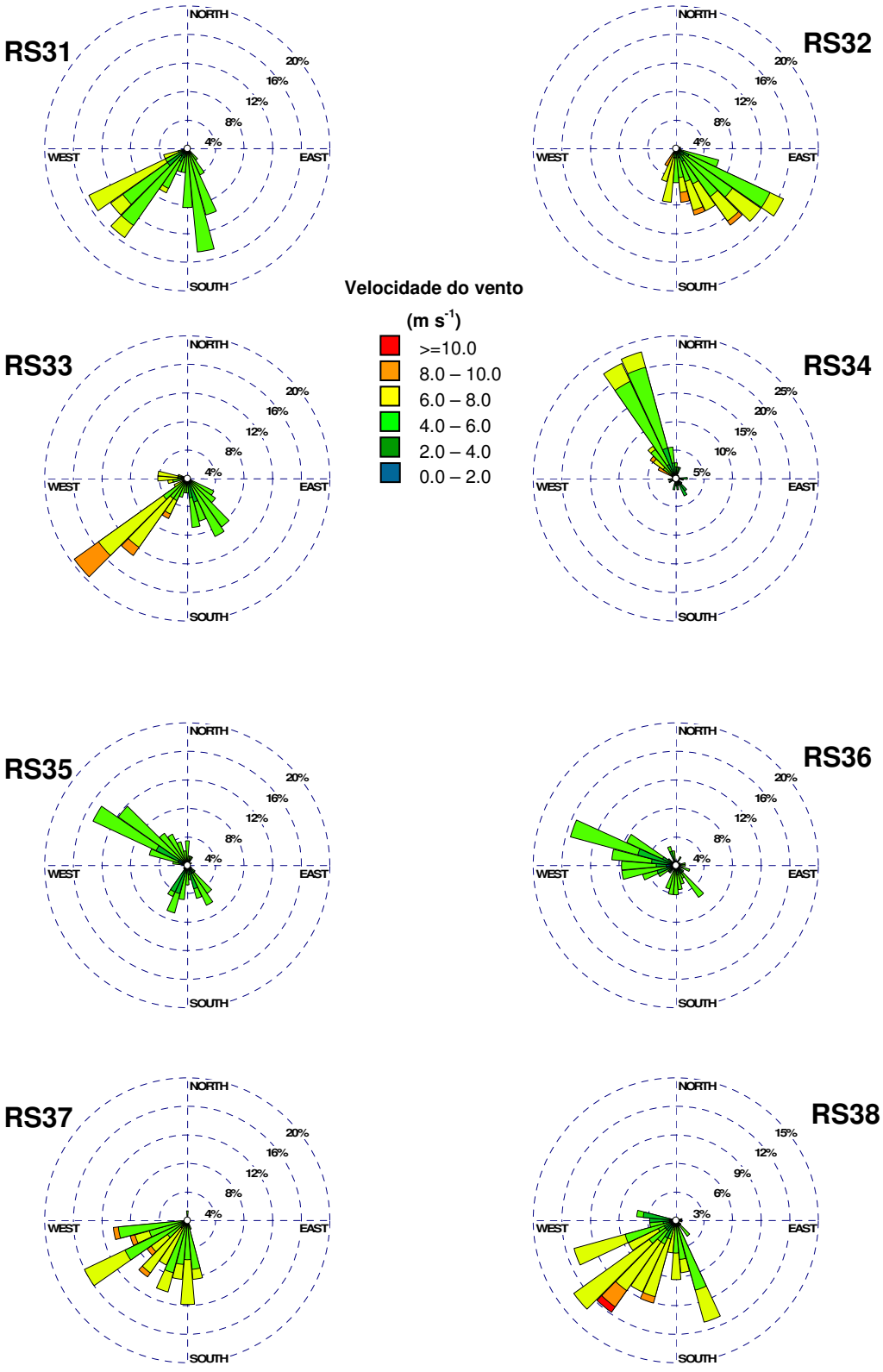

Figure 2.4 Wind Roses, with indication of percentages of distribution of wind velocity in function of its direction, associated to each rainwater sample (to be continued).

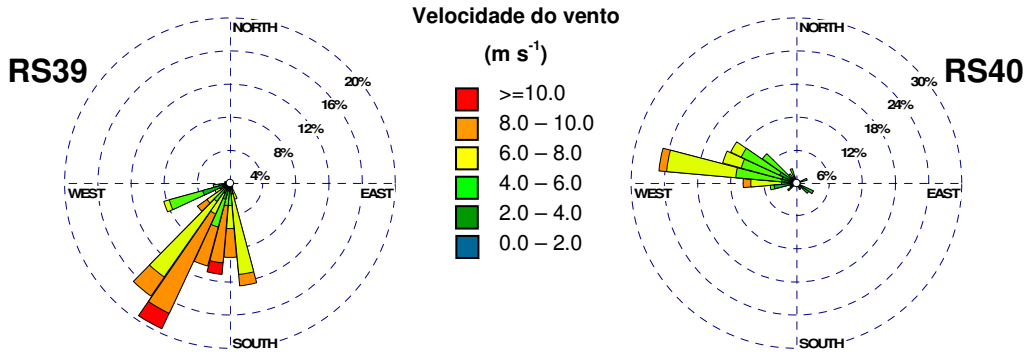

Figure 2.4 Wind Roses, with indication of percentages of distribution of wind velocity in function of its direction, associated to each rainwater sample (to be continued).

In order to compare the wind directions, shown in Figure 2.4 for each rainwater sample, with the origin of air masses, the air masses trajectories were calculated during the sampling periods. The general characteristics of air masses during the sampling period were evaluated by using Hybrid Single Particle Lagrangian Integrated Trajectory Model (HYSPLIT) developed by Draxler and Rolph (2003) at the National Oceanic Atmospheric Administration—Air Resources Laboratory (NOAA/ARL) (available at www.arl.noaa.gov/HYSPLIT.php).

Figure 2.5 presents the air mass trajectories generated for a 48 h hind-cast starting at 10 and 500 m level, calculated every 6 h for each rainwater sample.

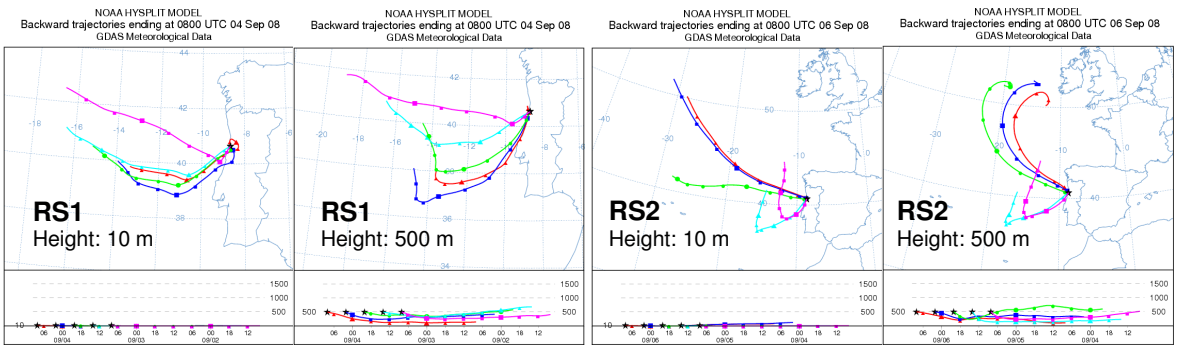

Figure 2.5 Air mass trajectories generated for a 48 h hind-cast starting at 10 and 500 m level, calculated every 6 h for each rainwater sample.

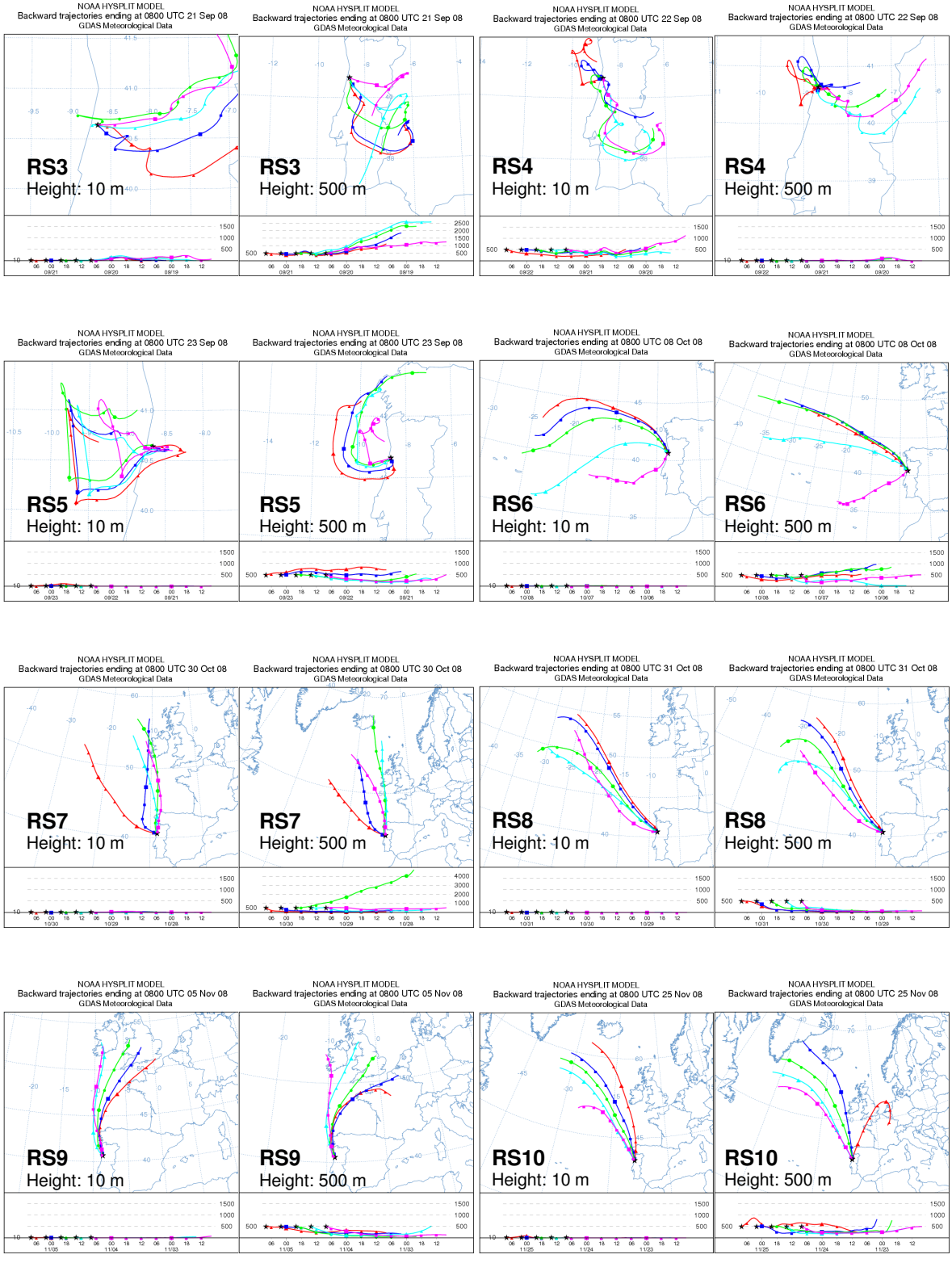

Figure 2.5 Air mass trajectories generated for a 48 h hind-cast starting at 10 and 500 m level, calculated every 6 h for each rainwater sample (to be continued).

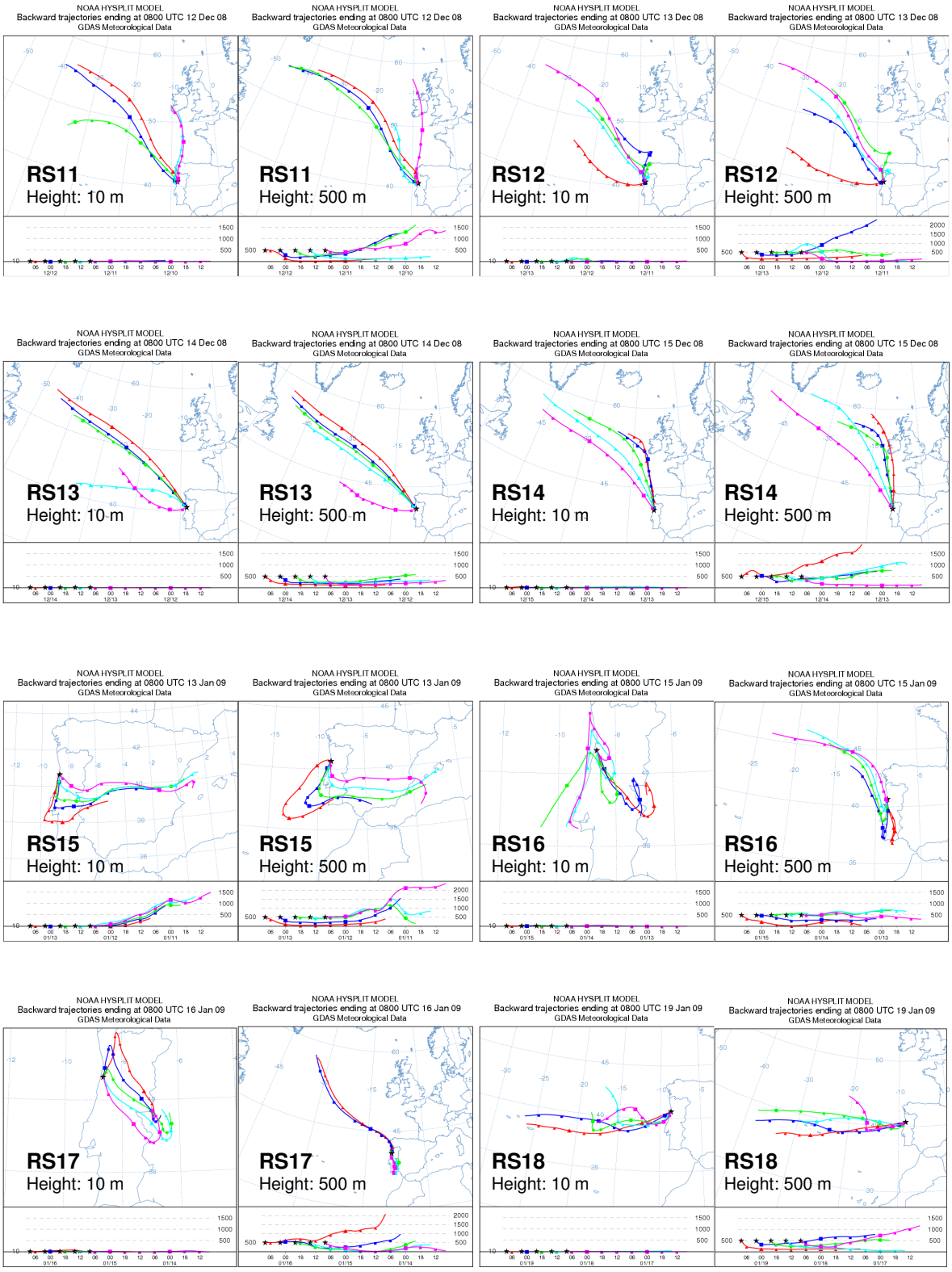

Figure 2.5 Air mass trajectories generated for a 48 h hind-cast starting at 10 and 500 m level, calculated every 6 h for each rainwater sample (to be continued).

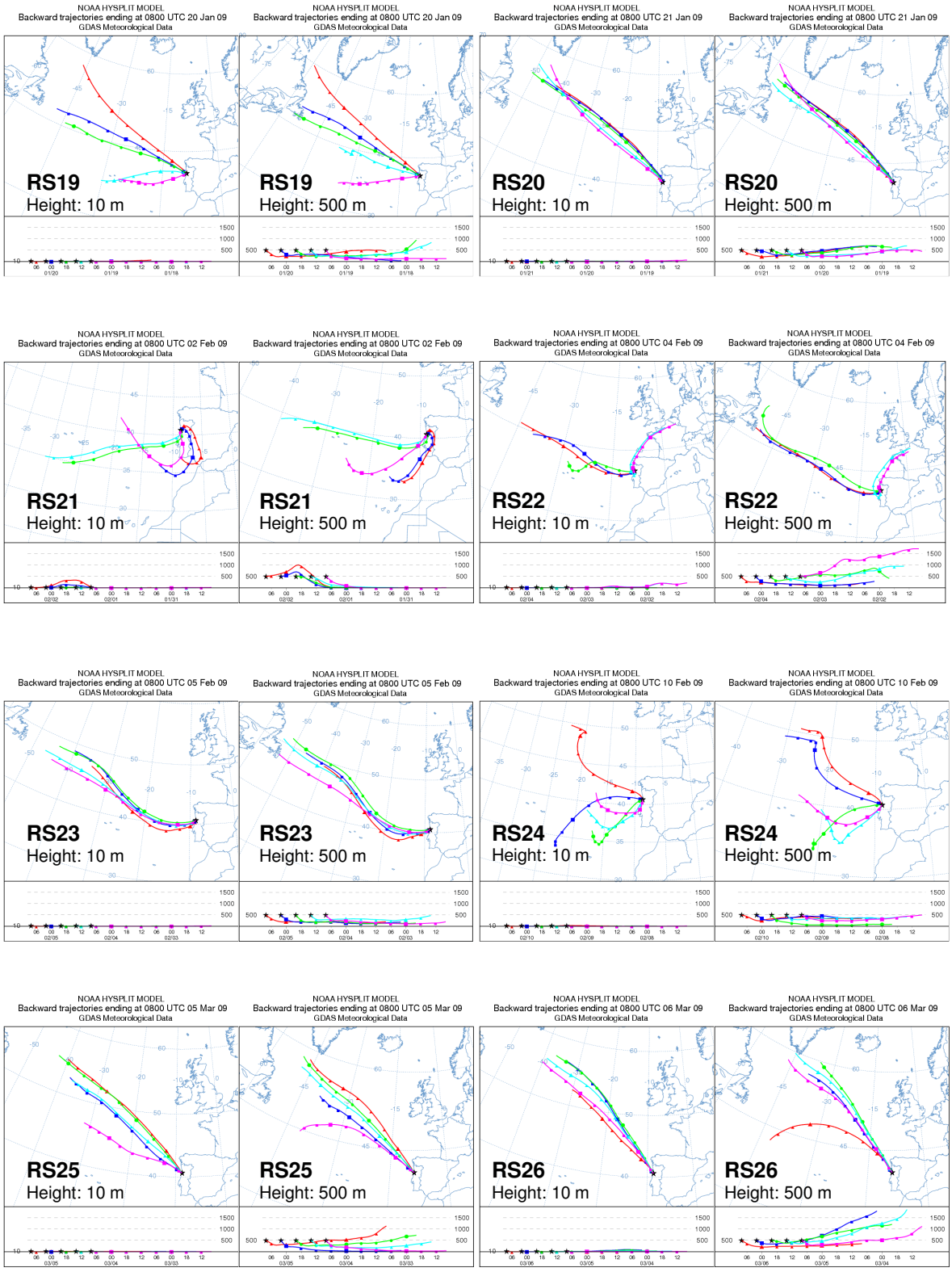

Figure 2.5 Air mass trajectories generated for a 48 h hind-cast starting at 10 and 500 m level, calculated every 6 h for each rainwater sample (to be continued).

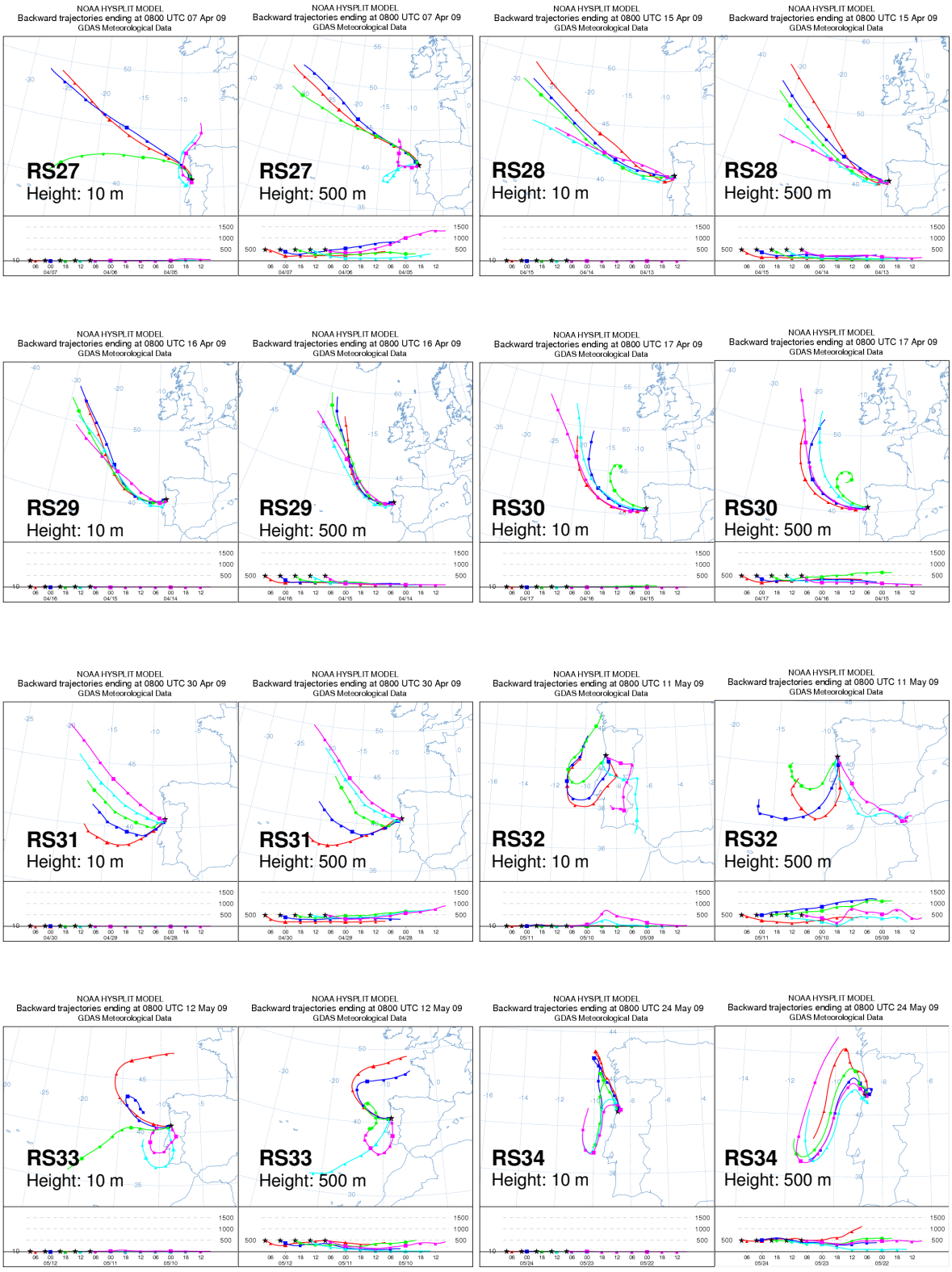

Figure 2.5 Air mass trajectories generated for a 48 h hind-cast starting at 10 and 500 m level, calculated every 6 h for each rainwater sample (to be continued).

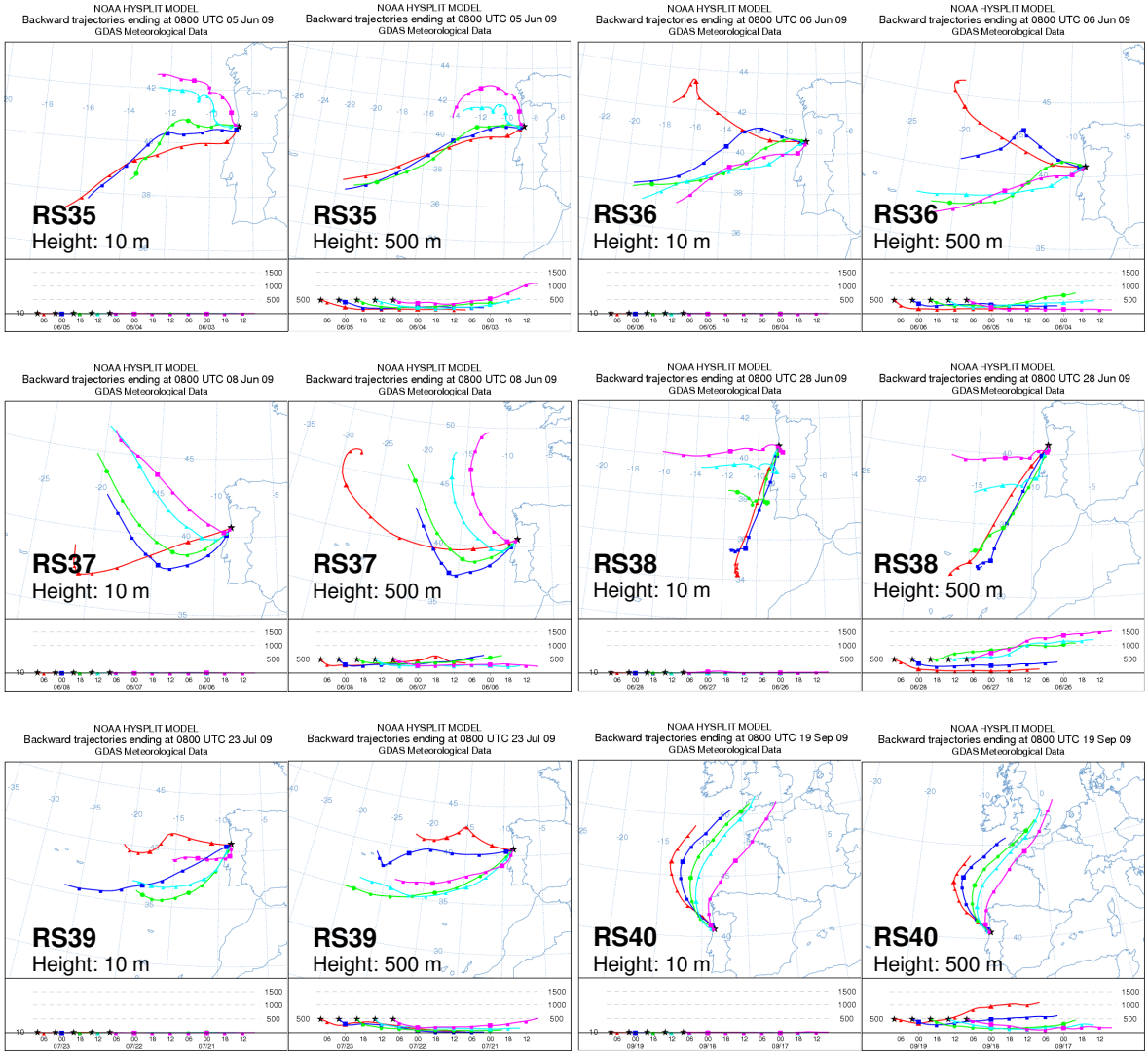

Figure 2.5 Air mass trajectories generated for a 48 h hind-cast starting at 10 and 500 m level, calculated every 6 h for each rainwater sample (to be continued).

As it may be seen in Figure 2.5, differences are observed for air mass trajectories between 10 m and 500 m of height for some samples, as for example for RS1, RS3, RS5, RS15, RS16, RS17, RS21 and RS32. Thus, it is important evaluate the air mass trajectories at 500 m, the approximate height of the low clouds and about half of the height of the atmospheric boundary layer, but also at 10 m because this height is more close of the height of rainwater collectors and is also more comparable with wind direction and intensity registered in meteorological station. The air mass trajectories at 10 m of height associated to each rainwater sample (Figure 2.5) are in accordance with the wind directions and intensities registered by meteorological station and presented in Figure 2.4.

Rainwater samples were classified into five groups according to the origin and trajectory of the air masses: class A contains samples related with air masses transported from the Atlantic Ocean; class B represents samples with origins in central and northern parts of industrialized Europe and transported to Portugal over the ocean; class C contains samples with similar origins that class B, but transported over land; class D refers to air masses transported from north Africa and the Mediterranean across the Iberian Peninsula; samples in which less than 60 % of the air-mass trajectories were from one section only, and had therefore a mixed origin, were agglomerated into class M. A similar way of classification had been previously used by Pio et al. (1991) for rainwater also collected at Aveiro (Portugal).

Figure 2.6 show the air mass trajectory analysis at 500 m level, for the rainwater samples RS40 to exemplify the classification of rainwater according to air-mass trajectories.

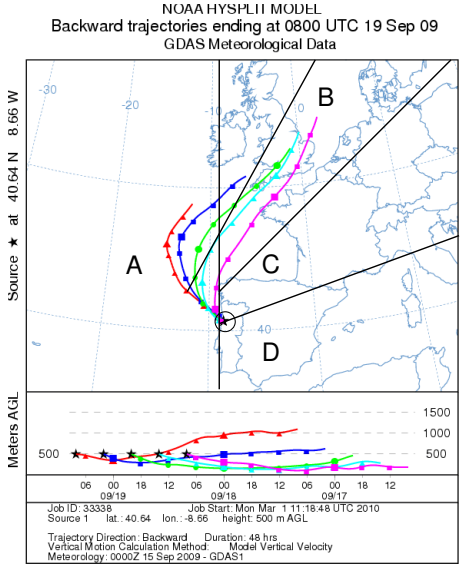

Figure 2.6 The air mass trajectory analysis at 500 m level, for the rainwater sample RS40 collected at 19 September 2009, to exemplify the classification of rainwater according to air-mass origins and trajectories.

The classification of collected rainwater according to air mass trajectories and recurring also to wind direction and speed (Figure 2.5) showed that 30 samples had a maritime influence (RS1-RS2, RS6-RS8, RS10-RS14, RS18-RS20, RS22-RS31, RS33-RS39; class A), 3 samples had origins in parts of Industrialized

Europe and transported to Portugal over the ocean (RS5, RS9, RS40; class B) and 7 samples were associated with air masses from the Mediterranean area (RS3-RS4, RS15-RS17, RS21, RS32; class D). Table 2.2 summarizes the meteorological data for each rainwater sample.

Table 2.2 Summer of meteorological data observed for each rainwater sample.

Season	Sample	Accumulated Precipitation (mm H_2O)	Temperature (ºC) [a]	Relative Humidity (%) [a]	Wind Speed (m/s) [b]	Air Mass Trajectory
Summer 2008	**RS1**	3.3	18.3	92.5	6.0	A
	RS2	23.2	16.6	100.0	8.7	A
	RS3	1.3	19.8	95.0	7.8	D
Autumn 2008	**RS4**	6.2	18.8	98.0	5.5	D
	RS5	5.9	18.1	99.5	2.7	B
	RS6	7.2	15.7	99.0	7.2	A
	RS7	7.1	12.2	75.0	9.3	A
	RS8	7.6	13.2	94.0	7.5	A
	RS9	5.8	12.6	98.0	4.0	B
	RS10	1.7	9.0	88.0	11.6	A
	RS11	13.8	10.1	92.0	9.2	A
	RS12	12.7	9.5	92.0	6.5	A
	RS13	13.2	10.2	85.0	11.3	A
	RS14	5.9	7.3	84.5	11.4	A
Winter 2009	**RS15**	19.8	9.7	71.0	6.9	D
	RS16	9.2	9.0	83.0	6.0	D
	RS17	9.7	8.7	100.0	3.6	D
	RS18	10.9	13.5	100.0	7.6	A
	RS19	8.4	10.3	87.0	12.2	A
	RS20	4.6	5.6	92.0	14.1	A
	RS21	11.2	9.0	95.0	5.1	D
	RS22	32.9	9.9	89.5	6.3	A
	RS23	18.9	9.1	91.0	9.8	A
	RS24	7.9	12.2	87.0	8.9	A
	RS25	10.4	11.7	82.0	14.6	A
	RS26	2.9	12.0	78.0	13.7	A
Spring 2009	**RS27**	1.0	11.9	75.5	6.8	A
	RS28	17.9	9.6	87.0	7.8	A
	RS29	20.5	10.1	88.5	6.3	A
	RS30	4.1	11.9	82.0	6.2	A
	RS31	6.9	14.2	84.0	5.3	A
	RS32	11.8	15.5	81.0	6.4	D
	RS33	9.3	15.2	88.5	6.8	A
	RS34	4.2	15.8	85.0	6.5	A
	RS35	4.0	18.0	78.4	2.9	A
	RS36	14.4	17.1	79.4	3.2	A
	RS37	37.4	17.2	75.0	6.0	A
Summer 2009	**RS38**	9.0	21.9	64.2	7.7	A
	RS39	14.4	20.1	88.5	8.4	A
	RS40	0.1	17.3	88.5	5.8	B

[a] median value
[b] maximum value

Air mass trajectories were also calculated for events whose rainwater was not collected between September 2008 and September 2009 (Annex I), to evaluate the representativeness of the collected samples.

The classification of rainwater amount according to air-mass trajectories during all sampling period is shown in Table 2.3.

Table 2.3 Percentage of total and seasonal rainwater amount discriminated according to air-mass trajectories for all precipitation events between September 2008 and September 2009.

	Total	A	B	C	D	M
Total	100	82	2	1	15	0
Autumn	27	87	6	1	6	0
Winter	44	73	0	1	26	0
Spring	22	94	0	0	6	0
Summer	7	97	1	0	2	0

As it may be seen, 82 % of precipitation was related with air masses transported from the Atlantic Ocean (A) while the rest of precipitation was related to air masses with anthropogenic and terrestrial contributions (B, C and D). Pio et al. (1991) had also observed that around 80 % of the precipitation in Aveiro between 1986 and 1989 was associated to air masses with an Atlantic origin. Moreover, no rainwater sample was attributed to a mixed origin (M). On the other hand, Table 2.3 also shows that 44 % of precipitation occurred during winter, while only 7 % occurred during summer. Autumn and spring presented similar percentages of rainwater volume. It must be pointed out that, during spring, except for a small percentage of class D air mass related precipitation (6%), rainwater was exclusively class A. On the contrary, autumn was the season when precipitation was most heterogeneous according to related air masses (87 % A, 6 % B, 1 % C and 6 % D).

The classification of collected rainwater amount according to air-mass trajectories during all sampling period is shown in Table 2.4.

Table 2.4 Percentage of total and seasonal rainwater amount discriminated according to air-mass trajectories for collected rainwater events between September 2008 and September 2009.

	Total	A	B	C	D	M
Total	100	81	3	0	16	0
Autumn	21	80	13	0	7	0
Winter	35	66	0	0	34	0
Spring	31	91	0	0	9	0
Summer	13	96	1	0	3	0

Comparing Tables 2.3 and 2.4, similar percentages of rainwater volume discriminated according to air-mass trajectories are observed, except for rainwater with origins in central and northern parts of industrialized Europe and transported to Portugal over land (class C), because few events with this trajectories occurred in all sampling period. Therefore, results show that collected rainwater is representative of the whole rainwater during the sampling period.

3. Molecular fluorescence analysis of rainwater: effects of sample preservation

Very different filtration and preservation procedures may be found in the literature on the study of the rainwater dissolved organic fraction. Thus, the influence of sample filtration and preservation procedures on the fluorescence of rainwater dissolved organic matter (DOM) was studied in this work. Rainwater was filtered through different filters (quartz 0.22 μm or PVDF 0.45 μm) and excitation (λ_{em}= 415 nm) and synchronous ($\Delta\lambda$ = 70 nm) fluorescence spectra were obtained at the same day of collection, or after preservation by refrigeration (1 to 7 days) or by freezing (1 to 4 weeks). The excitation-emission matrix (EEM) spectra of rainwater showed six types of fluorescent bands: two corresponding to humic-like bands, and four resembling proteins. Then, the excitation and synchronous spectra were chosen in order to monitor changes in the humic-like and protein-like bands, respectively. The filtration procedures adopted in this work did not affect the fluorescence properties of the rainwater samples. However, these properties were differently preserved by refrigeration or freezing: after refrigeration, filtered rainwater maintained the original fluorescent properties for at least four days, while after freezing fluorescent properties were not always preserved since it occurred a decrease of protein-like fluorescence intensity.

Santos, P.S.M., Otero, M., Santos, E.B.H., Duarte, A.C., 2010. Molecular fluorescence analysis of rainwater: effects of sample preservation. Talanta 82, 1616–1621.

3.1 Introduction

Molecular fluorescence spectroscopy is an excellent tool for tracing the origin and nature of chromophoric dissolved organic matter (CDOM) and may be used to reveal important information about its composition and biogeochemical cycling (Burdige et al., 2004). Compared with other spectroscopic techniques, fluorescence spectroscopy is a simple, sensitive, non-destructive, and rapid analytical technique that does not require separation, and needs only a small volume of aqueous sample (Miano et al., 1988).

Given its sensitiveness, fluorescence spectroscopy results may be affected by sample processing before analysis, namely, filtration and preservation. Dissolved organic matter (DOM) is operationally defined as the organic matter that passes through the pores of filters, usually of 0.2 to 0.7 μm pore size (Benner et al., 1993). Although there is an almost universal consensus about 0.45 μm (Zsolnay, 2003; Peuravuori and Pihlaja, 2007), the size limit that is used to differentiate DOM from particulate organic matter is somewhat arbitrary. On the other hand, DOM fluorescence is sensitive to changes in the environmental conditions and, ideally, water samples should be analyzed immediately after sample collection. However, it is often desirable, or necessary, because of logistical constraints, to store water samples before processing.

Regarding rainwater, the work by Willey et al. (2000) was key to highlighting the importance of the study of the dissolved organic fraction. Table 3.1 shows the subsequent works published on this matter together with the filtration and preservation procedures adopted. A few of these works have highlighted the valuable properties of molecular fluorescence for the characterization of rainwater DOM (Kieber et al., 2006; Kieber et al., 2007; Miller et al., 2008; Muller et al., 2008; Miller et al., 2009; Santos et al., 2009a; Santos et al., 2009b) and it has been demonstrated that fluorescence has a great potential for fingerprinting of rainwater DOM (Muller et al., 2008).

Although references in Table 3.1 are all quite recent, separation and preservation procedures used differ a lot. Filters of different materials and pore sizes, or, also, no filtration, have been used to separate DOC and different ways

Table 3.1 Works published on the rainwater dissolved organic fraction during the last decade.

Sample filtration	Preservation procedure	Time until analysis	Fluorescence analysis	Origin	References
N.F.	dark at 4ºC	N.S.	none	São Paulo State (Brasil)	Lara et al., 2001
N.F.	Freezing	N.S.	none	South Island (New Zealand)	Kieber et al., 2002
0.45 µm (Gelman GN-6)	4ºC	within 24 h	none	Guandaushi Forest (Taiwan)	Liu and Sheu, 2003
0.7 µm (Whatman GF/F)	Freezing	N.S.	none	New Brunswick, NJ (USA)	Seitzinger et al., 2003
0.45 µm (Gelman GN-6)	4ºC	within 24 h	none	Hui-Sun Forest (Taiwan)	Wang et al., 2004
N.F.	N.S.	within minutes	none	Wilmington, NC (USA)	Kieber et al., 2005
N.F.	N.S.	within 12 h	none	Wilmington, NC (USA)	Avery et al., 2006
0.2 µm (Supor® polysulfonone)	dark at 4ºC	within hours (2-3)	EEM	Wilmington, NC (USA)	Kieber et al., 2006
N.F.	N.S.	within minutes	none	Wilmington, NC (USA)	Willey et al., 2006
0.7 µm (Millipore GF/F)	4ºC	7 days[Ø]	none	Riberão Preto and Araraquara (SP, Brasil)	Campos et al., 2007
N.F.	N.S.	N.S.	none	N.S.	Ćosović et al., 2007
0.2 µm (Supor® polysulfonone)	dark at 4ºC	within hours (2-3)	EEM	Wilmington, NC (USA)	Kieber et al., 2007
0.6 µm (Whatman GF/F)	Freezing	N.S.	none	Twin Cays (Belize)	Wanek et al., 2007
0.45 µm (Millipore cellulose acetate)	Freezing	N.S.	none	Riberão Preto and Araraquara (SP, Brasil)	Coelho et al., 2008
N.F.	N.A.	immediately	EEM	Wilmington, NC (USA)	Miller et al., 2008
N.F.	N.S.	within 24 h	EEM	Birmingham (UK)	Muller et al., 2008
0.7 µm (Whatman GF/F)	dark at 4ºC	N.S.	none	Šibenik (Croatia)	Plavšić et al., 2008
1 µm (Glass fiber filters)	N.S.	within 48 h	none	Guangzhou (China)	Xu et al., 2008
0.2 µm (Supor® polysulfonone)	dark at 4ºC	N.S.	EEM	Wilmington, NC (USA)	Miller et al., 2009
0.7 µm (Whatman GF/F)	dark at 4ºC	N.S.	none	Zagreb and Šibenik (Croatia)	Orlović-Leko et al., 2009
0.45 µm (Millipore PVDF)	Freezing	N.S.	EEM	Aveiro (Portugal)	Santos et al., 2009
0.45 µm (Millipore PVDF)	N.S.	within few hours	EEM	Aveiro (Portugal)	Santos et al., in press
0.45 µm (membrane filters)	at 4ºC	within 1 month	none	Tönnersjöheden (Sweden)	Rosenqvist et al., 2010
0.45 µm (Sartorius Minisart SRP)	Freezing	N.S.	none	Beijing, Baoding , Cangzhou, Luancheng, Tianjin, Tanggu, Tangshan, Xinglong, Yucheng and Yangfang (China)	Pan et al., 2010

N.F. = Not Filtered
N.S. = Not Specified
N.A. = Not Applicable
EEM = Excitation-Emission Matrix
[Ø] DOC integrity was proved

of sample preservation have been followed by different research groups. Still, different procedures have been followed in different works by the same research group. Even when focussing only on those works using such a sensitive technique as molecular fluorescence spectroscopy, this situation remains. Kieber et al. (2006, 2007) and Miller et al. (2009) filtered rainwater samples through 0.2 µm filters (polysulfone) immediately after collection and kept them at 4ºC in the dark until fluorescence analysis, but, while Kieber et al. (2006) analysed the samples within 3h after collection, Miller et al (2009) did not specify the sample preservation time. Miller et al. (2008) and Muller et al. (2009) did analyse samples without filtration and analysed them by fluorescence spectroscopy immediately or within a maximum of 24h, respectively, but without specifying how samples were kept meanwhile. In order to use the same operational definition of DOM for its quantification and for its characterization by fluorescence spectroscopy, filtration through 0.45 µm has been used either for analysis within a few hours after collection (Santos et al., 2009a) or for analysis after freezing preservation (Santos et al., 2009b).

The production environmental data without the influence of operational variables such as filtration and storage of samples is of utmost importance, namely when applying molecular fluorescence spectroscopy to such a low concentration of DOM as in the case of rainwater. Thus, this work aims to study the effects of filtration and preservation procedures on the fluorescence properties of DOM from samples of rainwater in order to choose the most appropriate procedures.

3.2 Experimental

3.2.1 Rainwater sampling and preservation

Rainwater samples were collected in spring and autumn, during April (A08) and October 2008 (O08), respectively, at a sampling station (40º38' N, 8º39' W) in the western part of the town of Aveiro, Portugal. Samples were collected at 70 cm above the ground, through glass funnels (30 cm diameter) into glass bottles (5 L).

Sampling containers were left out open in order to collect both wet and dry depositions on a 24 h basis. Prior to use, all glass materials were immersed for 30 min, in a solution of NaOH (0.1 M), then rinsed with distilled water, followed by another immersion for 24 hours in a solution of HNO_3 (4 M), and finally rinsed with ultrapure (Milli-Q) water. Rainwater samples, after finishing the sampling period of 24 h, were transported within less than 1 hour to the laboratory for further processing.

Figure 3.1 shows a diagram of the experimental procedure adopted in this work.

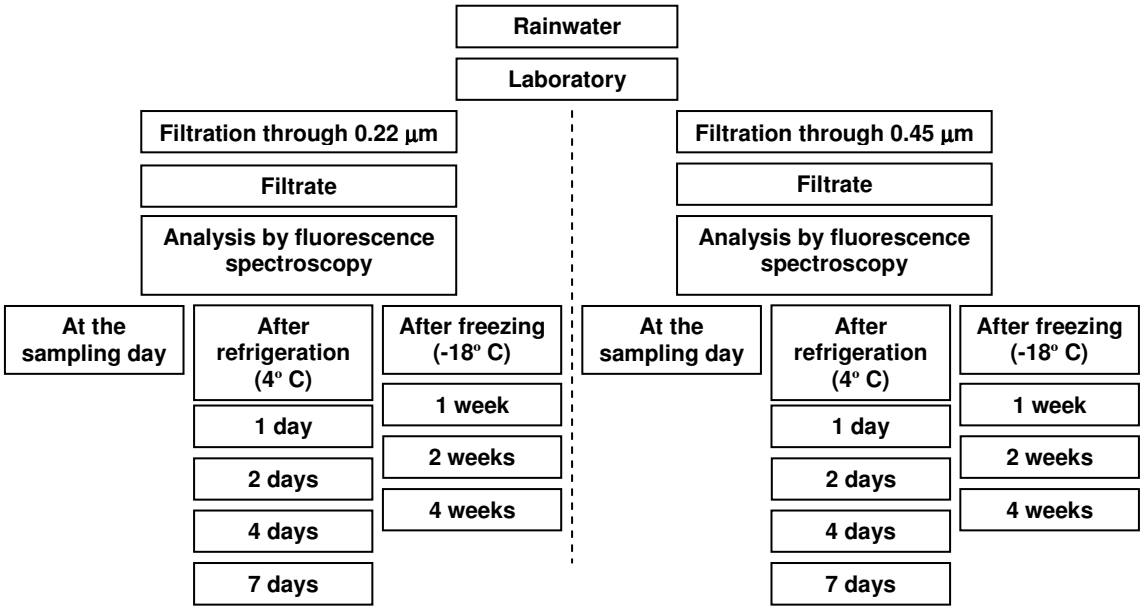

Figure 3.1 Schematic diagram of the experimental procedure adopted.

Once in the laboratory, rainwater was divided into two aliquots. One of the aliquots was filtered through 0.22 µm quartz filters, GSWP Millipore, in a glass filtration apparatus and the other one was filtered through 0.45 µm hydrophilic PVDF Millipore membrane filters in a stainless steel filtration apparatus. For both filtration systems, blanks (Milli-Q water) were obtained and analysed by fluorescence spectroscopy in the same way as samples. The filtrate from each aliquot was then divided in eight sub-aliquots, one to be analysed at the day, four to be analysed 1 to 7 days under refrigeration (4ºC), and three to be analysed 1 to 4 weeks freezing (-18 ºC). In the case of samples from April, they were only filtered through 0.45 µm and then subjected to the subsequent preservation

procedures here considered (Figure 3.1). In all cases, rainwater was stored in glass vials. Optical measurements were conducted within 2-3 hours of rainwater collection and/or after reaching room temperature (20ºC), in the cases of refrigerated and/or frozen sub-aliquots.

3.2.2 Laboratory analytical procedures

The molecular fluorescence spectra were obtained by a Fluoromax 3 (JobinYvon-Spex Instruments S.A., Inc, now HORIBA Jobin Yvon Inc, Edison, NJ, USA) with a xenon lamp source. Fluorescence analyses were carried out under thermostated 20ºC conditions and spectra were recorded using 1 cm cells and 5 nm bandpasses on both the excitation and emission monochromators. Excitation-emission matrix (EEM) fluorescence spectra were obtained by concatenating emission spectra measured every 5 nm from 290 to 510 nm using excitation wavelengths (λ_{ex}) from 240 to 400 nm (5 nm intervals). Synchronous spectra ($\Delta\lambda$ = 70 nm) and excitation spectra (λ_{em} = 415 nm) were also acquired using λ_{ex} from 240 to 400 nm (5 nm intervals). Scans were corrected for instrument configuration using factory supplied correction factors (Coble et al, 1993). Data were normalized to a daily-determined water Raman intensity ($275_{ex}/303_{em}$, 5 nm bandpasses) and converted to Raman normalized quinine sulphate (QS) equivalents in ppb (Coble et al., 1998). For each way of filtration, the corresponding averaged blank (Milli-Q water) spectrum was subtracted from rainwater spectra. Replicate scans within 5% agreement in terms of intensity and within bandpass resolution in terms of band location were obtained. However, at low excitation wavelengths ($\lambda_{ex} \leq 250$ nm), instrumental variability on fluorescence intensity was always higher than at $\lambda_{ex} > 250$ nm.

3.3 Results and discussion

Figure 3.2 shows the EEM fluorescence spectra of A08 and O08 rainwater samples filtered through 0.45 µm.

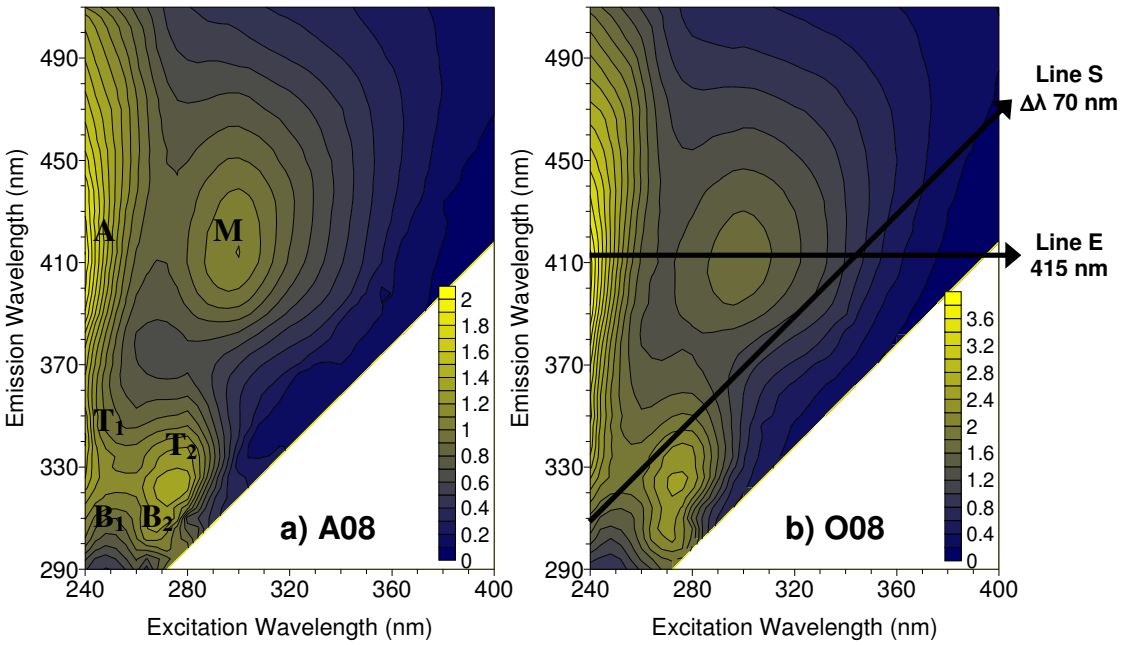

Figure 3.2 EEM fluorescence contour profiles of a) A08 and b) O08 rainwater samples. Fluorescence intensities are presented in ppb QS. The line S indicates the spectral range covered by the synchronous mode using Δλ = 70 nm. The line E corresponds to the excitation spectrum at λ_{em}=415 nm.

The corresponding spectra were obtained at the day of sample collection. Both samples have the same fluorescent bands: two humic-like bands, A ($\lambda_{ex}/\lambda_{em}$ ≈ 240/415 nm) and M ($\lambda_{ex}/\lambda_{em}$ ≈ 300/415 nm); and four protein-like bands, B_1 ($\lambda_{ex}/\lambda_{em}$ ≈ 240/305 nm), B_2 ($\lambda_{ex}/\lambda_{em}$ ≈ 270/305 nm), T_1 ($\lambda_{ex}/\lambda_{em}$ ≈ 240/340 nm) and T_2 ($\lambda_{ex}/\lambda_{em}$ ≈ 275/330 nm). Bands in the same range as A have already been identified in the emission-excitation matrix (EEM) fluorescence spectra of rainwater dissolved organic matter and have being assigned to humic-like compounds (Kieber et al., 2006; Muller et al., 2008; Santos et al., 2009a). A band at similar $\lambda_{ex}/\lambda_{em}$ of M has already been identified in the EEM fluorescence spectra of rainwater, being assigned also to marine humic-like compounds (Kieber et al.,

2006; Santos et al., 2009a). B and T bands are attributed to protein-like compounds, such as tyrosine and tryptophan, respectively (Coble, 1996; Burdige et al., 2004).

The $\Delta\lambda$ = 70 nm for the synchronous spectra was chosen in order to highlight the protein-like fluorescence, and the excitation spectra with λ_{em} = 415 nm was chosen to study the behaviour of the humic-like bands (Santos et al, 2009a). These spectra are represented in Figure 3.2 by the lines E and S, corresponding to excitation and synchronous spectra, respectively.

The comparison between spectra was done and the determination of the percentage differences calculated using the fluorescence intensities, as described below:

$$Percentage \quad difference \quad (\%) = \frac{x_i - \mu}{\mu} \times 100$$

where x_i is the fluorescence intensity of the rainwater spectrum to compare with μ that is the fluorescence intensity of the spectrum of reference, at the same wavelength. The percentage difference was calculated for all excitation wavelengths in the range 240-400 nm.

Figure 3.3 shows the fluorescence spectra corresponding to the O08 rainwater sample obtained for the two filtrates (0.22 and 0.45 μm) after refrigeration (4ºC) during 1 to 7 days. Excitation and synchronous spectra at the sampling day were compared for rainwater filtered through quartz 0.22 μm and through PVDF 0.45 μm, obtaining a difference in fluorescence intensity lower than 7%. This value approximates the replication error, so the effect of rainwater filtration through different filters (quartz 0.22 μm and PVDF 0.45 μm) may be considered no significant.

Excitation spectra in Figure 3.3 a) and 3.3 b) show that, for both types of filters used, spectra keep the same until four days under refrigeration (differences in fluorescence intensity lower than 5%). However, when rainwater is preserved under refrigeration during 7 days, an intensity increase (up to 17%) of the excitation spectra was observed in the case of rainwater filtered through quartz 0.22 μm. For rainwater filtered through PVDF 0.45 μm, both an intensity increase

of fluorescence (up to 21%) at low λ_{ex} and a shift to longer λ_{ex} were observed after 7 days under refrigeration. The A08 rainwater sample also kept the original spectra until four days under refrigeration, showing an intensity increase (up to 15%) at low λ_{ex} and a shift to longer λ_{ex} after 7 days under refrigeration.

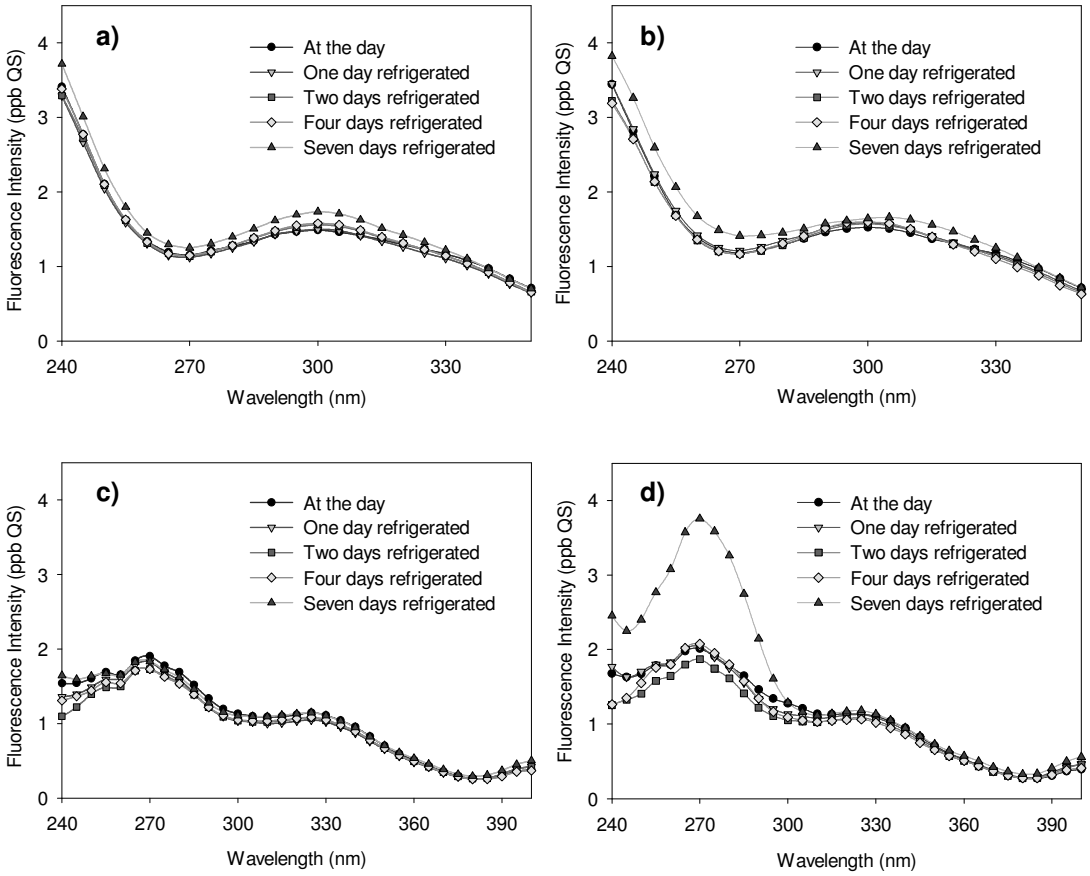

Figure 3.3 Excitation, (a) and (b), and synchronous, (c) and (d), fluorescence spectra corresponding to O08 rainwater analysed after refrigeration (1 to 7 days), for the two filtrates (0.22 and 0.45 µm).

Synchronous spectra in Figures 3.3 c) and 3.3 d), show a marked increase of intensity of the protein-like fluorescence (87% at λ_{ex} = 270 nm) in the 0.45 µm sub-aliquot after seven days under refrigeration while the spectra of the 0.22 µm sub-aliquots generally keep the original spectra obtained for rainwater at the day of sampling. The same behaviour was observed for the A08 rainwater sample filtered through 0.45 µm, which showed a slightly lower intensity increase than O08 (70% at λ_{ex} = 270 nm) after 7 days under refrigeration, but also kept the

original spectrum for 4 days under refrigeration. Differences between filtrates may be related to differences on biological activity due to the different pore size of filters. Some bacteria, which may be trapped by the 0.22 µm filter, can pass through the 0.45 µm filter (Lead and Wilkinson, 2006) and refrigeration may hold-up their activity but not completely stopped it (Weber and Marahiel, 2003; Elliott et al., 2006). Then, the fluorescence intensity increase in the 0.45 µm sub-aliquots may be related to microbiological activity, which may transform DOM to give new fluorophores, as it was pointed by Moran et al. (2000).

Figure 3.4 shows the fluorescence spectra corresponding to the O08 rainwater sample obtained for the two filtrates (0.22 and 0.45 µm) after freezing (-18ºC) during 1 to 4 weeks.

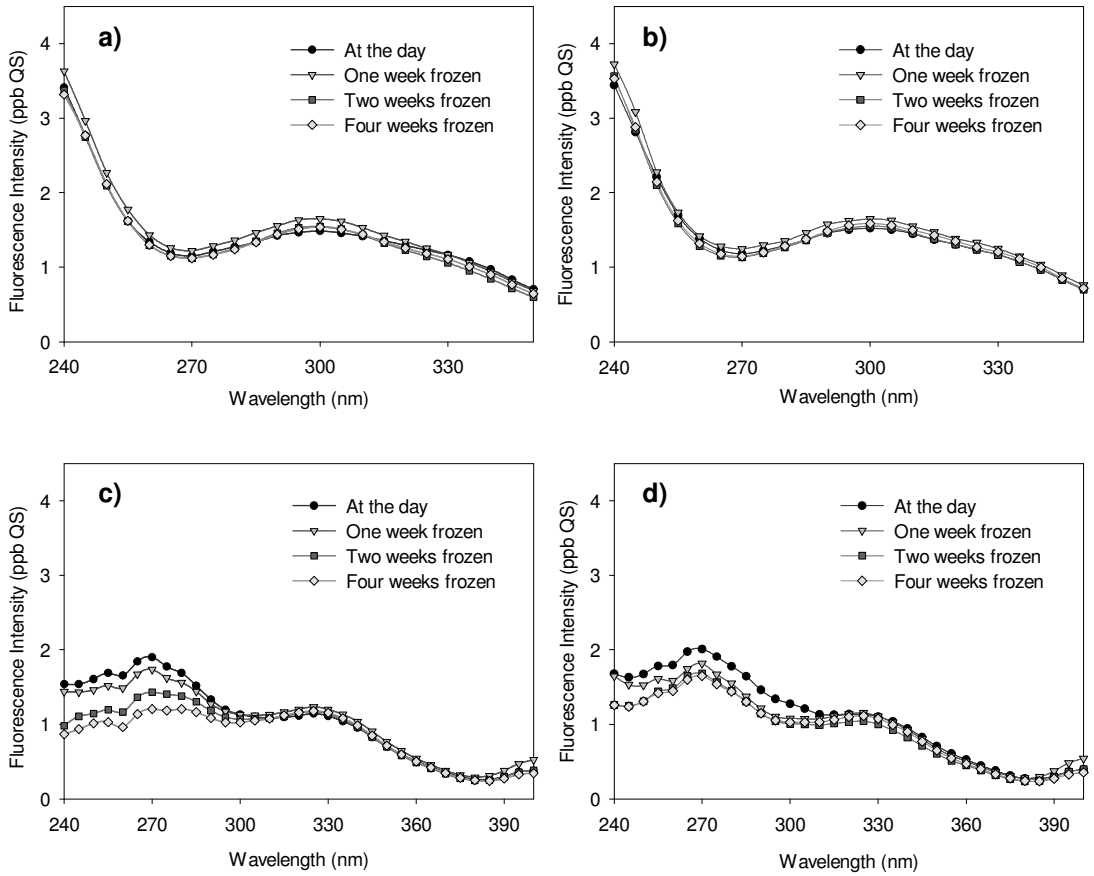

Figure 3.4 Excitation, (a) and (b), and synchronous, (c) and (d), fluorescence spectra corresponding to O08 rainwater analysed after freezing (1 to 4 weeks), for the two filtrates (0.22 and 0.45 µm).

In Figures 3.4 a) and 3.4 b), for both types of filters used, excitation spectra maintain unaltered (differences in fluorescence intensity lower than 5%) for rainwater preserved under freezing during 4 weeks. However, synchronous spectra in Figures 3.4 c) and 3.4d) show that, although there are not important changes in humic-like fluorescence related to freezing, that is not the case for the protein-like fluorescence. Rainwater freezing caused a gradual decrease in intensity of the protein-like bands with time. The decrease after four weeks frozen was 37% and 18% at λ_{ex} = 270 nm for the rainwater filtered through 0.22 and 0.45 μm, respectively. These results confirm that the protein-like fraction of fluorescent DOM may be less stable in response to the freezing process in comparison to the humic-like fractions, which has been already proved by Spencer et al. (2007). The intensity decrease may be related to the cold denaturation of protein-like fluorophores, when water is not in liquid state (Privalov, 1992; Strambini and Gonnelli, 2007). The protein-like fluorophores may lose their 3D structure and then their spectral properties are altered (Lakowicz, 2006; Strambini and Gonnelli, 2007) therefore affecting fluorescence intensity. The intensity decrease of the protein-like fluorescence after freezing and thawing was more remarkable for the O08 rainwater filtered through 0.22 μm than for that filtered through 0.45 μm. On the other hand, the decrease of the protein-like fluorescence intensity was not verified for the A08 rainwater sample, filtered through 0.45 μm, which fluorescence excitation and synchronous spectra, after freezing (up to 4 weeks) and thawing, kept unaltered (differences in fluorescence intensity lower than 5%). In a study on estuarine pore waters, no changes on fluorescence DOM (separated by filtration through 0.45 μm Durapore membranes) were found upon freezing (Otero et al., 2007). Also, Spencer et al. (2007) when studying the freeze/thaw effects on freshwater DOM (separated by filtration through 1.2 μm Whatman GF/C filters) from 35 different UK locations found large and variable responses of spectrophotometric measurements. Spencer et al. (2007) highlighted that knowledge of the original properties could not be used to determine the amount of DOM fluorescence change that would occur with freezing and subsequent thawing.

3.4 Conclusions

Different filtration and preservation procedures have been adopted in different published works for the study of the dissolved organic fraction of rainwater. However, in the present work, on rainwater collected in Aveiro (Portugal), it has been found that these procedures may affect rainwater fluorescent properties:

1) No significant differences were observed in original fluorescence properties between rainwater filtered through quartz 0.22 µm or PVDF 0.45 µm.
2) No matter the filter used for DOM separation (quartz 0.22 µm or PVDF 0.45 µm), fluorescence properties keep unaltered for rainwater preserved under refrigeration during 4 days.
3) Freezing may preserve rainwater fluorescent properties but may also cause an intensity decrease of the original protein-like fluorescence, depending on the rainwater sample. Differences must be related to the nature of the rainwater protein-like fluorophores, which may be less or more sensitive to denaturation.

The above results confirm that rainwater DOM fluorescent properties, mainly those related to the presence of protein-like compounds, are very sensitive and may be altered depending on the way of preservation and the time elapsed until analysis.

On the whole, authors would recommend filtration through 0.45 µm to separate the soluble from the particulate organic matter since this is the pore size which gets more consensus for the operational definition of dissolved organic matter and it has been shown that there are no alterations in samples filtered through 0.45 µm during the time recommended for preservation (4 days maximum). With respect to preservation, rainwater samples should be kept at dark 4ºC after collection and until molecular fluorescence analysis, which should be carried out as soon as possible but no longer than four days after collection. In any case, results on rainwater DOM fluorescence should always refer, apart from the

filter type used for DOM separation, the preservation procedure, proving that it did not affect the original properties.

References

Avery Jr., G.B., Willey, J.D., Kieber, R.J., 2006. Carbon isotopic characterization of dissolved organic carbon in rainwater: terrestrial and marine influences. Atmos. Environ. 40, 7539–7545.

Benner, R., von Bodungen, B., Farrington, J., Hedges, J., Lee, C., Mantoura, F., Suzuki, Y, Williams, P.M., 1993. Measurement of dissolved organic carbon and nitrogen in natural waters: workshop report. Mar. Chem. 41, 5-10.

Burdige, D.J., Kline, S.W. and Chen, W., 2004. Fluorescent dissolved organic matter in marine sediment pore waters. Mar. Chem. 89, 289-311.

Campos, M.L.A.M., Nogueira, R.F.P., Dametto, P.R., Francisco, J.G., Coelho, C.H., 2007. Dissolved organic carbon in rainwater: Glassware decontamination and sample preservation and volatile organic carbon. Atmos. Environ. 41, 8924–8931.

Coble, P.G., Schultz, C.A., Mopper K., 1993.Fluorescence contouring analysis of DOC Intercalibration Experiment samples: a comparison of techniques. Mar. Chem. 41, 173-178.

Coble, P.G., 1996. Characterization of marine and terrestrial DOM in seawater using excitationemission matrix spectroscopy. Mar. Chem. 51, 325-346.

Coble, P.G., Del Castillo, C.E., Avril, B., 1998. Distribution and optical properties of CDOM in the Arabian Sea during the 1995 Southwest Monsoon. Deep-Sea Res. II 45, 2195–2223.

Coelho, C.H., Francisco, J.G., Nogueira, R.F.P., Campos, M.L.A.M., 2008. Dissolved organic carbon in rainwater from areas heavily impacted by sugar cane burning. Atmos. Environ. 42, 7115–7121.

Ćosović, B., Orlović-Leko, P., Kozarac, Z., 2007. Rainwater dissolved organic carbon: characterization of surface active substances by electrochemical method. Electroanal. 19, 2077–2084.

Elliott, S., Lead J.R., Baker, A., 2006. Characterisation of the fluorescence from freshwater, planktonic bacteria. Water Res. 40, 2075 – 2083.

Kieber, R.J., Peake, B., Willey, J.D., Avery, G.B., 2002. Dissolved organic carbon and organic acids in coastal New Zealand rainwater. Atmos. Environ. 36, 3557–3563.

Kieber, R.J., Long, M.S., Willey, J.D., 2005. Factors influencing nitrogen speciation in coastal rainwater. J. Atmos. Chem. 52, 81-99.

Kieber, R.J., Whitehead, R.F., Reid, S.N., Willey, J.D., Seaton, P.J., 2006. Chromophoric dissolved organic matter (CDOM) in rainwater, Southeastern North Carolina, USA. J. Atmos. Chem. 54, 21-41.

Kieber, R.J., Willey, J.D., Whitehead, R.F. and Reid, S.N, 2007. Photobleaching of chromophoric dissolved organic matter (CDOM) in rainwater. J. Atmos. Chem. 58, 219-235.

Lakowicz, J. R., 2006. Principles of fluorescence spectroscopy, third ed., Springer, New York, USA.

Lara, L.B.L.S., Artaxo, P., Martinelli, L.A., Victoria, R.L., Camargo, P.B., Krusche, A., Ayers, G.P., Ferraz, E.S.B., Ballester, M.V., 2001. Chemical composition of rainwater and anthropogenic influences in the Piracicaba River Basin, Southeast Brazil. Atmos. Environ. 35, 4937-4945.

Lead J.R., Wilkinson K.J., 2006. Aquatic Colloids and Nanoparticles: Current Knowledge and Future Trends. Environ. Chem. 3, 159–171.

Liu,C.P., Sheu, B.H., 2003. Dissolved organic carbon in precipitation, throughfall, stemflow, soil solution, and stream water at the Guandaushi subtropical forest in Taiwan. Forest Ecol. Manag. 172, 315-325.

Miano, T.M., Sposito, G., Martin, J.P., 1988. Fluorescence spectroscopy of humic substances. Soil Sci. Soc. Am. J. 52, 1016–1019.

Miller, C., Willey, J.D., Kieber, R.J., 2008. Changes in rainwater composition in Wilmington, NC during tropical storm Ernesto. Atmos. Environ. 42, 846-855.

Miller, C., Gordon, K.G., Kieber, R.J., Willey, J.D., Seaton, P.J., 2009. Chemical characteristics of chromophoric dissolved organic matter in rainwater. Atmos. Environ. 43, 2497-2502.

Moran, M.A., Sheldon, W.M., Zepp, R.G., 2000. Carbon loss and optical property changes during long-term photochemical and biological degradation of estuarine dissolved organic matter. Limnol. Oceanogr. 45, 1254-1264.

Muller, C.L., Baker, A., Hutchinson, R., Fairchild I.J., Kidd, C., 2008. Analysis of rainwater dissolved organic carbon compounds using fluorescence spectrophotometry. Atmos. Env. 42, 8036-8045.

Otero, M., Mendonça, A., Válega, M., Santos, E.B.H., Pereira, E., Esteves, V.I., Duarte, A., 2007. Fluorescence and DOC contents of estuarine pore waters from colonized and non-colonized sediments: effects of sampling preservation. Chemosphere 67, 211–220.

Orlović-Leko, P., Plavšić, M., Bura-Nakić, E., Kozarac, Z., Ćosović, B., 2009. Organic matter in the bulk precipitations in Zagreb and Šibenik, Croatia. Atmos. Environ. 43, 805–811.

Pan, Y., Wang, Y., Xin, J., Tang, G., Song, T., Wang, Y., Li, X., Wu, F., 2010. Study on dissolved organic carbon in precipitation in Northern China. Atmos. Environ. 44, 2350-2357.

Peuravuori, J., Pihlaja, K., 2007. Characterization of Freshwater Humic Matter. In: Handbook of Water Analysis. Editor Leo M.L. Nollet. CRC Press. Taylor & Francis Group LLC, Boca Raton, 2nd Edition, pp. 436-437.

Plavšić, M., Orlović-Leko, P., Kozarac, Z., Bura-Nakić, E., Strmečki, S., Ćosović, B., 2008. Complexation of copper ions in atmospheric precipitation in Croatia. Atmos. Res. 87 (2008) 80–87.

Privalov, P.L., 1990. Cold Denaturation of Proteins. Biochem. Mol. Biol. 25, 281-306.

Rosenqvist, L., Kleja, D.B., Johansson, M.-B., 2010. Concentrations and fluxes of dissolved organic carbon and nitrogen in a *Picea abies* chronosequence on former arable land in Sweden. Forest Ecol. Manag. 259, 275-285.

Santos, P.S.M., Otero, M., Duarte, R.M.B.O., Duarte, A.C., 2009. Spectroscopic characterization of dissolved organic matter isolated from rainwater. Chemosphere 74, 1053-101.

Santos, P.S.M., Duarte, R.M.B.O., Duarte, A.C., 2009b. Absorption and fluorescence properties of rainwater during the cold season at a town in Western Portugal. J. Atmos. Chem. 62, 45-57.

Seitzinger, S.P., Styles, R.M., Lauck, R., Mazurek, M.A., 2003. Atmospheric pressure mass spectrometry: a new analytical chemical characterization method for dissolved organic matter in rainwater. Environ. Sci. Technol. 37, 131–137.

Spencer, R.G.M., Boltond, L., Baker, A., 2007. Freeze/thaw and pH effects on freshwater dissolved organic matter fluorescence and absorbance properties from a number of UK locations. Water Res. 41, 2941–2950.

Strambini, G.B., Gonnelli, M., 2007. Protein Stability in Ice. Biophys. J. 92, 2131-2138.

Wanek, W., Hofmann, J, Feller, I.C., 2007. Canopy interactions of rainfall in an off-shore mangrove ecosystem dominated by Rhizophora mangle (Belize). J. Hydrol. 345, 70–79.

Wang, M.C., Liu, C.P., Sheu, B.H., 2004. Characterization of organic matter in rainfall, throughfall, stemflow, and streamwater from three subtropical forest ecosystems. J. Hydrol. 289, 275–285.

Weber, M.H.W., Marahiel, M.A., 2003. Bacterial cold shock responses. Sci. Prog. 86, 9–75.

Willey, J.D., Kieber, R.J., Eyman, M.S., Avery, G.B., 2000. Rainwater dissolved organic carbon: concentrations and global flux. Global Biogeochem. Cy. 14, 139-148.

Willey, J.D., Kieber, R.J. and Avery, G.B., 2006. Changing chemical composition of precipitation in Wilmington, North Carolina, U.S.A.: Implications for the Continental U.S.A. Environ. Sci. Technol. 40, 5675-5680.

Xu, T., Song, Z., Liu, J., Wang, C., Wei, J., Chen, H., 2008. Organic composition in the dry season rainwater of Guangzhou, China. Environ. Geochem. Health 30, 53–65.

Zsolnay, A., 2003. Dissolved organic matter: artefacts, definitions and functions. Geoderma 113, 187-209.

4. Comparison between DAX-8 and C-18 solid phase extraction of rainwater dissolved organic matter

Rainwater is a very low concentrated matrix and, for dissolved organic matter (DOM) characterization, an efficient extraction procedure is essential. Isolation procedures based on the adsorption onto XAD-8 and C-18 sorbents have been used in the literature for rainwater DOM isolation, but a comparison between these procedures is lacking. In this work, UV-visible and molecular fluorescence spectroscopies highlighted differences between rainwater DOM isolated by DAX-8 (replacement for XAD-8) and by C-18. It was possible to recover higher rainwater DOM percentage by the C-18 based procedure than by the DAX-8 one. Rainwater protein-like compounds were better concentrated by the C-18 procedure than by the DAX-8 one, while humic-like compounds were similarly concentrated by both procedures. Furthermore, rainwater DOM extracted by the C-18 procedure was more representative of the global matrix, while DAX-8 preferentially extracted humic-like compounds.

Santos, P.S.M., Otero, M., Filipe, O.M.S., Santos, E.B.H., Duarte, A.C., 2010. Comparison between DAX-8 and C-18 solid phase extraction of rainwater dissolved organic matter. Talanta, 83, 505-512.

4.1 Introduction

DOM is defined operationally, almost universal consensus, as the organic matter that passes through a filter of 0.45 μm pore diameter (Zsolnay, 2003; Peuravuori and Pihlaja, 2007). Although there are techniques that can be applied directly to rainwater samples for the characterization of DOM, such as fluorescence spectroscopy, a deeper knowledge of DOM requires a previous extraction from samples. Ultrafiltration or solid-phase extraction, using XAD or C-18 sorbents, are the main ways used to concentrate and isolate DOM from water samples for further analysis (Simjouw et al., 2005). However, there is no single technique that can achieve quantitative isolation of all organic solutes from water (Leenheer, 1981) and properties of DOM isolated with different techniques may differ markedly (Benner et al., 1992; Repeta et al., 2002; Maurice et al., 2002; Simjouw et al., 2005). Besides, some isolation techniques allow for the selective isolation of a certain DOM fraction, which may be advantageous when the aim is obtaining more homogeneous fractions for further characterization.

A vast literature exists on solid phase extraction of organic matter (OM) from matrixes such as soil, freshwater or marine water. Unlike soil and freshwater OM, there is neither a robust protocol for the quantitative isolation of marine DOM nor any commercially available marine reference sample with which to compare extraction efficacy or DOM characteristics of the isolate (Mopper et al., 2007) so the debate on this topic remains. A similar situation has also been already created for water soluble organic matter (WSOM) from aerosols (Graber and Rudich, 2006), although research on this OM is quite recent, compared with that on marine DOM. Regarding rainwater, the study of the dissolved organic fraction was especially pushed by Willey et al. (2000) and most of the references on this matter have been published subsequently. Among these references, even when rainwater is a very low concentrated matrix and, thus, concentration is particularly relevant for the study of DOM, to our best knowledge, DOM extraction has only been referred in four published works (Wang et al., 2004; Kieber et al., 2006; Miller et al., 2009; Santos et al., 2009a).

Wang et al. (2004), in a work not exclusively focussed in rainwater, applied the methodology used for the isolation of aquatic humic substances, which was based on the fractionation of the dissolved organic carbon (DOC) of the water samples into hydrophobic and hydrophilic fractions using Amberlite XAD-8 resin.

Kieber et al. (2006) extracted chromophoric dissolved organic matter (CDOM) from rainwater using C-18 cartridges by a method previously described for the isolation of marine DOM (Amador et al., 1990). Then, Miller et al. (2009), carried out solid phase extraction of CDOM from rainwater by C-18 cartridges, stating that they were employing the extraction technique previously described by Kieber et al. (2006). Both works highlighted that C-18 was chosen because earlier studies had found that, relatively to XAD, C-18 was able to better retain the UV-visible and fluorescence characteristics of isolated chromophoric organic material, which was supported by referring the work by Amador et al. (1990). However, Amador et al. (1990) is a work on extraction of humic substances (HSs) from seawater and the elution procedure was different from the one used by Kieber et al (2006). Furthermore, the International Humic Substance Society (IHSS) (http://www.ihss.gatech.edu) operationally defined dissolved HSs on the base of adsorption on XAD-8 (Thurman and Malcolm, 1981). Also, seawater and rainwater are very different matrixes. Thus, rigorously, conclusions on HSs from seawater by Amador et al. (1990) should not be taken as valid for CDOM from rainwater.

Finally, the procedure used for the isolation and extraction of DOM from rainwater by Santos et al. (2009) was adapted from the one used by Duarte and Duarte (2005) for isolating WSOM from atmospheric aerosols. Santos et al. (2009) highlighted that XAD-8 was able to isolate the most hydrophobic macromolecular rainwater organic solutes.

The present work aims at comparing DAX-8, the available replacement for XAD-8 (Peuravuori et al, 2001; Filella, 2009), and C-18 procedures for the isolation of rainwater DOM. For this first comparison, UV-visible and molecular fluorescence spectroscopies were used because they can be applied to rainwater samples with low DOC concentrations, without pre-concentration, allowing to follow the DOM isolation process. Moreover, the techniques are rapid and non-destructive, and the molecular fluorescence spectroscopy is a very sensitive

technique which detects subtle differences in properties and distribution of fluorophores. Thus, spectra were determined for rainwater and the effluents and eluates from each of the applied isolation procedures. Finally, since research on rainwater DOM is still progressing, this work will be a major contribution for choosing the adequate method of DOM extraction from rainwater.

4.2 Experimental

4.2.1 Rainwater sampling and sample preparation

Rainwater was collected at a sampling station (40º38' N, 8º39' W) located in the western part of the town of Aveiro, Portugal: one sample was collected in June of 2009 (J09) and two samples were collected in October of 2009 (O09a and O09b). Collection was carried out 70 cm above the ground, through glass funnels (30 cm diameter) into glass bottles (5 L). Sampling containers were left out open in order to collect both wet and dry depositions on a 24 h basis. Prior to use, all glass materials were immersed for 30 min, in a solution of NaOH (0.1 M), then rinsed with distilled water, followed by another immersion for 24 hours in a solution of HNO_3 (4 M), and finally rinsed with ultrapure (Milli-Q) water. After collection, samples were transported to the laboratory where they were filtered through hydrophilic PVDF Millipore membrane filters (0.45 μm). In all cases, rainwater was dark stored in glass vials at 4ºC for a maximum of four days, which was verified not to alter the optical properties of samples.

4.2.2 Fulvic acids solution preparation

For further comparison of the DOM isolation procedures considered in this work, in what concerns their capacity to isolate the humic fraction from rainwater or from other aqueous samples, both procedures were also applied to a known and previously characterized sample of fulvic acids. Fulvic acids (FA) extracted (Santos and Duarte, 1998) from river Vouga at Carvoeiro, Aveiro, Portugal, were

used for this purpose. That sample of fulvic acids has been isolated using the XAD-8 procedure recommended by the IHSS. It is worth to notice that the DAX-8 isolation procedure used in the present work uses a different elution procedure, with methanol/water instead of NaOH 0,1 M. Solutions of 2 ppm of these FA were prepared in ultrapure water and three replicate extractions of DOM were carried out as described below, exactly in the same way as for rainwater.

4.2.3 Extraction of dissolved organic matter (DOM)

Rainwater samples (500 mL) and FA solutions (500 mL) were subjected to two different procedures for the isolation and extraction of DOM: one based on the use of Supelite^{TM} DAX-8 resin (considered the substitute of XAD-8 since the production of the latter stopped (Peuravuori et al, 2001)), and another one based on the use of C-18 sorbent (Supelclean envi-18 cartridges, Supelco, 500 mg mass, volume size 6 mL).

The SupeliteTM DAX-8 resin is comprised of a poly(methyl methacrylate) resin (pore size = 225 Å; surface area = 160 m^2/g), which is slightly polar, while C-18 sorbent is constituted by alkyl chains of C-18 covalently bonded to a silica substrate (pore size = 60 Å; surface area = 475 m^2/g) being non polar (highly hydrophobic). DAX-8 and C-18 isolation procedures separate DOM into polar and non polar fractions taking into account the molecular size of the solutes and interactions between them and the sorbents.

The isolation procedure based on DAX-8 was adapted from the one described by Santos et al. (2009a) for the extraction of DOM from rainwater. Figure 4.1a) represents the schematic diagram of the experimental procedure adopted in the present work. A glass column containing DAX-8 resin (15 mL - bed volume) was prepared for adsorption of DOM. The resin was thoroughly cleaned by Soxhlet extraction as described elsewhere (Malcolm, R.L., 1989). Former to usage, the resin column was rinsed, first with ultrapure water (≈ 100 bed volumes), then with 60 mL of a methanol solution (40%) and with ultrapure water (≈ 50 bed volumes), after that with 0.1 M NaOH (1 bed volume), followed by 0.1 M HCl (1 column volume) and finally with 0.01 M HCl (1 bed volume). Rainwater and FA

solutions were acidified to pH = 2.2 ± 0.2, with a solution of HCl 6M, before being pumped to the DAX-8 column at a flow rate of ≈1.3 mL/min for DOM concentration. After pumping 500 mL of sample, the inorganic matter retained in the DAX-8 column void volume was down washed with ultrapure water (1 bed volume) pumped at ≈1.3 mL/min. The OM adsorbed in DAX-8 was then back eluted with 60 mL of a methanol solution (40%) at a flow rate of ≈0.4 mL/min (1/3 of the rate of fixation). Eluate was evaporated almost to dryness (volume ≤ 1 mL) in a rotary evaporator at 30 ºC, and then transferred to a volumetric flask (20 mL). Ultrapure water was then used to make up the flask volume.

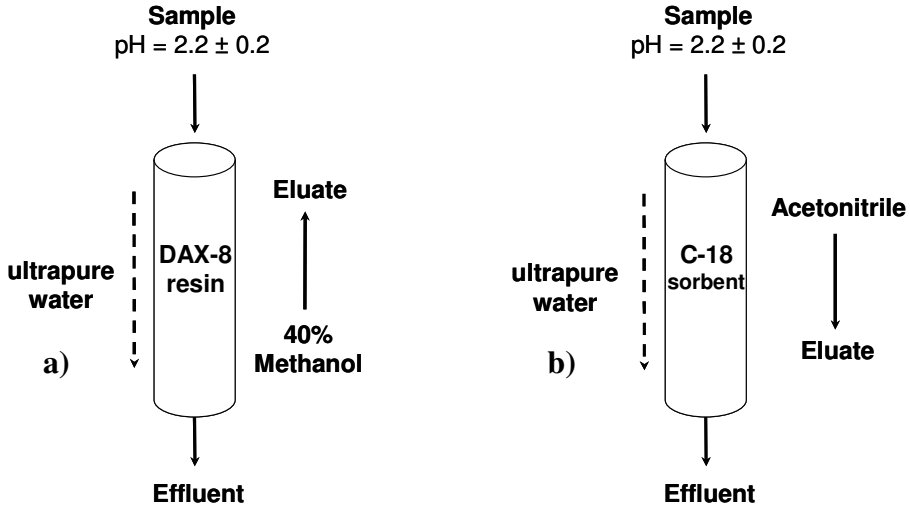

Figure 4.1 Schematic diagram of the experimental procedures adopted for DOM isolation.

The isolation procedure based on C-18 was adapted from the one described by Kieber et al. (2006) for the extraction of DOM from rainwater. Figure 4.1b) represents the schematic diagram of the experimental procedure adopted in the present work. As indicated by the manufacturer, C-18 cartridges were preconditioned by washing with methanol (6 mL) followed by ultrapure water (6 mL) and dried under N_2; cartridges were then washed with acetonitrile (2 x 5 mL) and by ultrapure water (2 x 5 mL). Then, 500 mL of acidified (pH = 2.2 ± 0.2) rainwater or FA solutions were pumped at a flow rate of 15-20 mL/min for DOM concentration. After the adsorption stage, the cartridge was washed with ultrapure water (2 x 5 mL) to remove salts and then dried under N_2. DOM was then eluted

with acetonitrile (2 x 3 mL) into volumetric glass flasks (20 mL) and dried under N_2. Ultrapure water was then used to make up the flask volume.

For optical analysis, aliquots of rainwater, FA solutions and the corresponding DAX-8 and C-18 eluates and effluents were acidified to pH = 3.0 ± 0.2, with solutions of HCl 6M or HCl 1M or NaOH 1M depending of the pH of the fraction.

For DAX-8 and C-18 extraction procedures, blanks (ultrapure water) were carried out and analysed in the same way than rainwater and FA solutions in order to be possible to subtract an averaged blank from each sample or solution spectrum.

Both the above procedures include few steps of sample handling, which constitutes an advantage for preventing possible modifications of samples chemical composition. However, with respect to operation time, the C-18 based procedure is less time-consuming than the DAX-8 one.

4.2.3 Optical analysis

UV–visible spectra (in the range of 200–600 nm) of rainwater samples, FA solutions and the corresponding effluents and eluates from DAX-8 and C-18 were recorded on a Shimadzu (Dusseldorf, Germany) Model UV 210PC spectrophotometer. Quartz cells of different path lengths were used depending on the observed absorbance: 5 cm (for the rainwater samples, FA solutions, effluents and rainwater eluates) and 1 cm (for the FA eluates). Ultrapure water was used as reference and to obtain the baseline.

The spectral slope coefficients (S) were inferred from the obtained UV–visible spectra. For comparison with S values published for rainwater DOM (Kieber et al., 2006; Santos et al., 2009), S values (μm^{-1}) were calculated from non-linear least-square regressions of the absorption coefficients (a_λ) vs. wavelength for the range between 240 and 400 nm using the equation of Markager and Vincent (2000): $a_\lambda = a_{\lambda 0} e^{S(\lambda 0 - \lambda)} + K$, where λ is the reference wavelength (300 nm) and K is a background parameter to improve the goodness of fit. Absorption coefficients (a_λ, m^{-1}) at each wavelength (λ) were calculated as $a_\lambda = 2.303\ A_\lambda / l$, where A_λ is

the corrected spectrophotometer absorbance reading at wavelength λ and l (m) is the optical pathlength. The maximum wavelength for spectral slope calculations was 400 nm because it was the highest wavelength where absorbance values were consistently above the detection limit.

The molecular fluorescence spectra corresponding to rainwater and FA fractions were obtained by a Fluoromax 3 (JobinYvon-Spex Instruments S.A., Inc, now HORIBA Jobin Yvon Inc, Edison, NJ, USA) spectrophotometer with a xenon lamp source. Fluorescence analyses were carried out under thermostated 20ºC, using a water bath connected to the fluorometer, which most approximates the room temperature in the laboratory. Spectra were recorded using 5 nm bandpasses on both the excitation and emission monochromators and 1 cm cells. Synchronous spectra ($\Delta\lambda$ = 70 nm) were acquired using λ_{ex} from 240 to 400 nm (5 nm intervals). Scans were corrected for instrument configuration using factory supplied correction factors (Coble et al, 1993). Data were normalized to a daily-determined water Raman intensity ($275_{ex}/303_{em}$, 5 nm bandpasses) and converted to Raman normalized quinine sulphate (QS) equivalents in ppb (Coble et al., 1998). In all cases, replicate scans within 5% agreement in terms of intensity and within bandpass resolution in terms of band location were obtained.

The corresponding averaged blank spectra were subtracted from samples/solutions spectra.

4.3 Results and discussion

Figure 4.2 shows the UV–visible spectra obtained for the FA solutions (average spectrum) and for the rainwater samples J09, O09a and O09b, for the blank (average spectrum), together with the spectra corresponding to their DAX-8 and C-18 effluents and eluates.

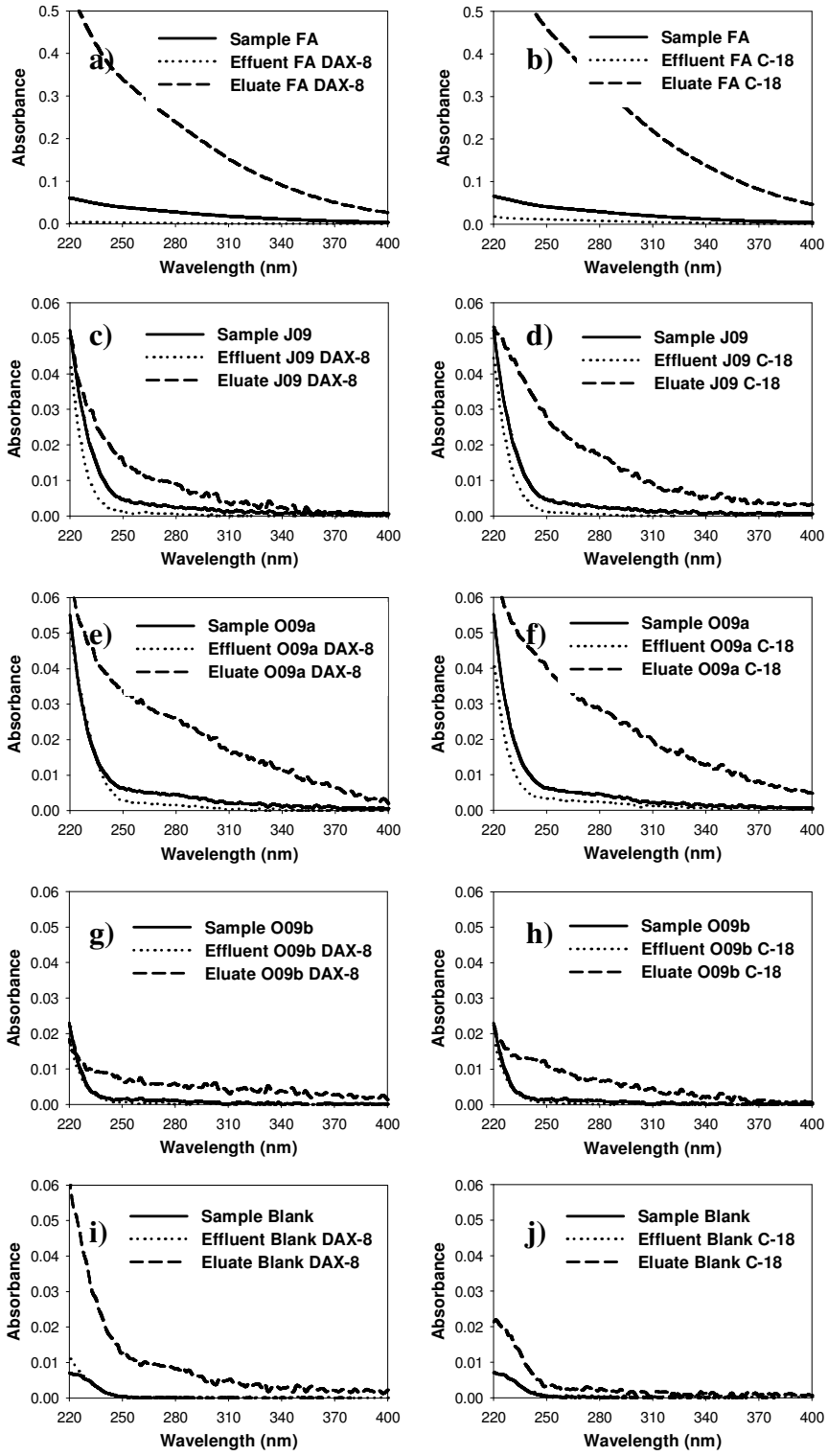

Figure 4.2 UV-Visible spectra, with blank subtraction, obtained for the different fractions of FA solution (averages spectrum; a) and b)) and rainwater (J09, c) and d); O09a, e) and f); O09b, g) and h)), by each of the isolation procedures considered. The blanks of the procedures (averages spectrum) are presented in the graphs i) and j).

The absorbance values were normalized for a 1 cm pathlength. In all the spectra, the absorbance decreased with increasing wavelength, following a trend similar to that already described for rainwater samples (Kieber et al., 2006, Santos et al, 2009). The UV-visible spectra show that the isolation procedure based on C-18 is able to recover more DOM, either from FA solutions or rainwater, than the one based on DAX-8.

The values of spectral slope coefficients (S) determined for the different FA and rainwater samples and fractions, obtained by the DAX-8 and C-18 isolation procedures here used, are shown in Table 4.1.

Table 4.1 Spectral slope coefficients (μm^{-1}) calculated for the different fractions of FA solution and rainwater, obtained by the DAX-8 and C-18 isolation procedures.

Matrixes	Phase Solid	Sample name	Fractions					
			Sample	Sample average	Effluent	Effluent average	Eluate	Eluate average
FA solution	DAX-8 resin	FA1	13.5	13.5 (± 0.1)	16.0	15.4 (± 0.8)	13.9	13.8 (± 0.1)
		FA2	13.4		14.5		13.7	
		FA3	13.6		15.8		13.8	
	C-18 sorbent	FA1	12.9	13.1 (± 0.4)	17.4	15.5 (± 1.9)	12.6	12.8 (± 0.2)
		FA2	12.9		13.5		12.8	
		FA3	13.6		15.6		13.0	
Rainwater	DAX-8 resin	J09	19.2	---	25.3	---	22.3	---
		O09a	17.7		32.7		11.9	
		O09b	18.5		29.3		10.2	
	C-18 sorbent	J09	19.2	---	34.8	---	18.2	---
		O09a	17.7		19.4		12.1	
		O09b	18.5		26.8		15.1	

Note: Standard deviations are indicated between brackets.

The S has been used as a proxy for molecular weight (MW) in a broad range of samples and it has been found that it is inversely related to the MW of the CDOM (Helms et al., 2008). For rainwater samples, the S values are higher than for the river FA sample, which suggests that rainwater DOM had lower molecular weight. With respect to FA solutions, the S values of the eluates are very close to those obtained for the FA solutions, suggesting that the eluates are representative of the FA sample for both isolation procedures. In the case of rainwater eluates, with the unique exception of DAX-8 eluate of sample J09, S values are lower than those obtained for rainwater samples, which indicates that the higher molecular weight OM is preferentially extracted, either by DAX-8 or C-18. This is in agreement with the fact that the S values of the effluents are always higher than the S values of the samples suggesting that the effluents must be represented by compounds with lower molecular weight than those retained in DAX-8 and C-18 sorbents during the concentration stage.

The molecular fluorescence synchronous spectra ($\Delta\lambda$ = 70 nm) obtained for the FA solutions (average spectrum) and J09, O09a and O09b, for the blank (average spectrum), together with the spectra of their DAX-8 and C-18 eluates, are shown in Figure 4.3. The $\Delta\lambda$ = 70 nm for the synchronous spectra was chosen in order to highlight the protein-like and the humic-like fluorescence (Santos et al., 2009b). Fluorescence emission-excitation matrix (EEM) have been used to characterize DOM in rainwater (Kieber et al., 2006; Muller et al., 2008; Santos et al., 2009a,b) and may exhibit the presence of seven fluorescent bands, as described in Table 4.2. These fluorescence bands that may be present in rainwater have been found in most EEMs of aquatic samples, even though the limits for the ranges of their λ_{exc} and λ_{em} maxima can be slightly different from those presented in Table 4.2 for rainwater samples (Coble, 1996; Burdige et al., 2004). Bands A and C have been usually assigned to humic-like compounds, while the band M has been usually assigned to marine humic-like compounds. Bands at the same λ_{ex}/ λ_{em} than B_1, B_2 and T_1, T_2 are attributed to protein-like compounds, such as tyrosine (B_1, B_2) and tryptophan (T_1, T_2). Burdige et al. (2004) used the nomenclature S and R for designating the bands B_1 and T_1, and B and T for designating B_2 and T_2.

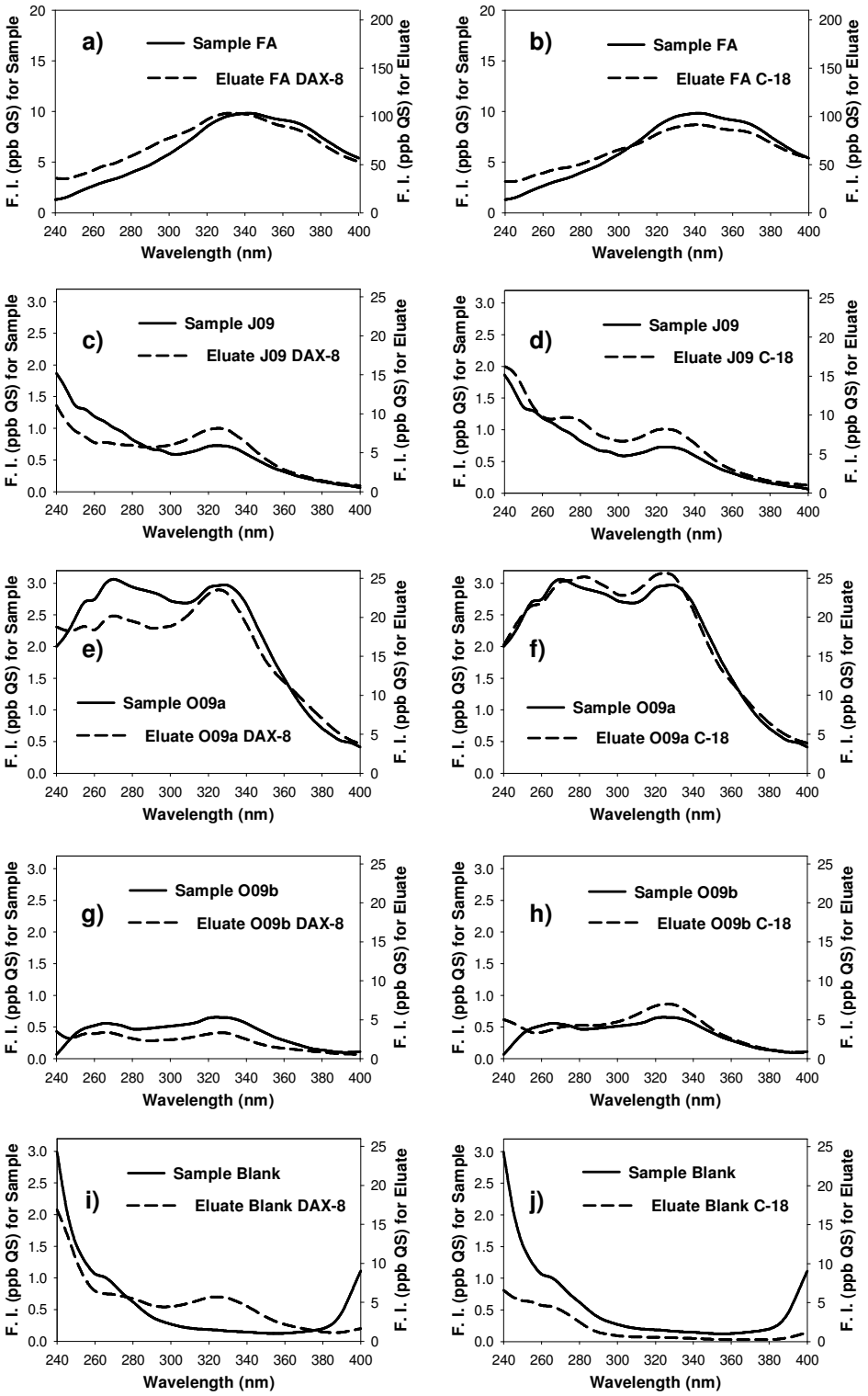

Figure 4.3 Synchronous spectra of fluorescence, with blank subtraction, obtained for the different fractions of FA solutions (averages spectrum; a) and b)), rainwater (J09, c) and d); O09a, e) and f); O09b, g) and h)), by each of the isolation procedures considered. The blanks of the procedures (averages spectrum) are presented in the graphs i) and j).

Table 4.2 Band, excitation/emission wavelength maxima range and attribution of fluorescent DOM in rainwater based in previous works (Kieber et al., 2006; Muller et al., 2008; Santos et al., 2009a,b).

Band	λ_{ex} max (nm)	λ_{em} max (nm)	Attribution
A [a,c]	220-260	380-460	Humic-like
M [a,c]	280-310	370-420	Marine humic-like
C [a,c]	320-360	390-475	Humic-like
T_1 [c]	220-230	335-360	Tryptophan-like, protein-like
T_2 [a,b,c]	260-295	330-370	Tryptophan-like, protein-like
B_1 [c]	220-230	295-310	Tyrosine-like, protein-like
B_2 [b]	265-285	295-315	Tyrosine-like, protein-like

[a] Kieber et al. (2006)
[b] Muller et al. (2008)
[c] Santos et al. (2009a,b)

Fluorescence spectra obtained for FA (Figures 4.3 a) and b)) contain three bands: one protein-like band, T_2 (λ_{ex} ≈ 270 nm); and two overlapped humic-like bands at λ_{ex} = 340-370 nm, M (λ_{ex} ≈ 340 nm) and C (λ_{ex} ≈ 370 nm). Regarding fluorescence spectra obtained for rainwater (Figures 3c) to 3h)), they contain two protein-like bands B_1 (λ_{ex} ≈ 240 nm) and T_2 (λ_{ex} ≈ 270 nm); and one humic-like band, M (λ_{ex} ≈ 325 nm). The lower excitation wavelength of the marine humic-like band (M) in rainwater than in FA solutions suggest that rainwater samples contain a lower amount of conjugated aromatic π-bond systems with electron-withdrawing functional groups (Chen et al, 2002).

Synchronous spectra in Figures 4.3a) and 4.3b) show that both isolation procedures allow a similar recovery of protein-like and humic-like compounds from FA solutions, since the fluorescence intensities of the eluates are similar for both isolation procedures. In the case of rainwater, as it may be seen in Figures 4.3c) to 4.3h), the C-18 based procedure allows a more efficient recovery of protein-like compounds than DAX-8 based procedure, while the humic-like compounds were similarly extracted by both procedures, except for O09b (Figures 4.3g) and 4.3h)). The lower efficiency of recovery of the humic-like compounds by the DAX-8 based procedure observed for O09b, may be due to the influence of

subtraction of blanks whose intensity are higher for DAX-8 than for C-18, affecting more significantly the samples like this one with less DOM.

Table 4.3 shows the percentages of retention of DOM from FA solutions and rainwater samples obtained by the DAX-8 and C-18 isolation procedures, expressed as percentages of UV absorbance at 250 nm (UV_{250nm}) and of fluorescence intensities (FI) at 270 and 325 or 340 nm ($FI_{270\ nm}$ and $FI_{325\ nm}$ or $FI_{340\ nm}$, respectively) of the original samples. UV_{250nm} was chosen because it may be used as a way of assessing OM content (Duarte and Duarte, 2005). On other hand, $FI_{270\ nm}$ corresponds to the maximum of protein-like fluorescence and $FI_{325\ nm}$ or $FI_{340\ nm}$, to the maximum of humic-like band (M) for rainwater or FA, respectively, as observed in Figure 4.3. The recoveries after elution, also shown in Table 4.3, and expressed in terms of UV absorbance or of FI were calculated using the equation:

$$\%\,\mathrm{Recovery} = \frac{(UV\ or\ FI)_{el}\ x\ V_{el}}{(UV\ or\ FI)_{in}\ x\ V_{in}}\ x\ 100$$

where UV or FI are the UV absorbance at 250 nm or the fluorescence intensities at 270 and 325 or 340 nm, respectively. V_{in} is the initial volume of sample that passes through the DAX-8 and the C-18 columns, while V_{el} is the eluate volume. The percentages of retention and recovery of DOM from FA solutions and rainwater samples obtained by the DAX-8 and C-18 isolation procedures were compared recurring to the one sided students t-tests, with the significance level of 5 %: t-test for means in the case of FA solutions and paired t-test for rainwater samples.

Results in Table 4.3 show that, in the case of FA, DAX-8 retained more DOM than C-18, as evaluated by UV_{250nm} ($p = 0.002$) and by both protein-like ($p = 0.006$) and humic-like ($p < 0.001$) fluorescence. However, the recovery percentages depend not only on the retention capacity but also on the elution efficiency. As can be seen in Table 4.3, the recoveries of DOM from FA solutions, expressed as UV_{250nm}, are higher ($p = 0.001$) by the C-18 based isolation procedure than by the DAX-8 one. However, when expressed as FI (FI_{270nm} or

Table 4.3 Percentages of DOM retention and recovery obtained from the DAX-8 and C-18 isolation procedures.

Matrixes	Fractions	Sample name	%							
			UV_{250nm}	UV_{250nm} average	FI_{270nm}	FI_{270nm} average	FI_{325nm}	FI_{325nm} average	FI_{340nm}	FI_{340nm} average
FA solution	Retained in DAX-8 resin	FA1	93.9	93.3 (± 0.6)	89.8	90.5 (± 1.4)	---	---	87.4	87.6 (± 0.8)
		FA2	92.8		89.5		---		86.9	
		FA3	93.3		92.1		---		88.5	
	Retained in C-18 sorbent	FA1	60.8	68.5 (± 7.1)	72.6	67.6 (± 9.1)	---	---	55.4	58.2 (± 3.8)
		FA2	74.7		73.1		---		62.5	
		FA3	70.1		57.0		---		56.6	
	Recovery from DAX-8 resin	FA1	37.6	36.9 (± 0.7)	54.1	58.1 (± 4.6)	---	---	44.4	44.1 (± 3.2)
		FA2	36.3		57.1		---		40.7	
		FA3	36.8		63.1		---		47.1	
	Recovery from C-18 sorbent	FA1	44.3	47.2 (± 2.6)	52.0	59.0 (± 7.1)	---	---	35.4	39.2 (± 3.2)
		FA2	49.2		66.3		---		40.8	
		FA3	48.2		58.8		---		41.3	
Rainwater	Retained in DAX-8 resin	J09	78.7	---	76.4	---	69.8	---	---	---
		O09a	53.3		57.6		56.7		---	
		O09b	73.1		60.9		68.5		---	
	Retained in C-18 sorbent	J09	72.6	---	68.2	---	77.0	---	---	---
		O09a	47.3		51.9		67.3		---	
		O09b	63.0		52.1		74.9		---	
	Recovery from DAX-8 resin	J09	15.1	---	27.6	---	50.8	---	---	---
		O09a	21.6		26.9		32.4		---	
		O09b	18.9		25.2		21.5		---	
	Recovery from C-18 sorbent	J09	27.4	---	46.3	---	49.2	---	---	---
		O09a	25.9		33.4		35.0		---	
		O09b	31.5		35.5		43.6		---	

Note: Standard deviations are indicated between brackets.

FI_{340nm}), similar recoveries were obtained by both the isolation procedures used ($p = 0.429$ for FI_{270nm} and $p = 0.069$ for FI_{340nm}). These results suggest that fluorescent bands do not represent all the OM that absorbs.

Regarding rainwater, for each of the samples, and according with $UV_{250\ nm}$ values, DAX-8 retained more DOM than C-18 ($p = 0.016$), which is in agreement with results obtained for FA. However, according with FI_{270nm} and FI_{325nm}, DAX-8 retained more protein-like ($p = 0.008$) but less humic-like ($p = 0.012$) fluorescence than C-18 for each of the separate samples, which evidence a different nature of rainwater humic matter relatively to the river FA, also suggested above by the lower MW of OM attributed by the spectral slope and the lower fluorescence excitation wavelength of marine humic-like compounds for rainwater (M). Anyway, the percentages of DOM recovery from rainwater, either expressed by UV_{250nm} or FI, were higher for the C-18 based isolation procedure than for the DAX-8 one, except for the humic-like band of the sample J09. Differences between both procedures recoveries showed to be significant for the UV_{250nm} ($p = 0.035$) and the protein-like band (FI_{270nm}; $p = 0.041$) and not significant for the humic-like band (FI_{325nm}; $p = 0.201$). It must be pointed out that rainwater samples, as well as their DOM content, are different and the % results differ among them. On other hand, it must be noticed that the blanks from DAX-8 are higher than those from C18 and special concern must be taken with DAX-8 isolation procedure for obtaining low blanks that may affect more the samples with lower DOM content.

Comparing the isolation procedures used in this work, results in Table 4.3 emphasize what has been already seen in Figures 4.2 and 4.3: the C-18 isolation procedure allows for a higher concentration of a DOM that is more representative of the global rainwater matrix, recovering a higher percentage of protein-like compounds and a similar percentage of humic-like compounds than the DAX-8 isolation procedure, which preferentially separates humic-like compounds. The possible reasons behind the preferential concentration of protein-like compounds by the C-18 procedure and the similar concentration of humic-like compounds by DAX-8 and C-18 procedures may be associated with the interactions between the compounds and the sorbents, being stronger between the protein-like compounds and the DAX-8 sorbent, as evidenced by the higher retention and lower recovery

(elution) of this fraction. The results emphasize that the humic-like and protein-like compounds may have different chemical properties such as the molecular size or functional groups conducting to the different results obtained on the isolation of the compounds.

4.4 Conclusions

In the present work, rainwater DOM isolated by two different procedures, the DAX-8 and the C-18 ones, was compared using UV-visible and molecular fluorescence spectroscopies, evidencing that:

1) With respect to molecular weight (inferred by S), both isolation procedures extracted preferentially the larger molecular weight DOM.
2) The C-18 based isolation procedure applied allowed for the isolation of a higher percentage of DOM from rainwater than the DAX-8 based one. Also, a higher percentage of protein-like compounds were extracted by the C-18 procedure compared with the DAX-8 one, while the percentages of humic-like compounds extracted by both procedures were in the same range.
3) Furthermore, protein-like and humic-like compounds were equally extracted from rainwater by the C-18 based isolation procedure, which thus allows to concentrate DOM that is more representative of the global matrix. On the contrary, the DAX-8 procedure extracts the humic-like compounds preferentially than the protein-like ones.

UV-visible and molecular fluorescence have been very useful to highlight that caution must be taken when comparing DOM fractions isolated from rainwater by the DAX-8 or by the C-18 procedures. However, further work, using other analytic techniques, such as high-resolution mass spectrometry, or nuclear magnetic resonance spectroscopy, should be carried out to further compare DAX-8 and C-18 solid phase extraction of rainwater DOM.

References

Amador, J.A., Milne, P.J., Moore, C.A., Zika, R.G., 1990. Extraction of chromophoric humic substances from seawater. Mar. Chem. 29, 1–17.

Benner, R., von Bodungen, B., Farrington, J., Hedges, J., Lee, C., Mantoura, F., Suzuki, Y, Williams, P.M., 1993. Measurement of dissolved organic carbon and nitrogen in natural waters: workshop report. Mar. Chem. 41, 5-10.

Burdige, D.J., Kline, S.W. and Chen, W., 2004. Fluorescent dissolved organic matter in marine sediment pore waters. Mar. Chem. 89, 289-311.

Chen, J., Gu, B., LeBoeuf, E.J., Pan, H., Dai, S., 2002. Spectroscopic characterization of the structural and functional properties of natural matter fractions. Chemosphere 48, 59–68.

Coble, P.G., Schultz, C.A., Mopper K., 1993.Fluorescence contouring analysis of DOC Intercalibration Experiment samples: a comparison of techniques. Mar. Chem 41, 173-178.

Coble, P.G., 1996. Characterization of marine and terrestrial DOM in seawater using excitation emission matrix spectroscopy. Mar. Chem. 51, 325-346.

Coble, P.G., Del Castillo, C.E., Avril, B., 1998. Distribution and optical properties of CDOM in the Arabian Sea during the 1995 Southwest Monsoon. Deep-Sea Res. II 45, 2195–2223.

Duarte, R.M.B.O., Duarte, A.C., 2005. Application of non-ionic solid sorbents (XAD resins) for the isolation and fractionation of watersoluble organic compounds from atmospheric aerosols. J. Atmos. Chem. 51, 79–93.

Filella, M., 2009. Freshwaters: which NOM matters?. Environ. Chem. Lett. 7, 21-35.

Graber, E.R., Rudich, Y., 2006. Atmospheric HULIS: How humic-like are they? A comprehensive and critical review. Atmos. Chem. Phys., 6, 729–753.

Helms, J.R., Stubbins, A., Ritchie, J.D., Minor, E.C., Kieber, D.J., Mopper, K., 2008. Absorption spectral slopes and slope ratios as indicators of molecular weight, source, and photobleaching of chromophoric dissolved organic matter. Limnol. Oceanogr. 53, 955–969.

Imai, A., Fukushima, T., Matshihige, K., Kim, Y.H., 2001. Fractionation and characterization of dissolved organic matter in a shallow eutrophic lake, its inflowing rivers, and other organic matter sources. Water Res. 35, 4019-4028.

Kieber, R.J., Whitehead, R.F., Reid, S.N., Willey, J.D., Seaton, P.J., 2006. Chromophoric dissolved organic matter (CDOM) in rainwater, Southeastern North Carolina, USA. J. Atmos. Chem. 54, 21-41.

Leenheer, J.A., 1981. Comprehensive Approach to Preparative Isolation and Fractionation of Dissolved Organic Carbon from Natural Waters and Wastewaters. Environ. Sci. Technol. 15, 578-587.

Malcolm, R.L., 1989. Factors to be considered in the isolation and characterization of aquatic humic substances. In: Allard, B., Boren, H., Grimvall, A. (Eds.), Humic Substances in the Aquatic and Terrestrial Environment: Proceedings of an International Symposium, Linlöping, Sweden, pp. 9–36.

Markager, S., Vincent, W.F., 2000. Spectral light attenuation and the absorption of UV and blue light in natural waters. Limnol. Oceanogr. 45, 642–650.

Maurice, P.A., Pullinb, M.J., Cabanissb, S.E., Zhouc, Q., Namjesnik-Dejanovicc,K., Aiken, G.R., 2002. A comparison of surface water natural organic matter in raw filteredwater samples, XAD, andreverse osmosis isolates. Water Res. 36, 2357–2371.

Miller, C., Gordon, K.G., Kieber, R.J., Willey, J.D., Seaton, P.J., 2009. Chemical characteristics of chromophoric dissolved organic matter in rainwater. Atmos. Environ. 43, 2497-2502.

Mopper, K., Stubbins, A., Ritchie, J.D., Bialk, H.M., Hatcher, P.G., 2007. Advanced instrumental approaches for characterization of marine dissolved organic matter: Extraction techniques, mass spectrometry, and nuclear magnetic resonance spectroscopy. Chem. Rev. 107, 419 – 442.

Peuravuori, J., Ingman, P., Pihlaja, K., Koivikko, R., 2001. Comparisons of sorption of aquatic humic matter by DAX-8 and XAD-8 resins from solid-state 13C NMR spectroscopy's point of view. Talanta 55, 733-742.

Repeta, D.J., Quan, T.M., Aluwihare, L.I., Accardi, A., 2002. Chemical characterization of high molecular weight dissolved organic matter in fresh and marine waters. Geochim Cosmochim. Acta 66, 955–962.

Santos, E.B.H., Duarte, A.C., 1998. The influence of pulp and paper mill effluents on the composition of the humic fraction of aquatic organic matter. Wat. Res. 32, 597-608.

Santos, P.S.M., Otero, M., Duarte, R.M.B.O., Duarte, A.C., 2009a. Spectroscopic characterization of dissolved organic matter isolated from rainwater. Chemosphere 74, 1053-101.

Santos, P.S.M., Duarte, R.M.B.O., Duarte, A.C., 2009b. Absorption and fluorescence properties of rainwater during the cold season at a town in Western Portugal. J. Atmos. Chem. 62, 45-57.

Simjouw, J.-P., Minor, E.C., Mopper, K., 2005. Isolation and characterization of estuarine dissolved organic matter: comparison of ultrafiltration and C18 solid phase extraction techniques. Mar. Chem. 96, 219–235.

Thurman, E.M., Malcolm, R.L., 1981. Preparative isolation of aquatic humic substances. Environ. Sci. Technol. 15, 463-466.

Wang, M.C., Liu, C.P., Sheu, B.H., 2004. Characterization of organic matter in rainfall, throughfall, stemflow, and streamwater from three subtropical forest ecosystems. J. Hydrol. 289, 275–285.

Willey, J.D., Kieber, R.J., Eyman, M.S., Avery, G.B., 2000. Rainwater dissolved organic carbon: concentrations and global flux. Global Biogeochem. Cy. 14, 139-148.

Williams, D.H., Fleming, I.: Spectroscopic methods in organic chemistry, 2nd edn. McGraw-Hill, London, UK (1973).

5. Seasonal and air mass trajectory effects on rainwater dissolved organic matter at a coastal town on the southwest of Europe

Rainwater contains a complex mixture of organic compounds which may influence the climate, the terrestrial and maritime ecosystems and thus the human health. In this work, the characteristics of rainwater at a coastal town on the southwest of Europe were assessed by UV-visible and three-dimensional excitation-emission matrix (EEM) fluorescence spectroscopies and by dissolved organic carbon (DOC) content. The seasonal and air mass trajectory effects on rainwater dissolved organic matter (DOM) were evaluated. The UV-Visible spectra of the rainwater samples were very similar to those obtained for other natural humic substances, decreasing monotonically with increasing wavelength. All rainwater samples showed humic-like and protein-like fluorescent bands. There was a strong positive correlation between UV_{250nm} and integrated fluorescence suggesting that these optical properties are directly interconnected and that most chromophoric dissolved organic matter (CDOM) is likely to fluoresce. Moreover, CDOM was an important contributor of DOC in rainwater, and there was more CDOM present in summer and autumn seasons than in winter and spring. Rainwater associated to terrestrial air masses contained a higher CDOM content than rainwater related to marine air masses, thus highlighting the contribution of terrestrial/anthropogenic sources. The similarity between rainwater and other natural waters observed either by absorbance spectra or by EEM fluorescence spectra, highlight that compounds that make part of rainwater CDOM may be derived from surface sources and/or from processes that originate or modify the organic compounds in the atmosphere.

5.1 Introduction

Dissolved organic carbon (DOC) is a ubiquitous component of rainwater, and is a major component of both marine (23 μM) and continental rain (161 μM) (Willey et al., 2000). Furthermore, rainwater is a globally important removal mechanism for atmospheric DOC, with a carbon flux (0.3 Gt yr^{-1}) equal to approximately 6% of the fossil fuel influx (5.5 Gt yr^{-1}) to the atmosphere (Willey et al., 2000). On other hand, dissolved organic matter (DOM) in rainwater is a complex mixture of organic compounds (Seitzinger et al., 2003).

Recent studies (Kieber et al., 2006; Muller et al., 2008; Miller et al., 2009; Santos et al., 2009a,b) have demonstrated that chromophoric dissolved organic matter (CDOM) is an important constituent of rainwater. CDOM is also an important fraction of the water-soluble organic matter (WSOM) in atmospheric particles (Facchini et al., 1999; Zappoli et al., 1999; Decesari et al., 2000; Duarte et al., 2005) exhibiting intense absorbance in the lower visible to UV range and, therefore, they might also be important in atmospheric absorption of solar radiation (Hoffer et al. 2004). These organic constituents were found to be important contributors to cloud condensation nuclei (CCN) (Facchini et al., 1999; Gysel et al., 2004) and droplet clouds are effective reflectors of incoming solar radiation, and small perturbations in their properties can significantly impact the amount of solar radiation absorbed by the planet, and thus affect climate (Andreae et al., 2005). In view of the potentially important role played by WSOM in the environmental impact of atmospheric particles, one can anticipate that DOM in rainwater may perform similar functions. Moreover, DOM in rainwater is also important since rain is the predominant source of all the fresh water and may affect both the terrestrial and aquatic ecosystems.

DOM in rainwater is still poorly characterized with respect to the chemical compounds present, their sources, temporal and spatial patterns of variation and the subsequent impact on climate and the environment (Muller et al., 2008); and to the best of our knowledge, only four recent studies have addressed the optical properties of CDOM in the original rainwater with the purpose of evaluating some

of the above mentioned points (Kieber et al., 2006; Muller et al., 2008; Santos et al., 2009b; Cheng et al., 2010).

Kieber et al. (2006) determined the DOC content and analysed the UV-visible and excitation-emission matrix (EEM) fluorescence properties of rainwater in Wilmington (North Carolina, USA) to study the CDOM and its variation with air mass back trajectories and seasonality. Muller et al. (2008) also determined the EEM fluorescence properties of rainwater in Birmingham (UK) and analysed its variations with meteorological patterns (storm type, source area and air mass type). Santos et al. (2009b) evaluated the variability of the optical properties of CDOM in rainwater of Aveiro (Portugal), for similar air mass trajectories (maritime), between autumn and winter events, using the DOC content, and the UV-visible and the EEM fluorescence spectroscopies. Cheng et al. (2010) analysed the optical characteristics of CDOM in rain collected in Xiamen Island (China), during the rainy season of 2007, using also the UV-visible and the EEM fluorescence spectroscopies.

Since little is known about the rainwater DOM, its sources, temporal patterns of variation, and the subsequent impact on the climate and the environment, the aim of this work is to characterize the DOM present in rainwater at a coastal town (Aveiro, Portugal) on the southwest of Europe, collected between September 2008 and September 2009. For such purpose, forty rainwater samples were assessed by the UV-visible and EEM fluorescence spectroscopies and by its DOC content. The data set is unique because it was collected for a long period and becomes one of the first detailed studies of rainwater DOM in Western Europe. Furthermore, another research aim was to evaluate how rainwater DOM was affected by seasons, type of air mass type and source area using back-trajectory analysis.

5.2 Experimental

5.2.1 Rainwater sampling and sample preparation

Rainwater was collected at a sampling station (40º38' N, 8º39' W) located in the western part of the town of Aveiro, Portugal, between September 2008 and September 2009. The sample collection was carried out at 70 cm above the ground, through glass funnels (30 cm diameter) into glass bottles (5 L). The sampling containers were left out open in order to collect both wet and dry depositions on a 24 h basis. Prior to use, all glass materials were immersed for 30 min, in a solution of NaOH (0.1 M), then rinsed with distilled water, followed by another immersion for 24 hours in a solution of HNO_3 (4 M), and finally rinsed with ultrapure (Milli-Q) water. After collection, samples were transported to the laboratory where they were filtered through hydrophilic PVDF Millipore membrane filters (0.45 µm). For all the sampling episodes, one aliquot of rainwater was stored in glass vials in the dark at 4ºC for a maximum of four days, for subsequent optical analysis, and another aliquot of rainwater was frozen for subsequent analysis of DOC content. The storage of samples in the dark at 4ºC was proved to be adequate for keeping the optical properties of the samples unchanged in case the storage time does not exceed 4 days (Santos et al., 2010).

5.2.3 Measurements of dissolved organic carbon (DOC)

The concentrations of total carbon (TC) and inorganic carbon (IC) were measured for each rainwater sample by means of a Shimadzu TOC-5000A analyzer. The DOC content of the samples was calculated as the difference TC-IC. For TC quantification, standards were prepared from reagent grade potassium hydrogen phthalate in ultra pure water in the range of 0.5 to 2 mg C L^{-1}. For IC measurements, standards were performed from reagents grade sodium hydrogenocarbonate plus sodium carbonate in ultra pure water, also in the range of 0.5 to 2 mg C L^{-1}. Control standards were generally within 5% agreement in

terms of TC and IC content. For each sample, three replicates were analysed for determining the average DOC content.

5.2.4 Optical analysis

UV–visible spectra (in the range of 200–600 nm) of rainwater samples were recorded on a Shimadzu (Dusseldorf, Germany) Model UV 210PC spectrophotometer using quartz cells of 10 cm path lengths. Ultrapure water was used as reference in order to obtain the baseline.

The spectral slope coefficients (S) were inferred from the obtained UV–visible spectra, and for comparison with S values published for rainwater DOM (Kieber et al., 2006; Santos et al., 2009a), S values (μm^{-1}) were calculated from non-linear least-square regressions of the absorption coefficients (a_λ) *versus* wavelength for the range between 240 and 400 nm using the equation of Markager and Vincent (2000): $a_\lambda = a_{\lambda 0} e^{S(\lambda 0 - \lambda)} + K$, where λ is the reference wavelength (300 nm) and K is a background parameter to improve the goodness of fit. Absorption coefficients (a_λ, m^{-1}) at each wavelength (λ) were calculated as $a_\lambda = 2.303\ A_\lambda / l$, where A_λ is the corrected spectrophotometer absorbance reading at wavelength λ and l (m) is the optical pathlength. The maximum wavelength considered for spectral slope calculations was 400 nm, since this was the highest wavelength whose absorbance values were consistently above the detection limit.

The molecular fluorescence spectra were obtained by a Fluoromax 3 (JobinYvon-Spex Instruments S.A., Inc, now HORIBA Jobin Yvon Inc, Edison, NJ, USA) with a xenon lamp as source of radiation. Fluorescence intensity measurements were carried out under thermostated conditions at 20ºC and spectra were recorded using 1 cm cells, and 5 nm bandpasses on both the excitation and the emission monochromators. Excitation-emission matrix (EEM) fluorescence spectra were obtained by concatenating emission spectra measured every 5 nm from 290 to 510 nm using excitation wavelengths (λ_{ex}) from 240 to 400 nm increasing also at 5 nm intervals. Scans were corrected for instrument configuration using factory supplied correction factors (Coble et al, 1993), and data were normalized to a daily-determined water Raman intensity ($275_{ex}/303_{em}$, 5 nm

bandpasses) and converted to Raman normalized quinine sulphate (QS) equivalents in ppb (Coble et al., 1998). For each sample a daily blank (Milli-Q water) spectrum was subtracted from rainwater spectrum. Replicate scans within 5% agreement in terms of intensity and within bandpass resolution in terms of band location were obtained.

5.2.5 Trajectories of air masses and meteorological data

The general characteristics of air masses during the sampling period were evaluated by using Hybrid Single Particle Lagrangian Integrated Trajectory Model (HYSPLIT) developed by Draxler and Rolph (2003) at the National Oceanic Atmospheric Administration—Air Resources Laboratory (NOAA/ARL) (available at www.arl.noaa.gov/HYSPLIT.php). Trajectories were generated for a 48 h hind-cast starting at 10 and 500 m level, calculated every 6 h for every day when sampling of precipitation occurred.

Rainwater samples were classified into five groups according to the origin and trajectory of the air masses: class A contains samples related to air masses transported from the Atlantic Ocean; class B represents samples with origins in central and northern parts of industrialized Europe and transported to Portugal over the ocean; class C contains samples with similar origins to those of class B, but transported over land; class D refers to air masses transported from north Africa and the Mediterranean across the Iberian Peninsula; samples in which less than 60 % of the air mass trajectories were from one section only, and had therefore a mixed origin, were agglomerated into class M. A similar way of classification had been previously used by Pio et al. (1991) for rainwater also collected at Aveiro (Portugal). Figures 5.1a) and 5.1b) show the air mass trajectory analysis at 10 and 500 m level, respectively, for one of the rainwater samples (RS1) collected for this study in order to exemplify the classification of rainwater according to air mass origins and trajectories.

A meteorological station at the sampling site (at 10 m height) supplied the following information during the sampling period: direction and velocity of wind, relative humidity, air temperature and amount of precipitation.

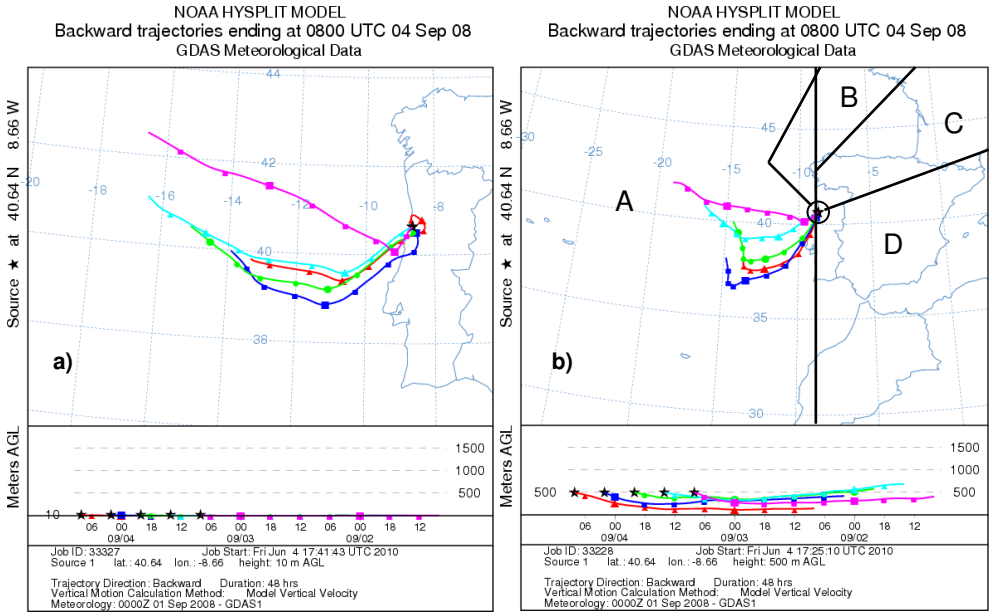

Figure 5.1 The air mass trajectory analysis at 10 m (a) and 500 m (b) level, for the rainwater sample (RS1) collected at 04 September 2008, to exemplify the classification of rainwater according to air-mass origins and trajectories into four groups A, B, C and D.

5.3 Results and discussion

Forty rainwater samples were collected between September 2008 and September 2009. During this sampling period, approximately 423 mm of rainwater were collected, which represents approximately 50% of the total precipitation (839 mm). 81 % of the collected rainwater amount (RA) was related with air masses transported from the Atlantic Ocean (class A) while the rest of precipitation was related to air masses with anthropogenic and terrestrial contributions (3 % of class B; and 16 % of class D). A similar distribution was obtained considering all the rainfall events of the sampling period instead of only those corresponding to the samples collected. Pio et al. (1991) had also observed that around 80 % of the rainfall amount in Aveiro between 1986 and 1989 was associated to air masses with an Atlantic origin. Regarding to the RA by season for the collected samples, 13 % occurred in summer (96 % of class A, 1 % of class B and 3 % of class D), 21 % in autumn (80 % of class A, 13 % of class B and 7 % of class D), 35 % in winter

(66 % of class A and 34 % of class D) and 31 % in spring (91 % of class A and 9 % of class D).

The volume-weighted average (VWA) DOC concentration and volume-weighted standard deviation for the forty rainwater samples was 0.66 ± 0.09 mg L^{-1}. The range of DOC varied from a low limit of 0.15 mg L^{-1} to a high limit of 6.75 mg L^{-1}. The VWA DOC concentration of rainwater samples is in the range of those measured at Aveiro in 2005-2006, 0.93±0.87 mg L^{-1} (Santos et al., 2009b).

The VWA absorbance spectra for all rainwater events are shown in Figure 5.2 along with the VWA spectra for samples of the autumn, winter, spring and summer events (Figure 5.2 a)) and with the VWA spectra for samples of the classes A, B and D (Figure 5.2 b)).

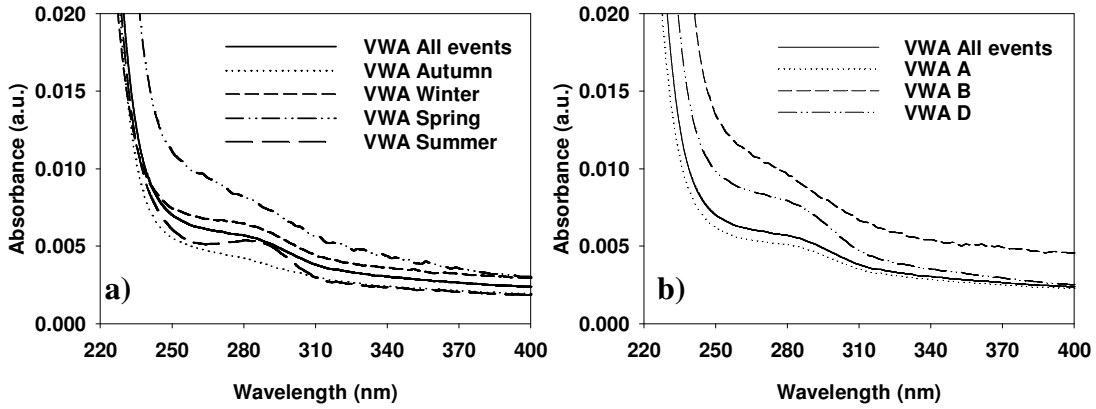

Figure 5.2 Volume-weighted average (VWA) UV-Visible spectra (absorbance units) *versus* wavelength (nm) of rainwater from: Autumn, Winter, Spring, Summer and all events (a); classes of trajectories A, B, D and all events (b).

The UV-Visible spectra of the rainwater samples are very similar to those obtained for other natural humic substances, decreasing monotonically with increasing wavelength (Senesi et al., 1989), as well as similar to the UV-Visible spectra obtained previously for rainwater (Kieber et al., 2006; Santos et al., 2009b). It should be recalled, however, that absorbance at shorter wavelengths (<240 nm) has also a contribution from inorganic species, specifically nitrate, which are likely to be present in rainwater samples (Pio et al., 1991). The VWA

absorbance spectra of the samples exhibit a shoulder in the 250–300 nm (~280 nm) region. In aquatic humic substances, absorbance in this UV region is usually attributed to π-π* electronic transitions in phenolic arenes, aniline derivatives, polyenes and polycyclic aromatic hydrocarbons with two or more rings (Chin et al., 1994; Peuravuori and Pihlaja, 1997).

Figure 5.3 presents the EEM fluorescence spectrum of a rainwater sample, which may be representative of spectra of all collected samples (Annex II). Seven bands at different $\lambda_{excitation}/\lambda_{emission}$ ($\lambda_{ex}/\lambda_{em}$) can be highlighted: three humic-like bands, A ($\lambda_{ex}/\lambda_{em}$ ≈ 240/405 nm), M ($\lambda_{ex}/\lambda_{em}$ ≈ 300/410 nm), and C (≈330/420 nm); and four protein-like bands, B_1 ($\lambda_{ex}/\lambda_{em}$ ≈ 240/305 nm), B_2 ($\lambda_{ex}/\lambda_{em}$ ≈ 270/305 nm), T_1 ($\lambda_{ex}/\lambda_{em}$ ≈ 240/340 nm) and T_2 ($\lambda_{ex}/\lambda_{em}$ ≈ 275/330 nm). These fluorescence bands that have been found in rainwater (Kieber et al., 2006; Muller et al., 2008; Santos et al., 2009a,b) have been also found in most EEMs of aquatic samples, even though the limits for the ranges of their λ_{exc} and λ_{em} maxima can be slightly different from those observed for rainwater samples (Coble, 1996; Burdige et al., 2004). Bands A and C have been generally assigned to humic-like compounds, while the band M has been usually assigned to marine humic-like compounds. Bands at the same $\lambda_{ex}/\lambda_{em}$ than B_1, B_2 and T_1, T_2 are attributed to protein-like compounds, such as tyrosine (B_1, B_2) and tryptophan (T_1, T_2). Burdige et al. (2004) used the nomenclature S and R for designating the bands B_1 and T_1, and B and T for designating B_2 and T_2. The humic-like band C does no show up in all the EEM fluorescence spectra of rainwater from Aveiro, appearing clearly only in some events (Santos et al., 2009b) and varying its emission wavelength maximum much more than observed for other bands, as will be discussed below. The variation of emission wavelength of bands may be due to the degree of condensed aromatic rings and other unsaturated bond systems associated (Chen et al., 2002). However, as shown in Figure 5.3, fluorescent CDOM is a common component in collected rainwater samples.

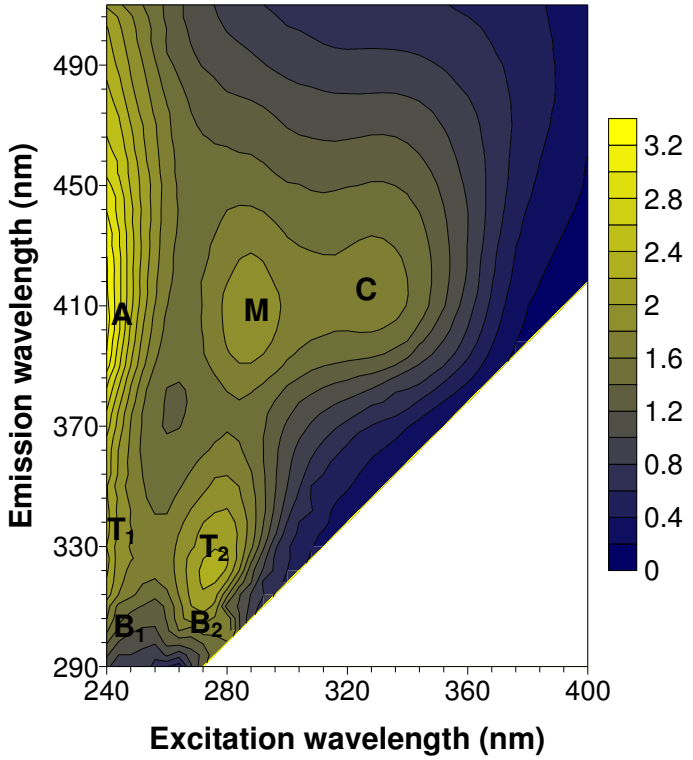

Figure 5.3 Representative EEM fluorescence spectrum of rainwater CDOM. The scale is in ppb QS. The EEM spectrum is from rainwater sample RS39, which was collected in summer and was associated with air-mass trajectories with a maritime origin (class A). The sample had [DOC] = 0.66 mg L^{-1}, UV_{250nm} = 0.009 (a.u.), ε_{280nm} = 18.6 $Lg^{-1}C\ cm^{-1}$, S = 11.5 μm^{-1}, entire scan integrated fluorescence = 33.8 x 10^3, and A:M ratio = 1.7.

Figure 5.4a) shows the absorbance at 250 nm (UV_{250nm}) and the entire scan integrated fluorescence for each rain event as functions of DOC. UV_{250nm} was chosen because it may be used as a way of assessing OM content (Duarte and Duarte, 2005). The entire scan integrated fluorescence was determined integrating the volume of the three-dimensional surface of EEM fluorescence spectrum.

A significant positive correlation between UV_{250nm} ($r = 0.826$, $p < 0.001$) and integrated fluorescence ($r = 0.832$, $p < 0.001$) with DOC concentration was observed, which may suggest that CDOM is an important contributor of DOC in rainwater. On other hand, the entire scan integrated fluorescence for each rain event was also plotted against the UV_{250nm} values as shown in Figure 5.4b), and a strong positive correlation was found between these two parameters ($r = 0.819$, $p < 0.001$) suggesting that these optical properties are directly interconnected and that most of the DOM is capable of fluoresce.

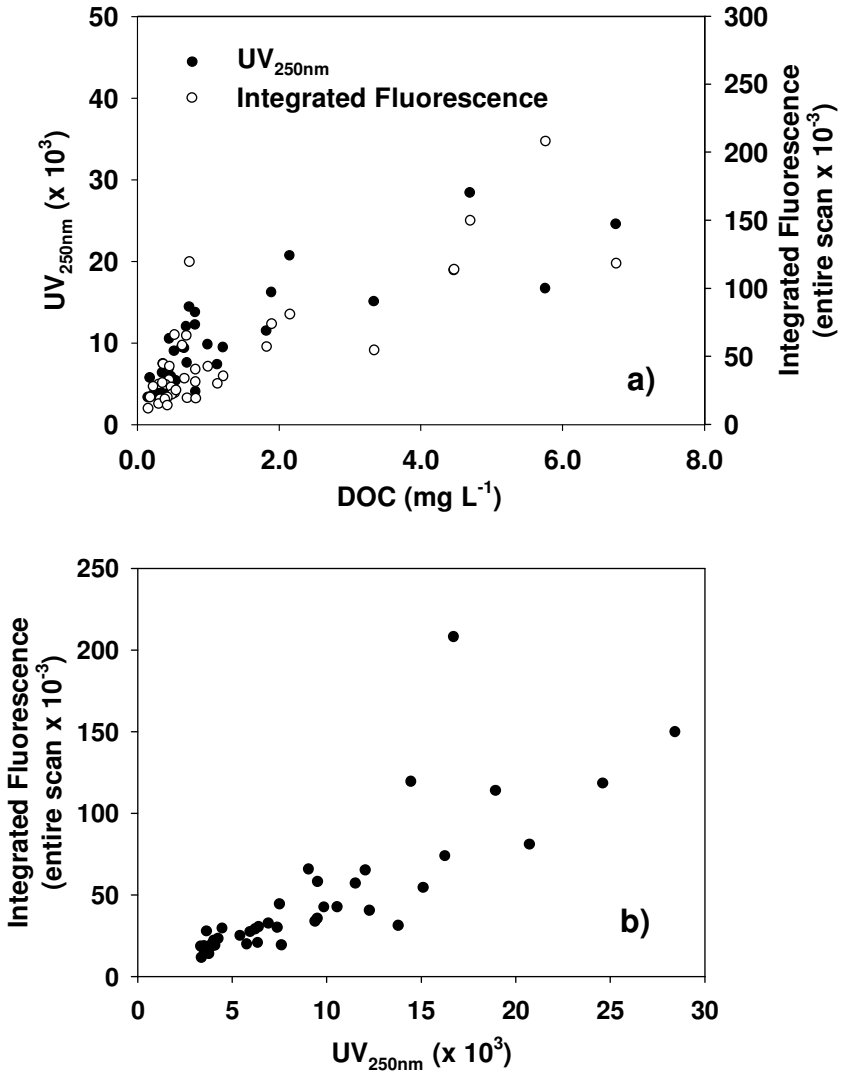

Figure 5.4 The relationships between absorbance at 250nm and DOC (absorbance units; r = 0.826, p < 0.001), and between entire scan integrated EEM fluorescence and DOC (integrated fluorescence units; r = 0.832, p < 0.001). b) The relationship between the entire scan integrated EEM fluorescence (integrated fluorescence units) with the absorbance at 250nm (absorbance units) (r = 0.819, p < 0.001).

Figure 5.5 shows the relationships between the DOC, the UV_{250nm} and the entire scan integrated fluorescence with the rainwater amount. As shown in Figure 5.5, inverse relationships were found between DOC, UV_{250nm} and entire scan integrated fluorescence with the rainwater amount, highlighted by the curves fitting of the first order exponential decay. These findings suggest that most of CDOM

present in rainwater was washed out from the atmosphere during the precipitation events. The sample with highest value of integrated fluorescence and also with the second highest value of DOC (RS1) also showed some differences in fluorescence properties relatively to the other samples, as will be discussed regarding data presented in Table 5.2, and thus, it may be considered an outlier. The data corresponding to sample RS1 is shown in Figure 5.5 as a cross mark and it was not considered for purpose of curve fitting.

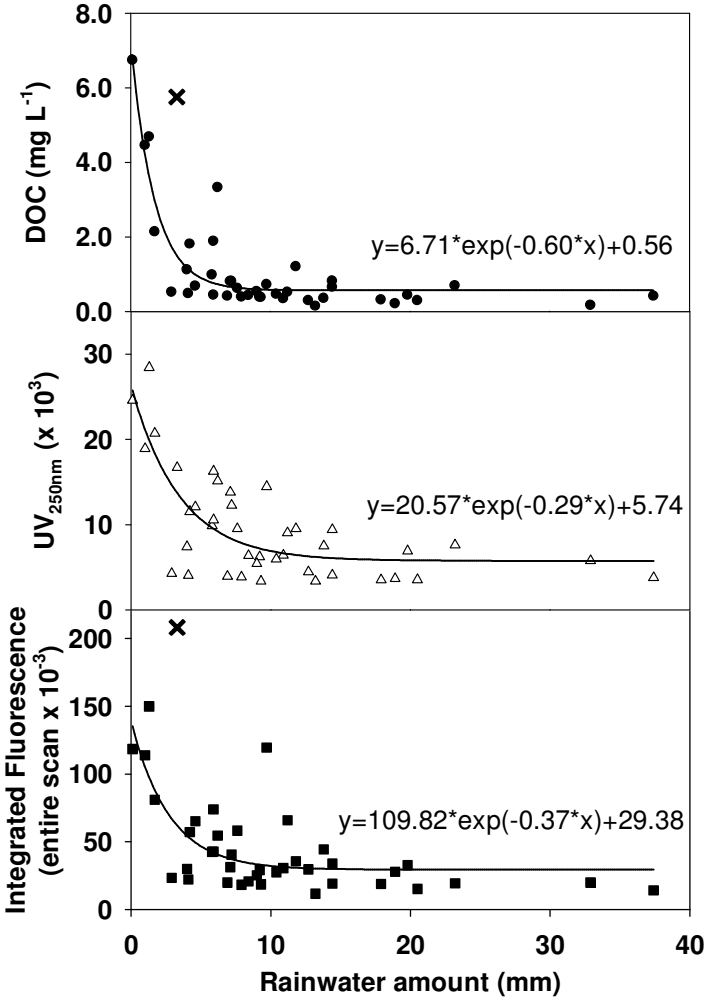

Figure 5.5 The variation of DOC concentration (mg L^{-1}; Adj R^2 = 0.802, $p < 0.001$)), absorbance at 250 nm (absorbance units; Adj R^2 = 0.570, $p < 0.001$) and entire scan integrated EEM fluorescence (integrated fluorescence units; Adj R^2 = 0.493, $p < 0.001$) with rainwater amount (mm).

The VWA of DOC, of UV_{250nm}, of specific absorptivity at 280 nm (ε_{280nm}), of spectral slope coefficient (S), of integrated fluorescence and of A:M ratio for the

total of samples collected, for the samples of the hydrological year 2009, for samples grouped by seasons and for samples grouped by air mass trajectories, are shown in Table 5.1.

Table 5.1 Rainwater VWA DOC concentrations (mg L^{-1}), UV absorbance at 250 nm (UV_{250nm}; absorbance units), specific absorptivity at 280 nm (ε_{280nm}; $Lg^{-1}C\ cm^{-1}$), spectral slope coefficient (S; μm^{-1}), integrated fluorescence for the entire scan (integrated fluorescence units) and A:M ratio for the total of samples collected, for the samples of the hydrological year 2009, for samples grouped by seasons and for samples classified according to their air masses trajectories (class).

Sampling period/ class	DOC (mg L^{-1})	UV_{250nm} x 10^3	ε_{280nm} ($Lg^{-1}C\ cm^{-1}$)	S (μm^{-1})	Integrated fluorescence x 10^{-3}	A:M ratio
Total (n = 40)	0.63 (± 0.07)	6.9 (± 0.7)	12.3 (± 2.5)	9.5 (± 1.0)	32.6 (± 3.4)	2.2 (± 0.3)
2009 (n = 35)	0.50 (± 0.06)	6.4 (± 0.7)	12.7 (± 2.7)	9.6 (± 1.1)	30.5 (± 3.8)	2.2 (± 0.3)
Autumn (n = 11)	0.82 (± 0.20)	9.3 (± 0.9)	12.7 (± 3.0)	9.6 (± 1.5)	40.3 (± 5.4)	2.0 (± 0.3)
Winter (n = 12)	0.38 (± 0.05)	6.7 (± 1.2)	17.2 (± 6.0)	7.6 (± 1.1)	36.1 (± 7.4)	2.6 (± 0.6)
Spring (n = 11)	0.60 (± 0.12)	4.7 (± 1.0)	6.6 (± 2.3)	11.7 (± 2.2)	20.8 (± 3.5)	2.0 (± 0.5)
Summer (n =6)	1.10 (± 0.33)	8.9 (± 3.1)	10.7 (± 5.6)	9.0 (± 3.0)	40.1 (± 11.6)	2.1 (± 1.0)
Class A (n = 30)	0.53 (± 0.07)	6.0 (± 0.7)	12.3 (± 3.0)	9.1 (± 1.1)	27.2 (± 2.8)	2.2 (± 0.3)
Class B (n = 3)	1.49 (± 0.77)	13.2 (± 6.9)	6.6 (± 3.3)	11.2 (± 5.4)	58.8 (± 31.2)	1.6 (± 0.8)
Class D (n = 7)	0.96 (± 0.23)	9.8 (± 1.5)	12.3 (± 3.6)	11.0 (± 2.1)	54.4 (± 12.9)	2.4 (± 0.7)
Autumn/Class A (n = 8)	0.48 (± 0.06)	8.1 (± 1.0)	14.6 (± 3.2)	9.2 (± 2.0)	35.9 (± 6.5)	2.1 (± 0.4)
Winter/Class A (n = 8)	0.31 (± 0.04)	5.6 (± 1.5)	18.2 (± 9.3)	6.5 (± 1.4)	25.6 (± 5.8)	2.6 (± 0.8)
Spring/Class A (n =10)	0.54 (± 0.11)	4.2 (± 1.0)	6.8 (± 2.5)	11.2 (± 2.4)	19.4 (± 3.6)	2.0 (± 0.5)
Summer/Class A (n = 4)	0.99 (± 0.26)	8.3 (± 2.5)	10.8 (± 4.9)	8.9 (± 1.8)	37.1 (± 7.6)	2.2 (± 0.9)
Spring/Summer/Autumn Class D (n = 3)	2.13 (± 0.66)	12.6 (± 3.5)	4.3 (± 2.5)	14.3 (± 8.0)	49.4 (± 10.2)	1.6 (± 0.8)
Winter Class D (n = 4)	0.51 (± 0.09)	8.7 (± 1.6)	15.4 (± 1.8)	9.7 (± 0.7)	56.3 (± 14.7)	2.8 (± 0.5)

n = number of rain events.
The standard deviations are indicated between brackets.

As shown in Table 5.1, the VWA DOC was higher in summer and autumn, than in winter and spring. Santos et al (2009b) also observed in rainwater of Aveiro that the VWA DOC concentration of autumn rainwater samples was higher than that of winter. On other hand, higher VWA of UV_{250nm} and integrated fluorescence were also observed for the summer and autumn seasons (Table 5.1), which suggest that there was more CDOM present in these seasons than in winter and spring. Kieber et al. (2006) also observed that there was more CDOM present in winter rainwater than in summer even though the VWA DOC concentrations are virtually identical for the two seasons. Relatively to the S, which has been used as a proxy for molecular weight (MW) in a broad range of samples, it has been found that it is inversely related to the MW of the CDOM (Helms et al., 2008), while the ε_{280nm} has been positively correlated with DOM MW of aquatic humic substances (Chin et al, 1994). Thus, the results of S and ε_{280nm} presented in Table 5.1 suggest that in winter there was higher MW of DOM than in summer and autumn, and in turn higher than in spring. The lower MW observed in spring, summer and autumn events may result from increased DOM photodegradation due to the higher irradiance during these seasons, comparatively with winter. In the case of spring samples, the photodegradation may have originated low content of chromophoric compounds due to the lower absorbance (UV_{250nm}) and fluorescence (integrated fluorescence) as observed in Table 5.1. The A:M ratio, an indicative of the relative predominance of fluorescent band A over M, was similar for spring, summer and autumn events, suggests that in these seasons there was a similar proportion of the compounds with higher degree of conjugation and aromaticity (M) and of the compounds with lower degree of conjugation and aromaticity (A) (Chen et al., 2002). Moreover, the A:M ratio was higher in winter than in the other seasons, signifying higher predominace of A fluorophores relatively to the M fluorophores comparatively to the other seasons. These findings suggest that in spring, summer and autumn samples A fluorophores are more readily photodegraded than M fluorophores. The results obtained for the class A events in the different seasons (Table 5.1) confirm the occurrence of higher A:M ratio in winter events, probably due to the lower photodegradation of A fluorophores, suggesting the presence of higher MW compounds. Kieber et al. (2006) also found, in rainwater samples from

Wilmington, a shift to lower MW CDOM and lower A:M ratio in the summer months.

Table 5.1 also shows some differences in CDOM for the samples grouped according to classes of air mass trajectories. Rainwater related with air masses with a maritime origin (class A) showed lower VWA values of DOC, UV_{250nm} and integrated fluorescence, suggesting lower content of CDOM than rainwater with a terrestrial contribution (classes B and D). Rainwater from class A is associated with air masses transported directly from the Atlantic Ocean and the VWA values found should approximately represent background concentrations. On other hand, when air masses come from continental Europe and transported over the ocean (class B), VWA of DOC, UV_{250nm} and integrated fluorescence present the highest values, suggesting that anthropogenic sources are important contributors of CDOM and that this CDOM is efficiently transported long from the sources over the sea. Rainwater related to air masses from Mediterranean area (class D) had the intermediate VWA values of DOC, UV_{250nm} and integrated fluorescence, suggesting smaller terrestrial/pollutant input when compared with the air masses from continental Europe, transported over the ocean (class B). Kieber et al. (2006) also observed that air mass back-trajectory analysis indicated elevated CDOM levels in continentally influenced rainwater relative to marine dominated events implying that anthropogenic and/or terrestrial sources are important contributors to CDOM levels in precipitation. The S and the ε_{280nm} also suggest that rainwater DOM from continental Europe and transported over the ocean (class B) have lower MW than rainwater DOM from ocean (class A) and from Mediterranean area (class D). As samples of class B were all collected in summer and autumn, the lower MW of DOM may be due to the photodegradation of DOM that occur with the higher irradiance during these seasons, as suggested above. Moreover, separating the events of the class D in spring/summer/autumn and winter events (Table 5.1), it was also observed lower MW of DOM for the seasons of higher irradiance. On other hand, the A:M ratio is lower for DOM from rainwater of class B and of class D in spring/summer/autumn than for DOM of class A, indicating higher relative predominance of organic compounds with higher degree of

conjugation or aromaticity, which may be due to the origin of air mass trajectory and respective anthropogenic/terrestrial sources.

Comparing the results obtained for the rainwater of Aveiro with that obtained by Kieber et al. (2006) for the rainwater of Wilmington, besides similar DOC content for the total of samples at both sites, the DOM of rainwater of Aveiro have higher MW (> ε_{280nm} and < S) and higher predominance of fluorophores with lower degree of conjugation and aromaticity (>A:M). In a recent study, Santos et al. (2009a) concluded that the DOM in Aveiro rainwater of autumn consists of a complex mixture of hydroxylated and carboxylic acids with a predominantly aliphatic character, containing a minor component of aromatic structures. The authors also suggested that the oxidation of volatile organic compounds directly emitted into the atmosphere, either by anthropogenic or biogenic sources, may have an important contribution to the polyacidic nature of rainwater DOM through in-cloud and/or precipitation scavenging of aerosol particles.

Table 5.2 shows the average excitation and emission wavelength maxima of the fluorescence of the humic-like bands (A, M, C) and their VWA of fluorescence intensity (FI) and of specific fluorescence intensity (SFI) for samples grouped by seasons and for samples grouped by air masses trajectories (class).

As shown in table 5.2, the average values of excitation/emission wavelengths maxima for each of the humic-like bands (A, M and C) were similar for all the samples: A ($\lambda_{ex}/\lambda_{em}$ ≈ 240/405 nm), M ($\lambda_{ex}/\lambda_{em}$ ≈ 300/410 nm), and C ($\lambda_{ex}/\lambda_{em}$ ≈ 330/420) nm. On other hand, while the ranges of excitation wavelengths were small for all bands, the ranges of emission wavelengths maxima were large in summer for bands A and M when air mass trajectories were maritime (class A) and large for band C in all seasons and in all classes of air mass trajectories. Analysing in more detail rainwater samples, it was verified that only one sample (RS1) of summer, with maritime air mass associated (class A), was responsible for increasing the emission wavelength range of the humic-like bands: of 415 to 455 nm in band A; of 425 to 455 nm in band M; and of 445 to 460 nm in band C. That sample is presented in Figure 5.1 and as it may be seen, the trajectories of air mass at 10 m of height highlight the passage for the city of Coimbra (at south of Aveiro), and for the industrialized area at north of Aveiro (town of Estarreja). Thus,

this rainwater sample may have been affected by anthropogenic sources and consequently humic-like bands were shifted to longer emission wavelengths comparatively to the other samples, indicating the presence of more condensed aromatic rings and other unsaturated bond systems (Chen et al., 2002). Although without this sample (RS1) the ranges of emission wavelengths decrease for bands A and M in summer, being small, for band C the ranges continue large, which may be due to its large uncertainty resultant of the bad definition in some samples. Nevertheless, no clear relationship was found between locations of emission wavelengths maxima of band C of samples with the seasons and air mass trajectories.

Table 5.2 also shows that the VWA FI of bands A, M and C is lower for spring than for the other seasons, which means low content of fluorescent organic matter in spring. This fact is not only due to lower concentration of DOM, because as seen in Table 5.1, the DOC concentration in spring is higher than in winter. On other hand, VWA SFI shows that for the same concentration of DOC, winter season presents the highest fluorescence for the three bands and about the double of the intensity of spring. Thus, the A, M and C fluorophores are more fluorescent in winter than in spring, and also than in summer and autumn. Moreover, the SFI of the three bands are lower and closer for spring and summer, and higher and closer for autumn and winter, except for the band A where the SFI of autumn is much less intense than in winter. These facts may be due to the occurrence of higher photodegradation of all bands in spring and summer relatively to autumn and winter, as well as of band A for autumn relatively to winter but in lower extent, which is in accordance with the lower MW and lower A:M ratio observed for spring, summer and autumn and presented in Table 5.1.

Table 5.2 also shows that rainwater related with air masses with a maritime origin (class A) have lower VWA FI of the fluorescent bands, A, M, and C, than rainwater from Mediterranean area (class D) and than rainwater related to air masses from continental Europe and transported over the ocean (class B).

Table 5.2 Average excitation and emission wavelength maxima (± standard deviation) of the fluorescence of humic-like bands and its VWA of fluorescence intensity (FI; ppb QS) and specific fluorescence intensity (SFI; $g^{-1}C$ L ppb QS) for samples collected at the different seasons and for samples grouped by air masses trajectories (class). The standard deviations of VWA FI and VWA SFI are indicated between brackets.

Band	Sampling period/ Class	λ_{ex} max (nm)	λ_{em} max (nm)	FI (ppb QS)	SFI ($g^{-1}C$ L ppb QS)	Attribution
A	Autumn (n = 11)	240±0	405±6 (395-410)	4.4 (±0.6)	8,322 (±2,334)	Humic-like
	Winter (n = 12)	240±0	399±7 (390-415)	4.4 (±0.9)	12,062 (±3,158)	
	Spring (n = 11)	240±0	408±8 (395-420)	2.5 (±0.4)	4,853 (±1,326)	
	Summer (n =6)	240±0	405±11 (390-455)	4.3 (±1.0)	3,937 (±1,587)	
	Class A (n = 30)	240±0	406±12 (395-455)	3.1 (±0.3)	7,668 (±1,618)	
	Class B (n = 3)	240±0	407±3 (405-410)	6.6 (±3.4)	4,475 (±2.221)	
	Class D (n = 7)	240±0	400±8 (390-410)	6.6 (±1.5)	10,241 (±3,184)	
	Autumn/Class A (n = 8)	240±0	404±6 (395-410)	3.9 (±0.7)	9,548 (±2,642)	
	Winter/Class A (n = 8)	240±0	401±7 (395-415)	3.1 (±0.8)	11,569 (±4,808)	
	Spring/Class A (n =10)	240±0	408±8 (395-420)	2.3 (±0.4)	4,968 (±1,458)	
	Summer/Class A (n = 4)	240±0	419±22 (400-455)	3.6 (±0.5)	3,964 (±1,162)	
	Spring/Summer/Autumn/Class D (n = 3)	240±0	408±2 (405-410)	5.7 (±1.5)	3,056 (±1,886)	
	Winter/Class D (n = 4)	240±0	394±2 (390-395)	6.9 (±1.4)	13,020 (±1,760)	
M	Autumn (n = 11)	294±5 (290-305)	410±0	2.4 (±0.3)	4,167 (±1,079)	Marine Humic-like
	Winter (n = 12)	299±4 (295-305)	409±9 (395-425)	1.7 (±0.3)	4,533 (±1,145)	
	Spring (n = 11)	299±2 (295-300)	412±3 (410-415)	1.3 (±0.3)	2,419 (±683)	
	Summer (n =6)	296±5 (285-305)	412±9 (395-455)	2.7 (±0.7)	1,969 (±794)	
	Class A (n = 30)	297±5 (285-305)	414±10 (395-455)	1.6 (±0.2)	3,404 (±627)	
	Class B (n = 3)	292±3 (290-295)	410±0	4.1 (±2.2)	2,740 (±1,357)	
	Class D (n = 7)	295±6 (285-300)	406±4 (400-410)	2.9 (±0.5)	3,937 (±1,096)	

Table 5.2 To be continued.

Band	Sampling period/ Class	λ_{ex} max (nm)	λ_{em} max (nm)	FI (ppb QS)	SFI ($g^{-1}C$ L ppb QS)	Attribution
M	Autumn/Class A (n = 8)	295±6 (290-305)	410±0	1.9 (±0.3)	4,655 (±1,240)	Marine Humic-like
	Winter/Class A (n = 8)	299±5 (290-305)	413±9 (395-425)	1.2 (±0.3)	4,437 (±1,742)	
	Spring/Class A (n =10)	299±2 (295-300)	412±3 (410-415)	1.2 (±0.3)	2,441 (±754)	
	Summer/Class A (n = 4)	291±5 (285-300)	425±18 (410-455)	2.1 (±0.6)	1,972 (±592)	
	Spring/Summer/Autumn/Class D (n = 3)	292±6 (285-300)	410±0	3.7 (±1.0)	1,919 (±1,092)	
	Winter/Class D (n = 4)	298±3 (295-300)	401±4 (395-405)	2.5 (±0.6)	4,717 (±705)	
C	Autumn (n = 11)	328±6 (320-340)	420±13 (405-445)	2.0 (±0.3)	3,677 (±972)	Humic-like
	Winter (n = 12)	330±0	418±14 (395-445)	1.4 (±0.3)	3,826 (±920)	
	Spring (n = 11)	331±2 (330-325)	424±10 (415-445)	0.9 (±0.2)	1,641 (±440)	
	Summer (n =6)	330±4 (320-340)	422±13 (395-460)	3.6 (±1.3)	1,778 (±655)	
	Class A (n = 30)	330±3 (320-340)	423±13 (405-460)	1.4 (±0.2)	2,779 (±508)	
	Class B (n = 3)	325±5 (320-330)	428±15 (415-445)	3.6 (±2.0)	2,360 (±1,175)	
	Class D (n = 7)	331±2 (330-335)	414±12 (395-435)	2.3 (±0.4)	3,296 (±935)	
	Autumn/Class A (n = 8)	326±9 (305-335)	417±11 (405-445)	1.7 (±0.3)	4,137 (±1,111)	
	Winter/Class A (n = 8)	323±11 (305-330)	421±13 (405-445)	1.0 (±0.2)	3,715 (±1,402)	
	Spring/Class A (n =10)	332±3 (330-340)	425±9 (415-445)	0.8 (±0.2)	1,658 (±489)	
	Summer/Class A (n = 4)	330±4 (325-335)	433±18 (415-460)	2.5 (±1.3)	1,770 (±445)	
	Spring/Summer/Autumn/Class D (n = 3)	332±2 (330-335)	422±9 (415-435)	2.8 (±0.4)	1,365 (±681)	
	Winter/Class D (n = 4)	324±6 (315-330)	410±9 (395-420)	2.2 (±0.5)	4,042 (±518)	

n = number of rain events.
The values in parenthesis for the excitation and emission wavelengths are the observed ranges for data sets.

This fact support the idea that rainwater associated with air masses transported directly from the Atlantic Ocean (class A) may represent background VWA FI values, as above mentioned. Muller et al. (2008) also observed that the highest humic-like substances (HULIS) fluorescence intensities were associated with events of continental origin and suggested the influence of terrestrial/anthropogenic sources. On other hand, the SFI values obtained for all seasons of class A highlight that local sources may have contributed to the fluorescent DOM found in rainwater, as suggested by the inverse correlation between the integrated fluorescence and rainwater amount (Figure 5.6). The value of SFI of band A associated to samples of class B (that occurred in summer and autumn seasons) is higher but more close of the SFI of spring/summer/autumn samples of class D, suggesting some similar fluorophores, which may be associated with a terrestrial/anthropogenic origin. On other hand, for the bands M and C the SFI values indicate that fluorophores fluoresce more when rainwater is from continental Europe and transported over the ocean (class B) than when is from the Mediterranean area (class D) for the seasons spring, summer and autumn, highlighting slightly more fluorescent organic matter present. Results confirm that fluorescent compounds of bands A, M and C were efficiently transported long from the sources over the sea and that terrestrial/anthropogenic sources are important contributors of them. On other hand, results highlight that rainwater samples associated with terrestrial air masses (classes B and D) presented higher CDOM content than rainwater samples with marine air masses (class A), which may be due to the contribution of terrestrial/anthropogenic sources.

5.4 Conclusions

Rainwater DOM at a coastal town on the southwest of Europe (Aveiro) was characterized by the UV-visible and molecular fluorescence spectroscopies and by its DOC content. The seasonal and air mass effects on rainwater DOM were evaluated. The results allowed the following conclusions:

1) CDOM is an important contributor of DOC in rainwater, where compounds with lower degree of conjugation and aromaticity predominate.
2) Rainwater presented similar optical properties to natural waters, signifying that compounds that make part of rainwater CDOM may be derived from surface sources and/or from processes that originate or modify organic compounds in the atmosphere.
3) Rainwater from summer and autumn presented higher content of CDOM and of compounds with higher degree of conjugation and aromaticity (> FI of bands M and C) than rainwater from winter and spring. Furthermore, rainwater of spring, summer and autumn presented lower MW and lower A:M ratio than rainwater of winter, which may be due to the higher DOM photodegradation of fluorophores with lower degree of conjugation and aromaticity (A).
4) Rainwater related with air masses with a maritime origin showed low content of CDOM than rainwater with terrestrial/anthropogenic contributions. Moreover, rainwater samples associated with air masses that come from continental Europe and transported over the ocean presented higher content of CDOM and of organic compounds with higher degree of conjugation or aromaticity than rainwater from the Mediterranean area, indicating that anthropogenic sources are important contributors of CDOM and that CDOM was efficiently transported long from the sources over the sea.

Chromophoric compounds showed to be important constituents of rainwater DOM and the presence of these highly absorbing and fluorescing compounds may exert a determining effect on atmospheric absorption of solar radiation. On other hand, the presence of chromophoric compounds in rainwater DOM affects the terrestrial and aquatic ecosystems, since rainwater is the predominant source of all the fresh water, which consequently may affect the human health.

References

Andreae, M.O., Jones, C.D., Cox, P.M., 2005. Strong present-day aerosol cooling implies a hot future. Nature 435, 1187–1190.

Burdige, D.J., Kline, S.W. and Chen, W., 2004. Fluorescent dissolved organic matter in marine sediment pore waters. Marine Chemistry 89, 289-311.

Chen, J., Gu, B., LeBoeuf, E.J., Pan, H., Dai, S., 2002. Spectroscopic characterization of the structural and functional properties of natural matter fractions. Chemosphere 48, 59–68.

Cheng, Y.-y., Guo, W.-d., Long, A.-m., Chen, S.-y., 2010. Study on optical characteristics of chromophoric dissolved organic matter (CDOM) in rainwater by fluorescence excitation-emission matrix and absorbance spectroscopy. Spectroscopy and spectral analysis 30, 2413-2416.

Chin, Y.-P., Alken, G., O'Loughlin, E., 1994. Molecular weight, polydispersity, and spectroscopic properties of aquatic humic substances. Environ. Sci. Technol. 28, 1853–1858.

Coble, P.G., Schultz, C.A., Mopper K., 1993.Fluorescence contouring analysis of DOC Intercalibration Experiment samples: a comparison of techniques. Marine Chemistry 41, 173-178.

Coble, P.G., 1996. Characterization of marine and terrestrial DOM in seawater using excitation emission matrix spectroscopy. Marine Chemistry 51, 325-346.

Coble, P.G., Del Castillo, C.E., Avril, B., 1998. Distribution and optical properties of CDOM in the Arabian Sea during the 1995 Southwest Monsoon. Deep-Sea Research II 45, 2195–2223.

Decesari, S., Facchini, M.C., Fuzzi, S., Tagliavini, E., 2000. Characterization of water-soluble organic compounds in atmospheric aerosols: a new approach. J. Geophys. Res. 105, 1481–1489.

Draxler, R.R., Rolph, G.D., 2003. HYSPLIT (Hybrid Single-Particle Langrangian Integrated Trajectory), www.arl.noaa.gov/HYSPLIT.php. NOAA Air Resources Laboratory, Silver Spring.

Duarte, R.M.B.O., Duarte, A.C., 2005. Application of non-ionic solid sorbents (XAD resins) for the isolation and fractionation of watersoluble organic compounds from atmospheric aerosols. J. Atmos. Chem. 51, 79–93.

Duarte, R.M.B.O., Pio, C.A., Duarte, A.C., 2005. Spectroscopic study of the water-soluble organic matter isolated from atmospheric aerosols collected under different atmospheric conditions. Anal. Chim. Acta 530, 7-14.

Facchini, M.C., Fuzzi, S., Zappoli, S., Andracchio, A., Gelencsér, A., Kiss, G., Krivácsy, Z., Mészáros, E., Hansson, H.C., Alsberg, T., Zebühr, Y., 1999. Partitioning of the organic aerosol component between fog droplets and interstitial air. J. Geophys. Res. 104(26), 26 821–26 832.

Gysel, M., Weingartner, E., Nyeki, S., Paulsen, D., Baltensperger, U., Galambos, I., Kiss, G., 2004. Hygroscopic properties of water-soluble matter and humic-like organics in atmospheric fine aerosol. Atmos. Chem. Phys. 4, 35–50.

Helms, J.R., Stubbins, A., Ritchie, J.D., Minor, E.C., Kieber, D.J., Mopper, K., 2008. Absorption spectral slopes and slope ratios as indicators of molecular weight, source, and photobleaching of chromophoric dissolved organic matter. Limnology and Oceanography 53, 955–969.

Hoffer, A., Kiss, G., Blazsó, M., Gelencsér, A., 2004 Chemical characterization of humic-like substances (HULIS) formed from a lignin-type precursor in model cloud water. Geophys. Res. Lett. 31, L06115. doi:10.1029/2003GL018962

Kieber, R.J., Whitehead, R.F., Reid, S.N., Willey, J.D., Seaton, P.J., 2006. Chromophoric dissolved organic matter (CDOM) in rainwater, Southeastern North Carolina, USA. J. Atmos. Chem. 54, 21-41.

Markager, S., Vincent, W.F., 2000. Spectral light attenuation and the absorption of UV and blue light in natural waters. Limnol. Oceanogr. 45, 642–650.

Miller, C., Gordon, K.G., Kieber, R.J., Willey, J.D., Seaton, P.J., 2009. Chemical characteristics of chromophoric dissolved organic matter in rainwater. Atmos. Environ. 43, 2497-2502.

Muller, C.L., Baker, A., Hutchinson, R., Fairchild, I.J., Kidd, C., 2008. Analysis of rainwater dissolved organic carbon compounds using fluorescence spectroscopy. Atmos. Environ. 42, 8036–8045.

Peuravuori, J., Pihlaja, K., 1997. Molecular size distribution and spectroscopic properties of aquatic humic substances. Anal. Chim. Acta 137, 133–149.

Pio, C.A., Salgueiro, M.L., Nunes, T.N., 1991. Seasonal and air-mass trajectory effects on rainwater quality at the South-Western European border. Atmos. Environ. 25A, 2259–2266.

Santos, P.S.M., Otero, M., Duarte, R.M.B.O., Duarte, A.C., 2009a. Spectroscopic characterization of dissolved organic matter isolated from rainwater. Chemosphere 74, 1053-101.

Santos, P.S.M., Duarte, R.M.B.O., Duarte, A.C., 2009b. Absorption and fluorescence properties of rainwater during the cold season at a town in Western Portugal. Journal of Atmospheric Chemistry 62, 45-57.

Seitzinger, S.P., Styles, R.M., Lauck, R., Mazurek, M.A., 2003. Atmospheric pressure mass spectrometry: a new analytical chemical characterization method for dissolved organic matter in rainwater. Environ. Sci. Technol. 37, 131–137.

Senesi, N., Miano, T.M., Provenzano, M.R., Brunetti, G., 1989. Spectroscopic and compositional comparative characterization of I.H.S.S. reference and standard fulvic and humic acids of various origins. Sci. Total Environ. 81, 143–156.

Willey, J.D., Kieber, R.J., Eyman, M.S., Avery, G.B., 2000. Rainwater dissolved organic carbon: concentrations and global flux. Global Biogeochem. Cy. 14, 139-148.

Zappoli, S., Andracchio, A., Fuzzi, S., Facchini, M.C., Gelencsér, A., Kiss, G., Krivácsy, Z., Molnár, Á., Mészáros, E., Hansson, H.C., Rosman, K., Zebühr, Y., 1999. Inorganic, organic and macromolecular components of fine aerosol in different areas of Europe in relation to their water solubility. Atmos. Environ. 33, 2733–2743.

6. Chemical features and seasonal variation of dissolved organic matter isolated from rainwater

The complexity of rainwater dissolved organic matter (DOM) and the large percent considered uncharacterized has made difficult to determine the role of rainwater DOM in regional and global carbon budgets. Recent studies have concentrated on determining the structural characteristics of the bulk DOM in rainwater, but a comparison between the structural characteristics of rainwater DOM from different seasons is lacking. In this work, DOM was extracted from rainwater by a procedure based on adsorption onto DAX-8 resin and a comparison between the spectroscopic characteristics of extracted DOM from rainwater was performed recurring to UV-Visible, excitation-emission matrix (EEM) fluorescence and ^{1}H NMR spectroscopies. Similar structural characteristics were observed for extracted DOM from the different seasons: high content of aliphatic structures, of hydroxy and alkoxy groups, of carbonyls groups and unsaturated carbon atoms, and low content in aromatic structures when compared with aliphatic structures. The obtained results allowed to suggest a model of chemical structures for the extracted DOM from rainwater, as consisting of an aromatic core bearing substituted by aliphatic chains, with –COOH, $-CH_2OH$, $-COCH_3$, or $-CH_3$ terminal groups.

6.1 Introduction

There is now a general consensus in the literature that the chemical composition of rainwater can no longer be reduced to the inorganic content. Organic and inorganic composition must be linked in order to understand and to model the physical and chemical processes occurring in the multiphase atmospheric system (aerosols, clouds and rainwater).

Dissolved organic carbon (DOC) is a ubiquitous component of rainwater and is a major component of both marine (23 μM) and continental rain (161 μM) (Willey et al., 2000). However, approximately 50% of rainwater DOC is considered uncharacterized at both the compound class and individual compound level (Willey et al., 2000).

Recent efforts have concentrated on the structural characteristics of the bulk dissolved organic matter (DOM) in rainwater (Wang et al., 2004; Decesari et al., 2005; Kieber et al., 2006; Miller et al., 2009; Santos et al., 2009a). These studies have reported the prevalence of DOM with characteristics resembling those of natural humic substances due to its polyacidic nature. In what concerns the origin of this type of macromolecular organic matter, atmospheric aerosols have been considered the main contributors of these macromolecular substances in the rainwater (Decesari et al., 2005). Nevertheless, Graber and Rudich (2006) showed that while sharing some important features such as the polyacidic nature, the atmospheric humic like substances (HULIS) differ substantially from terrestrial and aquatic humic substances. The major differences between atmospheric HULIS and humic substances pointed by Graber and Rudich (2006) include smaller average molecular weight, lower aromatic moiety content, greater surface activity, and better droplet activation ability.

The low concentration of all rainwater constituents has prompted the application of different analytical methodologies to isolate DOM from rainwater, such as the procedures based on the adsorption onto XAD-8 and C-18 sorbents (Wang et al., 2004; Kieber et al., 2006; Miller et al., 2009; Santos et al., 2009a). Santos et al. (2010a) showed that rainwater DOM extracted by the C-18 procedure was more representative of the global matrix, but DAX-8 (replacement for XAD-8)

preferentially extracted humic-like compounds. These isolation procedures combined with different analytical techniques (e.g. Fourier transform infrared (FTIR), nuclear magnetic resonance (NMR), UV-visible and fluorescence spectroscopies (Santos et al., 2009a)) constitutes new approaches for the elucidation of the chemical properties of the DOM from rainwater.

With the aim of assessing the seasonal variation of the bulk properties of DOM from rainwater, in this work rainwater samples were collected during about one year. An isolation procedure based on DAX-8 resin (Santos et al., 2009a) together with different analytical techniques, including UV-visible, excitation-emission matrix fluorescence and ^{1}H NMR spectroscopies, were applied to the elucidation of the structural features of the humic-like DOM from the collected rainwater. Owing to the small amounts of DOM usually extracted from rainwater, in this work, the DOM fractions extracted from the rainwater samples were combined for each sampling season prior to the ^{1}H NMR analysis.

6.2 Experimental

6.2.1. Rainwater sampling and sample preparation

Rainwater was collected at a sampling station (40º38' N, 8º39' W) located in the western part of the town of Aveiro, Portugal, between September 2008 and September 2009. The sample collection was carried out at 70 cm above the ground, through glass funnels (30 cm diameter) into glass bottles (5 L). The sampling containers were left out open in order to collect both wet and dry depositions on a 24 h basis. Prior to use, all glass materials were immersed for 30 min, in a solution of NaOH (0.1 M), then rinsed with distilled water, followed by another immersion for 24 hours in a solution of HNO_3 (4 M), and finally rinsed with ultrapure (Milli-Q) water. After collection, samples were transported to the laboratory where they were filtered through hydrophilic PVDF Millipore membrane filters (0.45 µm). Rainwater samples for subsequent DOM extraction, were stored in glass bottles in the dark at 4ºC for a maximum of four days, and an aliquot of

each sample was frozen for subsequent analysis of DOC content. The storage of samples in the dark at 4ºC was proved to be adequate for keeping the optical properties of the samples unchanged in case the storage time does not exceed 4 days (Santos et al., 2010b).

6.2.2. Extraction of dissolved organic matter (DOM)

Rainwater samples (2.5-5 L) were subjected to a procedure for the isolation and extraction of DOM based on the use of Supelite^{TM} DAX-8 resin (considered the substitute of XAD-8 since the production of the latter stopped; Peuravuori et al., 2001).

The isolation and extraction procedure is based on DAX-8 sorption, and it was adapted from the one described by Santos et al. (2009a) for the extraction of DOM from rainwater. A glass column containing DAX-8 resin (150 mL) was prepared accordingly for sorption of DOM. The resin was thoroughly cleaned by Soxhlet extraction as described elsewhere (Malcolm, 1991). Prior to usage, the resin in the column was rinsed, firstly with ultrapure water (≈ 100 column volumes), then with 600 mL of a methanol solution (40%), and with ultrapure water (≈ 50 column volumes); then it was rinsed with 0.1 M NaOH (1 column volume), followed by 0.1 M HCl (1 column volume) and finally with 0.01 M HCl (1 column volume). Rainwater samples were acidified to pH = 2.2 ± 0.2 before being pumped through the DAX-8 column at a flow rate of ≈13 mL min^{-1} for DOM concentration. After pumping the samples, the inorganic matter retained in the DAX-8 column void volume was down washed with ultrapure water (1 column volume) at a flow rate of ≈13 mL min^{-1}. The organic matter (OM) sorbed in DAX-8 was then back eluted with 600 mL of a methanol aqueous solution (40%) at a flow rate of ≈4 mL min^{-1} (1/3 of the of fixation flow rate). The eluate was evaporated almost to dryness (volume ≤ 1 mL) in a rotary evaporator at 30 ºC, and then transferred to a volumetric flask (50 mL). Ultrapure water was then used to make up the flask volume, and the eluate was then divided into two aliquots. One aliquot (5 mL) was used for UV-visible and EEM fluorescence spectroscopies, and for determining the DOC content. The second aliquot was concentrated (until a volume of 2-3 mL) in a

rotary evaporator at 30 ºC, then transferred to glass vials (of 4 mL) and dried under an atmosphere of N_2. The dried extracts were stored in an exsicator for further ^{1}H NMR spectroscopy analysis.

For the optical analysis, the aliquots of rainwater sample, the corresponding DAX-8 eluates and effluents were acidified to pH = 3.0 ± 0.2.

For DAX-8 procedure, blanks (ultrapure water) were processed in the same way as the samples of rainwater. The signal of the eluates of blanks in terms of DOC content were lower than 8 % of the signals of the eluates of samples, and they were considered negligible.

6.2.3 Measurements of dissolved organic carbon (DOC)

The concentrations of total carbon (TC) and inorganic carbon (IC) were measured for each rainwater sample by means of a Shimadzu TOC-5000A analyzer. The DOC content of the samples was calculated as the difference TC-IC. For TC quantification, standards were prepared from reagent grade potassium hydrogen phthalate in ultra pure water in the range of 0.5 to 2 mg C L^{-1}. For IC measurements, standards were performed from reagents grade sodium hydrogenocarbonate plus sodium carbonate in ultra pure water, also in the range of 0.5 to 2 mg C L^{-1}. Control standards were generally within 5% agreement in terms of TC and IC content. For each sample, three replicates were analysed for determining the DOC content.

6.2.4 Optical analysis

UV–visible spectra (in the range of 200–600 nm) of rainwater samples were recorded on a Shimadzu (Dusseldorf, Germany) Model UV 210PC spectrophotometer. Quartz cells of different path lengths were used depending on the observed absorbance: 10 cm (for the rainwater samples and effluents) and 1 cm (for the rainwater eluates). Ultrapure water was used as reference and to obtain the baseline. The spectral slope coefficients (S) were inferred from the obtained UV–visible spectra. For comparison with S values published for rainwater

DOM (Kieber et al., 2006; Santos et al., 2009a), S values (μm^{-1}) were calculated from non-linear least-square regressions of the absorption coefficients (a_λ) vs. wavelength for the range between 240 and 400 nm using the equation of Markager and Vincent (2000): $a_\lambda = a_{\lambda 0} e^{S(\lambda 0 - \lambda)} + K$, where λ is the reference wavelength (300 nm) and K is a background parameter to improve the goodness of fitting. Absorption coefficients (a_λ, m^{-1}) at each wavelength (λ) were calculated as $a_\lambda = 2.303\ A_\lambda / l$, where A_λ is the absorbance reading at wavelength λ and l (m) is the optical pathlength. The maximum wavelength considered for spectral slope calculations was 400 nm, since this was the highest wavelength whose absorbance values were consistently above the detection limit.

The molecular fluorescence spectra were obtained by a Fluoromax 3 (JobinYvon-Spex Instruments S.A., Inc, now HORIBA Jobin Yvon Inc, Edison, NJ, USA) with a xenon lamp as source of radiation. Fluorescence intensity measurements were carried out under thermostated conditions at 20ºC and spectra were recorded using 1 cm cells and 5 nm bandpasses on both the excitation and the emission monochromators. Excitation-emission matrix (EEM) fluorescence spectra were obtained by concatenating emission spectra measured every 5 nm from 290 to 510 nm using excitation wavelengths (λ_{ex}) from 240 to 400 nm increasing also at 5 nm intervals. Scans were corrected for instrument configuration using factory supplied correction factors (Coble et al, 1993), and data were normalized to a daily-determined water Raman intensity ($275_{ex}/303_{em}$, 5 nm bandpasses) and converted to Raman normalized quinine sulphate (QS) equivalents in ppb (Coble et al., 1998). For each sample a daily blank (Milli-Q water) spectrum was subtracted from rainwater spectrum. Replicate scans within 5% agreement in terms of intensity and within bandpass resolution in terms of band location were obtained, for $\lambda_{ex} > 250$ nm. However, at low excitation wavelengths ($\lambda_{ex} \leq 250$ nm), instrumental variability on fluorescence intensity was always higher than at $\lambda_{ex} > 250$ nm

6.2.5 ^{1}H NMR spectroscopy

The ^{1}H NMR spectra were recorded on a Bruker Avance 300 spectrometer with an operating frequency of 300.13 MHz. The acquisition of spectra was performed with spinning rate of 20Hz. The recycle delay was 1s and the length of the proton 90º pulses was 10.9 μs. For NMR analysis, the solid extracts of the samples were dissolved in D_2O. The identification of functional groups in the NMR spectra was based on their chemical shift (δ_H) relative to that of the water (4.7 ppm).

6.2.6 Trajectories of air air masses and meteorological data

The general characteristics of air masses during the sampling period were evaluated by using Hybrid Single Particle Lagrangian Integrated Trajectory Model (HYSPLIT) developed by Draxler and Rolph (2003) at the National Oceanic Atmospheric Administration—Air Resources Laboratory (NOAA/ARL) (available at www.arl.noaa.gov/HYSPLIT.php). Trajectories were generated for a 48 h hind-cast starting at 10 and 500 m level, calculated every 6 h for every day when sampling of precipitation occurred.

Rainwater samples were classified into five groups according to the origin and trajectory of the air masses: class A contains samples related to air masses transported from the Atlantic Ocean; class B represents samples with origins in central and northern parts of industrialized Europe and transported to Portugal over the ocean; class C contains samples with similar origins to those of class B, but transported over land; class D refers to air masses transported from north Africa and the Mediterranean across the Iberian Peninsula; samples in which less than 60 % of the air mass trajectories were from one section only, and had therefore a mixed origin, were agglomerated into class M. A similar way of classification had been previously used by Pio et al. (1991) for rainwater also collected at Aveiro (Portugal).

A meteorological station at the sampling site (at 10 m height) supplied the following information during the sampling period: direction and velocity of wind, relative humidity, air temperature and amount of precipitation.

6.3 Results and discussion

Forty rainwater samples were collected between September 2008 and September 2009 and from these, only fourteen were collected with enough volume (2.5-5 L) to proceed with the procedure for DOM isolation and extraction. The procedure adopted for the isolation of DOM from rainwater was the DAX-8 based procedure (Santos et al., 2009a) and it was chosen because it extracts preferentially the humic fraction of rainwater (Santos et al., 2010a).

Table 6.1 presents the fourteen samples that were subjected to the DOM isolation, and classified according to the season when they were sampled and their air mass trajectories. Table 6.1 shows the percentages of recovery of organic matter based on DOC content and absorbance at 250 nm (UV_{250nm}). The UV_{250nm} was chosen because it may be used as a way of assessing organic matter (OM) content (Duarte and Duarte, 2005a).

Table 6.1 Rainwater samples subjected to the DAX-8 based isolation procedure, classified according to the season and air mass trajectory associated, eluate DOC and percentage of recoveries of rainwater OM resulting from the isolation procedure based on DOC and UV_{250nm}.

Season /Air mass	Sample	Eluate DOC ($mg\ L^{-1}$)	Recovery from DAX-8 resin (%)	
			DOC	UV_{250nm}
Autumn / Class A	11 December 2008	8.7	30.1	22.9
	12 December 2008	18.5	78.1	21.2
	13 December 2008	7.7	71.6	37.6
Winter / Class D	12 January 2009	5.1	14.0	18.7
	01 February 2009	10.1	34.1	29.1
Winter / Class A	03 February 2009	6.2	36.2	25.2
	09 February 2009	5.5	27.2	64.9
	04 March 2009	7.1	20.1	30.0
Spring / Class A	14 April 2009	6.3	21.4	25.6
	15 April 2009	8.4	29.6	21.4
	11 May 2009	8.8	34.9	37.0
	05 June 2009	8.8	18.4	26.0
	07 June 2009	10.0	24.1	22.4
Summer / Class A	22 July 2009	41.0	62.7	18.7

As shown in Table 6.1, the percentages of recovery differ from sample to sample in a range from 14 to 78 % for the DOC, and 19-65 % for the UV_{250nm}. On other hand, the percentages of recovery in DOC were higher in autumn and summer (median = 67%) than in winter and spring (median = 26%). Therefore, when using the parameter UV_{250nm} the results were similar for summer and autumn (median = 22%) and for winter and spring (median = 26%). This variation of percentages of recovery may be associated to the DOM chemical characteristics of each sample, such as the molecular size of the solutes.

6.3.1 UV-visible spectra

Figure 6.1 shows the UV-visible spectra of the eluates (isolated fraction) of rainwater samples grouped by seasons. For the sake of easier comparison between different eluates the spectra are shown as absorptivity ($g^{-1}C\ L\ cm^{-1}$) *versus* wavelength (nm) in order to avoid the effects of different concentrations.

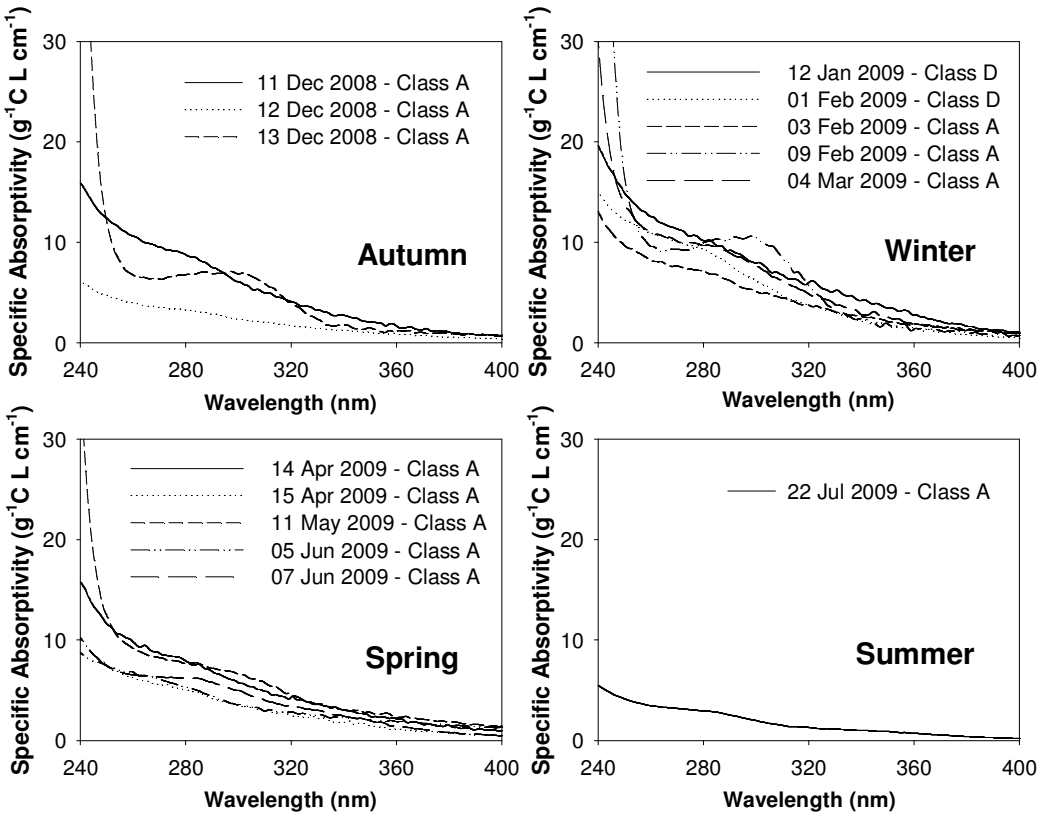

Figure 6.1 UV-visible spectra of rainwater eluates obtained from the isolation procedure of the rainwater DOM, grouped by seasons and presented as specific absorptivity (g^{-1} C L cm^{-1}).

The general decrease in specific absorptivity with increasing wavelength follows a trend similar to that already observed for rainwater samples (Kieber et al., 2006; Santos et al., 2009a,b), for aerosol samples (Duarte and Duarte, 2005a), and for other samples of natural humic substances (Senesi et al., 1989). The spectra of the eluates show a shoulder in the region 250-300 nm, which is usually attributed to $\pi \rightarrow \pi^*$ electron transitions of unsaturated systems (Peuravuori and Pihlaja, 1997).

Figure 6.2 shows the values of specific absorptivity at 280 nm (ε_{280}, g^{-1} C L cm^{-1}) and the values of spectral slope coefficients (S, μm^{-1}) associated to the eluates from rainwater.

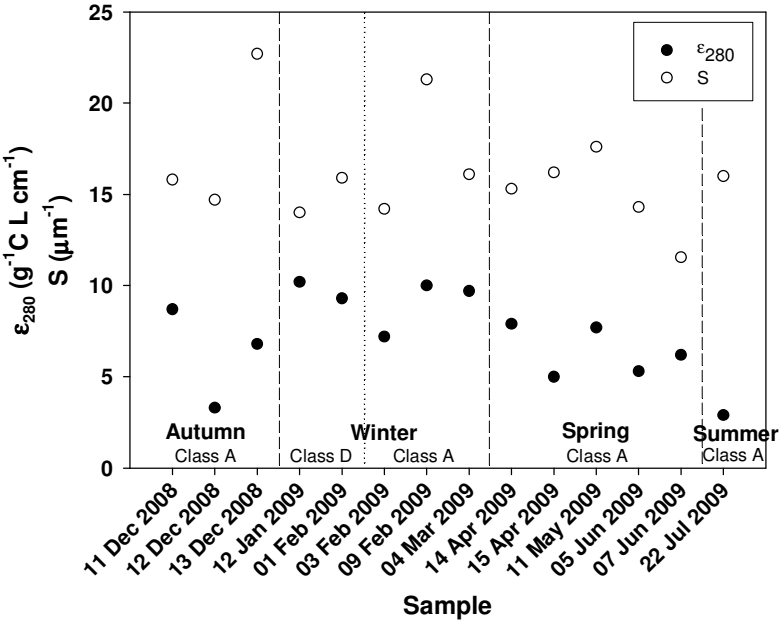

Figure 6.2 Specific absorptivity at 280 nm (ε_{280}, g^{-1}C L cm^{-1}) and spectral slope coefficient (S, μm^{-1}) of eluates obtained from the isolation procedure of the rainwater DOM.

Any effect of season and air mass trajectory on ε_{280} and S are not noticeable since no clear trend occurs for the values of ε_{280} and S of all eluates. Such observation in what concerns ε_{280} suggests, that the eluates contain compounds with similar complex unsaturated bond systems, where more than two π-bond orbitals overlap leading to a similarity in the absorptivity values (Williams and Fleming, 1973). In what concerns S, such observation may indicate that the eluates from different rainwater samples contain similar molecular weight, since S

can be considered inversely related to the molecular weight (MW) of DOM (Helms et al., 2008). The median of the S values of the eluates is 15.9 μm^{-1}, a value close of the average value (16.3 μm^{-1}) obtained by Miller et al. (2009) for the extract of rainwater of Wilmington applying the isolation procedure based on C-18 adsorption, suggesting similar MW of the DOM extracted from rainwater in both cases.

6.3.2 Excitation-emission matrix fluorescence spectra

Figure 6.3 shows the EEM fluorescence spectrum of the eluate from the sample collected on the 11th December 2008, which may be representative of spectra of all the eluates (Annex III). In order to avoid concentration effects, the fluorescence spectra were normalised to DOC content of the eluate (in g L^{-1}), and they are shown as specific fluorescence intensity (g^{-1}C L ppb QS).

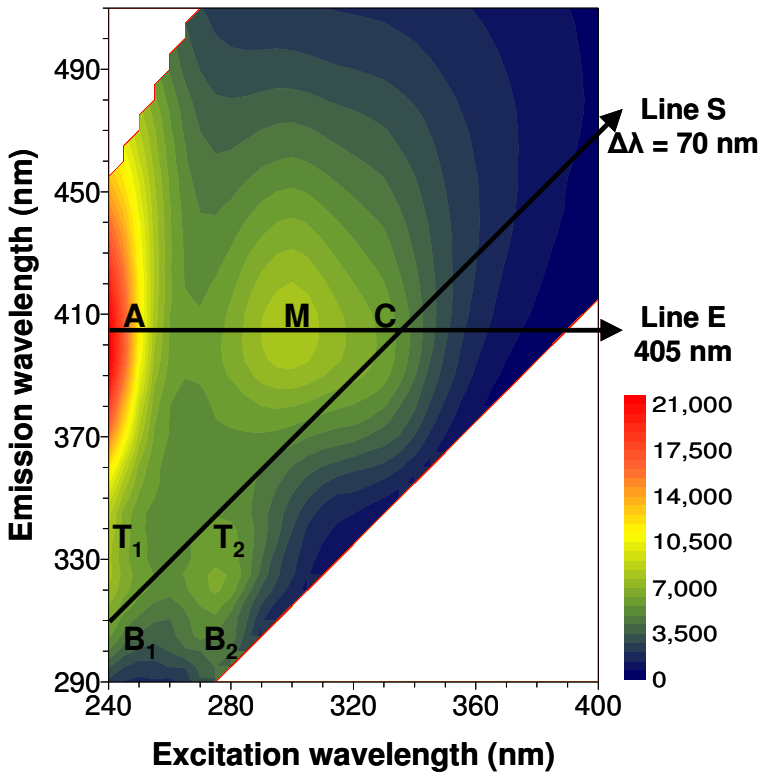

Figure 6.3 EEM fluorescence spectrum of the eluate from the sample collected on the 11th of December 2008, presented as specific fluorescence intensity (g^{-1}C L ppb QS).

The spectrum has the following fluorescent bands: three humic-like bands, A ($\lambda_{ex}/\lambda_{em}$ ≈ 240/400 nm), M ($\lambda_{ex}/\lambda_{em}$ ≈ 300/405 nm) and C ($\lambda_{ex}/\lambda_{em}$ ≈ 325/405 nm); and four protein-like bands, B_1 ($\lambda_{ex}/\lambda_{em}$ ≈ 240/305 nm), B_2 ($\lambda_{ex}/\lambda_{em}$ ≈ 270/305 nm), T_1 ($\lambda_{ex}/\lambda_{em}$ ≈ 240/340 nm) and T_2 ($\lambda_{ex}/\lambda_{em}$ ≈ 275/330 nm). Bands in the same range as A and C have been already identified in the emission-excitation matrix (EEM) fluorescence spectra of rainwater dissolved organic matter and have been assigned to humic-like compounds (Kieber et al., 2006; Santos et al., 2009a,b). A band at similar $\lambda_{ex}/\lambda_{em}$ of M has been already identified in the EEM fluorescence spectra of rainwater, being assigned also to marine humic-like compounds (Kieber et al., 2006; Santos et al., 2009a,b). B_1, B_2 and T_1, T_2 bands are attributed to protein-like compounds, such as tyrosine and tryptophan, respectively (Santos et al, 2010a).

The lines E and S shown in Figure 6.3 indicate the excitation and synchronous spectra chosen to compare the spectra of the eluates. The excitation spectra with λ_{em} = 405 nm was chosen to study the behaviour of the humic-like bands and the $\Delta\lambda$ = 70 nm for the synchronous spectra was chosen in order to highlight also the protein-like fluorescence. Figure 6.4 shows the excitation and synchronous fluorescence spectra for the eluates grouped by seasons.

In the excitation fluorescence spectra, as shown in Figure 6.4, the humic-like bands of the eluates show a similar trend independently of the season. The excitation spectra show that band A presents higher intensity than bands M and C for all eluates, which suggests that in all the eluates predominate compounds with low degree of conjugation or aromaticity. On other hand, in the majority of the excitation spectra, the band C appears more like a shoulder, suggesting low amount of conjugated aromatic π-bond systems with electron-withdrawing functional groups (Chen et al., 2002).

Regarding the synchronous fluorescence spectra, the most remarkable feature is the presence of the same fluorescent bands (bands B_1, T_2 and C) for all the eluates. Furthermore, no clear trend in fluorescence intensities of protein and humic bands was observed for the eluates either when analysed by seasons either when analysed by air mass trajectory.

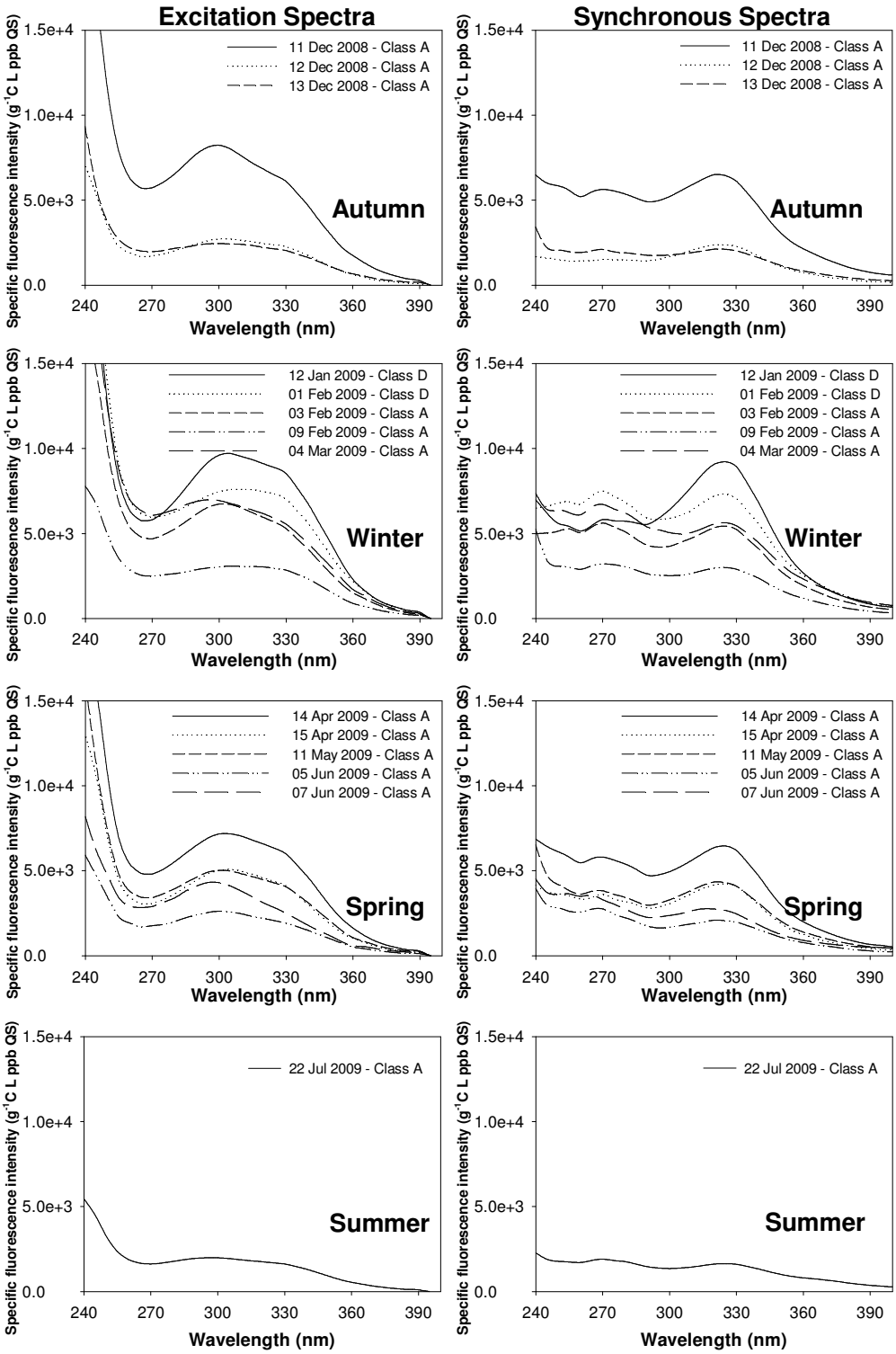

Figure 6.4 Excitation (left) and synchronous (right) fluorescence spectra for the eluates obtained from the isolation procedure of the rainwater DOM, grouped by seasons and presented as specific fluorescence intensity ($g^{-1}C$ L ppb QS).

6.3.3 ^{1}H NMR spectra

Proton NMR spectroscopy (^{1}H NMR) is applicable to the analysis of rainwater DOM (Kieber et al., 2009; Miller et al., 2009; Santos et al., 2009a), and spectra with a good signal-to noise ratio can be acquired for samples containing less than 1 mg of organic carbon (Decesari et al., 2000). ^{1}H NMR, as opposed to UV-visible or fluorescence spectroscopies, is also able to identify structural moieties in the bulk isolated DOM mixture. Another important characteristic of ^{1}H NMR spectroscopy is that quantitative analysis is straightforward, since the integrated area of the spectra is proportional to the moles of protons present in the samples (Decesari et al., 2000).

In order to obtain sufficient mass for the ^{1}H NMR spectroscopy analysis, the individual rainwater extracts were batched together according the season when they were sampled, and their air mass trajectories. Thus, as shown in Table 6.1 five groups of extracted samples were obtained: Autumn–Class A; Winter–Class D; Winter–Class A; Spring–Class A; Summer–Class A.

The ^{1}H NMR spectra of extracted DOM from these five groups of samples are shown in Figure 6.5.

The spectra exhibit some distinct peaks overlaying much broader bands, as would be expected from the NMR spectra of complex mixtures of structures. Despite the large variety of overlapping resonances, each ^{1}H NMR spectrum was investigated on the basis of the chemical shift assignments described in the literature for organic aerosols and rainwater DOM (Decesari et al., 2001; Decesari et al., 2005). Accordingly, four main regions of chemical shifts were considered and integrated in each spectrum: δ_H = 0.6–1.8 ppm (aliphatic protons, H–C); δ_H = 1.8-2.6 and 2.8–3.2 ppm (aliphatic protons in α position to carbonyl groups or unsaturated carbon atoms, H–C–C=); δ_H = 3.2–4.1 ppm (aliphatic protons on carbon atoms singly bound to oxygen atoms, H–C–O); and δ_H = 6.5–8.5 ppm (aromatic protons).

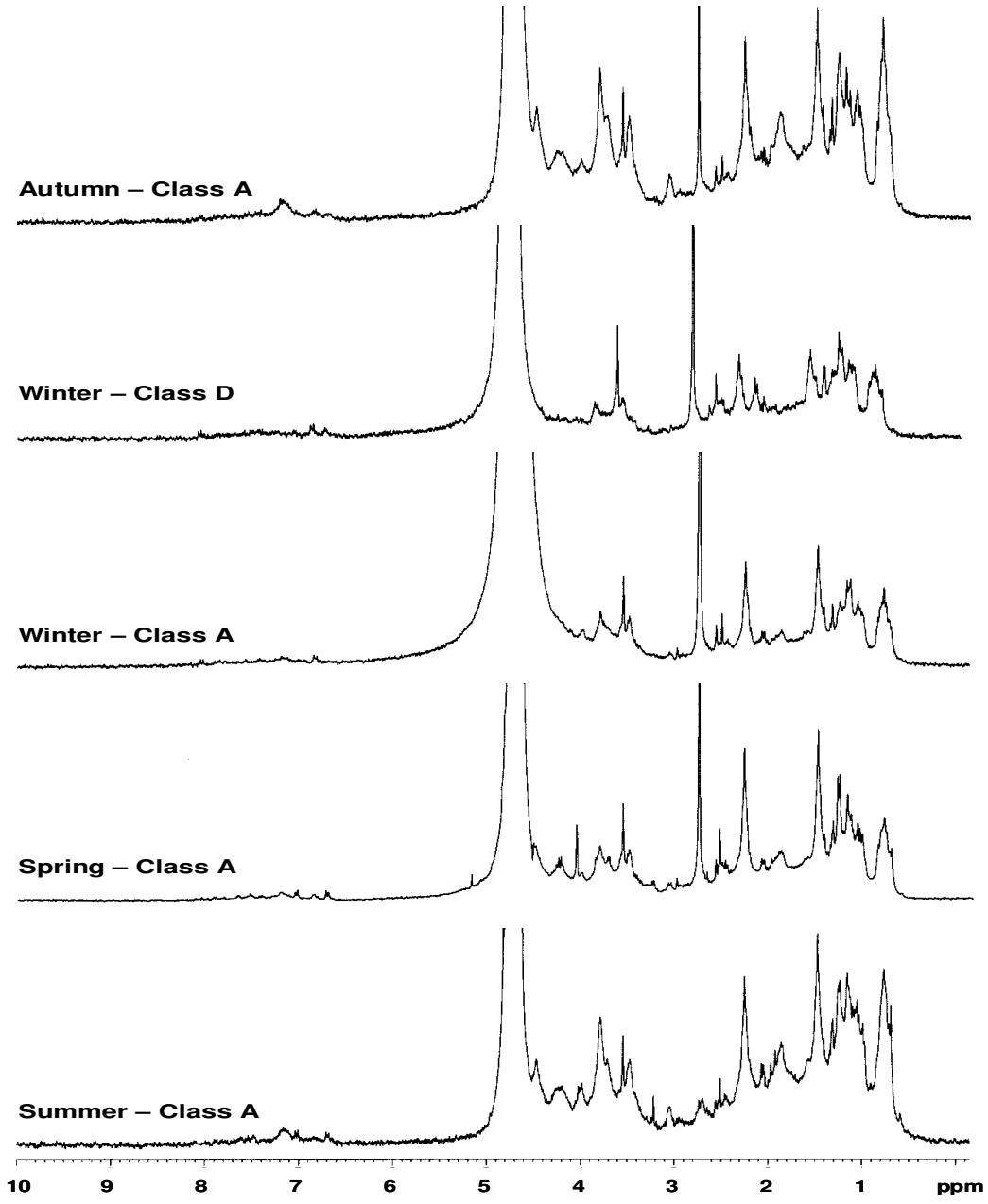

Figure 6.5 ^{1}H NMR spectra of the groups of extracted samples (Autumn–Class A; Winter–Class D; Winter–Class A; Spring–Class A; Summer–Class A). The peak at 4.7 ppm indicate the water signal.

Figure 6.6 shows the distribution of the different functional groups estimated from the partial integrals of the observed ^{1}H NMR bands for each group of samples.

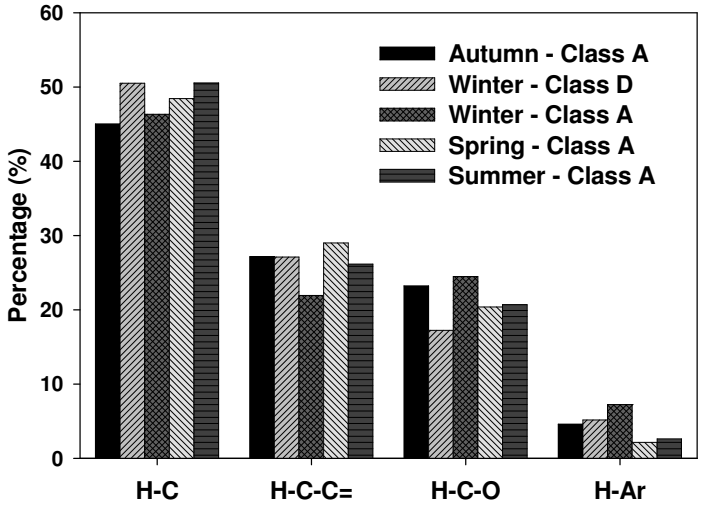

Figure 6.6 Functional group composition of the extracted samples: Autumn–Class A; Winter–Class D; Winter–Class A; Spring–Class A; Summer–Class A. Relative abundance of each functional group estimated as the partial integrals of the spectra reported in Figure 6.5. H-C: purely alkylic hydrogen atoms; H-C-C=: hydrogen atoms in α position to C=C or C=O groups; H-C-O: aliphatic C-H directly bound to an oxygen atom; H-Ar: aromatic hydrogen atoms.

The spectra of the extracted DOM from each group of samples exhibit quite similar patterns in terms of structural characteristics. Protons in the saturated aliphatic structures were found to be dominant moieties (45-51%) for all seasons and for both air mass trajectories. This fact suggests predominance of aliphatic moieties and it is consistent with previous works (Kieber et al., 2006; Miller et al., 2009; Santos et al., 2009a) where they also observed the predominance of saturated aliphatic structures in DOM extracts of rainwater.

The second most prominent signal in the spectra of Figure 6.5 arises from aliphatic protons linked to carbon atoms adjacent to C=C or C=O double bonds, including protons in aliphatic chains linked such as in aromatic rings, carbonyl and carboxyl groups, which accounts to 22-29% of the total integrated area of the spectra. Moreover, the spectra show at δ_H = 2.6-2.8 ppm an intense peak, except Summer–Class A spectrum where appears as a small peak. This peak was not integrated in all spectra due to its long shape, but its shift is attributed to the presence of dimethylsulfoxide (DMSO), which is usually tracer of marine air masses (Decesari et al., 2001). The small relatively peak of DMSO in Summer-

Class A may be due to the high DOC of the eluate (DOC = 41.0 mg L^{-1}, as shown in Table 6.1) that diluted the signal of the DMSO in the mixture of organic matter. On the other hand, the extract of Winter–Class D, associated with predominantly terrestrial air masses, also evidenced the presence of the long peak of DMSO, which may be related to a minor contribution of marine air masses and to the low DOC of the eluates (DOC = 5.1 and 10.1 mg L^{-1}, as shown in Table 6.1).

The ^{1}H NMR spectra of the DOM extracted from rainwater samples also exhibits resonance in the δ_H = 3.2-4.1 ppm region, which accounts to 17-24% of the total integral of the spectra. This region suggests the presence of the structures of polyols. The presence of polyols has been reported in the organic fraction of aerosols at Rondônia, Brazil (Decesari et al., 2006), and the occurrence of such structural fragments was associated to secondary formation from oxidation of volatile organic compounds emitted from pyrogenic and biogenic sources. Moreover, Duarte et al. (2005b) also found these types of structures (aliphatic carbons singly bonded to one oxygen) in the water-soluble organic matter (WSOC) isolated from atmospheric aerosols collected in a rural local near Aveiro. Nowadays, it is well established that atmospheric aerosols play an important role in climate and atmospheric chemistry, including the ability for providing condensation nuclei for cloud droplets. As water is the natural solvent in the atmosphere, is not unlikely that the oxygenated saturated aliphatic structures found in rainwater samples were scavenged from the aerosol particles from primary and/or secondary origin. However, one cannot disregard that this kind of structures could also be formed in cloud droplets through reactions (e.g. Fenton-type reactions) similar to those suggested in the literature for the formation of light-absorbing organic matter in cloud water (Gelencsér et al., 2003).

Finally, the aromatic protons are responsible for the very broad band in the δ_H = 6.5–8.5 ppm region. The relative abundance of functional groups reported in Figure 6.6 indicates that DOM extracted from rainwater samples exhibit a relatively low protons aromatic content (2-7%) in that spectral region, which may be associated to a very low content of aromatic structures or to a very high degree of substitution of these structures.

The high ratio (≈1) between unsubstituted aliphatic protons (H-C) and aliphatic protons near functional groups (H-C-C=O; H-C-O) for all samples is indicative of the presence of highly oxidized structures. The present results suggest the presence of a complex mixture of hydroxyl-acids that give rise to broad overlapping signals. Model structures consisting of an aromatic core bearing substituted aliphatic chains (with –COOH, $-CH_2OH$, $-COCH_3$, or $-CH_3$ terminal groups) properly fit the ^1H NMR features observed in all extracted samples. These results are consistent with previous findings concerning the presence of macromolecular humic-like organic compounds in aerosol and wet deposition samples (Decesari et al., 2001; Decesari et al., 2005).

6.4 Conclusions

In this work, to assess the seasonal influence into the chemical properties of the DOM from rainwater collected in a coastal town, the isolation procedure based on sorption onto DAX-8 resin was applied to rainwater samples. This isolation procedure allowed recoveries of 14-78% of the original pooled rainwater DOC and the spectroscopic characteristics of the extracted DOM allowed the following conclusions:

1) The UV-visible and fluorescence characteristics revealed that the extracted DOM contains a complex mixture of organic compounds, predominating compounds with low degree of conjugation or aromaticity.
2) The ^1H NMR features showed that the DOM extracted from rainwater samples of all seasons consists of a complex mixture of hydroxylated compounds and carboxylic acids with a predominantly aliphatic character, and a minor component of aromatics.
3) The similarity of spectroscopic characteristics observed for the DOM extracted from rainwater in all seasons, allowed to propose a model of chemical structures that consist of an aromatic core bearing substituted aliphatic chains, with –COOH, $-CH_2OH$, $-COCH_3$, or $-CH_3$ terminal groups.

Our proposed model for chemical structures of extracted DOM from rainwater supplies a less detailed picture compared to individual compound speciation. Nevertheless, certainly provides more comprehensive and useful information for modelling purposes and is particularly helpful when rainwater of bulk chemical characteristics is desired.

The results reported in this study highlight the importance of, in the near future, to improve the analytical procedure of DOM isolation from rainwater, for being possible to complete the structural characterization of rainwater DOM and eventually for establishing a spectroscopic fingerprint of the whole DOM.

References

Chen, J., Gu, B., LeBoeuf, E.J., Pan, H., Dai, S., 2002. Spectroscopic characterization of the structural and functional properties of natural matter fractions. Chemosphere 48, 59–68.

Coble, P.G., Schultz, C.A., Mopper K., 1993. Fluorescence contouring analysis of DOC Intercalibration Experiment samples: a comparison of techniques. Mar. Chem. 41, 173-178.

Coble, P.G., 1996. Characterization of marine and terrestrial DOM in seawater using excitation emission matrix spectroscopy. Mar. Chem. 51, 325-346.

Coble, P.G., Del Castillo, C.E., Avril, B., 1998. Distribution and optical properties of CDOM in the Arabian Sea during the 1995 Southwest Monsoon. Deep-Sea Research II 45, 2195–2223.

Decesari, S., Facchini, M.C., Fuzzi, S., Tagliavini, E., 2000. Characterization of water-soluble organic compounds in atmospheric aerosols: a new approach. J. Geophys. Res. 105, 1481–1489.

Decesari, S., Facchini, M.C., Matta, E., Lettini, F., Mircea, M., Fuzzi, S., Tagliavini, E., Putaud, J.-P., 2001. Chemical features and seasonal variation of fine aerosol water-soluble organic compounds in the Po Valley, Italy. Atmos. Environ. 35, 3691-3699.

Decesari, S., Facchini, M.C., Fuzzi, S., McFiggans, G.B., Coe, H., Bower, K.N., 2005. The water-soluble organic component of size-segregated aerosol, cloud water and wet deposition from Jeju Island during ACE-Asia. Atmos. Environ. 39, 211–222.

Decesari, S., Fuzzi, S., Facchini, M.C., Mircea, M., Emblico, L., Cavalli, F., Maenhaut, W., Chi, X., Schkolnik, G., Falkovich, A., Rudich, Y., Claeys, M., Pashynska, V., Vas, G., Kourtchev, I., Vermeylen, R., Hoffer, A., Andreae, M.O., Tagliavini, E., Moretti, F., Artaxo, P., 2006. Characterization of the organic composition of aerosols from Rondônia, Brazil, during the LBA-SMOCC 2002 experiment and its representation through model compounds. Atmos. Chem. Phys. 6, 375–402.

Draxler, R.R., Rolph, G.D., 2003. HYSPLIT (Hybrid Single-Particle Langrangian Integrated Trajectory), www.arl.noaa.gov/HYSPLIT.php. NOAA Air Resources Laboratory, Silver Spring.

Duarte, R.M.B.O., Duarte, A.C., 2005a. Application of non-ionic solid sorbents (XAD resins) for the isolation and fractionation of watersoluble organic compounds from atmospheric aerosols. J. Atmos. Chem. 51, 79–93.

Duarte, R.M.B.O., Pio, C.A., Duarte, A.C., 2005b. Spectroscopic study of the water-soluble organic matter isolated from atmospheric aerosols collected under different atmospheric conditions. Anal. Chim. Acta 530, 7-14.

Gelencsér, A., Hoffer, A., Kiss, G., Tombácz, E., Kurdi, R., Bencze, L., 2003. In-situ formation of light-absorbing organic matter in cloud water. J. Atmos. Chem. 45, 25–33.

Helms, J.R., Stubbins, A., Ritchie, J.D., Minor, E.C., Kieber, D.J., Mopper, K., 2008. Absorption spectral slopes and slope ratios as indicators of molecular weight, source, and photobleaching of chromophoric dissolved organic matter. Limnology and Oceanography 53, 955–969.

Kieber, R.J., Whitehead, R.F., Reid, S.N., Willey, J.D., Seaton, P.J., 2006. Chromophoric dissolved organic matter (CDOM) in rainwater, Southeastern North Carolina, USA. J. Atmos. Chem. 54, 21-41.

Malcolm, R.L., 1991. Factors to be considered in the isolation and characterization of aquatic humic substances. In: Allard, B., Boren, H., Grimvall, A. (Eds.),

Humic Substances in the Aquatic and Terrestrial Environment: Proceedings of an International Symposium, Linlöping, Sweden, pp. 9–36.

Markager, S., Vincent, W.F., 2000. Spectral light attenuation and the absorption of UV and blue light in natural waters. Limnol. Oceanogr. 45, 642–650.

Miller, C., Gordon, K.G., Kieber, R.J., Willey, J.D., Seaton, P.J., 2009. Chemical characteristics of chromophoric dissolved organic matter in rainwater. Atmos. Environ. 43, 2497-2502.

Muller, C.L., Baker, A., Hutchinson, R., Fairchild, I.J., Kidd, C., 2008. Analysis of rainwater dissolved organic carbon compounds using fluorescence spectroscopy. Atmos. Environ. 42, 8036–8045.

Peuravuori, J., Pihlaja, K., 1997. Molecular size distribution and spectroscopic properties of aquatic humic substances. Anal. Chim. Acta 137, 133–149.

Peuravuori, J., Ingman, P., Pihlaja, K., Koivikko, R., 2001. Comparisons of sorption of aquatic humic matter by DAX-8 and XAD-8 resins from solid-state 13C NMR spectroscopy's point of view. Talanta 55, 733-742.

Pio, C.A., Salgueiro, M.L., Nunes, T.N., 1991. Seasonal and air-mass trajectory effects on rainwater quality at the South-Western European border. Atmos. Environ. 25A, 2259–2266.

Santos, P.S.M., Otero, M., Duarte, R.M.B.O., Duarte, A.C., 2009a. Spectroscopic characterization of dissolved organic matter isolated from rainwater. Chemosphere 74, 1053-101.

Santos, P.S.M., Duarte, R.M.B.O., Duarte, A.C., 2009b. Absorption and fluorescence properties of rainwater during the cold season at a town in Western Portugal. J. Atmos. Chem. 62, 45-57.

Santos, P.S.M., Otero, M., Filipe, O.M.S., Santos, E.B.H., Duarte, A.C., 2010a. Comparison between DAX-8 and C-18 solid phase extraction of rainwater dissolved organic matter. Talanta 83, 505–512.

Santos, P.S.M., Otero, M., Santos, E.B.H., Duarte, A.C., 2010b. Molecular fluorescence analysis of rainwater: effects of sample preservation. Talanta 82, 1616-1621,.

Senesi, N., Miano, T.M., Provenzano, M.R., Brunetti, G., 1989. Spectroscopic and compositional comparative characterization of I.H.S.S. reference and

standard fulvic and humic acids of various origins. Sci. Total Environ. 81, 143–156.

Wang, M.C., Liu, C.P., Sheu, B.H., 2004. Characterization of organic matter in rainfall, throughfall, stemflow, and streamwater from three subtropical forest ecosystems. J. Hydrol. 289, 275–285.

Willey, J.D., Kieber, R.J., Eyman, M.S., Avery, G.B., 2000. Rainwater dissolved organic carbon: concentrations and global flux. Global Biogeochem. Cy. 14, 139-148.

Williams, D.H., Fleming, I., 1973. Spectroscopic methods in organic chemistry, 2nd edn. McGraw-Hill, London, UK.

7. Chemical composition of rainwater at a coastal town on the southwest of Europe: What changes in 20 years?

Rainwater was collected at the Portuguese west coast between September 2008 and September 2009, and analysed for pH, conductivity, Cl^-, NO_3^-, SO_4^{2-}, and NH_4^+ concentrations. Results of rainwater chemical composition were compared with those obtained at the same site between 1986-1989. In both collection periods rainwater was predominantly (≈ 80 %) associated to oceanic air masses. The rainwater concentration of H^+ was in the same range than twenty years ago. In both periods the highest concentration of NH_4^+, NO_3^- and non sea-salt sulphate (NSS-SO_4^{2-}) were associated to air masses transported from central and northern Europe over the ocean, evidencing that these pollutants can be transported long distances from the sources even over the ocean. However, a clear decrease of NSS-SO_4^{2-} was observed in 2008-2009 relatively to 1986-1989, not only in samples with origin in central and northern Europe, but also in samples from Atlantic Ocean and Mediterranean. This decrease indicates that SO_2 emissions were reduced, which may be due to a lower content of sulphur in oil by-products. A decrease was also observed in NH_4^+ concentration for the samples from all the origins in 2008-2009. On the contrary an increase of NO_3^- concentration was observed for samples of all origins in 2008-2009 relatively to 1986-1989, which was particularly high (more than 3 fold) for samples with origin in Atlantic Ocean, suggesting the incorporation of this ion by rainout at the sampling site. The contribution of local sources is indeed suggested by the moderate negative correlation of NH_4^+, NO_3^- and NSS-SO_4^{2-} with rainwater volume. The high increase of NO_3^- concentration can be attributed to the increase of local vehicular and industrial emissions in the sampling area.

7.1 Introduction

Rain is an efficient scavenging process for pollutants present in the atmosphere and provides a path for them reaching terrestrial and aquatic ecosystems. Furthermore, depending on the substances removed from the atmosphere, acid rain can form, which constitutes one of the major global environmental problems because of its important impact on these ecosystems, especially on vegetation and aquatic environments (Huang et al., 2010).

The study of rainwater chemical composition not only provides relevant information on the source types that contribute to rainwater chemistry but also enhances the understanding of local and regional dispersion of pollutants (Zunckel et al., 2003). Thus, precipitation chemistry has received special attention during the last decade (Lee et al., 2000; Lara et al., 2001; Zunckel et al., 2003; Khare et al., 2004; Mouli et al., 2005; Arsene et al., 2007; Das et al., 2010; Huang et al., 2010).

Land-use and industrial activities are major driving forces in the ongoing process of atmospheric and rainwater chemistry alteration (Lara et al., 2001). However, the chemical composition of precipitation may be affected by different factors such as pollutant transport processes or meteorological conditions (Arsene et al., 2007).

Europe has experienced a remarkable population growth, a strong industrialization, an increment of concentrated animal feeding operations and an extensive deforestation since the 60s and 70s, so affecting the atmosphere quality. However, the south-western coast of Europe, frequently subjected to relatively clean air masses transported from the Atlantic Ocean, is presumably less affected by anthropogenic emissions from the European continent (Pio et al., 1991).

The present study reports on data of the chemical composition of precipitation in Aveiro, a town on the south-western coast of Europe. Rainwater was sampled between September 2008 and September 2009 and samples were analysed for pH, conductivity, Cl^-, NO_3^-, SO_4^{2-}, and NH_4^+ concentrations. The general characteristics of air masses during the sampling period were registered

and rain samples were classified according to the trajectory of the air masses. Results on rainwater chemical composition were compared with those obtained by Pio et al. (1991) for rain collected at the same site between 1986-1989.

7.2 Experimental

7.2.1 Rainwater sampling and analysis

Rainwater was collected at a sampling station (40º38' N, 8º39' W) located in the western part of the town of Aveiro, Portugal, between September 2008 and September 2009. Collection was carried out 70 cm above the ground, through glass funnels (30 cm diameter) into glass bottles (5 L). Sampling containers were left out open (at 8:30h local hour) in order to collect both wet and dry depositions on a 24 h basis. Prior to use, all glass materials were immersed for 30 min, in a solution of NaOH (0.1 M), then rinsed with distilled water, followed by another immersion for 24 hours in a solution of HNO_3 (4 M), and finally rinsed with ultrapure (Milli-Q) water. After collection, samples were transported to the laboratory and divided into two aliquots. One aliquot was used for the measurements of pH and electrical conductivity (EC). A pH meter with a glass ROSS electrode (model 81-02) was used and was calibrated before each measurement with low ionic strength 4.10 and 6.97 buffers (ionic strength adjuster, Pure Water pHisa^{TM} from Thermo Orion, was added to each sample). Measurements were ± 0.01 pH units in the pH 4 range and ± 0.03 for samples with pH of 5 or above. The EC measurement was done by a WTW analyser (model LF 530). The other aliquot was filtered through sterilized nitrocellulose filters (MILLIPORE) of 0.45 µm pore size and frozen until the analysis of ion composition.

The anions Cl^-, NO_3^- and SO_4^{2-} were measured by ion chromatography, using a Dionex 2000i equipped with HPIC-4G4A guard column, HPIC-AS4A separating column, AMMS anion self-regenerating suppressor and conductivity detector. The samples were injected through 100 µL sample loop and eluted at 2.0

mL min^{-1} using Na_2CO_3 (2.25 mM)/$NaHCO_3$ (2.8 mM) in ultrapure water. The integrator SPECTRA Physics SPA 290 was used to collect data from Dionex. The corresponding peak areas were then used to calculate anions concentrations. These concentrations were measured with a relative standard deviation lower than 5%. Detection limits, corresponding to three times the residual standard deviation of the linear regression divided by the sensitivity of the method, were 0.54 µg mL^{-1} for Cl^-, 0.46 µg mL^{-1} for NO_3^- and 0.37 µg mL^{-1} for SO_4^{2-}. Non sea salt sulphate (NSS-SO_4^{2-}) that does not come from sea spray, was calculated from total SO_4^{2-} concentration by subtracting a fraction of 0.103 of chloride level, where 0.103 is the ratio, in equivalent basis, between sulphate and chloride in seawater (Pio et al., 1991).

Ammonium ion (NH_4^+) was determined spectrophotometrically using a Shimadzu (Dusseldorf, Germany) Model UV 210PC. Samples were colored with indophenol blue (citrate method; Hall and Lucas, 1981) and absorbance of the colored solution was measured at 640 nm in a quartz cell with 1.0 cm optical thickness. The ammonium concentration was measured with a relative standard deviation lower than 10%. Detection limit of ammonium concentration, corresponding to three times the residual standard deviation of the linear regression divided by the sensitivity of the method, was 49.3 µg L^{-1}.

7.2.2 Air mass trajectories and meteorological data

The general characteristics of air masses during the sampling period were evaluated by using Hybrid Single Particle Lagrangian Integrated Trajectory Model (HYSPLIT) developed by Draxler and Rolph (2003) at the National Oceanic Atmospheric Administration—Air Resources Laboratory (NOAA/ARL) of United States (available at www.arl.noaa.gov/HYSPLIT.php). Trajectories were generated for a 48 h hind-cast starting at 10 and 500 m level, calculated every 6 h for each rain day.

Rainwater samples were classified into five groups according to the trajectory of the air masses: class A contains samples related with air masses transported from the Atlantic Ocean; class B represents samples with origins in

central and northern parts of industrialized Europe and transported to Portugal over the ocean; class C contains samples with similar origins to those of class B, but transported over land; class D refers to air masses transported from north Africa and the Mediterranean across the Iberian Peninsula; samples in which less than 60 % of the air-mass trajectories were from one section only, and had therefore a mixed origin, were agglomerated into class M. A similar way of classification had been previously used by Pio et al. (1991) for rainwater also collected at Aveiro (Portugal).

A meteorological station at the sampling site (at 10 m height) supplied the following information during the sampling period: direction and velocity of wind, relative humidity, air temperature and amount of precipitation.

7.3 Results and discussion

Forty rainwater samples (417 mm) were collected during the sampling period (September 2008-September 2009), which represents approximately 50 % of the total precipitation (839 mm). 81 % of the collected rainwater amount (RA) was related with air masses transported from the Atlantic Ocean (class A) while the rest of precipitation was related to air masses with anthropogenic and terrestrial contributions (3 % of class B; and 16 % of class D). A similar distribution was obtained considering all the rainfall events of the sampling period instead of only those corresponding to the samples collected. Pio et al. (1991) had also observed that around 80 % of the rainfall amount in Aveiro between 1986 and 1989 was associated to air masses with an Atlantic origin. Regarding to the RA by season for the collected samples, 13 % occurred in summer (96 % of class A, 1 % of class B and 3 % of class D), 21 % in autumn (80 % of class A, 13 % of class B and 7 % of class D), 35 % in winter (66 % of class A and 34 % of class D) and 31 % in spring (91 % of class A and 9 % of class D).

The pH values of individual rainwater samples collected ranged from 4.48 to 6.88. Considering 5.60 as the neutral pH of unpolluted water due to equilibrium with atmospheric CO_2 (Seinfeld and Pandis, 1998), 57.5 % of samples were acid

rain, while 42.5 % of samples had pH above 5.60, which indicates the presence of alkaline species in the rainwater. However, the volume-weighted average (VWA) pH of all collected samples was 5.4. Since due to dissolution of naturally existing CO_2, NO_x and SO_2 in the cloud and rain drops, the VWA pH of rainwater in an unperturbed atmosphere is expected to be between 5.0 and 5.6 (Seinfeld and Pandis, 1998), the value obtained indicates that rain is not acid at the sampling site. Furthermore, 10 % of the collected samples had pH < 5.0, of which 7.5 % were associated to terrestrial air masses and consequently values may be related to anthropogenic emissions.

The VWA concentrations of the ions H^+, NH_4^+, NO_3^-, Cl^-, SO_4^{2-}, NSS-SO_4^{2-} and also of EC are shown in table 7.1. The ion Cl^- has much higher VWA concentrations than the rest of the ions, which is related to the proximity of the Atlantic Ocean (Seinfeld and Pandis, 1998). The lowest VWA concentration of H^+ was observed in winter as well as for NH_4^+, NO_3^- and NSS-SO_4^{2-}, suggesting that during this season rainwater was less affected by anthropogenic contributions. The highest VWA concentrations of H^+ and also of NO_3^- were observed in spring, which may indicate that HNO_3 was an important contributor for the higher values of H^+ observed in this season.

Table 7.1 also compare the values of the VWA concentration of ions in rainwater collected in 2008-2009 with values obtained in 1986-1989 and published by Pio et al. (1991). It is to highlight that, the ratio NSS-SO_4^{2-}/NO_3^-, which is usually used to indicate the relative contributions of NSS-SO_4^{2-} and NO_3^- ions to the precipitation acidity corresponding to 2008-2009 is much lower (<1) than those obtained twenty years before (>1). The most well known rainwater acidification mechanism is through SO_2 and NO_x, which, once emitted into the atmosphere, are oxidized to H_2SO_4 and HNO_3 through both gas and aqueous phase processes. Thus, this change on the anion composition of the wet precipitation indicates that the air pollution resulting from NO_x emission is more significant than it was during the eighties. Although the concentration of NO_3^-, which may be largely derived from the vehicle emissions and industrial activities (Arsene et al., 2007), is higher in 2008-2009 than it was 20 years ago, the NSS-SO_4^{2-} concentration is lower, which may be related to the reduction of the sulphur content in oil by-products

Table 7.1 Rainwater VWA EC and ion concentrations for the total of samples collected, for the samples of the hydrological year (2009) and for samples collected at the different seasons. Results obtained in this study are compared with those reported in the literature for rainwater collected in Aveiro and for rainwater collected at different sites on the south-western coast of Europe.

Local	Sampling period	EC ($\mu S\ cm^{-1}$)	H^+ ($\mu Eq\ L^{-1}$)	NH_4^+ ($\mu Eq\ L^{-1}$)	Cl^- ($\mu Eq\ L^{-1}$)	NO_3^- ($\mu Eq\ L^{-1}$)	SO_4^{2-} ($\mu Eq\ L^{-1}$)	NSS-SO_4^{2-} ($\mu Eq\ L^{-1}$)	NSS-SO_4^{2-}/ NO_3^-
This study, Aveiro (Portugal)	Total (n = 40)	18.7 (± 2.8)	5.1 (± 0.9)	13.2 (± 1.5)	145 (± 26.2)	28.0 (± 3.4)	23.5 (± 2.9)	8.6 (± 1.2)	0.37 (± 0.06)
	2009 (n = 35)	19.2 (± 3.0)	4.7 (± 0.9)	11.9 (± 1.5)	154 (± 28.0)	25.7 (± 3.5)	23.4 (± 3.2)	7.7 (± 1.2)	0.40 (± 0.07)
	Autumn (n = 11)	24.6 (± 5.1)	5.6 (± 2.1)	18.0 (± 3.2)	202 (± 57.5)	29.2 (±7.5)	31.5 (± 4.9)	10.8 (± 1.9)	0.54 (± 0.12)
	Winter (n = 12)	21.3 (± 5.6)	3.5 (± 1.0)	10.0 (± 2.0)	189 (± 53.5)	15.7 (± 3.0)	22.7 (± 6.0)	3.3 (± 0.8)	0.20 (± 0.09)
	Spring (n = 11)	14.1 (± 4.7)	6.3 (± 2.0)	12.4 (± 3.4)	87.8 (± 35.4)	39.5 (± 5.8)	20.1 (± 5.3)	11.1 (± 2.8)	0.36 (± 0.13)
	Summer (n =6)	13.2 (± 5.1)	5.3 (± 5.3)	15.8 (± 4.6)	66.9 (± 30.8)	31.6 (± 12.2)	20.8 (± 6.1)	13.9 (± 3.3)	0.62 (± 0.25)
Aveiro[1] (Portugal)	1986	21.6	5.9	23.7	217	8.6	36.9	23.4	3.2
	1987	23.8	6.5	22.3	127	7.4	39.5	27.3	5.2
	1988	27.9	4.0	18.5	159	9.0	41.5	25.2	4.7
	1989	24.6	3.8	27.9	130	14.8	68.5	56.1	4.4
	Autumn	22.0	5.1	20.2	136	7.3	33.8	25.1	3.9
	Winter	29.0	4.1	25.3	214	10.1	54.5	33.9	4.4
	Spring	22.8	7.2	23.9	119	11.4	49.3	37.0	5.0
	Summer	19.4	4.2	15.6	47	12.9	36.3	31.4	3.1
Illas Cíes[2] (Spain)	1999	163.7	0.15*	566	610	27	197	134*	5.0*
Lourizán[2] (Spain)	1999	44.6	0.63*	138	121	14	65	52*	3.7*
Xunqueira[2] (Spain)	1999	41.7	1.0*	42	210	19	70	48*	2.5*

n = number of rain events.
Standard deviations are indicated between brackets.
* approximate values (calculated with base in ion concentrations available in paper)
[1] Data from Pio et al. (1991).
[2] Data from Vázquez et al. (2003).

(Migliavacca et al., 2005). Therefore, the contribution of H_2SO_4 to the acidity of rainwater has decreased, contrary to that of HNO_3, the H^+ concentration in 2008-2009 being in the range of values for the years 1986-1989. As in the case of SO_4^{2-}, NH_4^+ ion concentration also decreased comparatively with the eighties values, which may be related to the reduction of the sources, such as the volatilization of animal residues, natural loss by plants and agricultural activities. Finally, the Cl^- concentrations are in the range of the values obtained during 1986-1989.

Table 7.1 also compares the ionic composition of rainwater determined in the present study with values reported for rainwater collected at three coastal sites (< 15 km of sea) also on the south-western coast of Europe (Vázquez et al., 2003). The concentrations of the ions NH_4^+, Cl^-, SO_4^{2-} and NSS-SO_4^{2-} in rainwater from these three coastal sites were much higher than those obtained in Aveiro, suggesting higher anthropogenic and maritime influences. On other hand, the concentrations of NO_3^- are comparable to those found in rainwater collected at Aveiro, so anthropogenic sources, mainly vehicle emissions and industrial activities, must have a similar contribution. The concentrations of H^+ in rainwater collected at the three sites considered are much lower than those in Aveiro. As concentrations of the NH_4^+ were much higher, so, very probably, NH_3 emissions have contributed to acid neutralization, resulting in lower values of H^+ concentrations. The NSS-SO_4^{2-} for the three coastal sites considered are also much higher than those obtained in the present study. Besides, the ratios NSS-SO_4^{2-}/NO_3^- for the three coastal sites considered are much higher than the ratio determined in this study, but close to the values obtained by Pio et al. (1991) for Aveiro twenty years ago. This indicates that pollution levels resulting from NSS-SO_4^{2-}emissions were lower in Aveiro during 2008-2009 than they were at the three considered sites.

Table 7.2 shows the values of VWA for EC and ions concentrations corresponding to rainwater classified according to air masses trajectories.

Table 7.2 Rainwater VWA ion concentrations and EC calculated corresponding to rainwater classified by dominant air masses trajectories.

Air mass	EC ($\mu S\ cm^{-1}$)	H^+ ($\mu Eq\ L^{-1}$)	NH_4^+ ($\mu Eq\ L^{-1}$)	Cl^- ($\mu Eq\ L^{-1}$)	NO_3^- ($\mu Eq\ L^{-1}$)	SO_4^{2-} ($\mu Eq\ L^{-1}$)	NSS-SO_4^{2-} ($\mu Eq\ L^{-1}$)	NSS-SO_4^{2-}/ NO_3^-
Class A (n=30)	21.0 (± 3.1)	4.2 (± 0.9)	10.3 (± 1.0)	171.9 (± 29.6)	28.3 (± 3.8)	25.5 (± 3.2)	7.8 (± 0.9)	0.42 (± 0.07)
Class B (n=3)	15.6 (± 8.4)	23.2 (± 15.4)	29.6 (± 17.5)	34.3 (± 21.1)	47.3 (± 3.8)	25.1 (± 13.4)	21.6 (± 12.8)	0.48 (± 0.23)
Class D (n=7)	8.1 (± 1.9)	6.3 (± 2.2)	24.3 (± 6.0)	30.7 (± 7.4)	23.2 (± 7.2)	13.5 (± 5.8)	11.1 (± 5.4)	0.21 (± 0.12)
Class A[1]	24.7	2.7	19.2	166	7.9	44.2	29.9	4.2
Class B[1]	24.2	41.0	41.5	141	38.3	75.4	60.9	1.9
Class D[1]	13.8	2.9	42.7	30	13.5	35.2	33.0	3.4

n = number of rain events.
[1] Data from Pio et al. (1991).

Rainwater related with air masses with a maritime trajectory (class A) had the lowest VWA values of acidity, NH_4^+ and NSS-SO_4^{2-}. On other hand, due to the maritime trajectories, class A rainwater had the highest VWA values of SO_4^{2-}, Cl^- and EC, suggesting that the majority of the SO_4^{2-} and Cl^- have a maritime origin and contribute significantly to EC values. Rainwater from class A is associated with air masses transported directly from the Atlantic Ocean so should approximately represent background concentrations. However, the NO_3^- VWA concentrations present in class A rainwater were high and considerably higher than twenty years ago, while NSS-SO_4^{2-}/NO_3^- ratio was significantly lower in 2008-2009. Since Aveiro is placed in an area that has being subjected to strong industrialization and population growth with an associated vehicular traffic, these results may be related to the increase of local anthropogenic emissions that are added to the atmosphere and rapidly washed by rainwater with short time for dilution. As it may be also observed in Table 7.2, when air masses come from continental Europe and transported over the ocean (class B), the rainwater acidity presented the highest VWA level, which had also been pointed out by Pio et al. (1991). The VWA concentrations of NH_4^+, NO_3^- and NSS-SO_4^{2-} are also highest in class B rainwater, which suggest that these ions are efficiently transported long from the sources over the sea. Thus, the higher acidity observed in rain events from class B is probably due to HNO_3 and H_2SO_4. The obtained results suggest

that, when air masses come from continental Europe transported over the ocean, there is not enough bases such as NH_3 to neutralize the emitted and produced acidity. Rainwater related to air masses from Mediterranean area (class D) had the lowest VWA values of EC, Cl^-, SO_4^{2-} and NO_3^- and the intermediate VWA values of acidity, NH_4^+ and NSS-SO_4^{2-}, suggesting small oceanic and terrestrial/pollutant input when compared with the air masses from continental Europe, transported over the ocean (class B). It is important to point out, that higher dispersion of values (standard deviation) was also observed for class B rainwater than for class A and class D rainwater (Table 7.2), possibly because samples of class B had terrestrial and maritime contributions with variable weights.

Table 7.3 shows the Pearson correlation coefficients for RA, EC and the concentrations of the ions H^+, NH_4^+, Cl^-, NO_3^-, SO_4^{2-} and NSS-SO_4^{2-}.

Table 7.3 Pearson correlation coefficients for rainwater volume, EC and ions concentrations.

	RA	EC	H^+	NH_4^+	Cl^-	NO_3^-	SO_4^{2-}	NSS-SO_4^{2-}
RA	1.000							
EC	-0.325 (0.040)	1.000						
H^+	-0.014 (0.933)	-0.274 (0.087)	1.000					
NH_4^+	-0.491 (0.001)	0.118 (0.467)	0.177 (0.275)	1.000				
Cl^-	-0.229 (0.154)	0.973 (0.000)	-0.352 (0.026)	-0.067 (0.682)	1.000			
NO_3^-	-0.441 (0.004)	0.141 (0.387)	0.180 (0.267)	0.451 (0.003)	0.028 (0.865)	1.000		
SO_4^{2-}	-0.477 (0.002)	0.916 (0.000)	-0.235 (0.144)	0.437 (0.005)	0.816 (0.000)	0.308 (0.053)	1.000	
NSS-SO_4^{2-}	-0.485 (0.002)	0.148 (0.361)	0.111 (0.496)	0.852 (0.000)	-0.066 (0.684)	0.488 (0.001)	0.524 (0.001)	1.000

The values between brackets are the significance levels.

Table 7.4 presents the source apportionment of ions in rainwater performed by factor analysis using SPSS Statistics 18.0 (SPSS Inc.), where the initial factors were extracted from a data set containing the ion composition associated to the

various samples and also to EC and RA, using the principal components algorithm followed by Varimax rotation.

Table 7.4 Varimax rotated factor matrix and communalities of metals in rainwater samples.

Metal	Factor 1	Factor 2	Factor 3	Communalities
RA	-0.32	**-0.66**	-0.08	0.54
EC	**0.98**	0.12	-0.00	0.98
H^+	-0.24	0.08	**0.92**	0.91
NH_4^+	-0.02	**0.92**	0.03	0.84
Cl^-	**0.99**	-0.08	-0.13	0.99
NO_3^-	0.14	**0.62**	0.38	0.56
SO_4^{2-}	**0.85**	0.47	-0.13	0.96
NSS-SO_4^{2-}	0.02	**0.94**	-0.03	0.88
% Variance	36	35	13	

As shown in Table 7.4, three factors were sufficient to explain 84% of the variance, and the communalities of the variables were higher than 0.5, what means that the retention of the three factors was sufficient to explain the majority of the variance of the variables. Factor 1 explains 36% of the total variance and has high loadings for EC, Cl^-, and SO_4^{2-}. Moreover, the EC showed a significant positive correlation with Cl^- ($p = 0.026$) and SO_4^{2-} ($p = 0.144$), indicating that Cl^- and SO_4^{2-} contribute significantly to EC values, while Cl^- and SO_4^{2-} also correlate positively and significantly ($p < 0.001$), suggesting that most of sulphate has a sea salt origin. Thus, results suggest that factor 1 is associated with marine sources (Sakihama et al., 2008). Factor 2, which explains 35% of total variance, has high loadings for RA, NH_4^+, NO_3^- and NSS-SO_4^{2-}, with a negative loading for RA. In addition, RA showed a moderate negative correlation with NH_4^+ ($p = 0.001$), NO_3^- ($p = 0.004$), and NSS-SO_4^{2-} ($p = 0.002$). These findings suggest that the concentrations of the ions NH_4^+, NO_3^- and NSS-SO_4^{2-} increased when the rainwater amount decreased, suggesting that these ions have been incorporated into the rainwater mainly by below-cloud scavenging of airborne particulate matter, highlighting the possibility of local influences. On other hand, the association of NH_4^+, NO_3^- and NSS-SO_4^{2-} in the second component together with the positive correlation of NH_4^+ with NO_3^- ($p = 0.003$) and NSS-SO_4^{2-} ($p < 0.001$), suggest acid

neutralization by NH_3 emissions with the consequent presence of ammonium sulphate and ammonium nitrate in rain. The NSS-SO_4^{2-} concentrations do also have a moderately positive correlation with NO_3^- concentrations (p=0.001), which may be attributed to some similar anthropogenic sources of their precursor gases SO_2 and NO_x and to their similar behaviour in precipitation (Hu et al., 2003; Zhang et al., 2007). The above results suggest that the second factor is associated with anthropogenic sources. Relatively to factor 3, it has a very high loading for H^+ and explains 13% of variance. Furthermore, the H^+ concentrations are not correlated with any of the ions analysed. Although the acidity of rainwater depends on the concentrations of acid-forming ions, it also depends on the concentrations of alkaline species, which had already been identified (Santos et al., 2008), and which may neutralize the acidity. The high loading for H^+ in the factor 3 suggests that complex processes of acid neutralization occur and, because of that, it is not possible to correlate H^+ with any of the other variables.

7.4 Conclusions

The chemical composition of rainwater collected between September 2008 and September 2009 in Aveiro, on the southwest coast of Europe, was compared with that collected at the same site 20 years ago. The results highlighted that at both sampling periods about 80 % of precipitation in Aveiro was associated to oceanic air masses, this is, associated to clean air masses.

1) In both periods the ion Cl^- had much higher VWA concentration than H^+, NH_4^+, NO_3^-, SO_4^{2-}, which is in agreement with the predominance of rain associated to oceanic air masses and related to the proximity of sampling site to the Atlantic Ocean.
2) The rainwater VWA concentration of H^+ in 2008-2009 was in the same range as twenty years ago. With respect to VWA concentrations of NH_4^+ and NSS-SO_4^{2-}, they were lower than twenty years ago, while the VWA concentration of NO_3^- was higher.

3) As observed in 1986-1989, in 2008-2009 the rainwater related to air masses from industrialized Europe showed the highest VWA concentrations of NH_4^+, NO_3^- and NSS-SO_4^{2-}, evidencing that these ions were efficiently transported long distances from the sources over the ocean. Moreover, in 2008-2009 the rainwater associated to air masses from the Atlantic Ocean also presented particularly high VWA concentration of NO_3^-, which reflects the influence of local emissions on rainwater composition.
4) Correlation coefficients analysis and factor analysis confirmed that the presence of NH_4^+, NO_3^- and NSS-SO_4^{2-} were mainly derived from anthropogenic sources and incorporated into the rainwater mainly by below-cloud scavenging of airborne particulate matter.
5) Since the sampling site is in an area that has being subjected to strong industrialization and vehicular traffic, the increase of NO_3^- concentrations in twenty years may be related with the increase of local NO_x emissions that are added to the atmosphere and washed by rainwater. On other hand, the decrease of NH_4^+ VWA concentrations may be due to the decrease of agricultural activities in the sampling area, while the decrease of SO_4^{2-} VWA concentrations may be associated with the reduction of SO_2 emissions due to the lower content of sulphur in oil by-products.

References

Arsene, C., Olariua, R.I., Mihalopoulos, N., 2007. Chemical composition of rainwater in the northeastern Romania, Iasi region (2003–2006). Atmos. Env. 41, 9452–9467.

Das, N., Das R., Chaudhury, G.R., Das, S.N., 2010. Chemical composition of precipitation at background level. Atmos. Res. 95, 108-113.

Draxler, R.R., Rolph, G.D., 2010. HYSPLIT (HYbrid Single-Particle Lagrangian Integrated Trajectory) Model access via NOAA ARL READY Website (http://ready.arl.noaa.gov/HYSPLIT.php). NOAA Air Resources Laboratory, Silver Spring, MD.

Hall, A., Lucas, M.F.M.B., 1981. Analysis of ammonia in brackish waters by indophenol blue technique: comparison of two alternative methods. Rev. Port. Quím. 23, 205-211.

Han, G., Liu, C.-Q., 2006. Strontium isotope and major ion chemistry of the rainwaters from Guiyang, Guizhou Province, China. Sci. Total Environ. 364, 165–174.

Hu, G.P., Balasubramanian, R., Wu, C.D., 2003. Chemical characterization of rainwater at Singapore. Chemosphere 51, 747–755.

Huang, X.-F., Li, X., He, L.-Y., Feng, N., Hu, M., Niu, Y.-W., Zeng, L.-W., 2010. 5-year study of rainwater chemistry in a coastal mega-city in South China. Atmos. Res. 97, 185-193.

Lara, L.B.L.S., Artaxo, P., Martinelli, L.A., Victoria, R.L., Camargo, P.B., Krusche, A., Ayers, G.P., Ferraz, E.S.B., Ballester, M.V., 2001. Chemical composition of rainwater and anthropogenic influences in the Piracicaba River Basin, Southeast Brazil. Atmos. Env. 35, 4937-4945.

Migliavacca, D., Teixeira, E.C., Wiegand, F., Machado, A.C.M., Sanchez, J., 2005. Atmospheric precipitation and chemical composition of an urban site, Guaíba hydrographic basin, Brazil. Atmos. Env. 39, 1829-1844.

Mouli, P.C., Mohan, S.V., Reddy, S.J., 2005. Rainwater chemistry at a regional representative urban site: influence of terrestrial sources on ionic composition. Atmos. Env. 39, 999-1008.

Pio, C.A., Salgueiro, M.L., Nunes, T.V., 1991. Seasonal and air-mass trajectory effects on rainwater quality at the south-western european border. Atmos. Env. 25A, 2259-2266.

Sakihama, H., Ishiki, M., Tokuyama, A., 2008. Chemical characteristics of precipitation in Okinawa Island, Japan. Atmos. Env. 42, 2320-2335.

Santos, P.S.M., Pereira, M.E., Duarte, A.C., 2008. Source assessment of metals in rainwater events at a town in western Portugal. Fresenius Environ. Bull. 17(12b), 2232-2239.

Seinfeld, J.H., Pandis, S.N., 1998. Atmospheric Chemistry and Physics: From air pollution to climate change. 1st ed., John Wiley & Sons, Inc, New York (United States of America).

Vázquez, A., Costoya, M., Pena, R.M., García, S., Herrero, C., 2003. A rainwater quality monitoring network: a preliminary study of the composition of rainwater in Galicia (NW Spain). Chemosphere 51, 375-386.

Yang, R., Hayashi, K., Zhu, B., Li, F., Yan, X., 2010. Atmospheric NH_3 and NO_2 concentration and nitrogen deposition in an agricultural catchment of Eastern China. Sci. Total Environ. 408, 4624–4632.

Zhang, M., Wang, S., Wu, F., Yuan, X., Zhang, Y., 2007. Chemical compositions of wet precipitation and anthropogenic influences at a developing urban site in southeastern China. Atmos. Res. 84, 311-322.

Zunckel, M., Saizar, C., Zarauz, J., 2003. Rainwater composition in northeast Uruguay. Atmos. Env. 37, 1601-1611.

8. Final considerations

The study of the chemical features of rainwater collected in Aveiro, a coastal town at the southwest of Europe, is the first study that explores the effects of the seasonality and air mass trajectories on organic chemical composition of rainwater in Europe, and certainly one of the very first carried out in the world. Besides, the inorganic composition of rainwater was determined and compared with to results found twenty years ago in order to detect any changes that might have occurred.

The collection of rainwater samples is a process that depends on the occurrence of precipitation events. On other hand, in this work the various analytical techniques applied to rainwater demanded high volumes of samples and an efficient time management for preservation of samples in their best conditions, that is, to maintain their representativeness.

The importance of studying the dissolved organic carbon (DOC) in rainwater was highlighted only recently by Willey et al. (2000). A review of the work published since then revealed that different filtration and preservation procedures have been adopted for the study of the dissolved organic fraction of rainwater. Taking this into account and due to the low concentrations of organic matter in rainwater the importance of analytical accuracy and the care needed to avoid contamination throughout the various analytical steps, the effects of filtration and preservation of dissolved organic matter (DOM) were evaluated using fluorescence spectroscopy. A comparison between two of the most used pore sizes of filters, 0.22 and 0.45 μm, was performed and results showed that DOM fluorescence properties of both filtrates are similar when analyses are performed at the day of sampling. The present study proposes the filtration of rainwater

through 0.45 µm to separate the soluble from the particulate organic matter since this is the pore size which attains consensus for the operational definition of DOM. With respect to preservation, rainwater samples should be kept at 4 ºC at dark, but no longer than four days after collection.

Another point studied in this work was the procedure of DOM isolation from rainwater. Two procedures, presented in the literature for the isolation of DOM from rainwater, the DAX-8 and the C-18 ones, were compared by using UV-visible and molecular fluorescence spectroscopies. Both isolation procedures extracted preferentially the larger molecular weight (MW) fraction of DOM. However, protein-like and humic-like compounds were equally extracted from rainwater by the C-18 procedure and the extracted DOM was representative of the bulk. On other hand, DAX-8 extracts preferentially the humic-like compounds relative to the protein-like ones, and this procedure may be useful when the interest is studying the humic fraction. Therefore, this was the isolation procedure adopted for the subsequent DOM isolation and extraction.

The rainwater collected between September 2008 and September 2009 in Aveiro, was mostly (80%) associated to oceanic air masses, while the rest was related to air masses with more anthropogenic and terrestrial characteristics.

The effects of seasonality and air mass trajectory on the bulk DOM of rainwater in Aveiro were first assessed applying the UV-visible and molecular fluorescence spectroscopies to the whole sample, without previous DOM extraction, besides DOC content of samples was determined. Chromophoric dissolved organic matter (CDOM) revealed to be an important contributor to the organic matter in rainwater. Rainwater showed similar optical properties to other natural waters, suggesting that compounds that make part of rainwater CDOM may be derived from surface sources and/or from processes that originate or modify humic-like substances in the atmosphere. Rainwater from summer and autumn showed a higher content of CDOM and DOC than rainwater from winter and spring. Furthermore, rainwater of spring, summer and autumn presented lower MW, which may be due to the higher DOM photodegradation occurring in these seasons, relatively to winter.

Rainwater related to air masses from maritime sources showed lower content of CDOM than rainwater with terrestrial/anthropogenic contributions. Moreover, rainwater samples associated to air masses from continental Europe, and transported over the ocean, presented higher CDOM content, and more predominance of organic compounds with higher degree of conjugation or aromaticity than rainwater from the Mediterranean area, indicating that anthropogenic/terrestrial sources are important contributors of CDOM which was efficiently transported long from the sources over the sea. The CDOM of maritime origin was the one with lowest degree of conjugation or aromaticity.

The influence of the seasons into the chemical properties of the humic-like fraction of the rainwater DOM by the procedure based on adsorption onto DAX-8 resin, was also assessed in this work, using UV-visible, molecular fluorescence and ^{1}H NMR spectroscopies. This isolation procedure allowed recoveries of 14-78 % of the original pooled rainwater DOC, showing that the methodology must be improved in order to obtain higher recoveries of DOM. The results showed that the DOM extracted from rainwater samples, consists of a complex mixture of hydroxylated compounds and carboxylic acids with a predominantly aliphatic character, containing a minor component of aromatic protons. As 80 % of the rainwater is of marine origin the majority of the samples isolated had that origin, and only two were from the Mediterranean area. The similarity of properties observed along all the seasons for all isolated humic-like substances suggest that these properties may be considered a fingerprint of these substances in the rainwater of Aveiro.

Relatively to the ionic composition of rainwater collected between September 2008 and September 2009 in Aveiro, the results were compared with those of rainwater collected at the same site between 1986 and 1989. Results showed that in both sampling periods the Cl^- volume weighted average (VWA) concentration was much higher than that of the ions H^+, NH_4^+, NO_3^-, SO_4^{2-}, due to the predominance of rain associated to oceanic air masses and due to the sampling local being coastal in nature. Moreover, comparing the VWA concentrations of the remaining ions in 2008-2009 with those found twenty years ago the following conclusions were drawn: H^+ concentration was in the same

range; NH_4^+ and NSS-SO_4^{2-} concentrations were lower, and the decrease of NH_4^+ VWA concentrations may be due to the decrease of agricultural activities in the sampling area, while the decrease of NSS-SO_4^{2-} VWA concentrations may be associated to the reduction of SO_2 emissions due to the lower content of sulphur in oil by-products; NO_3^- concentration was higher, which was attributed to the increase of industrialization in Aveiro as well as to the increase of vehicular traffic during the latest 20 years. In 2008-2009 the concentrations of NO_3^- were also high when air masses came from the Atlantic Ocean, highlighting the contribution of local sources to the ionic composition of rainwater. Correlation coefficients analysis and factor analysis confirmed that the presence of NH_4^+, NO_3^- and NSS-SO_4^{2-} were mainly derived from anthropogenic sources and incorporated into the rainwater mainly by below-cloud scavenging of airborne particulate matter. As observed in 1986-1989, in 2008-2009 the rainwater related to air masses from industrialized Europe showed also the highest VWA concentrations of NH_4^+, NO_3^- and NSS-SO_4^{2-}, evidencing that these ions were efficiently transported from long distances sources over the ocean, suggesting that the anthropogenic sources of these ions in industrialized Europe affect the ionic composition of rainwater at the southwest of Europe.

The determination of chemical composition of rainwater in Aveiro, provides an understanding of the source types that contribute to rainwater chemistry, and enhances the understanding of the local and regional dispersion of pollutants and their potential impacts on ecosystems through deposition processes.

The presence of CDOM, which has been demonstrated to be an important component of rainwater, may exert a determining effect on higher and lower atmospheric absorption of solar radiation, which consequently affects the amount of solar radiation absorbed by the planet and thus affect the climate. Besides the presence of chromophoric compounds in rainwater DOM affects the terrestrial and aquatic ecosystems, and consequently human beings, since rainwater is the predominant source of all the freshwater.

The rainwater in Aveiro was predominantly associated to clean air masses, Atlantic air masses, and the composition of rainwater should reflect the background levels. However, rainwater removed atmospheric aerosols from the

atmosphere in the region of Aveiro, which highlights the importance of the contribution of local sources for the chemical composition of rainwater. When air masses came from the industrialized parts of Europe rainwater was enriched with high contents of chemical constituents, both organic and inorganic, highlighting the contribution of anthropogenic/terrestrial sources. On the other hand, when air masses came from the Mediterranean area a low content of chemical constituents were found, but higher than was observed for the maritime air masses, indicating a low anthropogenic/terrestrial sources when compared with the rainwater of industrialized Europe.

The anthropogenic/terrestrial air masses have consequences for local human life due to the potential to alter the environmental distribution of chemical pollutants. In the future, the research will move towards on the identification of individual chemical constituents in rainwater and their specific sources, in order to anticipating the effects of chemical pollution in the rapidly changing environment, and identifying and mitigating effects in humans and most vulnerable ecosystems.

References

Willey, J.D., Kieber, R.J., Eyman, M.S., Avery, G.B., 2000. Rainwater dissolved organic carbon: concentrations and global flux. Global Biogeochem. Cy. 14, 139-148.

Annex I. Air mass trajectories calculated for events whose rainwater was not collected between September 2008 and September 2009

The air mass trajectories calculated for rainwater events whose rainwater was not collected between September 2008 and September 2009 are presented below. The air mass trajectories generated for a 48 h hind-cast starting at 500 m level, were calculated every 6 h for each rainwater sample.

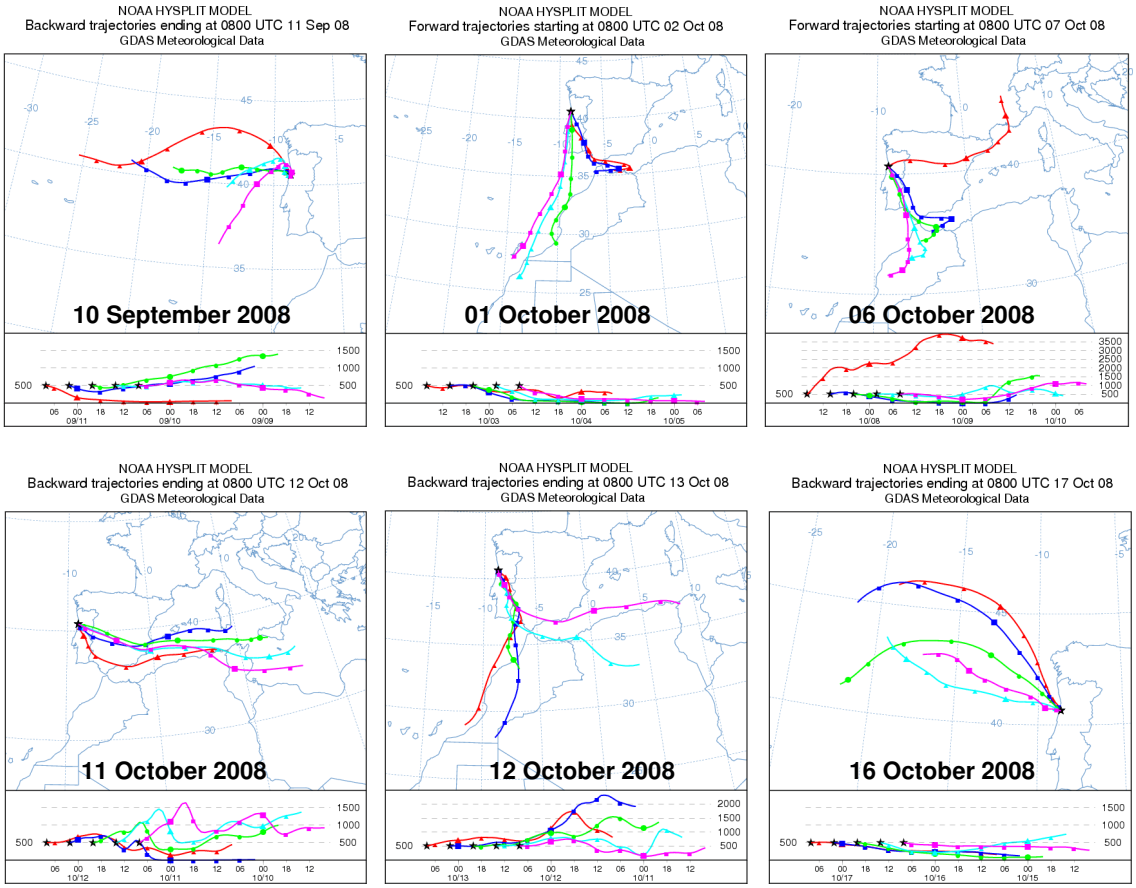

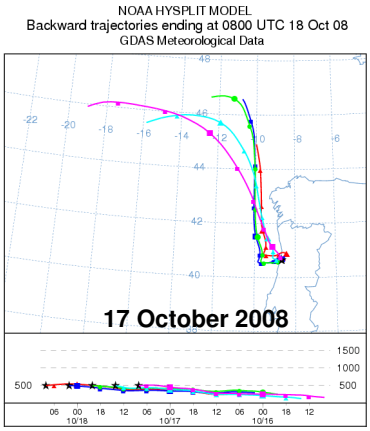
NOAA HYSPLIT MODEL
Backward trajectories ending at 0800 UTC 18 Oct 08
GDAS Meteorological Data
17 October 2008

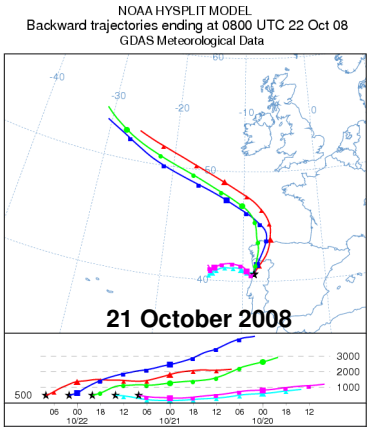
NOAA HYSPLIT MODEL
Backward trajectories ending at 0800 UTC 22 Oct 08
GDAS Meteorological Data
21 October 2008

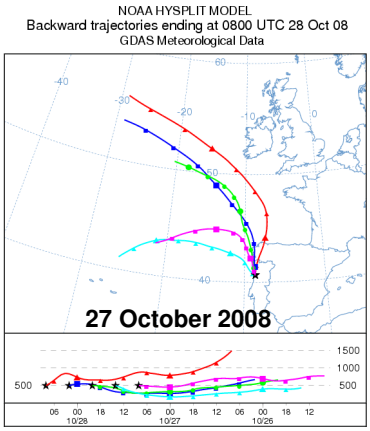
NOAA HYSPLIT MODEL
Backward trajectories ending at 0800 UTC 28 Oct 08
GDAS Meteorological Data
27 October 2008

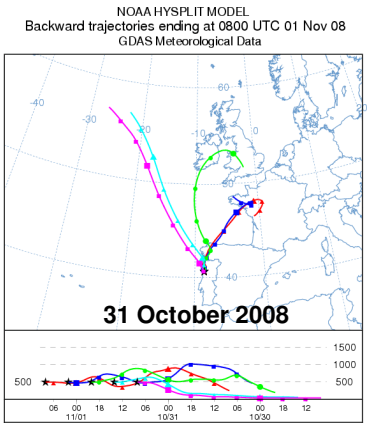
NOAA HYSPLIT MODEL
Backward trajectories ending at 0800 UTC 01 Nov 08
GDAS Meteorological Data
31 October 2008

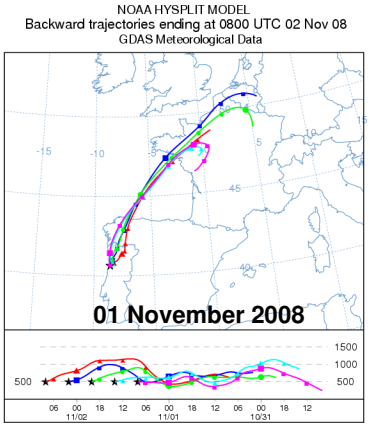
NOAA HYSPLIT MODEL
Backward trajectories ending at 0800 UTC 02 Nov 08
GDAS Meteorological Data
01 November 2008

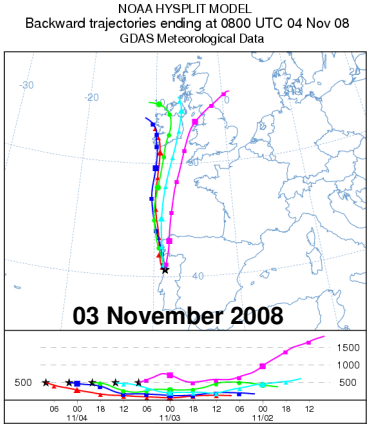
NOAA HYSPLIT MODEL
Backward trajectories ending at 0800 UTC 04 Nov 08
GDAS Meteorological Data
03 November 2008

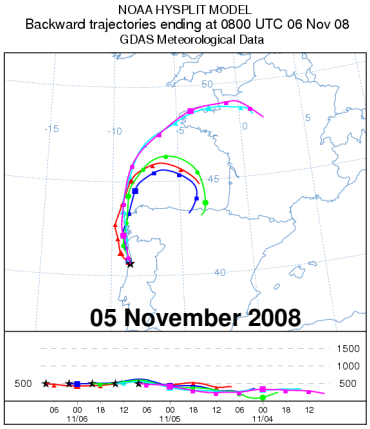
NOAA HYSPLIT MODEL
Backward trajectories ending at 0800 UTC 06 Nov 08
GDAS Meteorological Data
05 November 2008

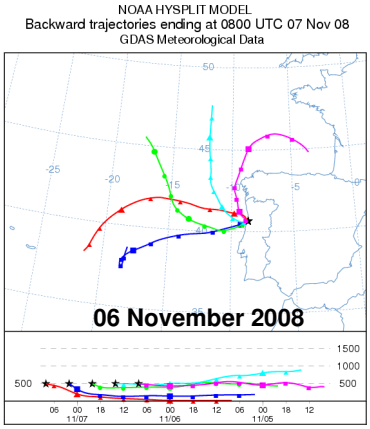
NOAA HYSPLIT MODEL
Backward trajectories ending at 0800 UTC 07 Nov 08
GDAS Meteorological Data
06 November 2008

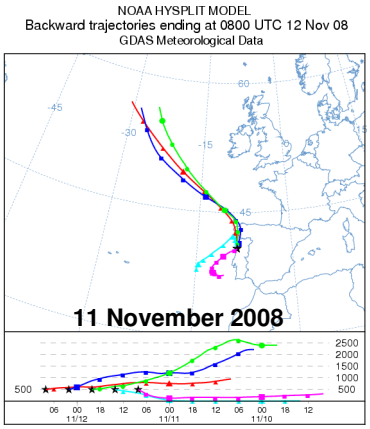
NOAA HYSPLIT MODEL
Backward trajectories ending at 0800 UTC 12 Nov 08
GDAS Meteorological Data
11 November 2008

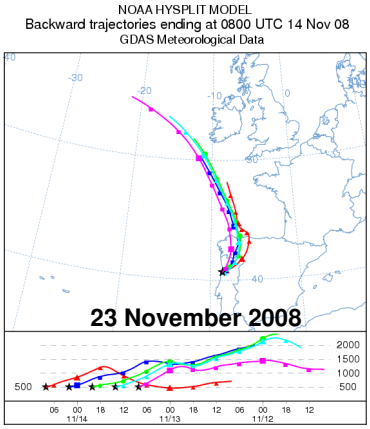
NOAA HYSPLIT MODEL
Backward trajectories ending at 0800 UTC 14 Nov 08
GDAS Meteorological Data
23 November 2008

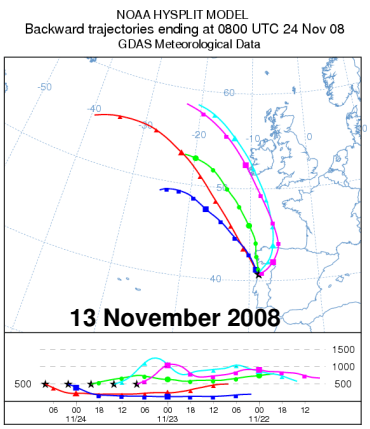
NOAA HYSPLIT MODEL
Backward trajectories ending at 0800 UTC 24 Nov 08
GDAS Meteorological Data
13 November 2008

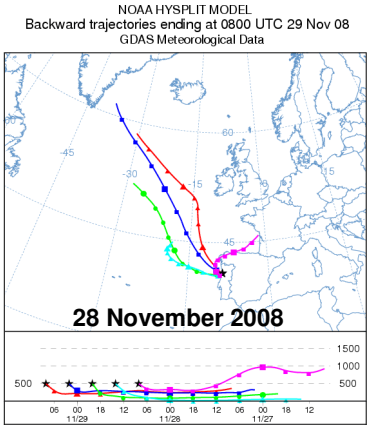
NOAA HYSPLIT MODEL
Backward trajectories ending at 0800 UTC 29 Nov 08
GDAS Meteorological Data
28 November 2008

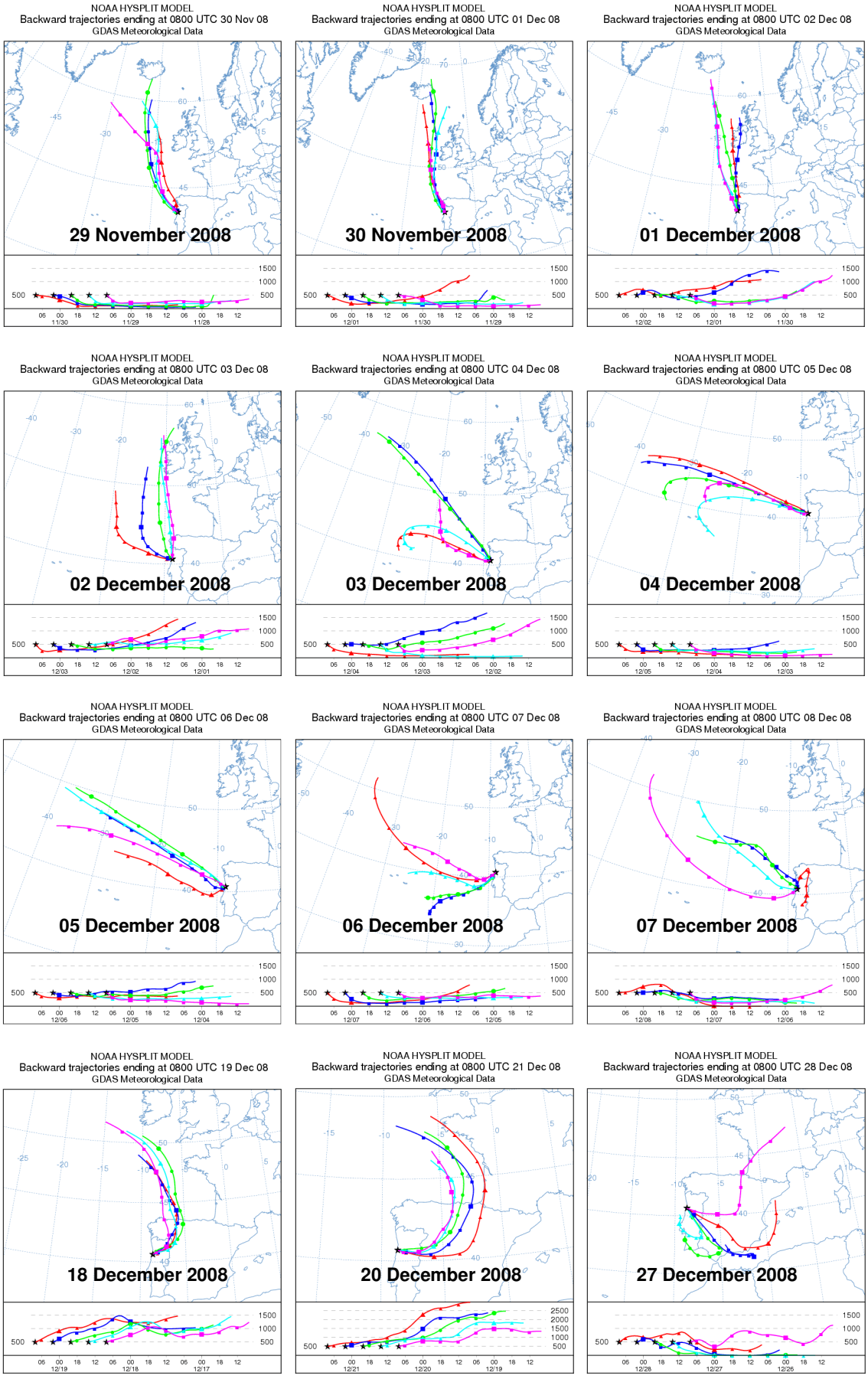
NOAA HYSPLIT MODEL
Backward trajectories ending at 0800 UTC 30 Nov 08
GDAS Meteorological Data
29 November 2008
NOAA HYSPLIT MODEL
Backward trajectories ending at 0800 UTC 01 Dec 08
GDAS Meteorological Data
30 November 2008
NOAA HYSPLIT MODEL
Backward trajectories ending at 0800 UTC 02 Dec 08
GDAS Meteorological Data
01 December 2008
NOAA HYSPLIT MODEL
Backward trajectories ending at 0800 UTC 03 Dec 08
GDAS Meteorological Data
02 December 2008
NOAA HYSPLIT MODEL
Backward trajectories ending at 0800 UTC 04 Dec 08
GDAS Meteorological Data
03 December 2008
NOAA HYSPLIT MODEL
Backward trajectories ending at 0800 UTC 05 Dec 08
GDAS Meteorological Data
04 December 2008
NOAA HYSPLIT MODEL
Backward trajectories ending at 0800 UTC 06 Dec 08
GDAS Meteorological Data
05 December 2008
NOAA HYSPLIT MODEL
Backward trajectories ending at 0800 UTC 07 Dec 08
GDAS Meteorological Data
06 December 2008
NOAA HYSPLIT MODEL
Backward trajectories ending at 0800 UTC 08 Dec 08
GDAS Meteorological Data
07 December 2008
NOAA HYSPLIT MODEL
Backward trajectories ending at 0800 UTC 19 Dec 08
GDAS Meteorological Data
18 December 2008
NOAA HYSPLIT MODEL
Backward trajectories ending at 0800 UTC 21 Dec 08
GDAS Meteorological Data
20 December 2008
NOAA HYSPLIT MODEL
Backward trajectories ending at 0800 UTC 28 Dec 08
GDAS Meteorological Data
27 December 2008

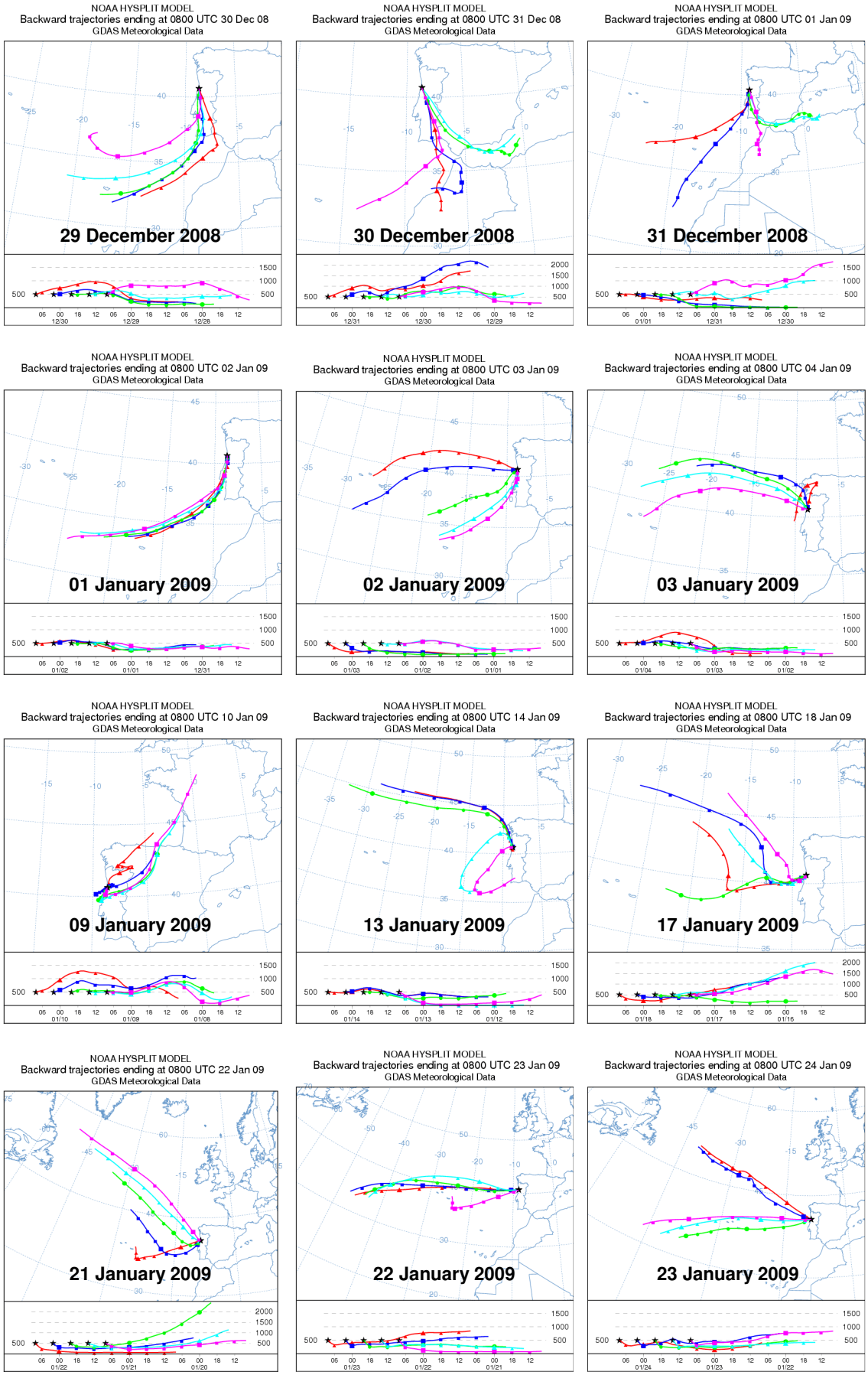
NOAA HYSPLIT MODEL
Backward trajectories ending at 0800 UTC 30 Dec 08
GDAS Meteorological Data
29 December 2008
NOAA HYSPLIT MODEL
Backward trajectories ending at 0800 UTC 31 Dec 08
GDAS Meteorological Data
30 December 2008
NOAA HYSPLIT MODEL
Backward trajectories ending at 0800 UTC 01 Jan 09
GDAS Meteorological Data
31 December 2008
NOAA HYSPLIT MODEL
Backward trajectories ending at 0800 UTC 02 Jan 09
GDAS Meteorological Data
01 January 2009
NOAA HYSPLIT MODEL
Backward trajectories ending at 0800 UTC 03 Jan 09
GDAS Meteorological Data
02 January 2009
NOAA HYSPLIT MODEL
Backward trajectories ending at 0800 UTC 04 Jan 09
GDAS Meteorological Data
03 January 2009
NOAA HYSPLIT MODEL
Backward trajectories ending at 0800 UTC 10 Jan 09
GDAS Meteorological Data
09 January 2009
NOAA HYSPLIT MODEL
Backward trajectories ending at 0800 UTC 14 Jan 09
GDAS Meteorological Data
13 January 2009
NOAA HYSPLIT MODEL
Backward trajectories ending at 0800 UTC 18 Jan 09
GDAS Meteorological Data
17 January 2009
NOAA HYSPLIT MODEL
Backward trajectories ending at 0800 UTC 22 Jan 09
GDAS Meteorological Data
21 January 2009
NOAA HYSPLIT MODEL
Backward trajectories ending at 0800 UTC 23 Jan 09
GDAS Meteorological Data
22 January 2009
NOAA HYSPLIT MODEL
Backward trajectories ending at 0800 UTC 24 Jan 09
GDAS Meteorological Data
23 January 2009

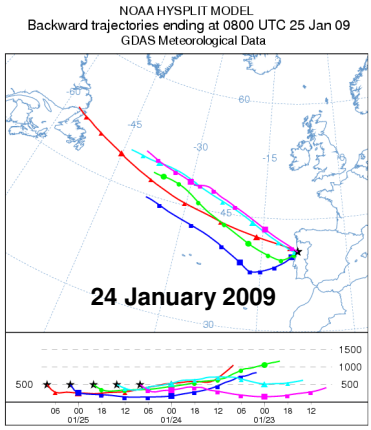
NOAA HYSPLIT MODEL
Backward trajectories ending at 0800 UTC 25 Jan 09
GDAS Meteorological Data
24 January 2009

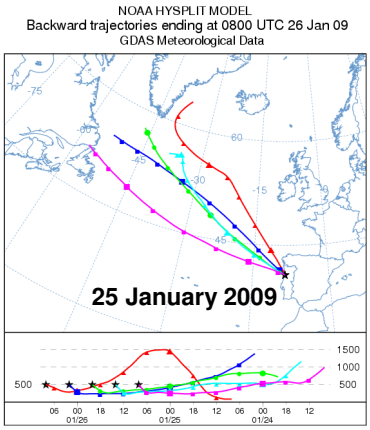
NOAA HYSPLIT MODEL
Backward trajectories ending at 0800 UTC 26 Jan 09
GDAS Meteorological Data
25 January 2009

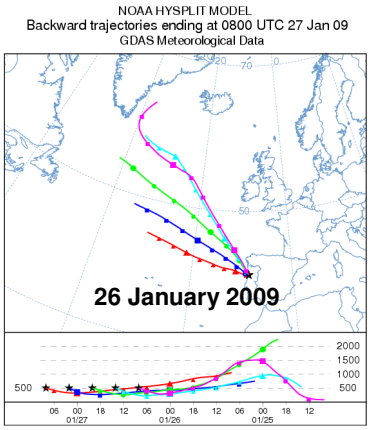
NOAA HYSPLIT MODEL
Backward trajectories ending at 0800 UTC 27 Jan 09
GDAS Meteorological Data
26 January 2009

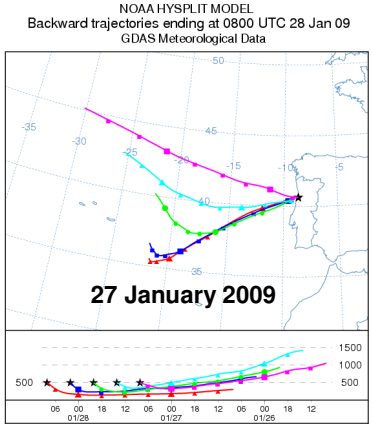
NOAA HYSPLIT MODEL
Backward trajectories ending at 0800 UTC 28 Jan 09
GDAS Meteorological Data
27 January 2009

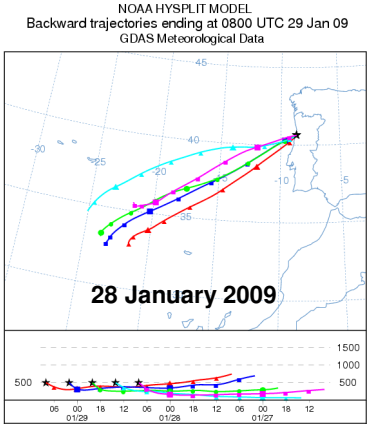
NOAA HYSPLIT MODEL
Backward trajectories ending at 0800 UTC 29 Jan 09
GDAS Meteorological Data
28 January 2009

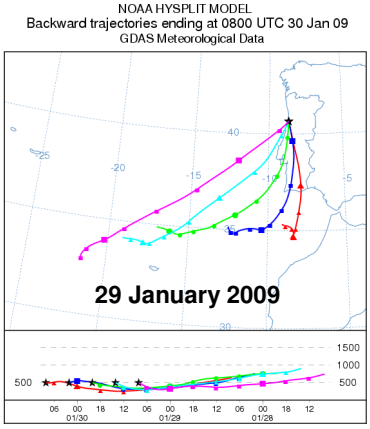
NOAA HYSPLIT MODEL
Backward trajectories ending at 0800 UTC 30 Jan 09
GDAS Meteorological Data
29 January 2009

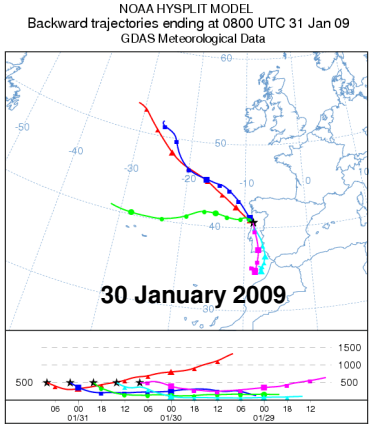
NOAA HYSPLIT MODEL
Backward trajectories ending at 0800 UTC 31 Jan 09
GDAS Meteorological Data
30 January 2009

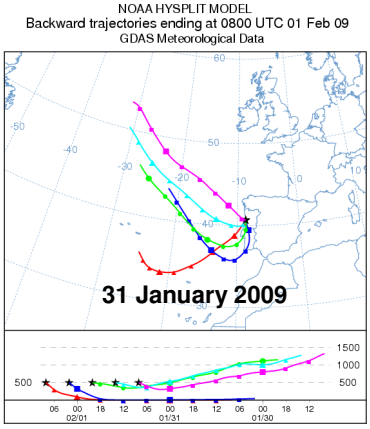
NOAA HYSPLIT MODEL
Backward trajectories ending at 0800 UTC 01 Feb 09
GDAS Meteorological Data
31 January 2009

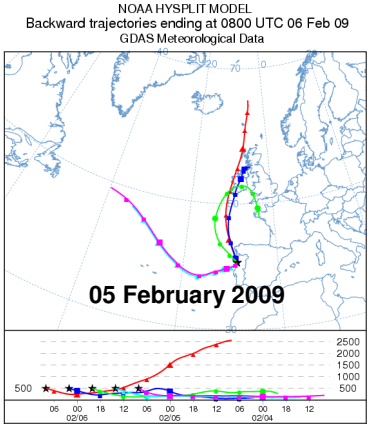
NOAA HYSPLIT MODEL
Backward trajectories ending at 0800 UTC 06 Feb 09
GDAS Meteorological Data
05 February 2009

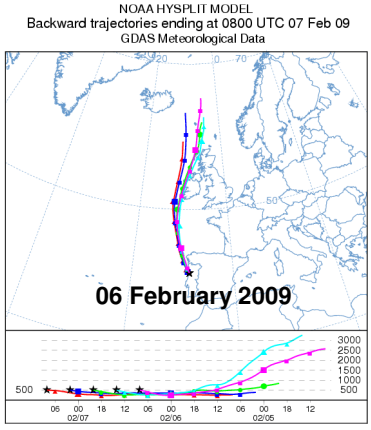
NOAA HYSPLIT MODEL
Backward trajectories ending at 0800 UTC 07 Feb 09
GDAS Meteorological Data
06 February 2009

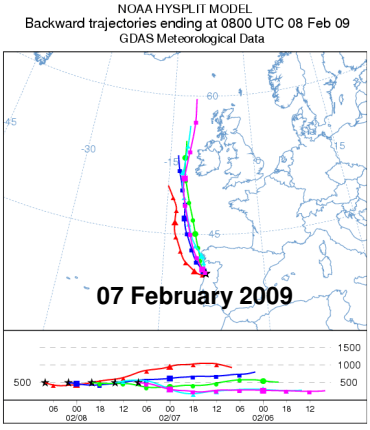
NOAA HYSPLIT MODEL
Backward trajectories ending at 0800 UTC 08 Feb 09
GDAS Meteorological Data
07 February 2009

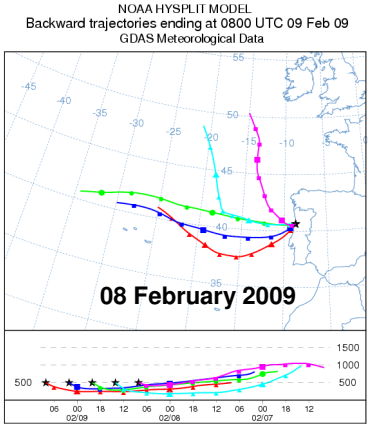
NOAA HYSPLIT MODEL
Backward trajectories ending at 0800 UTC 09 Feb 09
GDAS Meteorological Data
08 February 2009

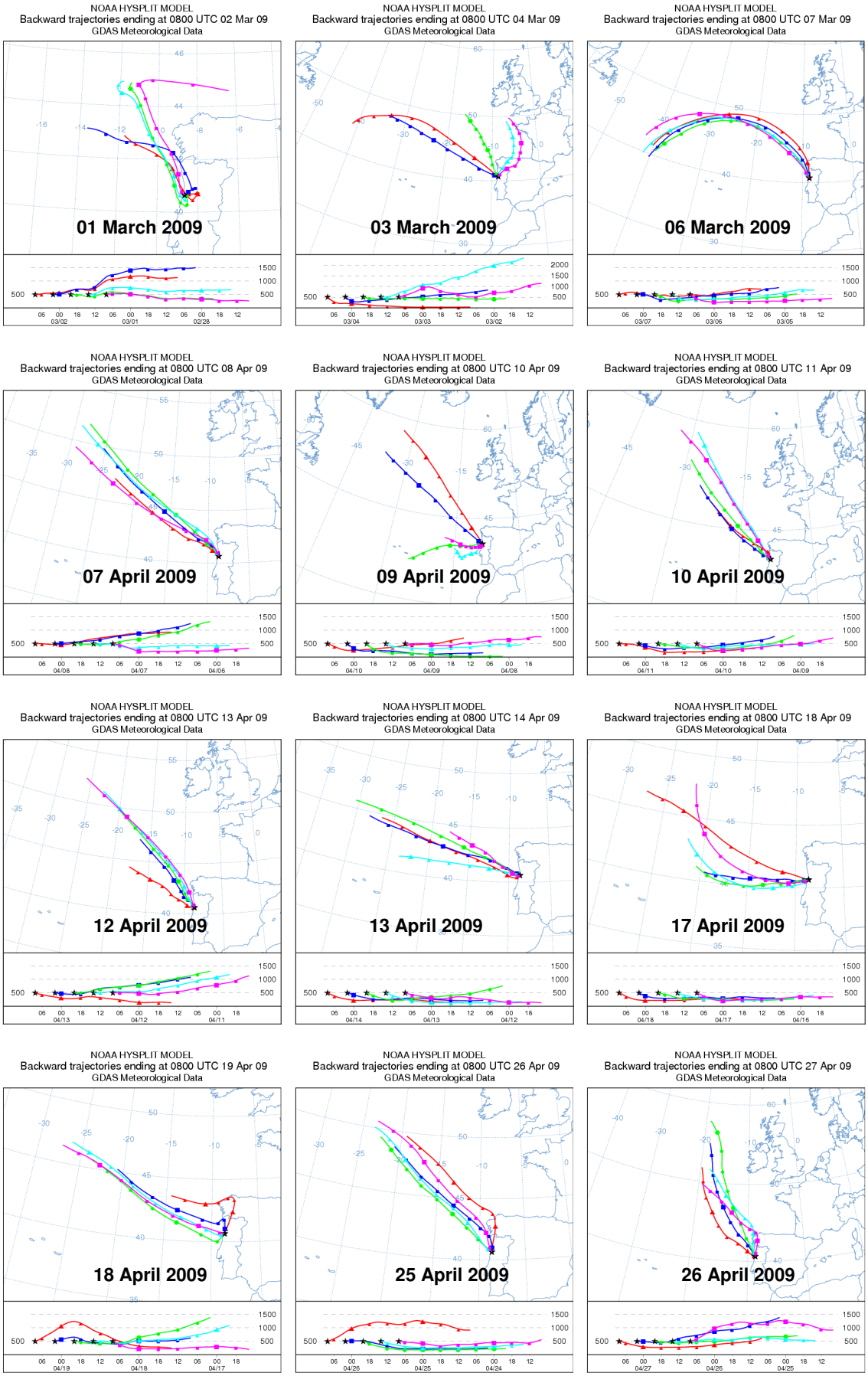
NOAA HYSPLIT MODEL
Backward trajectories ending at 0800 UTC 02 Mar 09
GDAS Meteorological Data
01 March 2009
NOAA HYSPLIT MODEL
Backward trajectories ending at 0800 UTC 04 Mar 09
GDAS Meteorological Data
03 March 2009
NOAA HYSPLIT MODEL
Backward trajectories ending at 0800 UTC 07 Mar 09
GDAS Meteorological Data
06 March 2009
NOAA HYSPLIT MODEL
Backward trajectories ending at 0800 UTC 08 Apr 09
GDAS Meteorological Data
07 April 2009
NOAA HYSPLIT MODEL
Backward trajectories ending at 0800 UTC 10 Apr 09
GDAS Meteorological Data
09 April 2009
NOAA HYSPLIT MODEL
Backward trajectories ending at 0800 UTC 11 Apr 09
GDAS Meteorological Data
10 April 2009
NOAA HYSPLIT MODEL
Backward trajectories ending at 0800 UTC 13 Apr 09
GDAS Meteorological Data
12 April 2009
NOAA HYSPLIT MODEL
Backward trajectories ending at 0800 UTC 14 Apr 09
GDAS Meteorological Data
13 April 2009
NOAA HYSPLIT MODEL
Backward trajectories ending at 0800 UTC 18 Apr 09
GDAS Meteorological Data
17 April 2009
NOAA HYSPLIT MODEL
Backward trajectories ending at 0800 UTC 19 Apr 09
GDAS Meteorological Data
18 April 2009
NOAA HYSPLIT MODEL
Backward trajectories ending at 0800 UTC 26 Apr 09
GDAS Meteorological Data
25 April 2009
NOAA HYSPLIT MODEL
Backward trajectories ending at 0800 UTC 27 Apr 09
GDAS Meteorological Data
26 April 2009

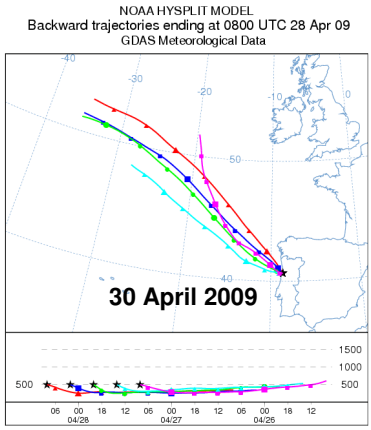
NOAA HYSPLIT MODEL
Backward trajectories ending at 0800 UTC 28 Apr 09
GDAS Meteorological Data
30 April 2009

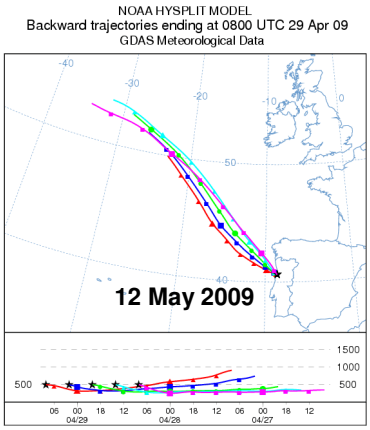
NOAA HYSPLIT MODEL
Backward trajectories ending at 0800 UTC 29 Apr 09
GDAS Meteorological Data
12 May 2009

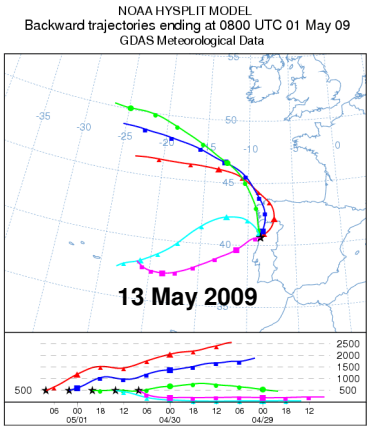
NOAA HYSPLIT MODEL
Backward trajectories ending at 0800 UTC 01 May 09
GDAS Meteorological Data
13 May 2009

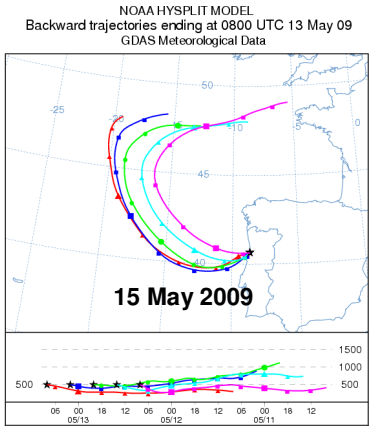
NOAA HYSPLIT MODEL
Backward trajectories ending at 0800 UTC 13 May 09
GDAS Meteorological Data
15 May 2009

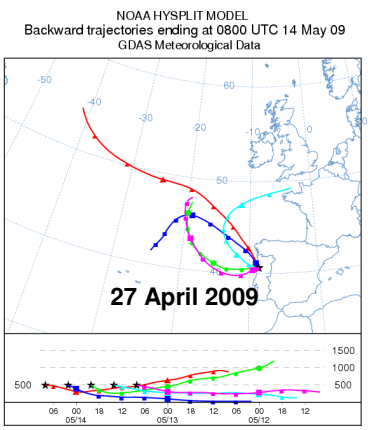
NOAA HYSPLIT MODEL
Backward trajectories ending at 0800 UTC 14 May 09
GDAS Meteorological Data
27 April 2009

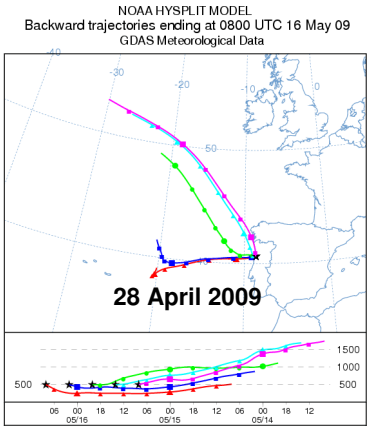
NOAA HYSPLIT MODEL
Backward trajectories ending at 0800 UTC 16 May 09
GDAS Meteorological Data
28 April 2009

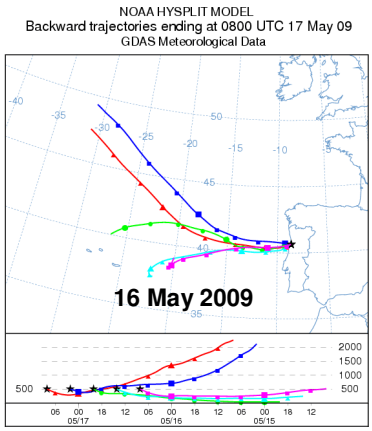
NOAA HYSPLIT MODEL
Backward trajectories ending at 0800 UTC 17 May 09
GDAS Meteorological Data
16 May 2009

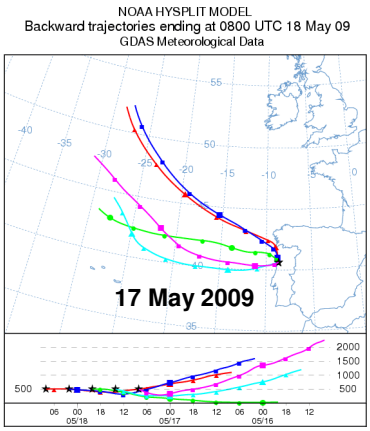
NOAA HYSPLIT MODEL
Backward trajectories ending at 0800 UTC 18 May 09
GDAS Meteorological Data
17 May 2009

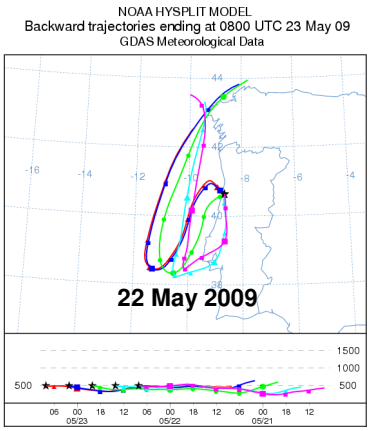
NOAA HYSPLIT MODEL
Backward trajectories ending at 0800 UTC 23 May 09
GDAS Meteorological Data
22 May 2009

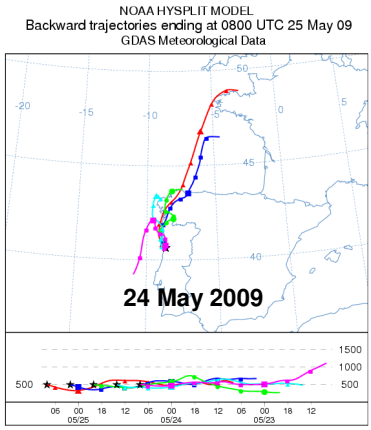
NOAA HYSPLIT MODEL
Backward trajectories ending at 0800 UTC 25 May 09
GDAS Meteorological Data
24 May 2009

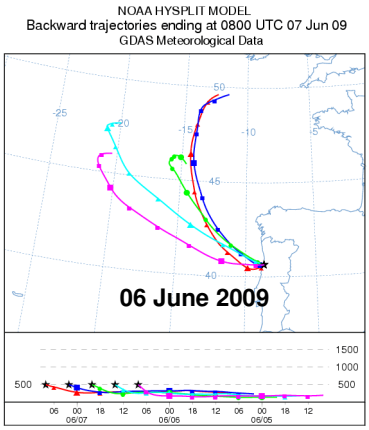
NOAA HYSPLIT MODEL
Backward trajectories ending at 0800 UTC 07 Jun 09
GDAS Meteorological Data
06 June 2009

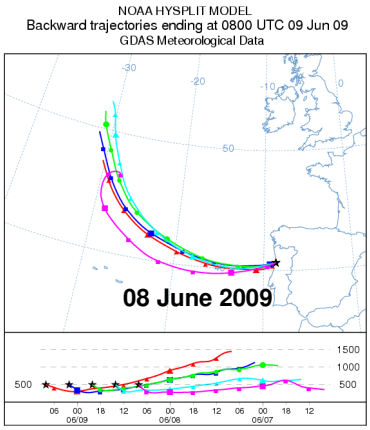
NOAA HYSPLIT MODEL
Backward trajectories ending at 0800 UTC 09 Jun 09
GDAS Meteorological Data
08 June 2009

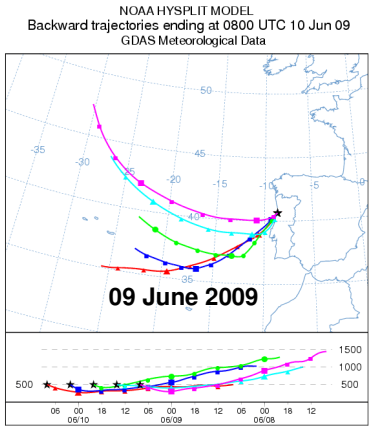
NOAA HYSPLIT MODEL
Backward trajectories ending at 0800 UTC 10 Jun 09
GDAS Meteorological Data
09 June 2009

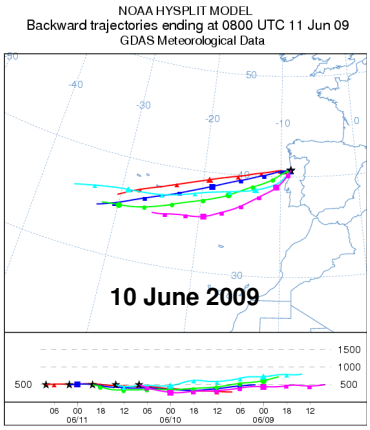
NOAA HYSPLIT MODEL
Backward trajectories ending at 0800 UTC 11 Jun 09
GDAS Meteorological Data
10 June 2009

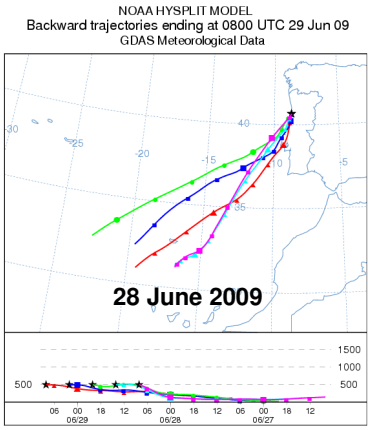
NOAA HYSPLIT MODEL
Backward trajectories ending at 0800 UTC 29 Jun 09
GDAS Meteorological Data
28 June 2009

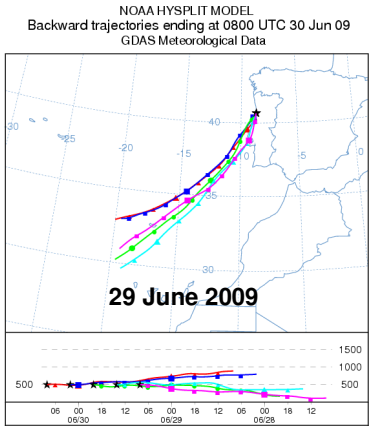
NOAA HYSPLIT MODEL
Backward trajectories ending at 0800 UTC 30 Jun 09
GDAS Meteorological Data
29 June 2009

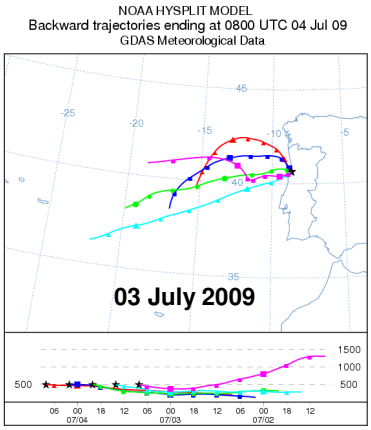
NOAA HYSPLIT MODEL
Backward trajectories ending at 0800 UTC 04 Jul 09
GDAS Meteorological Data
03 July 2009

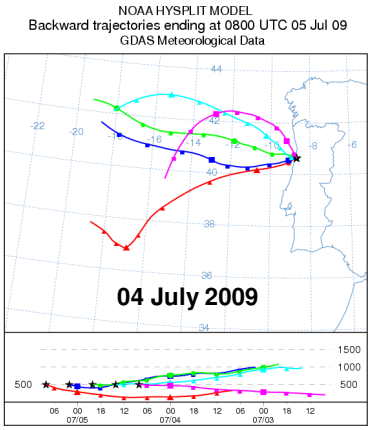
NOAA HYSPLIT MODEL
Backward trajectories ending at 0800 UTC 05 Jul 09
GDAS Meteorological Data
04 July 2009

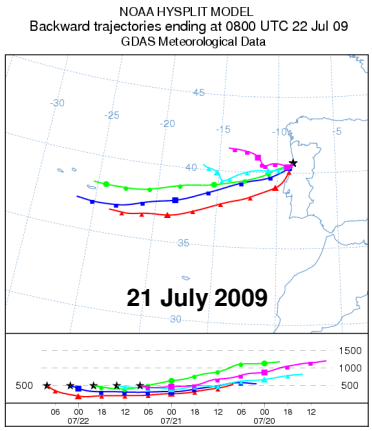
NOAA HYSPLIT MODEL
Backward trajectories ending at 0800 UTC 22 Jul 09
GDAS Meteorological Data
21 July 2009

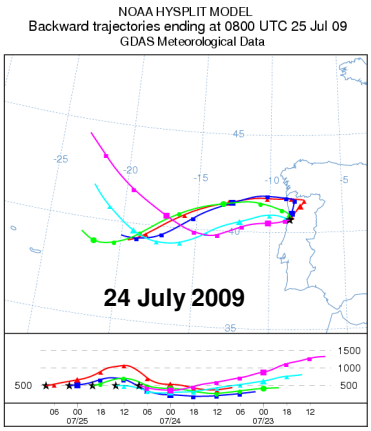
NOAA HYSPLIT MODEL
Backward trajectories ending at 0800 UTC 25 Jul 09
GDAS Meteorological Data
24 July 2009

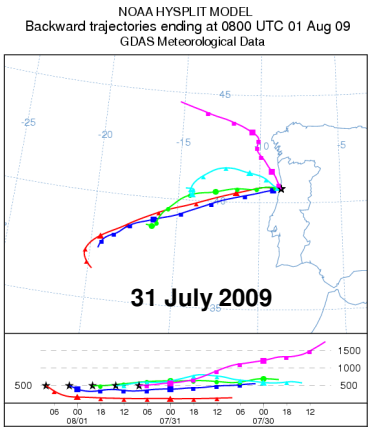
NOAA HYSPLIT MODEL
Backward trajectories ending at 0800 UTC 01 Aug 09
GDAS Meteorological Data
31 July 2009

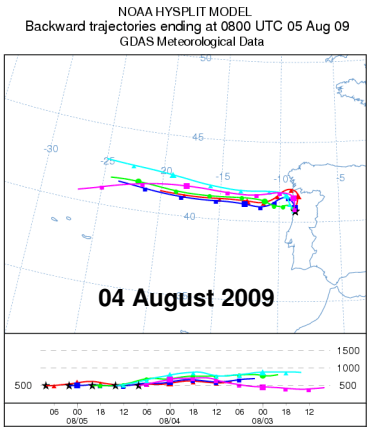
NOAA HYSPLIT MODEL
Backward trajectories ending at 0800 UTC 05 Aug 09
GDAS Meteorological Data
04 August 2009

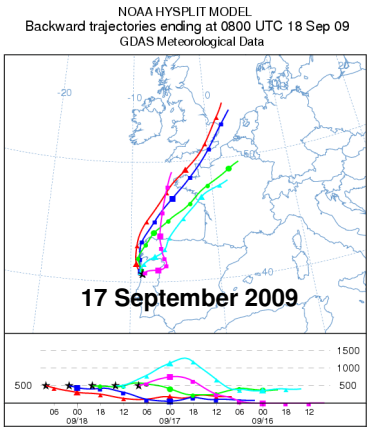
NOAA HYSPLIT MODEL
Backward trajectories ending at 0800 UTC 18 Sep 09
GDAS Meteorological Data
17 September 2009

Annex II. Excitation-emission matrix fluorescence contour and surface profiles of the collected rainwater samples

The excitation-emission matrix (EEM) fluorescence contour and surface profiles of the collected rainwater samples are presented below.

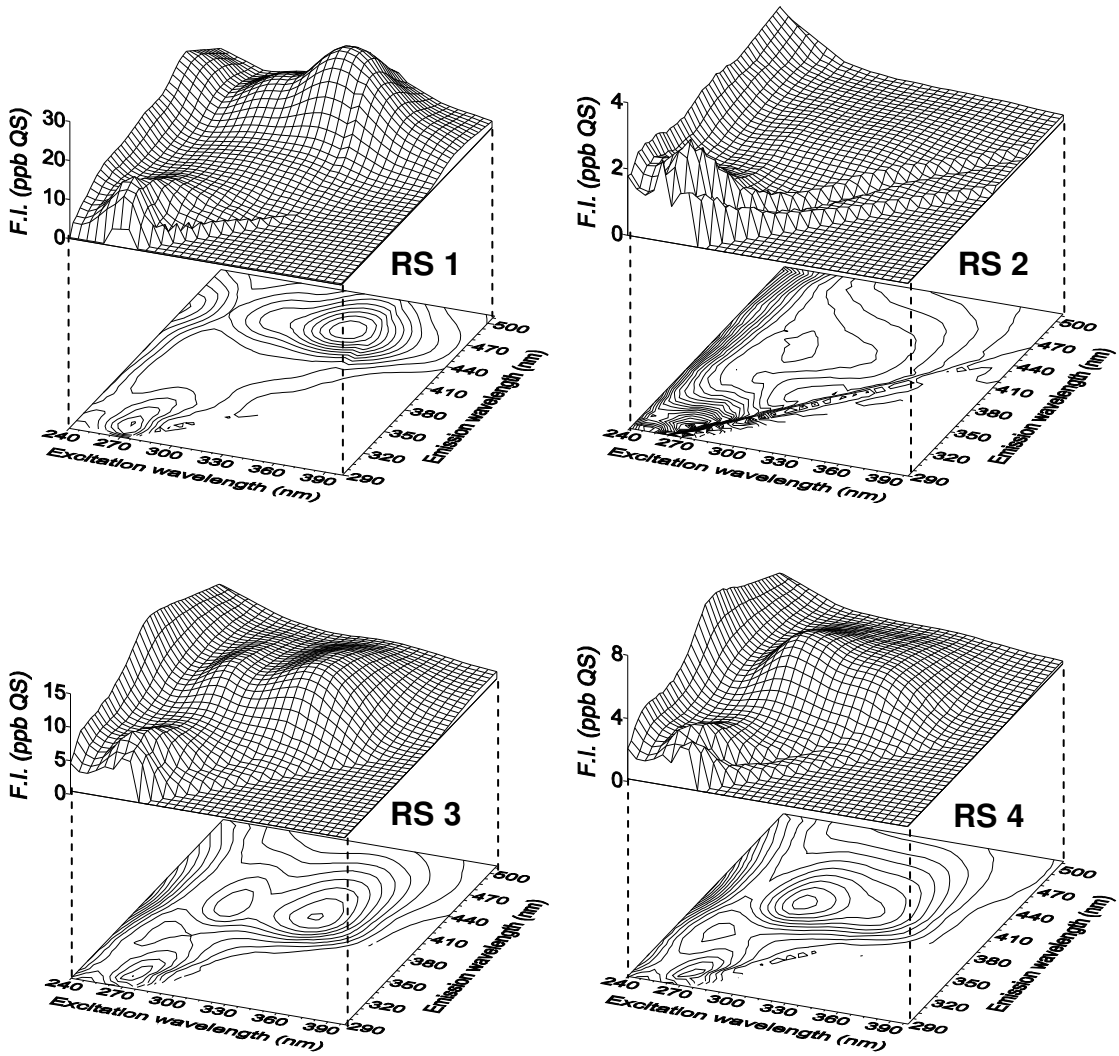

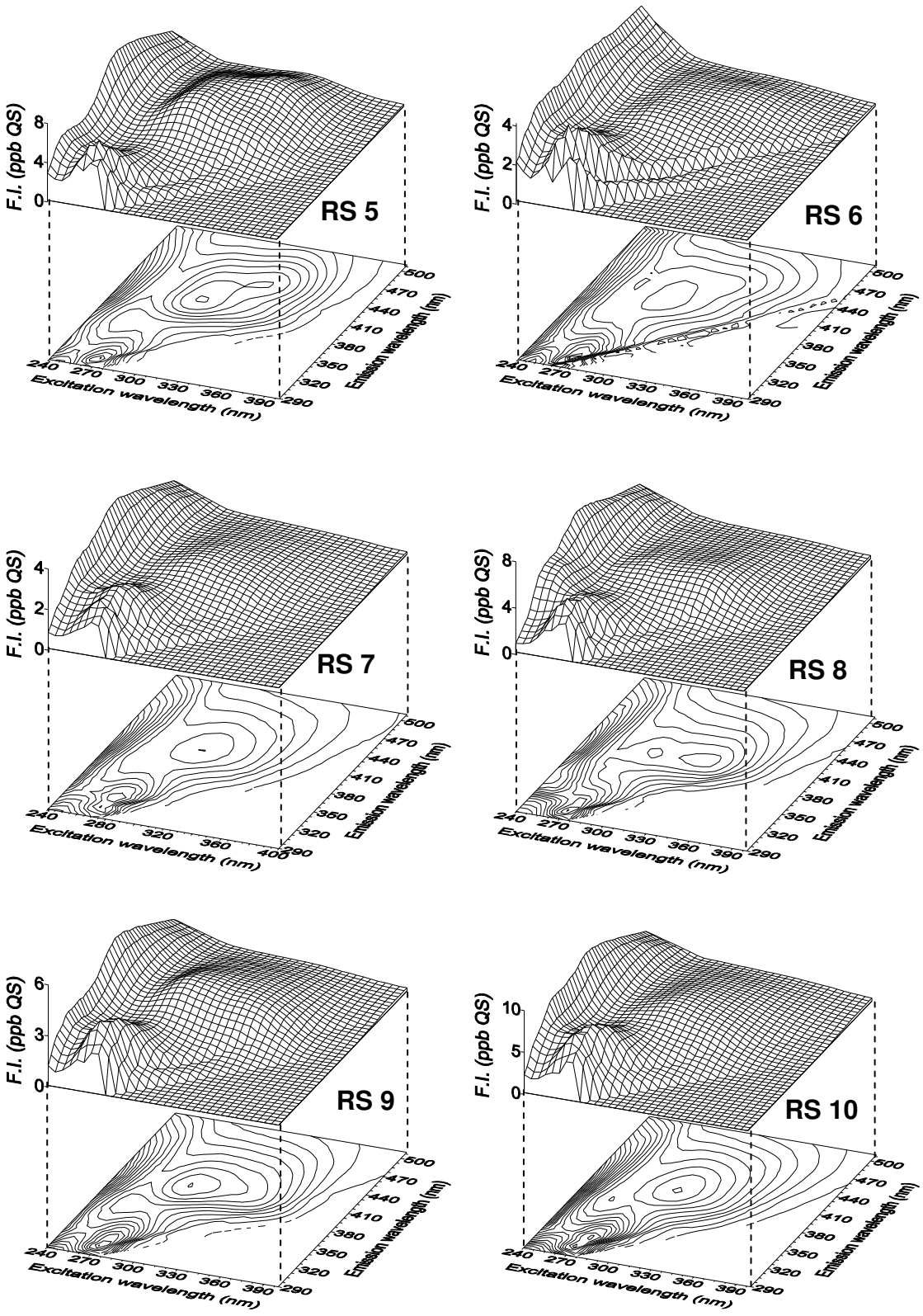
F.I. (ppb QS)
RS 5
RS 6
RS 7
RS 8
RS 9
RS 10
Excitation wavelength (nm)
Emission wavelength (nm)

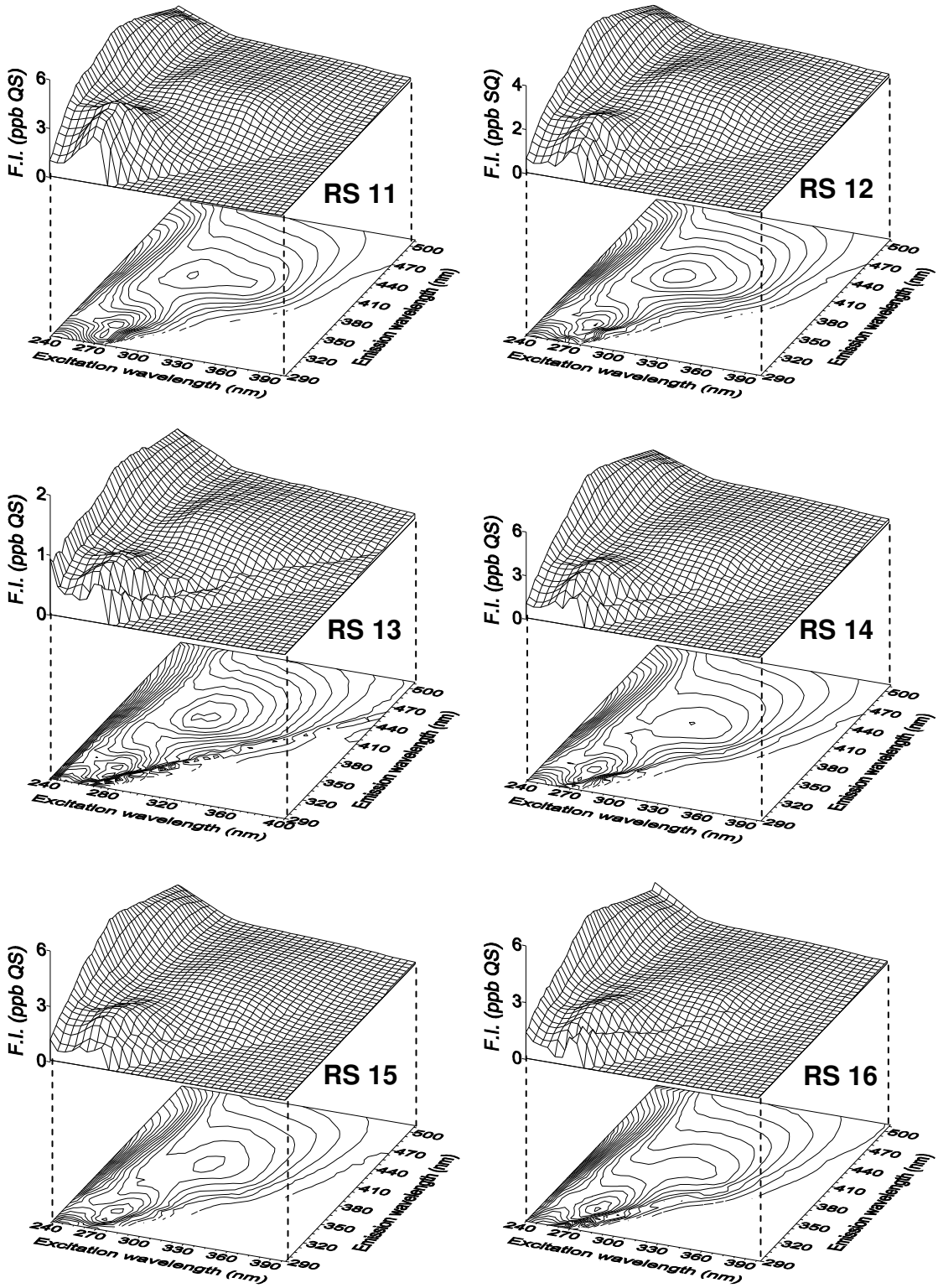
F.I. (ppb QS)
RS 11
F.I. (ppb SQ)
RS 12
RS 13
RS 14
RS 15
RS 16
Excitation wavelength (nm)
Emission wavelength (nm)

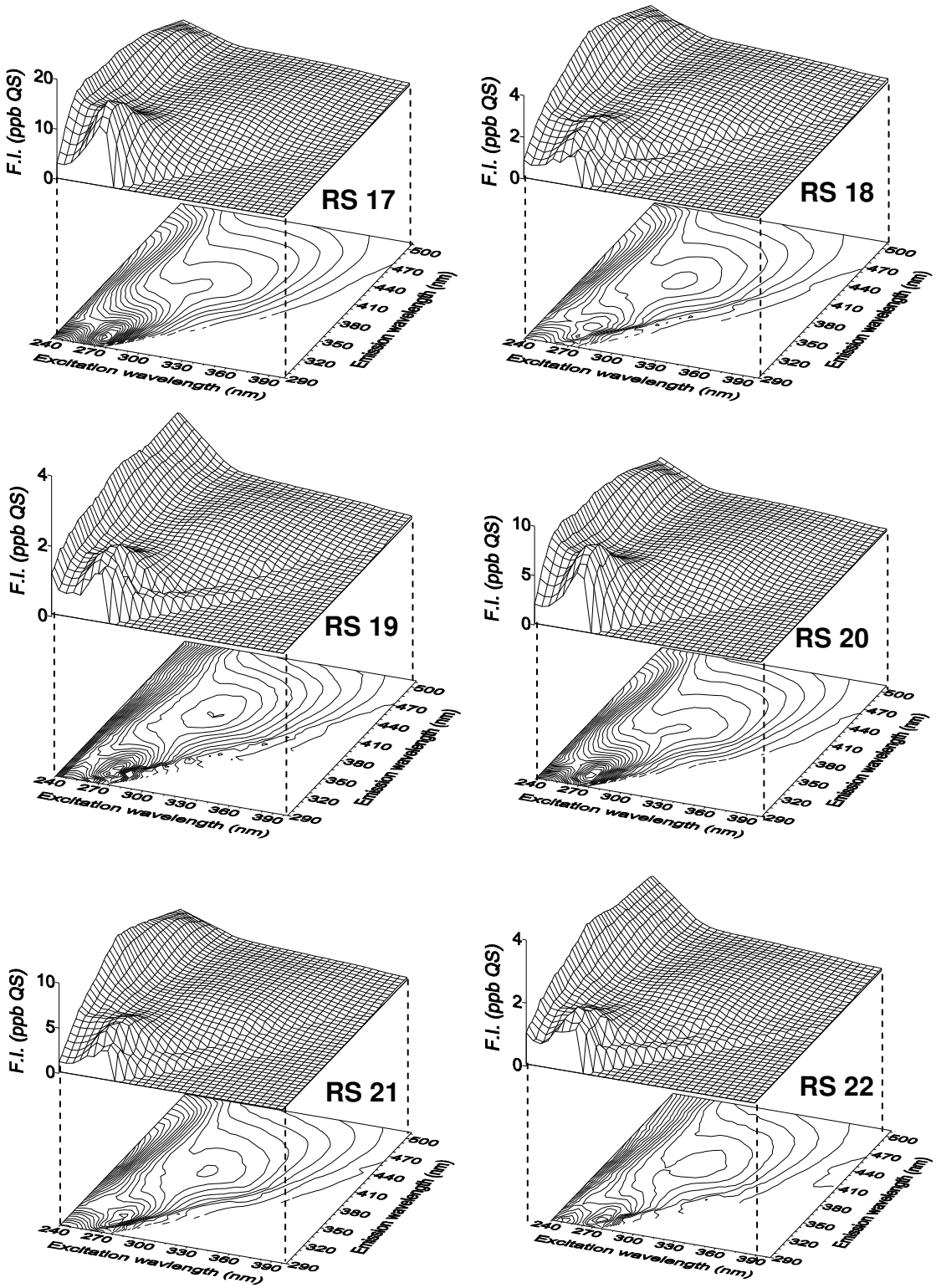
F.I. (ppb QS)
RS 17
RS 18
RS 19
RS 20
RS 21
RS 22
Excitation wavelength (nm)
Emission wavelength (nm)

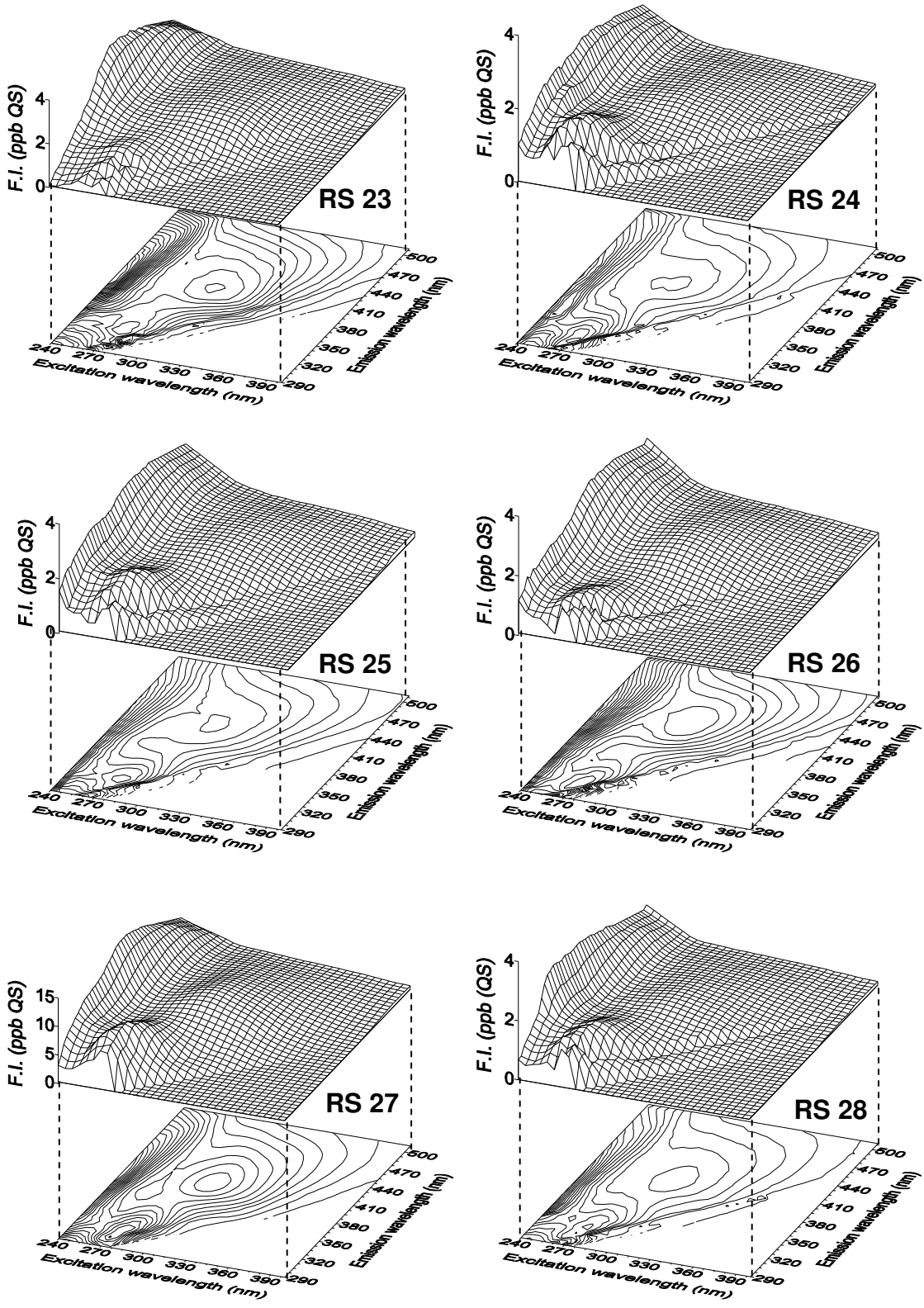
RS 23
RS 24
RS 25
RS 26
RS 27
RS 28
F.I. (ppb QS)
F.I. (ppb (QS)
Excitation wavelength (nm)
Emission wavelength (nm)

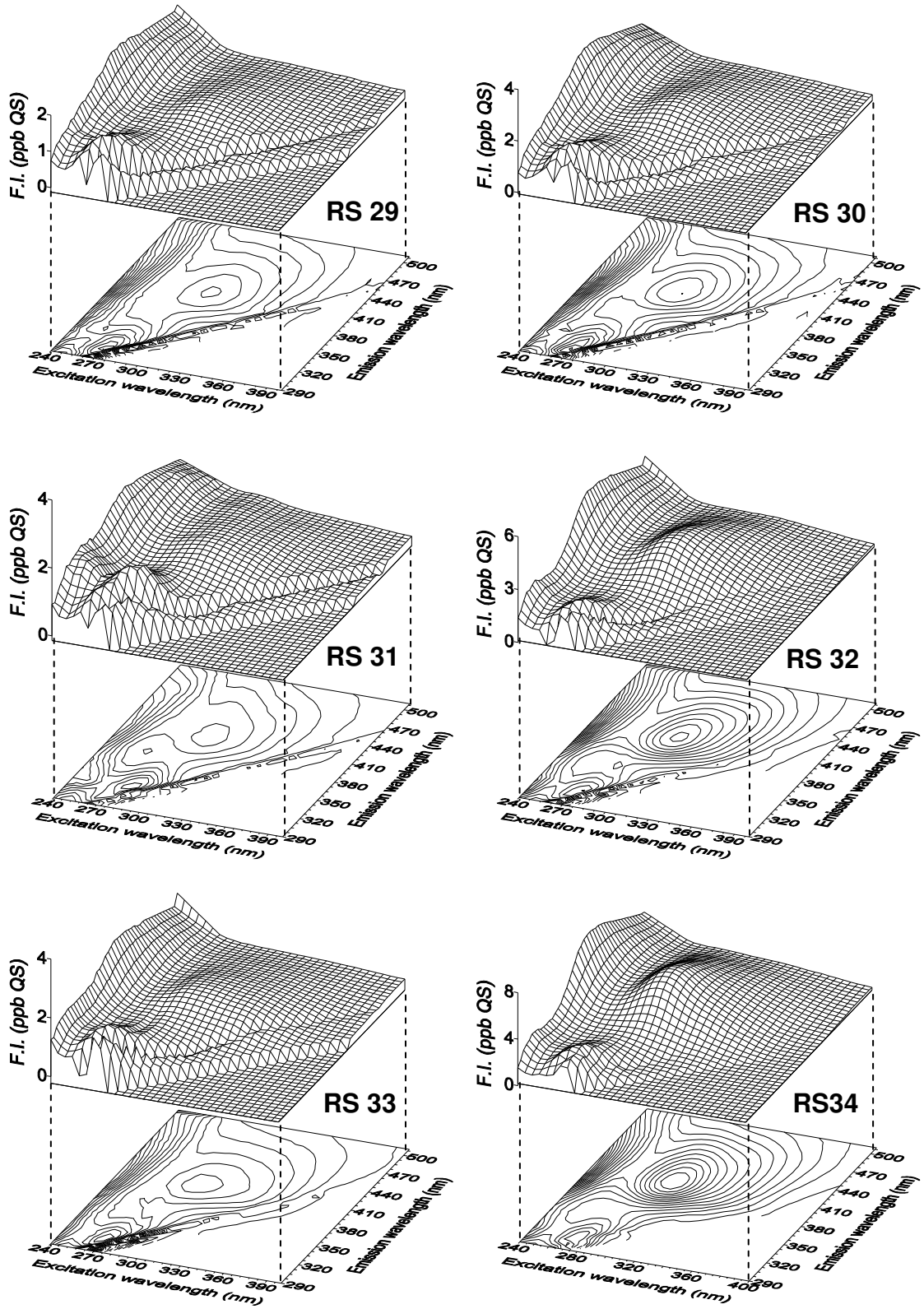
F.I. (ppb QS)
RS 29
RS 30
RS 31
RS 32
RS 33
RS34
Excitation wavelength (nm)
Emission wavelength (nm)

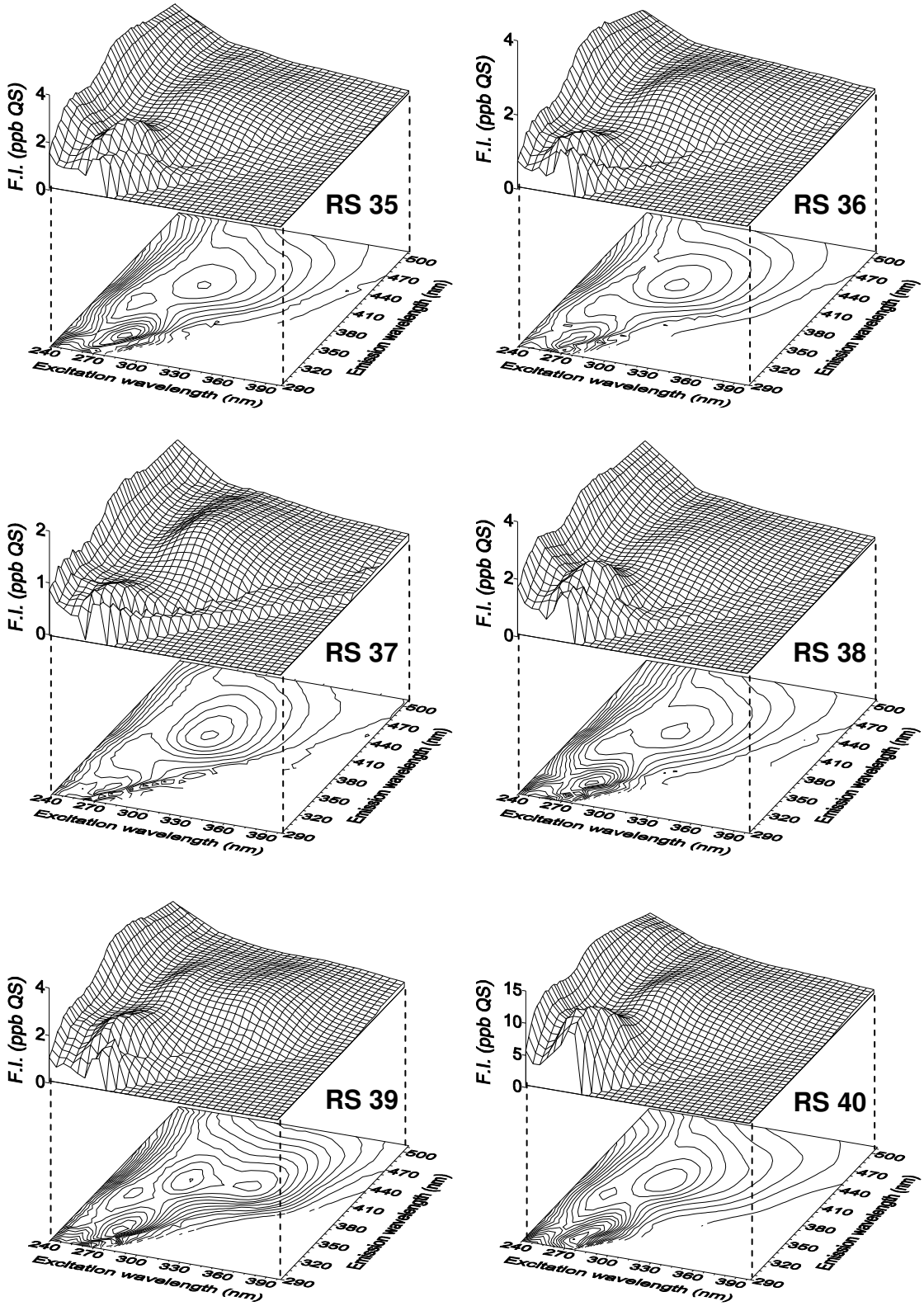
RS 35
RS 36
RS 37
RS 38
RS 39
RS 40
F.I. (ppb QS)
Excitation wavelength (nm)
Emission wavelength (nm)

Annex III. Excitation-emission matrix fluorescence contour and surface profiles of the eluates of rainwater samples

The excitation-emission matrix (EEM) fluorescence contour and surface profiles of the eluates obtained from the application of DAX-8 based procedure to the collected rainwater samples, are presented below. In order to avoid concentration effects, EEM fluorescence contour and surface profiles were normalised to dissolved organic carbon (DOC) content of the eluate (in g L^{-1}), and they are shown as specific fluorescence intensity (Spec. F.I.; g^{-1}C L ppb QS).

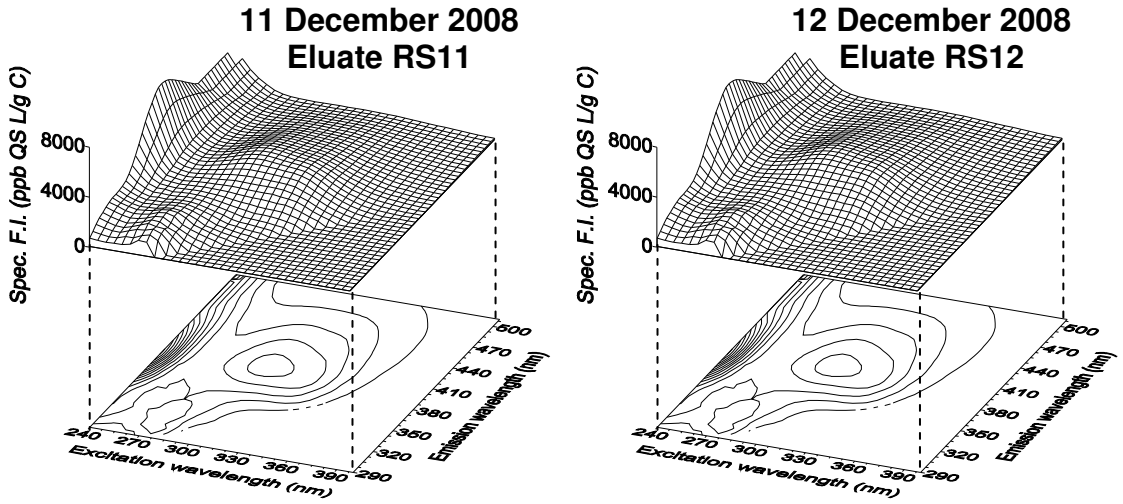

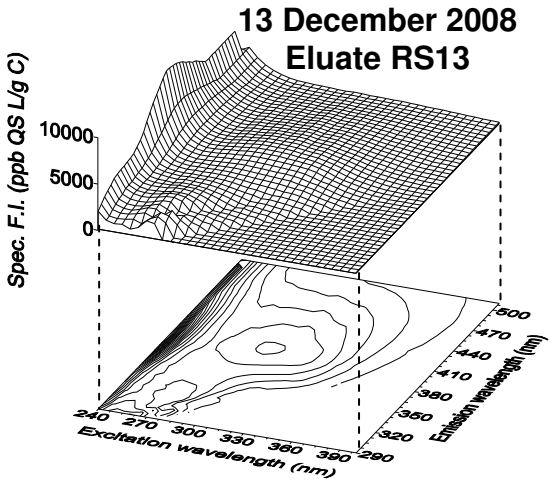
13 December 2008
Eluate RS13
Spec. F.I. (ppb QS L/g C)
10000
5000
0
240 270 300 330 360 390
Excitation wavelength (nm)
290 320 350 380 410 440 470 500
Emission wavelength (nm)

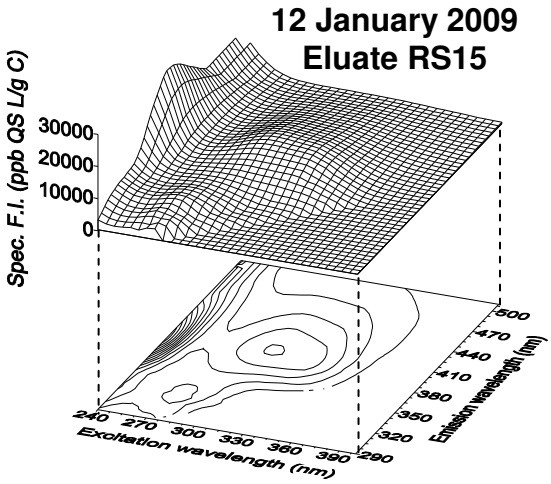
12 January 2009
Eluate RS15
Spec. F.I. (ppb QS L/g C)
30000
20000
10000
0
240 270 300 330 360 390
Excitation wavelength (nm)
290 320 350 380 410 440 470 500
Emission wavelength (nm)

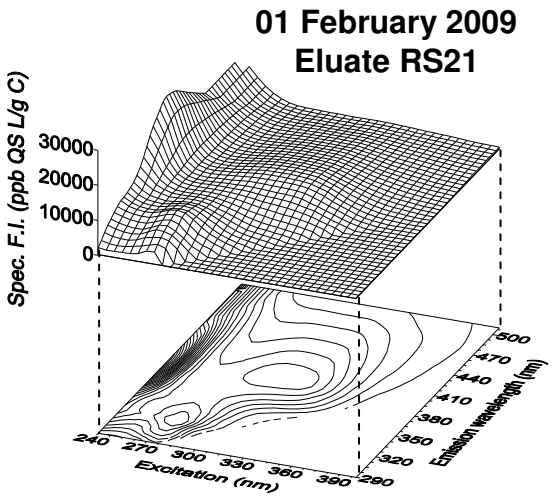
01 February 2009
Eluate RS21
Spec. F.I. (ppb QS L/g C)
30000
20000
10000
0
240 270 300 330 360 390
Excitation (nm)
290 320 350 380 410 440 470 500
Emission wavelength (nm)

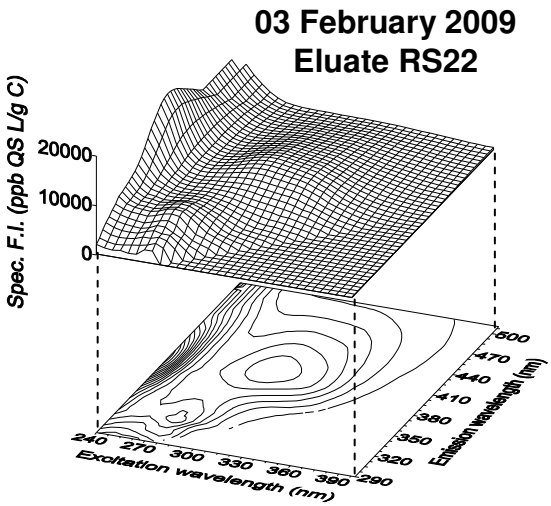
03 February 2009
Eluate RS22
Spec. F.I. (ppb QS L/g C)
20000
10000
0
240 270 300 330 360 390
Excitation wavelength (nm)
290 320 350 380 410 440 470 500
Emission wavelength (nm)

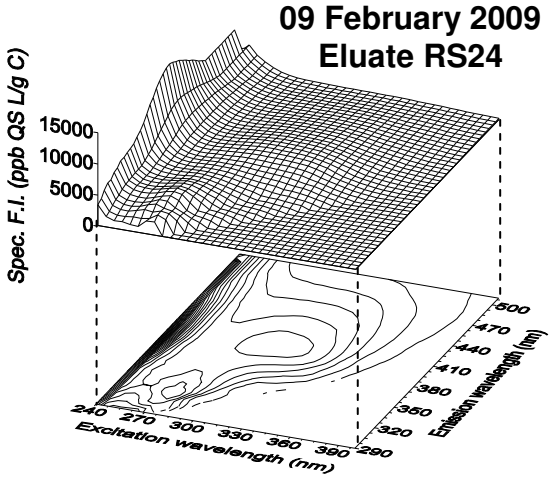
09 February 2009
Eluate RS24
Spec. F.I. (ppb QS L/g C)
15000
10000
5000
0
240 270 300 330 360 390
Excitation wavelength (nm)
290 320 350 380 410 440 470 500
Emission wavelength (nm)

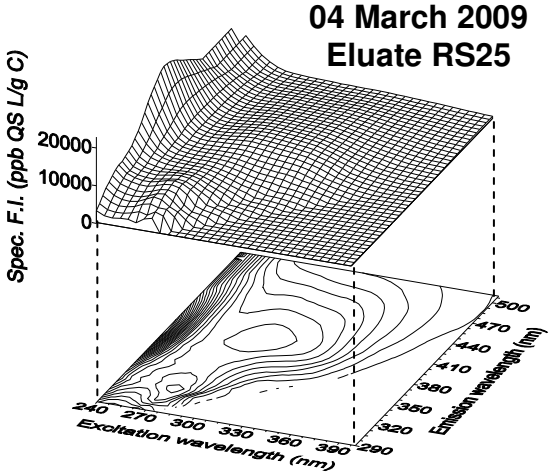
04 March 2009
Eluate RS25
Spec. F.I. (ppb QS L/g C)
20000
10000
0
240 270 300 330 360 390
Excitation wavelength (nm)
290 320 350 380 410 440 470 500
Emission wavelength (nm)

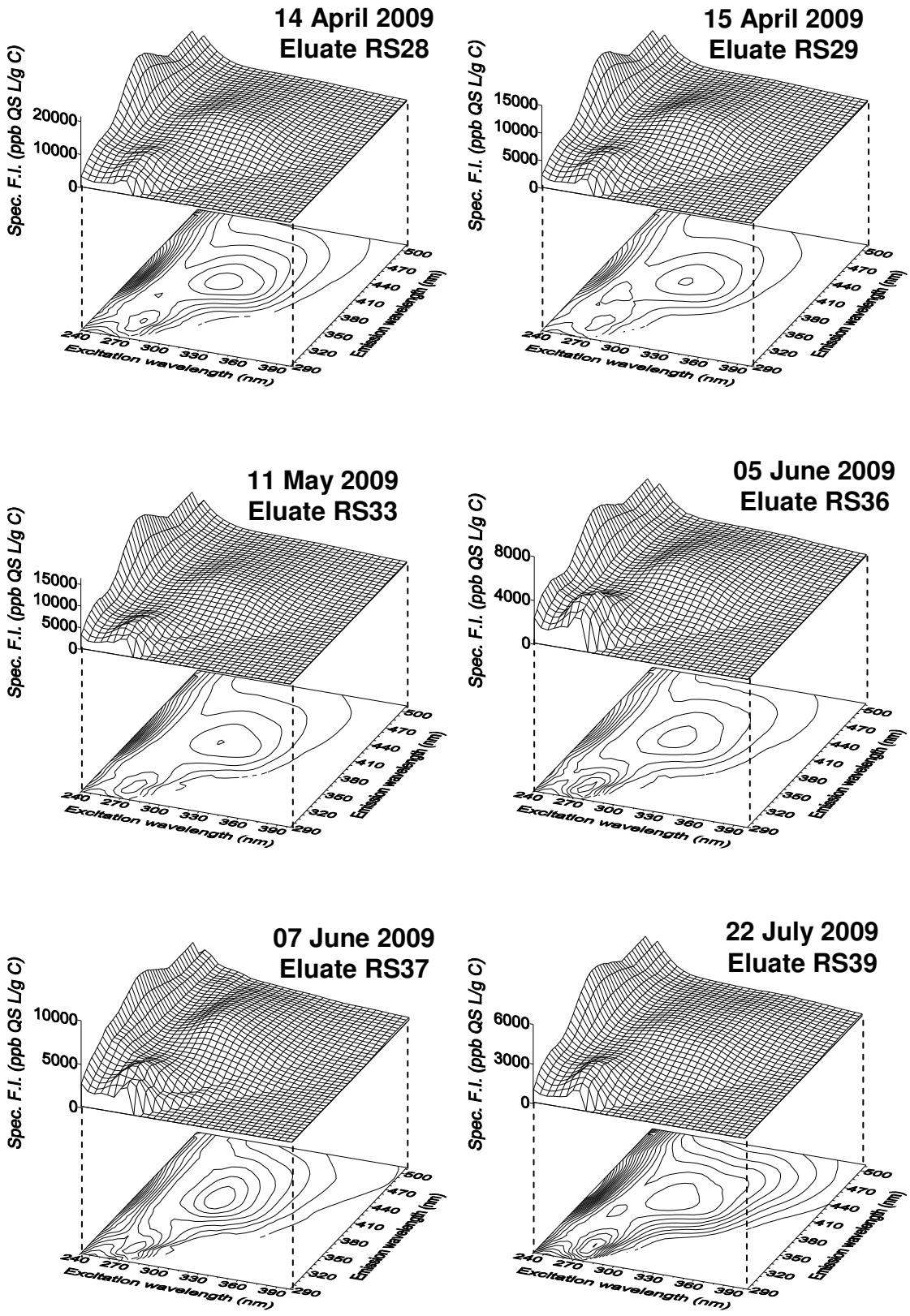
14 April 2009
Eluate RS28
15 April 2009
Eluate RS29
11 May 2009
Eluate RS33
05 June 2009
Eluate RS36
07 June 2009
Eluate RS37
22 July 2009
Eluate RS39
Spec. F.I. (ppb QS L/g C)
Excitation wavelength (nm)
Emission wavelength (nm)